University of Insubria, Como
Department of Science and High Technology

Ph.D. Program in Chemical and Environmental Sciences
(XXIX cycle) – Curriculum "Environment and Land"

Fine and ultrafine particulate: sampling, analysis and metal characterization for a risk assessment on human health

Supervisor
Prof. Domenico M. Cavallo

Ph.D. Coordinator
Prof. Norberto Masciocchi

External Supervisor
Prof. Andreas Limbeck

Ph.D. Candidate
Sabrina Rovelli

Academic Year 2015-2016

…A chi in questo mio percorso di vita
mi ha aiutata a crescere
professionalmente e personalmente…

…To those who supported
my professional and personal growth…

CONTENTS

Summary ***9***

Chapter 1 – Introduction ***13***

1.1 Background and Research Objectives **13**

1.2 Outline of the Thesis **17**

References **18**

Tables **25**

Figures **60**

Chapter 2 – Mass Concentration and Size-Distribution of Atmospheric Fine and Ultrafine Particles in an Urban Environment ***61***

1. Introduction **61**

2. Experimental Method **63**
2.1 Sampling Area Description and Sampling Strategy 63
2.2 Sampling Equipment 64
2.3 Statistical Analysis and Data Treatment 66

3. Results **67**
3.1 Sampling Information and Meteorological Conditions 67
3.2 Comparison Between DLPI and HI-$PM_{2.5}$ Mass Concentration 68
3.3 Ambient PM Mass Concentration and Temporal Trends 68
3.4 Particle Mass Size-Distribution 70

4. Discussion **70**
4.1 Comparison Between DLPI and HI-$PM_{2.5}$ Mass Concentration 70
4.2 Ambient PM Mass Concentration, Size-Distribution and Temporal Trends 71
4.3 Comparison of Ambient PM Concentrations with Literature Data 73
4.4 Strengths and Limitations of the Study 74

5. Conclusions **75**

References **76**

Tables **81**

Figures **90**

Chapter 3 – Multi-Element Analysis of Size-Segregated Fine and Ultrafine Particulate via Laser Ablation-Inductively Coupled Plasma-Mass Spectrometry ***99***

1. Introduction **99**

2. Experimental **101**
2.1 Collection of Size-Segregated Particles 101
2.2 Reagents, Standards and Reference Material 102
2.3 Wet Chemical Digestion and Conventional ICP-MS Analysis 102
2.4 LA-ICP-MS Procedure 104

3. Results and Discussion **106**

3.1 Validation of the Conventional ICP-MS Procedure 107
3.2 Development of an Accurate and Reproducible LA Procedure 108
3.2.1 Method improvement and optimization 108
3.2.2 Analytical performance 110

4. Conclusions **111**

References **112**

Tables **115**

Figures **126**

Chapter 4 – Toxic Trace Metals in Airborne Particulates: Mass Concentration, Size-Distribution and Health Risk Assessment ***135***

1. Introduction **135**

2. Materials and Methods **136**
2.1. Size-Segregated PM Collection and Analysis 136
2.2. Exposure Dose and Health Risk Assessment 137
2.3 Statistical Analysis and Data Treatment 139

3. Results and Discussion **140**
3.1. Elemental Mass Concentrations and Size-Distributions 140
3.2 Risk Characterization of Trace Metals in Size-Segregated PM via the Inhalation Exposure Route 141

4. Conclusions and Future Developments **143**

References **143**

Tables **147**

Figures **154**

Chapter 5 – Is Particulate Air Pollution at the Front Door a Good Proxy of Residential Exposure? ***159***

1. Introduction **159**

2. Methods **160**
2.1 Study Design 160
2.2 Instrumentation and Monitoring Procedure 161
2.3 QA/QC and Statistical Analysis 163
2.3.1 QA/QC 163
2.3.2 Statistical Analysis 163

3. Results and Discussion **163**
3.1 Meteorological Conditions and Air Exchange Rates 163
3.2 Comparison of Front and Back Monitoring Sites 164
3.2.1 Ultrafine Particles Number Concentrations 164
3.2.2 Particle Size Distribution 165
3.2.3 $PM_{2.5}$ Mass 166
3.2.4 Chemical Composition of $PM_{2.5}$ 167
3.3 Strengths and Weaknesses of the Study 168

4. Summary and Conclusions **169**

References **170**

Tables **177**

Figures **181**

Supplementary Material **185**

Chapter 6 – Occupational Exposure to Arsenic and Cadmium in Thin-Film Solar Cell Production ***193***

1. Introduction **193**

2. Materials and Methods **195**
2.1 Air Monitoring: Sampling and Analysis 195
2.2 Surface Contamination: Sampling and Analysis 196
2.3 Biomonitoring: Urine Collection and Analysis 196
2.4 Limit of Detection and Limit of Quantification 197
2.5 Statistical Analyses 197

3. Results **197**
3.1 Air Monitoring 197
3.2 Surface Contamination Monitoring 198
3.3 Biological Monitoring 198
3.4 Plant Life-Cycle Stage 198

4. Discussion **199**
4.1 Air Monitoring 199
4.2 Surface Contamination Monitoring 200
4.3 Biological Monitoring 200
4.4 Plant Life-Cycle Stage 201
4.5 Risk Management 201
4.6 Concluding Remarks 202

5. Conclusions **203**

References **204**

Tables **207**

Figures **211**

General Conclusions and Future Developments ***213***

Annex 1 – Participation in Funded Research Projects and Scientific Publication List ***215***

Summary

Background and Aims

The Particulate Matter (PM) is one of the main air pollutants typically present in urban environments with high population density and industrial activities. The scientific concern addressed to this complex mixture of organic and inorganic substances is mainly related to the well documented associations between PM concentration levels typically observed in urban and industrial areas and increased mortality and morbidity, as well as other adverse health outcomes.

Nevertheless, the particulate concentrations reported to be associated with adverse effects in epidemiological studies are much lower than those observed to cause health effects in laboratory toxicological studies and the biological mechanisms that are able to cause serious health damage even at such low concentrations are not yet clear. The problem is quite complex because of the great spatial and temporal variabilities in the PM concentration levels and because of the different composition of airborne particles that is not always adequately reflected in the results of epidemiological studies. Moreover, although current International Guidelines are focused on PM_{10} and $PM_{2.5}$, an emerging literature appears to demonstrate an increased toxicity for submicrometric (PM_1) and especially ultrafine ($PM_{0.1}$) particles compared to larger particulates on a per mass basis.

Motivated by this paradox, there is particular interest in examining those aspects that might be capable of producing injury while at the same time not contributing greatly to the measured airborne particle mass concentration, and information about the size-resolved chemical composition of airborne PM appear to be needed for an accurate evaluation of its toxicity.

Because of the great importance that this type of knowledge may have in terms of health concern and due to the limited information available on a local scale on this topic, a research project was specifically developed. Special emphasis was paid on the metal component of size-fractionated PM, because of its known adverse effects exerted on human health, as well documented in the scientific literature.

The general aim of the project could therefore be identified in the characterization of selected trace metals in fine, submicrometric and ultrafine particles. For these purposes, an experimental approach was specifically designed. Proper sampling lines and innovative analytical methods were developed and obtained findings were then used to characterize the study area in terms of mass concentrations, size-distributions, temporal variabilities. Moreover, the potential non-carcinogenic and carcinogenic risks for human health via the inhalation exposure route posed by the investigated metals were characterized.

Materials and Methods

To investigate the ambient mass concentration, size-distribution and temporal variability of atmospheric PM, an intensive long-scale monitoring campaign was undertaken at an urban background site in Como, Northern Italy. The experimental approach was designed to integrate different meteorological and environmental conditions that could potentially influence the PM mass and composition in the urban environment. For this reason, the total duration of the planned campaign was 10 months. Atmospheric sampling started at the end of May 2015 and was stopped at the end of March 2016, thus obtaining a large number of samples that could be used to characterize the study area and investigate temporal variations in the measured PM

concentration levels. Measurements generally started between 09:00–10:30 on Monday mornings and lasted until Friday mornings, using a 96-h sampling duration every sampling week. The sampling equipment consisted of different monitoring devices. A 13-stage Low Pressure Impactor (DLPI) was used for the collection of size-segregated particulates in the 0.028–10 μm size range. To evaluate DLPI performance and accuracy, during most of the sampling weeks $PM_{2.5}$ was also monitored via an Harvard-type Impactor (HI) and an external weather station was used to characterize meteorological conditions during the study period at the sampling site.

In order to characterize the total metal content in the size-segregated PM, a novel Laser Ablation-Inductively Coupled Plasma-Mass Spectrometry (LA-ICP-MS) measurement protocol was properly developed. Special efforts were made to improve and optimize sample pre-treatment steps and LA operating conditions in order to avoid some critical drawbacks encountered during analysis and make the particulate samples suitable for an accurate and reproducible LA-ICP-MS analysis, regardless of the mass loading on each dust filter. Under the optimum conditions, dust samples as well as blank filters and standards for calibration were analyzed by multiple line scan of each sample spot and quantitative analysis was accomplished with dried-micro droplets of aqueous standard solutions. The accuracy of LA-ICP-MS results was verified by comparison with conventional ICP-MS analysis of selected PM samples after complete sample mineralization with mineral acids. In this context, an alternative approach for sample pre-treatment in liquid ICP-MS analysis was developed, since the conventional microwave-assisted digestion approach utilizing *aqua regia* does not allow the complete dissolution of the filters used for particle collection in this study.

After method validation, the proposed LA-ICP-MS protocol was applied for the total metal content analysis of selected trace metals (Cr, Mn, Fe, Ni, Cu, Zn, Ba and Pb) on the extended set of size-segregated PM samples collected during the monitoring campaign.

Results and Conclusions

Despite some limitations, this thesis provides important insights about the concentration and size-distribution of airborne particles and metal components, that could be useful in developing larger air pollution and epidemiological studies.

As expected, the highest PM concentration levels were found during the heating period because of a joint effect of meteorological factors and variations in type and/or number of emission sources. One of the most interesting findings of this investigation was that the greatest increase effect in the PM concentration levels was registered for particles having aerodynamic diameter (a.d.) values between 0.15 and 1.60 μm (and mainly for particles having a.d. values between 0.4 and 0.9 μm - more related to the presence of additional sources of submicronic particles during the cold season), whereas no relevant and significant differences were found for particles > 1.60 μm.

The proposed LA-ICP-MS method for the metal characterization provided precise and accurate results, with a better sensitivity than the conventional ICP-MS technique. The LA treatment procedure identified for sample preparation allowed accurate and reproducible analysis with a simple and fast sample preparation, thus overcoming the laborious pre-treatment approach required for wet chemical digestion. With the proposed LA-ICP-MS approach, risks associated with sample contamination were minimized and the time needed for the application of the whole measurement protocol was reduced, with the possibility to analyze a greater number of

samples with several sample replicates in the same time required for the established ICP-MS protocol. Because of the less-laborious and fast sample preparation and analysis, this method could be used for routine application in order to monitor the elemental concentration and size-distribution of airborne particulates with a suitable precision and accuracy for health and sanitary purposes.

Regarding the elemental composition, the investigated elements accounted, on average, for a very small percentage of the total $PM_{2.5}$ mass concentration and results revealed characteristic size-distributions and great variations in the concentration levels of the analyzed toxic metals, with values differing by one or more orders of magnitude from element to element and between the different sampling periods.

Although based on the assumption that people living in the study area are exposed every day for a lifetime to the average metal concentrations monitored during the whole campaign, the estimated hazard quotients for each element and the overall estimate for non-carcinogenic effects posed by all of the metals under investigations were always < 1, suggesting no significant risks for the exposed population. Nevertheless, aerosol particles > 0.3 μm seemed to play the major role in the characterization of the overall non-carcinogenic risk, whereas lower contribution were found for particles < 0.3 μm, with percentage contribution values decreasing with decreasing aerosol particle size. Moreover, also the estimated $PM_{2.5}$ carcinogenic risks (CR) for Ni and Cr were below or within the acceptable range established in terms of regulatory purposes for the general population (10^{-6} or 10^{-5}), thus indicating a negligible cancer risk for people living in the study area. Nevertheless, it should be important taking into account that, although the estimated CRs for Ni were two orders of magnitude lower that the calculated CRs for Cr, the higher contributions to the total $PM_{2.5}$-CR for Ni were found to be mainly related to airborne particles that are able to more deeply penetrate into the respiratory system.

Therefore, despite some assumptions or limitations, results obtained from this investigation could represent important tools in epidemiological studies, as an innovative and alternative target with respect to the typical PM fractions on which these types of research are generally focused (PM_{10} or $PM_{2.5}$). Because of the type of sampling site used for particle collection (urban background) and the extended time series of size-segregated particle mass concentrations and elemental composition, these data could be used to better assess if the known and documented PM effects exerted on the general population (e.g., increased mortality or morbidity) could be related to specific size fractions and/or components of $PM_{2.5}$, with a particular focus on those particles that are able to reach the deepest parts of the respiratory tree, and if these effects are really greater than or independent from the effects induced by larger size particulates.

Chapter 1 – *Introduction*

1.1 Background and Research Objectives

In the recent years, the monitoring of air quality and air pollution in outdoor, as well as indoor or occupational environments, has become of increasing interest mainly because of the need to verify the compliance with recommended guideline or threshold limit values and assess the potential health risks for humans related to the exposure to various atmospheric contaminants.

Different chemical compounds are normally emitted in the atmosphere from natural as well as anthropogenic sources. The Particulate Matter (PM) is one of the main air pollutants typically present in urban environments with high population density and industrial activities and it may comprise primary particles – directly emitted as liquid or solids from sources such as biomass burning, incomplete combustion of fossil fuels, traffic related suspension phenomena of road or soil, sea salt and biological materials (plant fragments, micro-organisms, pollens) – or secondary particles – formed by gas to particle conversion in the atmosphere (Lohmann and Feichter, 2005; Pöschl, 2005). The PM composition is variable and it generally includes different compounds, from carbonaceous fractions (organic carbon, elemental carbon, carbonate carbon) to inorganic components (crustal elements, trace metals and ionic species) that undergo various physical and chemical interactions and transformations (atmospheric aging, coagulation, gas uptake).

The scientific concern addressed to this complex mixture of organic and inorganic substances is mainly related to the well documented associations between PM concentration levels typically observed in urban and industrial areas and increased mortality and morbidity (Pope *et al.*, 1995), as well as other adverse health outcomes. Aerosol particles are indeed recognised to have a strong impact on the environment and to be of concern in health-related effects. Numerous epidemiological and toxicological studies have found associations between measured particulate matter (PM) levels and adverse outcomes, as eye irritations, chronic respiratory and cardiopulmonary disease, lung cancer (Erdinger *et al.*, 2005; Schwarze *et al.*, 2006; Brook *et al.*, 2010; Stafoggia *et al.*, 2013; Raaschou-Nielsen *et al.*, 2016).

Nevertheless, the particulate concentrations reported to be associated with adverse effects in epidemiological studies are much lower than those observed to cause health effects in laboratory toxicological studies and the biological mechanisms that are able to cause serious health damage even at such low concentrations are not yet clear (Harrison and Yin, 2000; Raaschou-Nielsen *et al.*, 2016). The problem is quite complex because of the great spatial and temporal variabilities in the PM concentration levels and because of the different composition of airborne particles that is not always adequately reflected in the results of epidemiological studies (Harrison and Yin, 2000).

Motivated by this paradox, there is particular interest in examining those aspects that might be capable of producing injury while at the same time not contributing greatly to the measured airborne particle mass concentration. One of the main goal of the scientific research in this area is to understand if the mechanisms of particle toxicity are defined in specific size fractions and how the particulate chemical composition can affect it (Harrison and Yin, 2000; Kelly and Fussell, 2012).

Inhalation is the major pathway of exposure to airborne PM. The relation between the concentrations and characteristics of air contaminants and the resultant toxic doses and

potential hazards after their inhalation depends greatly on their patterns of deposition and the rates and pathways for their clearance from the deposition sites.
The distribution of deposition sites is firstly dependent on the aerodynamic diameter of particles. Particle size and shape are critical factors controlling the extent to which airborne PM penetrates the human respiratory tract (Lippmann *et al.*, 1980), and they influence the potential health toxicity, as well as other important variables. According to Yeh *et al.* (1976), since the initial deposition pattern of inhaled particles determines their future clearance and insult to tissue, the respiratory tract deposition plays a key role in assessing the potential toxicity of aerosols. Factors influencing the deposition efficiency of inhaled particles can be classified into three main areas: i) the physics of aerosols; ii) the anatomy of the respiratory tract and iii) the airflow patterns in the lung airways.
In the physics of aerosols, the forces acting on a particle and its physical and chemical properties, such as particle size and size distribution, density, shape, hygroscopic or hydrophobic character, chemical and physical reactions, will affect the deposition. With respect to the anatomy of the respiratory tract, important parameters are diameters, lengths and branching angles of airway segments, while physiological factors include airflow and breathing patterns. All these factors, together with the content of toxics, the total human exposure and the health status of the population, determine the potential particles toxicity.
Coarse particulate ($PM_{2.5–10}$) deposits in the upper respiratory tract while fine particles ($PM_{2.5}$) travel deeper into the lungs. The ultrafine fraction, defined as those fraction with aerodynamic diameter (a.d.) in the 1–100 nm range (UFPs, $PM_{0.1}$), is able to reach the alveolar region and it is consequently more difficult to eliminate through the mucociliary clearance and the physiological leaching mechanisms.
According to Lippmann *et al.* (1980), particle retention is a time-dependent variable equal to the difference between the amount of aerosol deposited and the amount cleared. Several mechanisms contribute to the particles clearance. The most important mechanism for insoluble particles is the mucociliary clearance. Soluble particulates, depending on their physicochemical properties, may either be incorporated into the mucus and be taken up by the airway epithelium, or pass through it to be cleared by the bronchial and pulmonary circulation. For a given individual, rates of clearance within the respiratory tract vary greatly from region to region. In the ciliated nasal passages and the tracheobronchial tree, clearance in normal individuals is completed in less than one day. In the alveolar zone, clearance proceeds by slower processes, most of which vary considerably with the particles' composition (Lippmann *et al.*, 1980).

For all the aforementioned reasons, in the last decade the knowledge about the chemical characterization of airborne particles in different size-fractions began to grow, with a particular focus on the smallest particle size ranges (submicronic (PM_1) and UFPs). Increasing toxicological and epidemiological evidences have indeed suggested strong correlations between health endpoints and ultrafine particles (Ibald-Mulli *et al.*, 2002; Oberdörster *et al.*, 2005; Karakoti *et al.*, 2006; Ostro *et al.*, 2015).
An emerging literature appears to demonstrate an increased toxicity for UFPs compared to larger particles on a per mass basis, especially if considering that the respiratory deposition fraction of these particles increases sharply with decreasing size (Montoya *et al.*, 2004). At a given mass, UFPs have 10^2 to 10^3 times more surface area than particles with aerodynamic

diameter in the 0.1–2.5 μm range and approximately 10^5 times more surface area than the coarse particulate (Harrison *et al.*, 2000). This surface area-to-mass ratio confers to submicron and ultrafine particles an important surface chemistry when in contact with epithelial cells (Donaldson *et al.*, 2002). Furthermore, although it makes a negligible contribution to particle mass levels, the ultrafine fraction dominates the atmospheric number concentration (Cass *et al.*, 2000), and it comprises particles having residence times in air that allow the atmospheric dispersion over a long distance from the original emission source, resulting in an enhanced level of ambient PM concentrations even at rural or background sites.
As well documented in the scientific literature, among all of the PM chemical constituents, a particular airborne PM component that is known to exert toxic effects on humans, even if at trace or ultra-trace levels, is the metallic fraction. Many elements, like Cd, Cr, Cu, Mn, Ni, Pb, V, Zn, are widely distributed in PM and hence are suspected to be an important source of PM toxicity. The concern becomes even more critical when considering the larger surface area of submicronic and UF particles and their higher deposition efficiency in the alveolar region. Investigations suggested that trace metals distributed throughout the lung on UFPs could catalyze the formation of oxidants within the lung, which in turn produce tissue damage (Li et al., 2003). Some metals, especially transition metals as Cd, Ni, Pb, or Tl, can injure the kidneys, the nervous and immune system as well as be teratogenic and carcinogenic (Sun *et al.*, 2001; Raaschou-Nielsen *et al.*, 2016).
Consequently, metals-containing UFPs are potentially more harmful when inhaled. Therefore, information about the size-resolved elemental composition of airborne PM appear to be needed for an accurate evaluation of its toxicity.

Until about fifteen years ago, most of the research studies carried out worldwide focused on the elemental characterization of Total Suspended Particulates (TSP), PM_{10} and $PM_{2.5}$ (Ayrault *et al.*, 2010; Hueglin *et al.*, 2005; Lonati *et al.*, 2008; Tahir *et al.*, 2013). A recent large-scale investigation provided a wide outlook on PM_1 mass concentration and chemical composition at three Italian urban sites, aiming at the identification of PM_1 major sources and the estimation of their contributions to mass concentrations (Vecchi *et al.*, 2008).
The increasing interest in the ultrafine component led the research to focus on this aspect, still little known until the beginning of the twentieth century. Different studies investigating the size-distribution of elements in the airborne PM were carried out in the United States, Asia, Europe. In order to find the main research studies dealing with this topic, a systematic research on three of the main scientific databases of peer-reviewed literature (PubMed, Scopus and Web of Science) was carried out.
For each database, a selected list of keywords, which were the same for the different databases, was used (Table 1). Keywords/phrases and the query's structure were arranged as a function of the specific database. Ambient aerosol terms (ambient aerosol, atmospheric particulate matter, atmospheric aerosol, airborne particulate matter, PM, particulate matter) were combined with sampling-type search terms (impactor, cascade impactor, DLPI, nano MOUDI), chemical composition referred terms (elemental composition, chemical characterization, chemical composition, metallic elements, elemental, speciation, OR metal*) and to terms about mass concentration (particle size distribution, mass concentration*, gravimetric*, gravimetric* analysis, size distribution) and referred to air or to atmosphere.

As shown in Fig. 1, 262, 311 and 78 papers were identified in Web of Science, Scopus and Pubmed, respectively (last search performed on July, 26th 2016). All these manuscripts were selected following the reported inclusion criteria:

- Papers in which atmospheric samplings were performed outdoor and during normal conditions (e.g. dust storm events or volcanic eruptions were excluded)
- Papers reported the elemental characterization of size-segregated particulate matter (elemental mass concentration and size-distribution)
- Papers between January 2000 and July 2016
- Papers written in English language

Among all of the considered manuscripts, 58 papers were found to meet all the selected inclusion criteria. These papers were then systematically reviewed. Information about sampling site and its characteristics, sampling period, analyzed elements, study design and methods, mass and elemental distribution of size-fractionated PM, correlations between elements (when possible) and other results were extracted. The main findings for all of the considered papers are reported in Table 2.

Nevertheless, up to now, in Italy there are still very few researches on the elemental composition and size distribution of atmospheric PM and such information are even more scarce and limited on a local scale. Indeed, no data regarding the mass size distribution and metal composition, especially for fine, submicronic and ultrafine particles, are available for the Como urban area (Northern Italy).

Therefore, motivated by the importance that this knowledge may have in understanding the particles' toxicity and their human health effects by inhalation, in determining their emission sources (Gugamsetty *et al.*, 2012; Vecchi *et al.*, 2008), in classifying their natural or anthropogenic origins (Lim *et al.*, 2010), the main goals of the research project have been defined as follows:

1. **Assessment of the ambient concentrations and distribution of size-resolved atmospheric particles in the Como urban area.**

2. **Elemental characterization of fine, submicronic and ultrafine particles in different sizes through high-sensitivity analytical techniques, with a special focus on those metals having a great toxicological concern (e.g. Cr, Mn, Ni, Pb).**

3. **Characterization of the elemental size-distribution in the measured particle fractions, to understand how the chemical components are distributed in the airborne PM.** This is of significant interest both in epidemiological and toxicological studies since different investigations suggest that some of the most toxic metals (e.g. Pb, Cd, Ni, V) have high proportions in the smallest particle size ranges (Mbengue *et al.*, 2014; Niu *et al.*, 2010; Sato *et al.*, 2008).

4. **Assessment of the potential health risks for the general population living in the study area.**

5. **Evaluation of the contribution of anthropogenic sources to the ambient levels by the use of Enrichment Factors (EFs).** EFs relative to the average composition of the

upper continental crust are widely employed in the atmospheric chemistry to classify the natural (EF values close to unity, tipically for elements of crustal origins as Al, Si, Fe) or anthropogenic (tipically, EFs > 5) origins of metals in the air (Mbengue *et al.*, 2014).

6. **Assessment of temporal variations in the measured levels of particles and metal components.**

1.2 Outline of the Thesis

After a brief introduction on the topic, as explained in the previous paragraph, chapter 2 describes the experimental approach specifically developed to investigate the ambient mass concentration, size-distribution and temporal variability of atmospheric particulate matter - from coarse particles to the smallest particulate ranges - in an urban environment. For this purpose, size-segregated PM was collected at an outdoor urban background site during an intensive long-scale monitoring campaign by means of a multistage low pressure impactor. Obtained results were then used to evaluate the performance of the particulate sampler, assess ambient mass concentration and size-distribution of atmospheric PM in the 0.028–10 μm size range, assess temporal and seasonal variations and evaluate the influence of meteorological and environmental conditions on the measured PM concentration levels.

Chapter 3 focuses on the development and optimization of a novel Laser Ablation-Inductively Coupled Plasma-Mass Spectrometry (LA-ICP-MS) measurement protocol for the elemental characterization of size-segregated PM samples collected as described in chapter 2. The analytical method was developed in collaboration with the Laboratory of Inorganic Trace Analysis, Division of Instrumental Analytical Chemistry, at the Institute of Chemical Technologies and Analytics, Vienna, under the supervision of Professor Andreas Limbeck. This chapter provides detailed information about the improvement of sample pre-treatment steps as well as the optimization of analytical operating conditions applied to obtain an accurate, reliable and reproducible LA-ICP-MS analytical method.

The proposed LA-ICP-MS protocol was then applied for the analysis of selected trace metals (Cr, Mn, Fe, Ni, Cu, Zn, Ba and Pb) on the extended set of size-segregated PM samples, as presented in chapter 4. Obtained findings were used for a preliminary assessment of ambient concentration levels, enrichment factors and size-distributions of the investigated elements. Moreover, results were used to evaluate their potential non-carcinogenic and carcinogenic risks for humans via the inhalation exposure route, based on the assumption that people living in the study area are exposed every day for a lifetime to the average metal concentrations monitored during the whole campaign.

The last two chapters present two others parallel research lines, equally focused on the importance of assessing the human exposure to airborne contaminants for a risk assessment and characterization in outdoor as well as indoor and occupational environments.

Specifically, chapter 5 describes a research study carried out in the framework of a main research project, funded by the Emilia-Romagna Region and the Regional Agency for the

Environmental Protection of Emilia-Romagna, that aims to develop and realize an accurate survey on the atmospheric pollution in the Emilia-Romagna Region, through the monitoring of physical, chemical and toxicological parameters, to improve the knowledge regarding the environmental and health aspects of air pollution, both indoors and outdoors, with a particular focus on fine and ultrafine particles. In particular, in this study an experimental approach to investigate the indoor/outdoor (I/O) and spatial variability of traffic-related pollutants simultaneously measured on the street- and back-side of a building in a trafficked urban area is presented. The main goal of the study is to underline differences and trends between the two opposite sides of the building, with a particular focus on $PM_{2.5}$ mass and chemical composition, size distribution and UFPs number concentration. Obtained findings could be used to assess the human health risk associated with a different proximity to traffic sources in urban areas, both indoor and outdoor, and could represent a valid support to avoid possible sources of misclassification in epidemiological studies.

Finally, chapter 6 presents a study focused on the assessment of human exposure in an occupational environment. Specifically, the monitoring protocol was developed in order to evaluate the workers' exposure to arsenic and cadmium in an industrial-scale plant devoted to the production of CdTe-based solar cells for different working task and throughout the plant history by means of environmental (air sampling) and biological (end-shift urine samples) monitoring. Further, surface sampling campaigns were performed to qualitatively evaluate the general workplace contamination.

References

Allen, A.G., Nemitz, E., Shi, J. P., Harrison, R.M. and Greenwood, J. C. (2001). Size distributions of trace metals in atmospheric aerosols in the United Kingdom. *Atmos. Environ.* 35(27): 4581–4591.

Almeida, S.M., Pio, C.A., Freitas, M.C., Reis, M.A. and Trancoso, M. A. (2006). Approaching $PM_{2.5}$ and $PM_{2.5–10}$ source apportionment by mass balance analysis, principal component analysis and particle size distribution. Sci. Total Environ. 368(2): 663–674.

Álvarez, F.F., Rodrıguez, M.T., Espinosa, A.F. and Dabán, A.G. (2004). Physical speciation of arsenic, mercury, lead, cadmium and nickel in inhalable atmospheric particles. *Anal. Chim. Acta* 524(1): 33–40.

Ayrault, S., Senhou, A., Moskura, M. and Gaudry, A. (2010). Atmospheric trace element concentrations in total suspended particles near Paris, France. *Atmos. Environ. 44*: 3700–3707.

Brook, R.D., Rajagopalan, S., Pope, C.A., Brook, J.R., Bhatnagar, A., Diez-Roux, A.V., Holguin, F., Hong, Y., Luepker, R.V., Mittleman, M.A., Peters, A., Siscovick, D., Smith, S.C., Whitsel, L. and Kaufman, J.D. (2010). Particulate matter air pollution and cardiovascular disease an update to the scientific statement from the American Heart Association. *Circulation* 121(21): 2331-2378.

Canepari, S., Padella, F., Astolfi, M.L., Marconi, E. and Perrino, C. (2013). Elemental concentration in atmospheric particulate matter: estimation of nanoparticle contribution. *Aerosol Air Qual. Res.* 13(6): 1619–1629.

Cass, G.R., Hughes, L.A., Bhave, P., Kleeman, M.J., Allen, J.O. and Salmon, L.G. (2000). The chemical composition of atmospheric ultrafine particles. *Phil. Trans. R. Soc. Lond. A* 358: 2581–2592.

Chen, S.-C., Hsu, S.-C., Tsai, C.-J., Chou, C.C.-K., Lin, N.-H., Lee, C.-T., Roam, G.-D. and Piu D.Y.H. (2013). Dynamic variations of ultrafine, fine and coarse particles at the Lu-Lin background site in East Asia. *Atmos. Environ.* 78: 154–162.

Cuccia, E., Bernardoni, V., Massabò, D., Prati, P., Valli, G. and Vecchi, R. (2010). An alternative way to determine the size distribution of airborne particulate matter. *Atmos. Environ.* 44(27): 3304–3313.

Donaldson, K., Tran, C.L. and ManNee, W. (2002). Deposition and effects of fine and ultrafine particles in the respiratory tract. *Eur. Respir. Monogr.* 21: 77–92.

Eleftheriadis, K. and Colbeck, I. (2001). Coarse atmospheric aerosol: size distributions of trace elements. *Atmos. Environ.* 35(31): 5321–5330.

Erdinger L., Dürr M. and Höpker K.A. (2005). Correlations between mutagenic activity of organic extractions of airborne particulate matter, NO_x, and sulphur dioxide in Southern Germany. *Environ. Sci. Pollut. Res.* 12(1): 10–20.

Espinosa, A.J.F., Rodríguez, M.T., de la Rosa, F.J.B. and Sánchez, J.C.J. (2001). Size distribution of metals in urban aerosols in Seville (Spain). *Atmos. Environ.* 35(14): 2595–2601.

Fang, G.C., Wu, Y.S., Wen, C.C., Lin, C.K., Huang, S.H., Rau, J.Y. and Lin, C.P. (2005). Concentrations of nano and related ambient air pollutants at a traffic sampling site. *Toxicol. Ind. Health* 21(9): 259–271.

Fang, G.C., Zhang, L. and Huang, C.S. (2012). Measurements of size-fractionated concentration and bulk dry deposition of atmospheric particulate bound mercury. Atmos. Environ. 61: 371–377.

Fang, G.C., Chang, C.Y., Tsai, J.H. and Lin, C.C. (2014). The Size Distributions of Ambient Air Metallic Pollutants by Using a Multi-Stage MOUDI Sampler. *Aerosol Air Qual. Res.* 14: 970–980.

Gokhale, S.B. and Patil, R.S. (2004). Size distribution of aerosols (PM_{10}) and lead (Pb) near traffic intersections in Mumbai (India). *Environ. Monit. Assess.* 95(1-3): 311–324.

Gugamsetty, B., Wei, H., Liu, C.-N., Awasthi, A., Hsu, S.-C., Tsai, C.-J., Roam, G.-D., Wu, Y.-C. and Chen, C.-F. (2012). Source characterization and apportionment of PM_{10}, $PM_{2.5}$ and $PM_{0.1}$ by using positive matrix factorization. *Aerosol Air Qual. Res.* 12: 476–491.

Han, J.S., Moon, K.J., Ryu, S.Y., Kim, Y.J. and Perry, K.D. (2005). Source estimation of anthropogenic aerosols collected by a DRUM sampler during spring of 2002 at Gosan, Korea. *Atmos. Environ.* 39(17): 3113–3125.

Harrison, R.M. and Yin, J. (2000). Particulate matter in the atmosphere: which particle properties are important for its effects on health? *Sci. Total Environ.* 249: 85–101.

Harrison, R.M., Shi, J.P., Xi, S., Khan, A., Mark, D., Kinnersley, R. and Yin, J. (2000). Measurements of number, mass and size distribution of particles in the atmosphere. *Philos. Trans. R. Soc. A* 358: 2567–2579.

Hays, M.D., Cho, S.H., Baldauf, R., Schauer, J.J. and Shafer, M. (2011). Particle size distributions of metal and non-metal elements in an urban near-highway environment. *Atmos. Environ.* 45(4): 925–934.

Hieu, N.T. and Lee, B.K. (2010). Characteristics of particulate matter and metals in the ambient air from a residential area in the largest industrial city in Korea. *Atmos. Res.* 98(2): 526–537.

Hueglin, C., Gehrig, R., Baltensperger, U., Gysel, M., Monn, C. and Vonmont, H. (2005). Chemical characterization of $PM_{2.5}$, PM_{10} and coarse particles at urban, near-city and rural sites in Switzerland. *Atmos. Environ.* 39: 637–651.

John, A.C., Kuhlbusch, T.A.J., Fissan, H. and Schmidt, K.G. (2001). Size-fractionated sampling and chemical analysis by total-reflection X-ray fluorescence spectrometry of PMx in ambient air and emissions. *Spectrochimica Acta Part B: Atomic Spectroscopy* 56(11): 2137–2146.

Ibald-Mulli, A., Wichmann, H.E., Kreyling, W. and Peters, A. (2002). Epidemiological evidence on health effects of ultrafine particles. *Journal of Aerosol Medicine* 15(2): 189–201.

Karakoti, A.S., Hench, L.L. and Seal, S. (2006). The potential toxicity of nanomaterials – the role of surfaces. *JOM – Journal of the Minerals Metals and Materials Society* 58: 77–82.

Kelly, F.J. and Fussell, J.C. (2012). Size, source and chemical composition as determinants of toxicity attributable to ambient particulate matter. *Atmos. Environ.* 60: 504–526.

Kertész, Z., Dobos, E., Fenyős, B., Keki, R. and Borbély-Kiss, I. (2008). Time and size resolved elemental component study of urban aerosol in Debrecen, Hungary. *X-Ray Spectrometry* 37(2): 107–110.

Kopanakis, I., Eleftheriadis, K., Mihalopoulos, N., Lydakis-Simantiris, N., Katsivela, E., Pentari, D., Zarmpas, P and Lazaridis, M. (2012). Physico-chemical characteristics of particulate matter in the Eastern Mediterranean. *Atmos. Res.* 106: 93–107.

Kuhn, T., Biswas, S. and Sioutas, C. (2005). Diurnal and seasonal characteristics of particle volatility and chemical composition in the vicinity of a light-duty vehicle freeway. *Atmos. Environ.* 39(37): 7154–7166.

Kuloglu, E. and Tuncel, G. (2005). Size distribution of trace elements and major ions in the eastern Mediterranean atmosphere. *Water Air Soil Poll.* 167(1-4): 221–241.

Kuzu, S.L., Saral, A., Demir, S., Summak, G. and Demir, G. (2013). A detailed investigation of ambient aerosol composition and size distribution in an urban atmosphere. *Environ. Sci. Pollut. Res.* 20(4): 2556–2568.

Li, N., Sioutas, C., Cho, A., Schmitz, D., Misra, C., Sempf, J., Wang, M., Oberley, T., Froines, J. and Nel, A. (2003) Ultrafine particulate pollutants induce oxidative stress and mitochondrial damage. *Environ. Health Persp.* 111: 455–460.

Lim, J.-M., Lee, J.-H., Moon, J.-H., Chung, Y.-S. and Kim, K.-H. (2010). Airborne PM_{10} and metals from multifarious sources in an industrial complex area. *Atmos. Res.* 96: 53–64.

Lin, C.C., Chen, S.J., Huang, K.L., Hwang, W.I., Chang-Chien, G.P. and Lin, W.Y. (2005). Characteristics of metals in nano/ultrafine/fine/coarse particles collected beside a heavily trafficked road. *Environ. Sci. Technol.* 39(21): 8113–8122.

Lippmann, M., Yeates, D.B. and Albert, R.E. (1980). Deposition, retention and clearance of inhaled particles. *Brit. J. Ind. Med.* 37: 337–362.

Lohmann, U. and Feichter, J. (2005). Global indirect aerosol effects: a review. *Atmos. Chem. Phys.* 5(3): 715–737.

Lonati, G., Giugliano, M. and Ozgen, S. (2008). Primary and secondary components of $PM_{2.5}$ in Milan. *Environ. Int.* 34: 665–670.

Liu, X., Zhai, Y., Zhu, Y., Liu, Y., Chen, H., Li, P., Peng, C., Xu, B., Li, C. and Zeng, G. (2015). Mass concentration and health risk assessment of heavy metals in size-segregated airborne particulate matter in Changsha. *Sci. Total Environ.* 517:215–221.

Ma, C.J., Oki, Y., Tohno, S. and Kasahara, M. (2004). Assessment of wintertime atmospheric pollutants in an urban area of Kansai, Japan. Atmos. Environ. 38(19): 2939–2949.

Maenhaut, W., Cafmeyer, J., Dubtsov, S. and Chi, X. (2002). Detailed mass size distributions of elements and species, and aerosol chemical mass closure during fall 1999 at Gent, Belgium. *Nuclear Instruments and Methods in Physics Research Section B: Beam Interactions with Materials and Atoms* 189(1): 238–242.

Malandrino, M., Casazza, M., Abollino, O., Minero, C. and Maurino V. (2016). Size resolved metal distribution in the PM matter of the city of Turin. *Chemosphere* 147: 477–489.

Masiol, M., Squizzato, S., Ceccato, D. and Pavoni, B. (2015). The size distribution of chemical elements of atmospheric aerosol at a semi-rural coastal site in Venice. (Italy). The role of atmospheric circulation. *Chemosphere* 119:400–406.

Mbengue, S., Alleman, L.Y. and Flament, P. (2014). Size-distributed metallic elements in submicronic and ultrafine atmospheric particles from urban and industrial areas in Northern France. *Atmos. Res.* 135: 35-47.

Miranda, R., and Tomaz, E. (2008). Characterization of urban aerosol in Campinas, São Paulo, Brazil. *Atmos. Res.* 87(2): 147–157.

Montoya, L.D., Lawrence, J., Murthy, G.G.K., Sarnat, J.A., Godleski, J.J. and Koutrakis, P. (2004). Continuous measurements of ambient particle deposition in human subjects. *Aerosol Sci. Tech.* 38: 980–990.

Nakamura, M. and Ise, H. (2002). Determination of the size distribution of carbon and trace elements in suspended particulate matter by ion beam analysis. *Nuclear Instruments and Methods in Physics Research Section B: Beam Interactions with Materials and Atoms* 189(1): 279–283.

Niu, J., Rasmussen, P.E., Hassan, N.M. and Vincent, R. (2010). Concentration distribution and bioaccessibility of trace elements in nano and fine urban airborne particulate matter: influence of particle size. *Water Air Soil Pollut.* 213(1-4): 211–225.

Ntziachristos, L., Ning, Z., Geller, M.D., Sheesley, R.J., Schauer, J.J. and Sioutas, C. (2007). Fine, ultrafine and nanoparticle trace element compositions near a major freeway with a high heavy-duty diesel fraction. *Atmos. Environ.* 41(27): 5684–5696.

Ny, M.T. and Lee, B.K. (2011). Size distribution of airborne particulate matter and associated metallic elements in an urban area of an industrial city in Korea. *Aerosol Air Qual. Res.* 11(6): 643–653.

Oberdörster, G., Oberdörster, E. and Obertörster J. (2005). Nanotoxicology: an emerging discipline evolving from studies of ultrafine particles. *Environ. Health Persp.* 113: 823–839.

Onat, B., Şahin, Ü.A. and Bayat, C. (2012). Assessment of particulate matter in the urban atmosphere: size distribution, metal composition and source characterization using principal component analysis. *J. Environ. Monitor.* 14(5): 1400–1409.

Ostro, B., Hu, J., Goldberg, D., Reynolds, P., Hertz, A., Bernstein, L. and Kleeman, M.J. (2015). Associations of mortality with long-term exposures to fine and ultrafine particles, species and sources: results from the California teachers study cohort. *Environ. Health Persp.* (Online) 123(6): 549.

Pakkanen, T.A., Kerminen, V.M., Korhonen, C.H., Hillamo, R.E., Aarnio, P., Koskentalo, T. and Maenhaut, W. (2001). Urban and rural ultrafine ($PM_{0.1}$) particles in the Helsinki area. *Atmos. Environ.* 35(27): 4593–4607.

Pakkanen, T.A., Kerminen, V.M., Korhonen, C.H., Hillamo, R.E., Aarnio, P., Koskentalo, T. and Maenhaut, W. (2001). Use of atmospheric elemental size distributions in estimating aerosol sources in the Helsinki area. *Atmos. Environ.* 35(32): 5537–5551.

Pakkanen, T.A., Loukkola, K., Korhonen, C.H., Aurela, M., Mäkelä, T., Hillamo, R.E., Aarnio, P., Koskentalo, T., Kousa, A. and Maenhaut, W. (2001). Sources and chemical composition of atmospheric fine and coarse particles in the Helsinki area. *Atmos. Environ.* 35(32): 5381–5391.

Pakkanen, T.A., Kerminen, V.M., Loukkola, K., Hillamo, R.E., Aarnio, P., Koskentalo, T. and Maenhaut, W. (2003). Size distributions of mass and chemical components in street-level and rooftop PM_1 particles in Helsinki. *Atmos. Environ.* 37(12): 1673–1690.

Pennanen, A.S., Sillanpää, M., Hillamo, R., Quass, U., John, A.C., Branis, M., Hůnová, I., Meliefste, K., Janssen, N.A.H., Koskentalo, T., Castaño-Vinyals, G., Bouso, L., Chalbot, M.-C., Kavouras, I.G. and Salonen, R.O. (2007). Performance of a high-volume cascade impactor in six European urban environments: mass measurement and chemical characterization of size-segregated particulate samples. *Sci. Total Environ.* 374(2): 297–310.

Pipalatkar, P.P., Gajghate, D.G. and Khaparde, V.V. (2012). Source identification of different size fraction of PM_{10} using factor analysis at residential cum commercial area of Nagpur city. *B. Environ. Contam. Tox.* 88(2): 260–264.

Pope, C.A., Dockery, D.W. and Schwartz, J. (1995). Review of epidemiological evidence of health effects of particulate air pollution. *Inhal. Toxicol.* 7: 1–18.

Pöschl, U. (2005). Atmospheric aerosols: composition, transformation, climate and health effects. *Angew. Chem. Int. Ed.* 44(46): 7520–7540.

Raaschou-Nielsen, O. *et al.* (2016). Particulate matter air pollution components and risk for lung cancer. *Environ. Int.* 87: 66-73.

Richard, A., Gianini, M.F.D., Mohr, C., Furger, M., Bukowiecki, N., Minguillón, M.C., Lienemann, P., Flechsig, U., Appel, K., DeCarlo, P.F., Heringa, M.F., Chirico, R., Baltensperger, U. and Prévôt, A.S.H. (2011). Source apportionment of size and time resolved trace elements and organic aerosols from an urban courtyard site in Switzerland. *Atmos. Chem. Phys.* 11(17): 8945–8963.

Salma, I., Maenhaut, W., Zemplén-Papp, É. and Záray, G. (2001). Comprehensive characterisation of atmospheric aerosols in Budapest, Hungary: physicochemical properties of inorganic species. *Atmos. Environ.* 35(25): 4367–4378.

Salma, I., Maenhaut, W. and Záray, G. (2002). Comparative study of elemental mass size distributions in urban atmospheric aerosol. *J. Aerosol Sci.* 33(2): 339–356.

Salma, I., Ocskay, R., Raes, N. and Maenhaut, W. (2005). Fine structure of mass size distributions in an urban environment. *Atmos. Environ.* 39(29): 5363–5374.

Sato, K., Tamura, T. and Furuta, N. (2008). Partitioning between soluble and insoluble fractions of major and trace elements in size-classified airborne particulate matter collected in Tokyo. *J. Environ. Monit.* 10: 211–218.

Schwarze, P.E., Øvrevik, J., Lãg, M., Refsnes, M., Nafstad, P., Hetland, R.B. and Dybing, E. (2006). Particulate matter properties and health effects: consistency of epidemiological and toxicological studies. *Hum. Exp. Toxicol.* 25: 559-579.

Smolik, J., Ždimal, V., Schwarz, J., Lazaridis, M., Havárnek, V., Eleftheriadis, K., Mihalopoulos, N., Bryant, C. and Colbeck, I. (2003). Size resolved mass concentration and

elemental composition of atmospheric aerosols over the Eastern Mediterranean area. *Atmos. Chem. Phys.* 3(6): 2207–2216.

Srivastava, A. and Jain, V.K. (2007). Size distribution and source identification of total suspended particulate matter and associated heavy metals in the urban atmosphere of Delhi. *Chemosphere* 68(3): 579–589.

Stafoggia, M., Samoli, E., Alessandrini, E., Cadum, E., Ostro, B., Berti, G., Faustini, A., Jacquemin, B., Linares, C., Pascal, M., Randi, G., Ranzi, A., Stivanello, E., Forastiere, F. and the MED-PARTICLES Study Group. (2013). Short-term associations between fine and coarse particulate matter and hospitalizations in Southern Europe: results from the MED-PARTICLES Project. *Environ. Health Perspect.* 121: 1026-1033.

Sulejmanović, J., Muhić-Šarac, T., Memić, M., Gambaro, A. and Selović, A. (2014). Trace metal concentrations in size-fractionated urban atmospheric particles of Sarajevo, Bosnia and Herzegovina. *Int. J. Environ. Res.* 8(3): 711–718.

Sun, G., Crissman, K., Norwood, J., Richards, J., Slade, R. and Hatch, G.E. (2001). Oxidative interactions of synthetic lung epithelial lining fluid with metals-containing particulate matter. *Am. J. Physiol. Lung Cell. Mol. Physiol.* 281: L807–L815.

Tahir, N.M., Suratman, S., Fong, F.T., Hamzah, M.S. and Latif, M.T. (2013). Temporal distribution and chemical characterization of atmospheric particulate matter in the eastern coast of peninsular Malaysia. *Aerosol Air Qual. Res.* 13: 584–595.

Taiwo, A.M., Beddows, D.C., Shi, Z. and Harrison, R.M. (2014). Mass and number size distributions of particulate matter components: Comparison of an industrial site and an urban background site. *Sci. Total Environ.* 475: 29–38.

Tan, J., Duan, J., Zhen, N., He, K. and Hao, J. (2016). Chemical characteristics and source of size-fractionated atmospheric particle in haze episode in Beijing. *Atmos. Res.* 167: 24–33.

Toscano, G., Moret, I., Gambaro, A., Barbante, C. and Capodaglio, G. (2011). Distribution and seasonal variability of trace elements in atmospheric particulate in the Venice Lagoon. *Chemosphere* 85(9): 1518–1524.

Vecchi, R., Chiari, M., D'Alessandro, A., Fermo, P., Lucarelli, F., Mazzei, F., Nava, S., Piazzalunga, A., Prati, P., Silvani, F. and Valli, G. (2008). A mass closure and PMF source apportionment study on the sub-micron sized aerosol fraction at urban sites in Italy. *Atmos. Environ.* 42: 2240–2253.

Verma, M.K., Chauhan, L.K.S., Sultana, S. and Kumar, S. (2014). The traffic linked urban ambient air superfine and ultrafine PM_1 mass concentration, contents of pro-oxidant chemicals, and their seasonal drift in Lucknow India. *Atmos. Pollut. Res.* 5(4): 677–685.

Zereini, F., Alt, F., Messerschmidt, J., Wiseman, C., Feldmann, I., von Bohlen, A., Müller, J., Liebl, K. and Püttmann, W. (2005). Concentration and distribution of heavy metals in urban airborne particulate matter in Frankfurt am Main, Germany. *Environ. Sci. Technol.* 39(9): 2983–2989.

Yang, J.Y., Kim, J.Y., Jang, J.Y., Lee, G.W., Kim, S.H., Shin, D.C. and Lim, Y.W. (2013). Exposure and toxicity assessment of ultrafine particles from nearby traffic in urban air in Seoul, Korea. *Environmental Health and Toxicology* 28.

Yang, Y., Yu, Y., Zhou, R., Ma, Z., Ren, L. and Zhang, L. (2014). Elemental Compositions and Size Distributions of PM Between Urban and Rural Site in Beijing During the Spring of 2012. *Asian J. Chem.* 26(11): 3180–3186.

Yeh, H.C., Phalen, R.F. and Raabe, O.G. (1976). Factors influencing the deposition of inhaled particles. *Environ. Health Persp.*15: 147–156.

Ynoue, R.Y. and Andrade, M.F. (2004). Size-resolved mass balance of aerosol particles over the Sao Paulo metropolitan area of Brazil. *Aerosol Sci. Technol.* 38(S2): 52–62.

Yun, H.J., Yi, S.M. and Kim, Y.P. (2002). Dry deposition fluxes of ambient particulate heavy metals in a small city, Korea. *Atmos. Environ.* 36(35): 5449–5458.

Tables

Table 1. Query' structure used for each scientific database.

DataBase	Search Query
Pubmed	((((((((((ambient aerosol) OR atmospheric particulate matter) OR atmospheric aerosol) OR airborne particulate matter) OR PM) OR particulate matter)) AND ((air) OR atmosphere*)) AND ((((impactor) OR cascade impactor) OR DLPI) OR nano MOUDI)) AND (((((((elemental composition) OR chemical characterization) OR chemical composition) OR metallic elements) OR elemental) OR speciation) OR metal*)) NOT indoor) AND (((((particle size distribution) OR mass concentration*) OR gravimetric*) OR gravimetric* analysis) OR size distribution)
Web of Science	((TS=("ambient aerosol" OR "atmospheric particulate matter" OR "atmospheric aerosol" OR "airborne particulate matter" OR "PM" OR "particulate matter")) AND (TS=(air OR atmosphere*)) AND (TS=(impactor OR "cascade impactor" OR DLPI OR "nano MOUDI")) AND (TS=("elemental composition" OR "chemical characterization" OR "chemical composition" OR "metallic elements" OR elemental OR speciation OR metal*)) NOT (TS=(indoor)) AND (TS=("particle size distribution" OR "mass concentration*" OR gravimetric* OR "gravimetric* analysis" OR "size distribution")))
Scopus	(((((TITLE-ABS-KEY ("ambient aerosol" OR "atmospheric particulate matter" OR "atmospheric aerosol" OR "airborne particulate matter" OR "PM" OR "particulate matter")) AND (TITLE-ABS-KEY (air OR atmosphere*))) AND (TITLE-ABS-KEY (impactor OR "cascade impactor" OR dlpi OR "nano MOUDI"))) AND (TITLE-ABS-KEY ("elemental composition" OR "chemical characterization" OR "chemical composition" OR "metallic elements" OR elemental OR speciation OR metal*))) AND NOT (TITLE-ABS-KEY (indoor))) AND (TITLE-ABS-KEY ("particle size distribution" OR "mass concentration*" OR gravimetric* OR "gravimetric* analysis" OR "size distribution"))

Table 2. Summary of research studies on the elemental composition of size-segregated PM.

Reference	Location	Site characterisation	Sampling period	Main Results	
				PM mass distribution	**Elemental characterization**
Malandrino *et al.* (2016)	Turin	Site localized near the historical centre (45° 3' 6,412" N; 7° 40' 51,919" E) at an elevation of 15 m with respect to the road level. Urban site	autumn-winter (2011-2012)	February sampling: PM_{10} distribution is bimodal, with modes around 5 μm and 1 μm (typical of urban aerosol)	Identification of three main bahavioural types: 1) elements associated with coarse particles (Cd, Cr, Cu, Fe, Mn, Mo, Sn). 2) Elements found within fine particles (As, Co, Pb, V). 3) Elements spread throughout the entire size range (Ni, Zn)
				February sampling: the accumulation mode (1 μm) is by far the highest	Most of the elements present lower concentrations in Turin than in other considered urban areas
				During February $PM_{2.5}$ represent 80% of the total mass of PM collected	The highest metal concentrations were reached by Cr (0.83 ng/m^3), Zn (32.7 ng/m^3), Cd (1.85 ng/m^3) and Sn (30.02 ng/m^3) in October sample. Co (0.06 ng/m^3), Ni (1.55 ng/m^3), Cu (2.52 ng/m^3), As (0.13 ng/m^3), Mo (0.34 ng/m^3), Pb (2.25 ng/m^3) in January sample. V (0.30 ng/m^3), Mn (3.10 ng/m^3), Fe (207 ng/m^3) in February sample
					There is a grater diference in elements size distribution between the firts sampling (October) and the last two (January and February)
					Co, V, Ni show a larger mode in the finest fraction (<1.6 μm) in winter than in autumn
					Zn presents a larger mode in the fine fraction (<2.7 um) in autumn
					Elements could be diveded into 3 groups: 1) elements are mostly concentrated in the coarse mode (2.7-11 μm: Cd, Cr, Cu, Fe, Mn, Mo, Sn); 2)elements show higher concentrations in the acumulation mode (<2.7 μm: As, Co, Pb, V); 3) elements presents several modes spread throughtoth the size distribution (Ni, Zn) -> these bheaviour is generally in line with the findings reported by other

					authors
Tan *et al.* (2016)	Beijing	Site localized on the rooftop of a building (5 m above the ground) in an urban area	December 27th 2006	4th-December	The size distributions of particle mass during heavy haze and normal days were both bimodal but slightly differet: these mode peaks were within the range of 0.32-1.0 μm and 3.2-5.6 μm	Ca>Si>Fe>Al>K>Mg>Na (consistent with the previous result in Beijing)
					The peak of accumultion mode shifted toward larger size during heavy haze period from 0.32 μm to 1.0 μm	The crustal elements (Ca, Si, Fe, Al, Mg) were mainly present in coarse mode and the proportions of their concentrations of coarse mode particles to the total mass concentrations were 70%, 65%, 68% and 73.1% respectively
					Averagely 51.5% and 74.1% of the total ambient aerosol mass was distribuited in the sub-micron and fine particle, rispectively	Atmospheric heavy metals (Pb, Zn, Cu, Ni) were of great concern
						Cr, Ni, Cu, Zn, Ga, Ge, As, Se, Mo, Ag, Cd, Sn, Sb, Cs, Hg, Ti, Pb were dominated by sub-micron particles (PM_1/PM_{10} >50%)
						Ti, V, Zr, Ba were dominated in fine particles ($PM_{2.5}/PM_{10}$ >50%)
						Si, Fe, Al, Ca, Mg, Sc, Co, Sr were dominated in coarse particles ($PM_{2.5}/PM_{10}$ <50%)
						Size distriubtion of elements wew classified into 4 main type. 1) elements whose mass was enriched mainly within accumulation mode (<1μm: Ge, Se, Ag, Sn, Sb, Cs, Hg, Ti, Pb); 2) those elements (K, Cr, Mn, Cu, Zn, As, Mo, Cd)were resided mainly within the accumulation mode, ranged from 1 to 2 μm; 3) Na, V, Co, Ni, Ga were distribuited among fine, intermediate and coarse modes; 4)those which

				were mainly found within particles larger than 2.7 µm (Al, Mg, Si, Ca, Sc, Ti, Fe, Sr, Zr, Ba)
				Crustal elements (Al, Mg, Si, Ca, Sc, Ti, Fe, Sr, Zr, Ba) exhibited a single modal size distribution, and their highest mass peaks appeared int he range of 3.2-5.6 µm
				4 main type: elements were enriched within the accumulation mode (<1 µm: Ge, Se, Ag, Sn, Sb, Cs, Hg, Ti, Pb). Those mass (K, Cr, Mn, Cu, Zn, As, Mo, Cd) was resided mainly within the accumulation mode, ranged from 1 to 2 µm. Na, V, Co, Ni, Ga were distibuited among fine, intermediate and coarse moed. Those which were mainly ofund within particles larger than 2.7 µm (Al, Mg, Si, Ca, Sc, Ti, Fe, Sr, Ba)
Masiol *et al.* (2015)	Venice	Semi-rural coastal site. 15 m above ground on a lighthouse (45,4227 N, 12,4368 E)	cold season (late autumn and winter); October 2007-January 2008	Antropogenic elements are strongly inter-correlated in the submicrometric (<1 µm): S, K, Mn, Cu, Fe, Zn and intermediate mode (1-4 µm). Mn, Cu, Zn, Ni
				In the intermediate mode, association having geochemical significance between marine (Na, Cl, Mg) and crustal (Si, Mg, Ca, Al, Ti, K)
				In the coarse mode (>4 µm) Fe an Zn are well correlated
				Basing on median values, sulfur is the most abundant element (746 $\mu g/m^3$), followed by Cl (469 ng/m^3), Ca(193 ng/m^3), K (183 ng/m^3) and Na (153 ng/m^3)
				Ti, Cl, Ni, Cu, Ca are more concentrated in the intermediate mode (1-4 µm)
				Sulfur, potassium, vanadium, manganese are mostly in the submicrometric range mode (<1 µm)
				Na, Mg, Al, Cr show bimodal distributions in both

				submicrometrical and coarse rages
				Distribution reproduce a general trend, showing the antropogenic elements linked to te finest fraction and those related with the coarse one
				Submicron-sized aerosol is usually attribuited to hight energy sources or secondary aerosl fomration process. Sulfurm potassium, manganese and iron present in the highest number of significant correlations among them, generally with titanium, copper, zinc
				In the intermediate mode, associations having geochemical significance exist between marine, crustal and anthropogenic elements
Liu *et al.* (2015)	Changsha	28,12°N; 112,59° E	April 13th-May 6th of 2014	Fe>Zn>Mn>Pb>Cr>Cd>Cu>Ni
				The most aubundant HM was Fe. The size distribution for Pb and Cu, they were concentrated in fine particles (<2.1 μm)
				Concentration of Ni and Cr were higher in the coarse particles
				Cd, Fe, Mn, Cr were presented a unifomr distribution in both fine and coarse particles wich indicated that they were contributed by antropogenic emissions and natural sources including soil dust re-suspension and second aerosol aggregation
Verma *et al.* (2014)	Lucknow	Traffic linked ambient air. 1.5 m above the ground (26,847°N; 80,947° E)	October 2011; December 2011; March 2012; April 2012, May 2012	Content of Fe was the greatest
				Fe accumulation was more in $PM_{0.8}$, $PM_{1.0}$, $PM_{0.18}$, $PM_{0.056}$ fraction and less in $PM_{0.56}$, $PM_{0.32}$, $PM_{0.1}$ fractions
				The contents of Ni in $PM_{1.8}$ to $PM_{0.1}$ exceeded the permitted levels marginally
				The contents of transitionals metal (Cu, Fe, Pb) were greater in $PM_{1.8}$ to $PM_{0.18}$

					Ni and Fe accumulated in $PM_{1.8}$; Cd in $PM_{1.0}$; Cr and Cu in $PM_{0.56}$; Pb in $PM_{0.32}$
					Contents of Cr, Ni, Cu, Fe on submicron fractions are below the recommended and permissible exposure levels
Sulejmanovic *et al.* (2014)	Sarajevo	Urban. 6 m from the ground	August 2008-December 2008	The average concentrations of particulate matter are 37% 18% 15% 8% 15% of total suspended particle for $PM_{<0.49}$, $PM_{0.95-0.49}$, $PM_{1.5-0.95}$, $PM_{3.0-1.5}$, $PM_{7.2-3.0}$ and $PM_{>7.2}$	The decreasing trend of average trace elements concentrations in the particulates revealed the following order: Fe> Mn>Cu>Co
				The highest average concentrations of PM was obtained in fraction <0.49	Fe showed the highest concentration and Co the lowest one
				Lowest average level of PM was obtained in fraction >7.2 µm	Maximum concentrations of all analyzed metals are found in the $PM_{7.2-3.0}$ µm with the values of 3.83 ng/m^3 for Co, 179.20 ng/m^3 for Cu, 6.82 ug/m^3 for Fe and 208.70 ng/m^3 for Mn
				For each month, except August, the highest average concentrations of PM were observed in fraction <0.49 µm	The trace element calue in the urban atmosphere of Sarajevo in comparison with some European urban sites were times higher
Onat *et al.* (2012)	Instanbul	Yenisbona: 40° 59' 60" N 28° 49' 24,93" E 14 m altitude. Goztepe: 40° 59' 32,82" N 29° 04' 26,96"E 19 m altitide (urban)	Yenisbona: January-July 2006; Goztepe: February-August 2007	Log-normal distributions showed that the particles at the Yenibosna site have a smaller size compared to the Goztepe samples and the size distribution of PM was represented the best by the tri-modal	The higher metal rte in fine and medium coarse PM ahowed that the antrhropogenic sources were the most significant polluted sources
				The fine particles (<3.3 µm) constitute a significant part of TSP and particulate size distribution was best rapresented as tri-modal	50-90% of the metal mass is concentrated in the fine PM
					The metal concentration at two site were variable

					V concentration value were similar at the two stations
					The higher value of all metals were determined at Goztepe station (except Pb)
					At Yenisbona the seasonal variation of Cd, V, Cr, Co, Cu, Ni and Pb have peak values during the hating season
					At Goztepe (except Pb) the seasonal concentration of Cd, V, Cr, Sn were similar during the heating and non-heating seasons
					The highest correlation was between Pb and Cd at Yenisbona
					At Yenisbona there are high correlations between Cd and V, Ni, Pb, As; between Ni and Co, Cu, V; between As and Sn, Co; between Cr and Co
					All of the metals (except Ni) are related by a high correlation at Goztepe site
Taiwo *et al.* (2014)	Port talbot (TB) and Birmingham (EROS)	PT: (costal) industrial (51°34'N 3° 46'W) ; EROS: urban background (1,93° W, 52,46°N)	EROS: March 30th-april 11th. PT: April 17th-May 16th 2012.	Port Talbot: bimodal peaks (0.5- and 2-6 μm). Highest mass concentration observed on April 23-26	Al and Fe were the metals with highest concentrations at both sites
				EROS: modal peaks in the fine and coarse PM ranges at 0.5 and 2-4 μm	Mean concentrations of Cr, Mn, Fe and Zn were higher at PT than EROS
				Particle mass, for wich the fine mode was very similar at both sites but the coarse mode was much more prominent at PT due largely to increase marine aerosol	The traffic signatures of Cu, Sb, Ba and Pb were particuulary prominent at EROS
				EROS was dominated by fine particles while PT showed an elevated coarse particle concentrations reflected in a higher ratio of $PM_{2.5}/PM_{10}$	EROS: all of the metals displayed at least two peaks covering fine and coarse PM fraction (excet Pb and Zn and Sb, where the two modes were both in the fine fraction). Multiple modes were observed for Al, V and Cr

				PT: the concentration of Fe was tge highestm followed by Al and Zn
				Generally the moeds in the size distributions were similar at the two sites. Notable differences: Calcium showed a fine mode at PT wich was not evident at EROS; alluminium showed a pronunced mode >10 µm at EROS wich has no parallel at PT; chromium shows a multi-modal behaviour at both sites, but the smallest mode at PT it is around 0.2 µm, whereas at EROS it is close to 0.5 um; manganese at PT shows a very pronunced coarse particle mode, while at EROS the mode is much broader, peaking at 1-2 µm; iron, for wich in both sites show a bimodal distribution
				EROS was dominated by fine particles while PT showed an elevated coarse particle concentration
Kuzu *et al.* (2013)	Instanbul	Urban	March 2009-March 2010.	Two prevalin particulate modes are found throughought PM_{10}. First mode in the fine mode is found to be between 0.43 and 0.65 um. The other peaks was observed between 3.3 and 4.7 µm	The maximum concentration of Fe are observed in rush hour sample between the size range of 1.1-4.7 µm
				The mean PM_{10} concentrations was determined as 41.2 µg/m^3. $PM_{0.43}$ has the highest mean concentration value of 10.67 ug/m^3, making up nearly one fourth of the total PM_{10} mass	For Cu, higher concentrations were monitored during day-time, between diameters of 0.65-0.43 µm
				The fine mode (0.43-1.1 µm); the coarse mode (5.8-9.0 µm)	Zn has a maerly unifrom distribution througthought the stages
					The maximum elemental composition comprised alkaline and alkaline earth metals (Na, K, Mg, Ca). The maximum concentrations of these elements were observed in rushhour sampples, between 1.1 and 4.3

				μm
Ny and Lee. Ulsan (2011)	Urban area of an industrial city. 12 m from the ground	April 2008-January 2009	Most of the fine and coarse particle mass was concentrated in the size range 0.7-1.1 μm and 9-10 μm respectively. PM mass showed two peaks in spring: the firts peak was observed for the smallest particles (<0.7 μm) and the second one was found in the coarse particles (2.1-10 μm). Fine particles (0.7-2.1 μm) showed the highest PM concentrations in winter	3 main group were determined: 1) heavy metals (Cd, Zn, Mn, Ni, Cr) which were present in high concentrations in fine particles (<2.1 μm) particulary at the size of 0.4-0.7 μm. 2) light metals (Na, Ca, K, Al) anf Fe which had high concentrations in coarse particles. Other heavy metals (Pb, Mg, Cu) showing high concentrations at size larger than 5.8 μm
				Metals (Cd, Zn, Mn, Ni, Cr) in group 1 had much higher concentrations in fine particles (<2.1 μm) as compared in coarse particles (>2.1 μm) and the metal concentrations decrease with increasing size of particles within the fine mode. group 2 including light metals (Na, Ca, Al, K) and Fe, showed increased concentrations with increase in particle size, wich is wella matched with the size characeristics identified in the previously studies. the metals in group 3 (Pb, Mg, Cu)showed increasing concentrations in the size group abovr 5.8 μm
Pipalatkar *et al.* (2012)	Nagpur Residential cum commercial area. 3m above ground level	winter period	The average concentration of PM_{10} and fine particulate matter (<2.2 μm) was found to be 300 and 136.7 $\mu g/m^3$ respectively, wich was exceeding limit of Central Pollution Control Board	Metals (Sr, Ni, Zn) were found to large proportions in below 0.7 μm particle size
			Maximum mass concentration of 41 $\mu g/m^3$ in size range of 9-10 μm amd minimum mass concentration of 19 $\mu g/m^3$ in size range 2.2-3.3	Maximum contribution of Sr (32%) and Mg (14%) were found in the bolow 0.4 μm

				µm was observed	
					Ni (31%) and Zn (21%) were found maximum in the particle size range 0.4-0.7 µm whike As (21%) and Ba (17%) were maximum in the size rane 0.7-1.1 µm. The remaing metals like fe, Pb, Si, Cu were observed maximum in seze range of 2.1-3.3 µm; 3.3-4.7 µm; 5.8-9.0 µm; 9.0-10 µm respectively. There was no significant variation for Mo (11-12%) in all size fractions
					Zn (45%), Sr (65%) and Ni (55%) contribute maximum and other metals varied from 30-45% in fine mode
					Percent contribution of Si (40.3%) and Pb (63.3%) was maximum in coarse mode and in medium mode, respectively
Hays *et al.* (2011)	North Carolina interstate	Near highway	26-31 July 2006; 3-10 August 2006	PM mass size distribution was trimodal with a major accumulation mode peak at 500-800 nm. PM mass levels reflected daily traffic activity, while mean near-highway PM_{10} (33 $\mu g/m^3$), $PM_{2.5}$ (29 $\mu g/m^3$) and $PM_{0.1}$ (1.4 $\mu g/m^3$) mas levels variede less than 24% over the two week samplig period. On average, the $PM_{2.5}$ fraction represent 86% of the total PM_{10} mass	Numerous metals (An, Cr, Ni, Co) showed a variety of dealy enrichment and size distributions, indicating that the raleigh near-highway PM is influenced by multiple source contributions
Kopanakis *et al.* (2012)	Akrotiri	Suburban/rural (35°31'48"N; 24° 03'36"E)	August 2007; July 2008	The mean PM_{10} conentration during the measuring period was equal to 36.1 μgm^3. The $PM_{2.5}$ concentration was equal to 23.6 $\mu g/m^3$	The concentration of antropogenic elements (Cu, Cr, Pb, Ni) are low, in comparison to the concentration of Fe (crustal element)

				The mean PM_{10} concentration during the first sampling period was equal to 28.3 $\mu g/m^3$ (10/08/2007-28/08/2007) whereas during the second sampling period (9/07/2008-19/07/2008) was 41.6 $\mu g/m^3$	A good pearson correlation has been shown between PM levels (PM_{10} and $PM_{2.5}$) and concentration of Fe, and also between $PM_{2.1}$ and concentration of Pb
				The measurenment showed a bimodal size distribution for the aerosol mass concentration	The average concentration of Fe is high and it is nearly equally distribuited in coarse ad fine PM fractions
				A significant decrease of $PM_{2.5}$ annual means (35.2%) was recorded between 2004 and 2007, alike other studies in the region of mediterranean sea	Copper chromium and lead showed the highest concentrations in the coarse PM fraction with aerodynamic diameters larger than 4.7 μm
					Nickel presented the highest concentration in the ultrafine PM fraction with aerodynamic diameters less than 0.4 μm
Kertész *et al.* (2008)	Debrecen	Downtown	before, during and after the Easter holdays		Two different kind of particles could be identified according to the size distribution
					In the size distribution of Al, Si ,Ca, Fe, Ba, Ti, Mn, Co one peak can be found around 3 μm (these are the elements of predominatly natural origin)
					The size distribution of elements like S, Cl, K and Zn has a bimodal shape. One peak can be observed at 0.25-0.5 μm and another at 2-4 μm, indicating different sources of these elements
					Concentration values are lower in the weekend than in the working days
					The result obtained are in good agreemeent with mass size distribution measured in other hungarian and European cities

Ntziaxhristos *et al*. (2007)	Southern california freeway	1 mile downwind of the freeway (I710 freeway in Los Angeles)	February-April (Monday-Friday)	2006	The freeway location exhibits significantly higher mass concentrations than the urban site for all particle size, with coarse PM mas consituting about 50% of PM_{10} at both samplig locations	The most abundant trace elements in the accumulation mode were S (138 ng/m^3), Na (129 ng/m^3), Fe (89 ng/m^3)
						S (35 ng/m^3) and Fe (35 ng/m^3) were the most abundant in the ultrafine mode
						The concentration of several trace elements, including Mg, Al, Zn and, in particular Ca, Cu, Pb, did not uniformly increase with size within fine PM. The most abundant elements in the $PM_{0.18-2.5}$ mode are S, Na, Fe, followed by Ca, K, Al and Mg
						In the $PM_{0.18}$ mode S and Fe are the most abundant, followed by Ca, Al, Na
						Most elements fall into two distinct concentration profile with particle size: several elements present a monotonic increase in their profile with size, such as Na, S, Ti, V, Mn, Fe, Sn, Ba. The second characteristic concentration profili reflects distribution that does not uniformly increase with size, i.e the distribution is "flatter" bacause concentration are similar across the lower aize ranges (Ng, Al, K, Ca, Cu, Zn, Pb)
						Nanoparticles (18-32 nm) appear to have a much higher fraction of mg, Ca, Cr, Ni, Cu, Zn, Sr, and Pb from all other size fractions whitin the ultrafine mode
						The concentration of most trace elements is below 100 ng/m^3
Hieu and Lee. (2010)	Ulsan	Urban, residential area	April-August 2008		The identified concentrations of $PM_{1.0}$; $PM_{2.5}$; PM_{10} were 18.5, 27.6 and 50.5 μg/m^3	Na, K, Ca, Mg, Al, Fe, Zn were detected in high concentrations in the coarse particles
					The highest value for the mean mass fraction (16.4%) was	Cd, Cr, Cu, Ni, Mn, Pb were found mainly in the fine particles

	observed in the size range of 9.0 to 10 μm, followed by the size ranges of 0.7 to 1.1 μm (14.3 μm) and 0.4 to 0.7 μm (12%)	
	The mean concentrations of $PM_{1.0}$, $PM_{2.5}$ and PM_{10} during the study period in the largest city of Korea were 18.5, 27.6 and 50.5 $\mu g/m^3$ respectively	The crustal elements were found in higher coincentration in the spring and the antropogenic elements were found in high concentrations in the summer
		Here were 2 distinct concentratio groups during the study period for the mean concentration of metals in PM_{10}
		The light metal group (Na, K, Ca, Mg, Al) was found in very high concentration as compared to the heavy meal group (except Fe and Zn) wich was found in trace concentrations
		For the light metals, the principal metal component was Ca followed by Al and Na
		For the geavy metals the concentration of Fe, Zn and Pb were much higher than the concentration of Cd, Cr, Cu, Mn, Ni, wich were less than 100 ng/m^3
		The difference in metal concentration between the two season was relatively small, except that for Pb wich was found at a concentration in summer that was twice as hight that in spring for all particle sizes
		There were fluctuations in the metallic element concentrations during the sampling periods, the concentration ratio of the metallic elements in the fine and coarse particles were very similar in both of the season except for the $PM_{2.5}/PM_{2.5\text{-}10}$ ratio in Ca, Cd, Mn, Ni
		The concentration of Al, K, Na,Zn, Ni were higher in spring than in summer

					Light metals and Fe and Zn trended to accumulate in coarse rather than fine particles
					Cd, Cr, Cu, Mn, Ni, Pb trended to accumulate in the fine particles rather than in the coarse particles
Niu *et al.* (2010)	Ottawa	Urban	ECH-93 (1992-1993) and ECH-2K (1999-2000)	Both EHC-93 and EHC-2K show the same distributiom pattern: the mass is concentrated in the coarse size fraction and decrease with decreasing particle size showing the lowest mass in the nano-size fraction	A general trend of increasing element concentration with decreasing aerodynamic diameter was observed for V, Mn, Ni, Cu, Zn, Se, Cd.-Fe, Sr, Mo, Sn, Sb, Ba, Pb were predominately concentrated in the fine-size range
					For the ECH-93 samples, Fe is the most abundant, followed by Zn and Pb. Manganese, Cu, Sn, Ba show moderate abundance. elements with lower median values include V, Ni and Sr
					For EHC-93 samples the best association exist between V, Mn, Cu, Zn, Se, Ba.The strong correlation remains in the finer particle size fractions for V with Cu, Zn and Se but no longer with Mn and Ba
					For EHC-2K samples elements concentration increase as aerodynamic particle size decrease for V, Mn, Ni, Cu, Zn, Cd, Se with maximum concentration in the nano-size fraction.Sn, Sb, Mo, Fe, Ba, Sr, Pb are dominated in the fine-size fraction
					V, Mn, Ni, Cu, Zn, Se and Cd exibithed the relative highest mass concentration in the nano size (<100 nm) and the lowest concentration in the coarse size(>1.0 nm) for these elements, a genarel trend of increasing element concentrations as aerodynamics particle size decrease was obsewrved. Other elements (Fe, Pb, Ba, Sn, Sb, Mo, Sr) predominatly occur in the fine-size fraction (100-1 nm)

Pakkanen *et al.* (2003)	Heliski	One sample at 3.5 m height and one sample at 20 m height	June 1997	The average concentrations of PM_1 were pratically the same, about 11 $\mu g/m^3$, at the two heights	Cu, Ba, Fe, Sb, Bi, Al were higher at street levelsuggesting that local trafic and road dust were importnt sources for these components
					Concentrations of Ca, Co, Li, Mo, Na, Ni, Pb, Rb, Se, Sr, Ti, Tl, V were similar at the two heights or higher at the rooftops site pointing
					Comparison of size distribution and concentration revealed several groups of correlating chemical components: Ti, As, Cd, B, Pb; V, Ni, Co, Mo; Ba, Cu, Fe, Sb; Zn, Rb, Pb, Mo
					At rooftop both the average concentrations and average mass fractions of fine particle (Co, Se, Ti) were >20% larger than lose at street level. The average concentrations and mass fractions of Li, Ni, Tl, V were slightly higher at he rooftop site
					The concentrations of Se, Li, Tl were larger at the rooftop site for all sampling periods
					The average submicron concentrations and mass fractions of Ag, Al, As, B, Ba, Bi, Cu, Fe, K, Mn, Sb, Th were clearly larger at street level
					The concentrations of Ba , Th, Fe, Mn, Pb and Sb were larger at street level for all sample pairs
Pakkanen *et al.* (2001)	Helsinki	One sample at an urban area. One sample at an rural site (3.5 m above the ground)	April 1996- June 1997	The average $PM_{2.3}$ (fine particle) concentrations at the urban and rural sites were 11.8 and 8.4 $\mu g/m^3$. The $PM_{2.3-15}$ (coarse particles) concentrations were 12.8 and about 5 $\mu g/m^3$ respectively	The average fine particle concentration of the chemical components appeared to be fearly similar at the two sites for most of these components. Exceptions were the average fine particlea Ba, Fe, Sb, V concentrations that weere clearly highest at the urban site pointing to traffic (Ba, Fe, Sb) and to combustion of heavy fuel oil (V)
				Average mass concentrations of coarse particles were 12.8 $\mu g/m^3$ at the urban site; 5.8 $\mu g/m^3$ at the rural site; 10.6 $\mu g/m^3$ at the semi-urban site	The strongest correlation at the urban site was between Ni e V. Mo had its strongest correlation with Ni, and Co with Mo. Ba, Cu and Fe formed a clear group at the urban site having their stronget correlations with each other. Sb had its strongest

					correlation with Ba, K and Cu but a weaker correlation with Fe
				Average mass concentration of PM_{15} particle were 25.5 µg/m^3 at the urban site; 14.4 µg/m^3 at the rural site; 18.9 µg/m^3 at the semi-urban site	The average concentrations were relatively low when compared to those reported in the literature for central and southern Europe and for the densely populated areas in North America
					The average Ba, Fe, Sb and V concentrations were clearly higher at the urban site. In coarse particles, there were strong to moderate correlations between the common major and minor crustal elements, including Al, Ba, Ca, Co, Fe,K, Li, Mn, Rb, Sr, Th, Ti, U, V
Alvarez *et al.* (2004)	24 areas of Seville (37° 23'N; 5° 58"W)	The different sampling points were classified into three categories: sites under the influence of industrial emissions, stations unedr the influence of vehicular emission, and peripheral stations under the influence of resuspended soils	January 2000-June 2001 (differnt days in each week)	Average PM_{10} level over the sampling period was 41.8 µg/m^3 (this concentration exceeds even the annual limit value of PM_{10} estabilished by the new european framework directive of evaluation and management of amient air quality)	The highest mean cincentration was obtained (in PM_{10}) for Pb, followed by As and Ni. The lowestr concentrations were obtained for Cd and especially for Hg. Toxic elements As and Pb were accumulated in the fine particles of <0,6 µm, as well the metals Cd and Ni. the size interval where Hg contents were higher than in $PM_{0,6}$ corresponded to a fine and a coarse mode, meanwhile Ni presentes similar percentage between all size range
				Two size dependent log-normal ditributions. One mode correspond to the accumulation mode, a fine mode below 1.3 µm, and other one correspond to mechanical erosions	In PM_{10} samples the highest concentration was obtained for lead. Arsenic and nikel presente medium levels. the lowest concentratins were obtained for cadmium and mercury
				The more abundant particles in air are the finest sizes, consiuting 48.4% of the total suspended particles	All metals were highly associated with fine particles. the resultas of distribution expressed as percentages were 74.8% for arsewnic, 69.0% for lead; 61.3% for cadmium, 57.5 for nickel and 40.4% for mercury

					Maximum percentages were obtained in particles between 1.3 and 0.61 um for cadmium and lead. Nickel presented a uniform distribution over all size ranges. Mercury shows a different profile from the other studied elements, with a maximum value in particles between 4.9 and 2.7 µm and similar values in particles between 2.7 and 0.6 µm. Mercury was mainly distribuited in a size range between 4.9 and 0.6 µm. Arsenic presented the mixmum value in the finest fraction (<0.6 µm)
Kuhn *et al.* (2005)	State route 110 (Pasedena)	Two diferent sites were used : site A (very close to the three northbound traffic lanes-2.5 m from the edge of the freeway) + site B (used to characterize background aerosol. 150 m from the freeway)	winter 2005 (weekdays)-12/01-25/01/2005 from 12 pm to 7 pm.	At site A, the mass concentrations were higher than site B in all three size modes. Contrary to the summer study, the mass concentrations in the accumulation mode were higher than the coarse mode. In the summer study the coarse mass concentrations were highest (23 and 21.5 $\mu g/m^3$ for site A and B respectively) compared to 19 ans 19.2 $\mu g/m^3$ in accumulation mode and 5.1 and 3.3 $\mu g/m^3$ in ultrafine mode for site A and B respectively	Na, Si, Cl, K, Ca, Ti, Fe, Cu, Ba were dominated by the coarse moed concentrations. All these species were much higher in summer
					Concentrations for other species (Na, Si, S, K, Ca, Fe) were similar or slightly higher at site B. most of these species are dominated by the coase mode concentrations
Lin *et al.* (2005)	Taiwan	Busy road	February-April 2004	The mean concentration of the nano, ultrafine, fine, coarse, and PM_{10} particles were 13, 31, 140, 51, 191 $\mu g/m^3$ respectively	The nano particles were found to contain more of traffic-related metals (Pb, Cd, Cu, Zn, Ba, Ni) than particle of other size, althought crustal metals accounted for over 90% of all the particulate metals
					Most crustal metals (Ba, Ni, Pb, Zn) in ultrafine particles displayed aitken modes

					Particle-bound Zn was more aboundant in the accumulation mode than in the nucleation/condensation mode, but the opposite was true for Ag, Cd, Sb
					The Ag, Ba, Cd, Pb, Sb, V and Zncontents in nano particles were strongly associated withdiesel fuel, while the Cu, Mn and Sr in particles <0.1 μm were more strongly associated with gasoline
					The metallic components were divided into 3 groups. Majour crostal metals (Si, Na, Mg, Al, K, Ca, Fe), sub-major metals (Cr, Ni, Zn, Sr, Ba, Pb), minor metals (Mn, Cu, Ag, Cd, V, Sb)
					K exhibited a trimodal size distributions, but the other major metals exhibited approximatly bimodal size distributions with primary peaks in the 3.2-5.6 μm range and secondary peaks in the nano size range. Some major metals, including Si, Al, Ca, e, Na, K, displayed Aitken modes in the ultrafine range
					Some sub-major metals, such as Ba, Pb, Zn exhibithes bimodal distributions
Fang *et al.* (2005)	Central Taiwan	Traffic site (1.7 m above the ground)	winter (November 2004-January 2005)	The mass size distribution of ambient suspended particles has two modes. The range of the sizes of the particles in the teo modes are between 1.0 and 1.8 and 3.2 and 5.6 μm	Concentrations followed the order Fe>Mg>Cr>Zn>Pb>Cu in PM_{10}, fine, ultrafine and nano-sized particles
				The distribution of the sized of the fine and coarse paricles were 0.18-1.8 and 1.8-10 μm espectively	The average metallic elements Fe and Zn have similar concentrations distributions:the concentrations decrease as the particle size fell in the nano size range
				The mean cumulative fractions of PM_{10}, $PM_{2.5}$, PM_{1}, $PM_{0.1}$ and nano-particles size of 0.018-0.056 μm were 94.4, 68.9, 50.13, 16.9 and	Mean metallic elements Fe and Zn exhibit similar trends in concentrations: the concetrations dropped as the particle size decrease in the nano-size range

				12.3%	
					Concentrations followed the order Fe> Mg> Cr> Zn>Pb> Cu in PM_{10}, fine, ultrafine, nano-sized ranges. This order was Fe>Mg>Cr>Zn>Pb>Cu for coarse particles
Pennanes *et al.* (2007)	6 urban sampling sites across Europe	Urban background environment	7 weeks campaign in 2002-2003: Diusburg (autumn:4 october-21 november 2002); Prague (winter: 29 november 2002- 16 january 2003); Amsterdam (winter: 24 january-13 march 2003); Helisinki (spring. 21 march-12 may 2003); Barcelona (spring: 28 march-19 may 2003), Athens (summer: 2 june-21 july 2003)		Common soil derived metals (Al, Fe) were generally more abundant in $PM_{10-2.5}$ size range compared with the asmples in $PM_{2.5-0.2}$ and $PM_{0.2}$ size ranges
					Some metals (Cr, Mn, Pb, Zn were consistenlt more abundant in Duisburg than elsewere in two or three size ranges
					The As content in particulate samples in thr three size ranges of Prague winter was strikingly much higher than that in all the other particulate samples. The Ni and V contents in the $PM_{2.5-0.2}$ and $PM_{0.2}$ samples were highest in Barcelona and Helsinki
Salma *et al.* (2002)	Budapest	4 sites: 1)KFKI (urban background); 2)Eotvos University (39 m above the street level); 3)Sezena Square (downtown. 4.5 m above the ground); 4)CD tunnel	April-June 1999		Typical coarse-mode elements (Na, Mg, Al, Si, P, Ca, Ti, Fe, Ga, Sr, Zr, Mo, Ba) exhibited unimodal size distributions at all four urban locations studied, with most of their mass in the coarse mode, and with little mass below 1 μm
					Elements typically related to high-temperature or anthropogenic aources (S, Cl, K, V, Cr, Mn, Ni, Cu, Zn, Ge, As, Se, Br, Rb, Pb) had a unimodal size distribution. Significant differences between the size distributions of four sampling sites were noted
					There was a clear tendency for the accumulation mode to decrease and for the coarse mode to increase with increasing total aerosol mass concentration
Nakamura and	Setagaya	Residential area	weekdays in Februay,		Table 3

Ise (2002)			March and April; on weekends in February and in the period of Asian dust events in March		During Asian dust events, the Al and Fe concentrations increased in comparison to other periods
John *et al.* (2001)	Dusseldorf	Traffic related site	17-21 November 1999 (6:00-20:00 and 20:00-6:00)	PM_{10} mass concentrations were 45 $\mu g/m^3$ on average during this measurement campaign; 34% of these data excedeed 50 $\mu g/m^3$	Sulfur: nearly 90% of the PM_{10} mas is already contained in the $PM_{2.5}$ fraction
					Silicon, iron, calcium are elements on the coarse-mode aerosol
					No distinct diurnal pattern could be observed for some elements (sulfur). In the case of other elements (calcium), the time period of day and night sampling revealed clear differences between the samples
Maenhaut *et al.* (2002)	Gent	Urban area (top roof)	6 September-30 October 1999		Sulphur was mainly in the fine size range, with maximum at 0.5 µm
					Other elements with mainly a fine mode were V, Ni, As, Se, Pb
					The crustal elements (Al, Si, Ti, Fe, Zr) exhibited mostly a unimodal coarse mode size distribution, with maximum at about 4 µm
					Other elements with mainly a coarse mode were Na, Mg, P, Ca, Cr, Mn, Cu, Ga, Sr
					K, Zn, Rb were generally bimodal
Kuloglu and Tuncel (2005)	Antalya	Mediterranean coast (30° 54' E; 36° 81' N). Rural station	August 1993-May 1994		Pollution derived elemets (As, Cd, Mo, Pb, Se, Zn) have MMD's between 1.25 and 1.01 µm
					Coarse component in concentraions of Cd, Pb, Sb and particulate Hg are due to adsorption of fine antrhopogenic particles on coarse crustal aerosol, whereas coarse fraction (Z, As, Se, In, Mo, Au) are crustal
					Bromine, Cr, Ni and V have bimodal distributions

					Approximately 30% or 40% of the mass of crustal elements (Al, Ca, Ce, Dy, Au, Fe, Gd, Hf, La, Lu, Mn, Nd, Rb, Sc, Sm, Ta, Tb, Th, Ti, Yb) occur in the second impactor stage (4.2 μm cut-off diameter)
					The first three stages, wich cover particle diameters larger than 2.1 μm include approximately 70% of the masses of soil related elements
					Majority of the masses of pollution-derived elements in the submicron range, apporoximately 10-30% of the masses of As, Cd, Mo, Pb, Sb, Se, Zn are found to be in the first three impactor stages
					Bromine, Ci, Ni, V have 27-48% of their masses in the first two stages of the impactor, and 29-42% of their masses on the last impactor stage and on the backup filter
					Crustal elements (Al, K, Mg, Ca, Fe, Sc, Co, Ti, La, Ce, Sm) are correlated with each other in both coarse (stage 1-3) and fine fraction particles (stage 4-6), as expected
					Marine elements (Na, Cl) are correlates with each other at every impactor stage. These element are also correlated with Mg and K in the coarse fraction
					K and Mg are not correlated with sea salt elements in the fine fractions
					Vanadium, Cr and Ni are correlated with Al in the coarse fraction
					Sulfate correlates with Al (and other crustal elements) in the second impactor stage
Pakkanen *et al.* (2001)	Helsinki	Vallila (urban); Luukki (rural)	12 June 1996-5 June 1997	In the Helsinki area, the average UFP mass was about 0.5 μg/m^3 at both sites	The average chemical composition of UFP was similar at the two sites
				The average UFP mass concentrations were 490 and 520 ng/m^3 at the urban and rural site,	The most important metals at both sites were Ca, Na, Fe, K, Zn

			respectively	
				Ni, V, Cu, Pb were important with average ultrafine concentrations between about 0.1 and 0.2 ng/m^3
				At both sites the contribution of ultrafine to fine was especially high for Se, Ag, B, Ni and at the rural site also for Co and Mo
				The Aitken modes of Ba, Ca, Mg, Sr were similar in several samples, suggesting a common local combustion source for these elements
				Of heavy metals, concentrations in the UFP size range were the highest (in decreasing order) for Zn, Ni, V, Cu, Pb
				The highest individual Aikne mode concentration sobserved were in the range 10-25 ng/m^3 for Ca, Na, Fe, K. Zn, Al, Mg, Cu, Ni, Pb showed maximum Aitken mode conecntrations between about 1 and 4 ng/m^3. Li, Th, Tl, U showed none or only few Aitken modes
				Compared to the urban site the UFP contribution to $PM_{2.5}$, was higher at the rural site for most of the components. The difference was especially high for Ni, Co, Mo, Bi, V, Cu, Al, Ti, Fe, Rb. Only Cd had a higher average and median UFP contribution at the urban site
				Compared to the rural site, the UFP concentration was higher at the urban site especially for Fe, B, Ba, V, Mn, Sb
Yang *et al.* (2013)	Seoul	Urban area	December 2007-December 2009 (except during unusual weather phenomena such as rain, snow, Asian dust)	The PM size distribution were bi-modal, peaking at 0.18 to 0.32 and 1.8 to 3.2 µm. During the sampling period, the annual level of PM_{10} was less than 100 µm/m^3 (the 24h air quailty standards in Korea), but excedeed 50 µm/m^3 (the annual air	The mass concentrations of the metals in fine particles (0.1 to 1.8 µm) accounted for 45.6 to 80.4% of the mass concentrations of metals in PM_{10}

				quality standard for PM_{10} in Korea)	
				The average montly sampling concentrations of PM_{10} and $PM_{2.5}$ on the nearby roadside were 34 to 124 μg/m^3 and 20 to 80 μm/m^3 respectively	The mass proportions of fine particles of the pollutants relatesd to traffic emission, lead (80.4%), cadmium (69.0%), and chromium (63.8%) were higher than those of other metals
				The average levels of PM_{10} and $PM_{2.5}$ were 77.7 and 45.6 μm/m^3 respectively	Iron was the dominant transition metal in fine particles, accounting for 64.3% of the PM_1 mass in all samples
				The percentage of UFP (<0.1 μm) , fine particles (0.1 to 1.8 μm) and coarse particles (1.8 to 10.0 μm) were 7%, 58.5% and 34.5% respectively	Weak correlations between PM mass and the concentrations of chromium, lead, and iron
Miranda and Tomaz (2008)	Campinas	Avenue with intense vehicle traffic	August 2003-August 2004. MOUDI: 8-12 December 2003; 9-13 August 2004	Result showed an annual mean of 20.85; 10.68; 10.17 μg/m^3 for PM_{10}, $PM_{2.5}$ and $PM_{2.5-10}$ respectively	The size distribution for chemiacl elements indicated soil-derived elements in the coarse fraction
				Concentrations for PM_{10} were higher in winter (August and September) than in summer. The annual mean was 20.85 ±16.61 μg/m^3; 10.68± 8.25 μg/m^3 and 10.17 ±10.00 μg/m^3 for PM_{10}, $PM_{2.5}$ and $PM_{2.5-10}$ respectively	Comparing the diurnal and nocturnal concentration sof two seasons, higher concentrations of soil-derived elements were observed during the day in summer and winter
Richard *et al.* (2011)	Zurich kaserme	Urban courtsyde (urban background)	28 November 2008-5 January 2009		Aerosol sample are segregated into three size ranges: the coarse fraction ($PM_{10-2.5}$), an intermediate size range ($PM_{2.5-1}$) and the fine fraction ($PM_{1-0.1}$)
					Fe, Cu, Sn, Sb how a related pattern to the rush-hour times of increased traffic activities

					No clear diurnal variations were found for fine mode S and K. Daytime concentrations of Si, K, Ca, Sr in $PM_{10-2.5}$, exceeded night-time mass concentrations without specific daily pattern
Srivastava and Jain (2007)	Delhi	6 differnt sites	3 diferent seasons: winter (1/01/2001-15/02/2001), summer (1/05/2001-15/06/2001), monson (1/07/2001-15/08/2001)	The impactor stage frectionations of particles shows that a major portion of TSPM concentrations is in the form of $PM_{0.7}$	Mn, Cr, Cd, Pb, Ni, Fe are concentrated in the $PM_{0.7}$ mode
				The 24h average TSPM levels are relatively high in winter and summer season at OK, wich is not unexpected since it is an industrial area	The only exceptions era size distribution spertaining to Cu and Ca
				Dominace of fine particles (<0.7 μm) at all sites for all seasons except DK, when the dominance of fine particles is confined in summer season only	Though, Cu is more in $PM_{0.7}$ mode, its presence in size intervals 5.4-1.6 μm and 1.6-0.7 μm is also significant
				Unimodal distribution	No specific trend for any metal is being observed in any particular season at any of the chosen sites
					The only important cocnlusion that can be drawn i that DK and VV (heavy traffic sites) are comparatively more affected whilst JNU and HK (residential areas) less affected sites
					Most of the metals are associated with the $PM_{0.7}$, except Ca, P, Cu, Cr
					Cu and Cr, apart form last stage, are also present in fourth stage
					Ca and Pb has no definite pattern of its association with various fractions of TSPM
Canepari *et al.* (2013)	Rome	Parking site	spring 2010		Elements that are maily relased into the atmosphere by natural sources or by re-suspension process (Ba, Li, Mg, Mn, Na, Sn, Sr) are mostly present in coarse particles

				Elements having significant contribution from combustive sources (As, Cd, K, Pb, Rb, Sb, Tl, V) show a bimodal distribution, with substantial contributes also from fine particles
				Some elements (Na, Li, Mg, Ba, Mn, Sr) show a dimensional distribution almost completely in the coarse stage of the impactor
				The size distribution of a second group of element (Rb, Tl, K) was mainly confined in the fine fraction
				A third group of elements (Sb, Cd, V, As, Sn, Pb) also exhibited a significant fine contribution, but the values obtained after thr elution were maredly lower than those obtained from the direct analysis
Cuccia *et al.* (2010)	Genoa	Urban area	March 2008-August 2008	Six sources were resolved: re-suspended soil (Al, Si); Sea Salt (Na, Cl, Br); Traffic (Cu, Zn, Pb); heavy oil combustion (V, Ni); secondary (S); unidentified sources
				Sea salt and re suspended soil show larger conctributions in the coarse fraction (0.6-6 µm)
				Secondary componunds are mailnly concentrated in the fine fraction
				Traffic PM is resolved in all size bins
				Heavy oil combustion sources shows a flat distributions up to 3 µm
Eleftheriadis and Colbeck (2001)	Colchester	Rural and urban area		Fraction for earth metals (Ca, K, Ti) is comparatively grater in the rural site than the urban site, while for trace metal (Mn, V, Cu, Cr) this fraction conctitutes a more significant part of the coarse mass at the urban site
				Most crustal elements (Fe, Ca, K, Ti) display a peak in their mass concentration between 3 and 7 µm. The shape of their respective size distributions is generally similar. The only exception in potassium

					which displays a clear second mode at around 10 μm at the rural location
					A clear distinction between the two sites is evident. All these elements (Co, V, Mn and Cu), excluding Cr, appear to have their ambient concentrations maximising between 2 and 3 μm at the rural site and between 4 and 6 μm at the refuse site
					Chromium displays a surprising bimodal distibution with a first peak similar to those of the other metals and a second peak at around 80 μm
Almeida *et al.* (2006)	Lisbon	Suburban area		The fine particulate mass concentrations varied between 2.4 and 30 $\mu g/m^3$ (mean value 14 $\mu m/m^3$)	Aerosol can be classified into eight types: crustal matter sea salt, ammonium, sulphate, nitrate, organic matter, black carbon, minor elements
				The coarse particulate mass concentrations veried between 4 and 88 $\mu g/m^3$ (mean value 18 $\mu g/m^3$)	Very similar size distribution fo La, Sm, Fe, Sc. They skewed to the larger size range and ha done peak in the coarse particle region (2-4 and 4-8 μm)
					The mass size distribution fo K is rapresented as a bimodal distribution having two peaks in the stages 0.25-0.5 and 2-4 μm
					The mass size distribution for Zn, As, Se, Sb, Hg did not present a common similar pattern
					Se and As skewed to the smaller size range and had only one peak in the fine fraction region
					Zn and Sb not only had similar mass size distributions with a peak in the fraction 2-4 μm
Ma *et al.* (2004)	Kansai	Urban Area	Wintertime	$PM_{2.5}$ levels are higher in the day time with an average level of 21.3 $\mu g/m^3$, while the levels are lower in the night time, with an averge level of 12.6 $\mu g/m^3$	Insuloble Si and Fe are enriched in coarse fraction (>2.05 μm) showing the bimodal distribution
				The number concentration of particles larger than 0.3 μm	K and Ca show the monomodal distribution with coarse fraction enrichment

				appears dominated by the ultrafine particles ranged between 0.3 and 0.5 μm	
					The size distribution of insoluble minor trace elements like Cu, V, Br display the bimodal with major peak in coarse fration and minor peak in fine fraction
					Soluble S showing the maximum concentration is prinicpally enriched in a range of 0.01-1.17 μm fine fraction and shows the bimodal distribution by border with 0.19 μm. Ti and Cu rapresent the multiple peaks. The soluble fraction of Fe shows dominant peak in coarse particle region
Yun *et al.* (2002)	Kunpo	Metropolitan area (12 m high)	February, May, September, October 2000	The total mass and elements concentrations during daytime were higher than nighttime	The average fluxe of total mass and elements measuring during daytime were higher than the nighttime fluxes
					The average fluxes of al and Ca were 1-2 orders of magnitude higher than Mn and antrhropogenic elements such as As, Cd, Cu, Ni, Pb, Zn
					The size distribution of the crustal elements (Al, Ca, Mn) showed two peaks, one in a small particles (<9 μm), the other large particles (>9 μm). The mass concentrations of Al and Ca were higher than those of Mn and anthropogenic elements in all measured periods
					The ambient concentration sof both Al and Ca were highest in October daytime
Zereini *et al.* (2005)	Frankfurt am Main	Three different sites with different traffic densities: 1) 32500 cars/day. 2) <1000 cars/day. 3)large garden on a hill	August 2001-July 2002	Coarse dust (>2.1 μm) dominates the particle distribution of urban air, with an average fraction of 60%	The highest airborne heavy metal concentrations occurred at the main street with a large number of traffic
				The fine dust fraction (<2.1 μm) dominates at the side street and rural sites, with an average fraction	With exception of Co, V, Ce, Mn, the heavy metals had an elevated enrichment factor compared to thei copncentation sin the continental crust

				of 55-64%	
					For As, Cd, Pb, V, the main fraction can be found in fine particles (<2.1 μm). Ce, Cr, Co, Ni occour mainly in coarse particles (>2.1 μm). Cu, Mn, Sb, Zn, Pt, Pd, Rh occour in high concentration sin the medium range (1.1-4.7 μm)
Salma *et al.* (2000)	Budapest	Urban background, two downtownsites, road tunnel	April-May 1996; June 1998; April-June 1999 (semi-consecutive days)	In the downtown, the median TSP was found to be higher by approximately 25% than the sum of the median PM for the coarse and fine size fractions	The elements can be classified into two groups: 1) Na, Mg, Al, Si, P, Ca, Ti, Fe, Ga, Sr, Zr, Mo, Ba. All these elements have essentially a unimodal size distribution for all data sets with most of their mass in he coarse mode, and with little mass below 1 um. 2) S, Cl, K, V, Cr, Mn, Ni, Cu, Zn, Ge, As, Se, Br, Rb, Pb. They either have a unimodal size distribution with their mass occurring primairly in the accumulation mode or exhibit clearly a bimodal size distribution at the urban background site
				At to the relatioship between the mass concentrations of PM_{10} and fine size fraction (PM_2), the latter makes up only 43% and 33% of the PM_{10} mass at the urban background and downtown	
Toscano *et al.* (2011)	Venice Lagoon	Three different sites. Site 1: influenced by industrial and urban sources. Site 2: efecteed by marine aerosol and long range sources. Site 3: located downwind from a mainland urban area close to Venice Airport	March 2002-July 2003	At all stations , particles with an aerodynamic diameter <3 μm were predominant (78% of the total aerosol mass concentration)	Similarity in size distribution of elements at all sites allowed the identification of three main behavioural types: 1) elements found mainly whitin coarse particles (Ca, Mg, Na, Sr); 2) elements found mainly whitin fine particles (As, Cd, Ni, Pb, V); 3) elements with several modes sread throughout the entire size range (Co, Cu, Fe, K, Zn, Mn)
				The general particulate distribution in the three sites in the warm and in the cold season was bimodal, registering the highest abundance in the 0.49-1.5 μm fraction	The highest metal concentrations for almost all elements was foun dat site 1

			Only at site 3 a unimodal with a maximum of the fine particulates was observed during the cold season	The distribution of na, Mg, Sr, Ca showed a large mode in the coarse fraction (3-10 μm) in all stations
				Cd, Pb, Ni, V, As showed a large mode between 0.49 and 1.5 μm at all sites. Cd, Ni, V and As showed an additional mode for dp< 0.49 μm at site 1
				Al, Fe, Mn, Cu, Zn, Co, K presented a bimodal distribution: the first at 0.95-1.5 μm and the second at 3-10 μm
Salma *et al.* Budapest (2005)	Downtown (7.5m above the street level). The site can be classified as kerbside	April 26th- May 5th 2002		For the crustal elements, two modes were identified in the mass size distributions: a major coarse mode and a intermediate mode, wich contained about 4% of the elemental mass
				The typical anthropogenic elements exhibited usually trimodal size distributions including a coarse mode and two submicrometer modes instead of a single acumulation mode
				An Aitken mode was unanbiguios observed for S, Zn, but in a few case only
				For Al, Si, Ca, Ti, Fe, the size distributions generally consisted of a large coarse mode with a GMAD of 4-5 μm containing about 96% of the elemental mass
				Correlation between the coarse-mode concentration pairs of the typical elements (Al, Si, Ca, Ti, Mn, Fe) was strong
				For Cl, Zn, Na, Mn, Ni, Cu, Pb, S, Br, the distributios were generally trimodal
				On average, more than half of the elemental mass for Cl, Zn, Na, Mn, Ni, Cu was observed in the coarse mode
				For K four modes were detected in the ize distribution, but the intermediate mode had a significantly larger mean

					The Aitken mode was observed only as an exception for S, K, Zn, but in general, it was missing
Yang *et al.* (2014)	Beijing	Urban site; rural site	April 9th- April 23th 2012		The total concentation of the elements at urba site was 1.4 times higher than that at the rural site
					Al, Ca, Mg, Fe, Ba, Th, Sr were mainly asociated with coarse particle with a peak at 4.7-5.8 μm
					Cd, As, Tl, Pb were found to be most dominant in fine particles with the peak at 0.43-1.1 μm
					Na, K, Ni, V, Zn, Cr, Se, Co, Mo, Cu, Mn, U had a multi-mode distribution
					The conecntrations of Na, Mg, Al, K, Ca, Fe contituted the major proportion in the measurements of particulate matter, occupying 95.5 and 95.6% of all the elements
					High elemental concentrations were still observed at both sites, especially for pollution elements such as Cu, Zn, As, Se, Pb
Chen *et al.* (2013)	Lu-Lin	Background	July-August 2009; September-November 2010	The $PM_{0.1}$ was 0.08-0.2 μg/m^3 at the LABS, much lower than that in uban area	K, Mn, Pb, As in sample f and the average distributions for other samples shows a bimodal pattern
Fang *et al.* (2012)	Taiwan	Traffic site (Hungkuang); wetland site (Gomei); industrial site (Quanxing)	November 2010-July 2011	PM_{10} contributed more than 50% to the bulk concenration at the traffic and the industrial sites, but only contribuoted 25% at the wetland site	At all three sites, PM_{10} and $PM_{10\text{-}2.5}$ dominated the total Hg(p) concentrations. However, their percentage contribution sto the total Hg(p) were different from site to site
				$PM_{2.5\text{-}10}$ contribuited 25%-50% to the bulk mass	PM_1 was the dominate mode at the traffic site and the industrial site
				Coarse fraction ($PM_{2.5\text{-}18}$) contribuited 7% at Hungkuang, 25% at Gaomei, 19% at Quandxing	$PM_{1\text{-}2.5}$ was the dominant mode at the wetland site
				Samples with very high bulk concentrations had larger fine fractions	

Smolik *et al.* (2003)	Finokalia	Coastal site (3 m above the ground)	10-31 July 2000; 7-14 January 2001	Time series for PM_1 and PM_{10} mass and elemental concentrations showed both daily and seasonal variation	The crustal elements and sea-salt had a unimodal distribution
				The mass size distribution swere predominanty bimodal with mode ean diameter around 0.4 and 5 μm and a minimum between both modes at around 1 μm	Sulphur was found predominantly in submicron fraction. K, V, Ni exhibited a bimodal distribution with a submicron mode
					Antropogenic elements had broad and not well-definited distributions
					Monomodal distribution with particle size >1 μm and a mode centred about 4 μm were tipical for Al, Si, Ca, Ti, Mn, Fe, Sr. Multimodal distribution of Al and Si was observed during winter. Also Cl exhibited monomodal distribution with particle size >1 μm and a mode around 5 μm
					S, Br, K, V, Ni exhibited bimodal distribution with modes at around 0.3 and 3 μm
					Cu, Cr, Zn and Pb showed rather flat multimodal distributions centered at abount 1 μm
Espinosa *et al.* (2001)	Seville	12 different areas	Spring 1996 (Apil-June)	Tipical bimodal distribution, one corresponding to the fine mode below 1 μm (55%) and the other to the coarse mode around 10 μm (32%)	Nickel, lead, cadmium are mainly accumulated in the smaller partiles, with percentages of 72.6, 69.4 and 63.8% respectively
				Two size dependent log-normal distribution, one corresponding to the accumulation mode (a fine mode below 1 μm) and the other to mechanical erosion, a coarse mode around 10 μm	One group of metal are present in high percentages in the fine particles (<0.61 μm): nickel, vanadium, lead, cadmium (except vanadium they correspond to the most toxic metals)
				Mean TSP levels obtained for the whole city over the sampling	One group is formed by the metal that have highest percentages in the coarse particles: iron, magnesium,

				period was 79 μm/m^3	titanium, manganese
				Aerosol particles of <0.61 μm predominate in all sampling sites. Particles <1.3 um account for over 55% of the total aerosol concentration of this area, aerosol particles of <10 μm represent 85% of the TSP particles and those of <2.7 μm represent 61%	
Ynoue and Andrade. (2004)	Sao Paulo	Metropolitan area	3-11 August 1999		Sodium, potassium, magnesium, chloride had total concentrations up to 2.6 times higher in nightime than in daytime sampling
Fang *et al.* (2014)	Taichung (Taiwan)	Westin Park+ Gung-Ming Junior High School	Semptember 2011-February 2012	Comparing the particle size of PM_{18}; PM_{18-10}; $PM_{10-2.5}$ revaled higher concentrations in Westin Park than those Gung-Ming Junior.	Zn, Ni, Cu, Cd, Pb in the ambinet air, the raletive concentrations were PM_{18}>$PM1_{8-10}$>$PM_{2.5-1}$>$PM_{10-2.5}$ for all sampling site
				At the Westin Park, the average concnetration of PM_{18}, PM_{18-10}, $PM_{10-2.5}$, $PM_{2.5-1}$ were19.67; 16.42; 16.09; 3.18 and 12.38 respectively	The relative concentrations of Zn particle were PM_{18}>$PM_{10-2.5}$>$PM_{2.5-1}$>PM_{18-10}
				At the Gung Ming sampling site, the mean particle concentrations of PM_{18}, PM_{18-10}; $PM_{10-2.5}$; $PM_{2.5-1}$ were 14.54; 9.90; 3.28: 12.70; 12.63 repectively	The relative concentratio of Ni particles were $PM_{10-2.5}$>PM_{18}>PM_{18-10}>$PM_{2.5-1}$
					The relaive concentrations od Cu and Hg particles were PM_{18}>PM_{18-10}>$PM_{10-2.5}$>$PM_{2.5-1}$
					The relative concentrations of Cd particles were $PM_{10-2.5}$>PM_{18}>$PM_{2.8-1}$>PM18-10
					Zn, Cu, Hg tended to associated in the particle size of PM_{10-18} during the sampling period of September-November 2011 at the Westin Park. Ni and Cd tended to associated in the particle size of $PM_{10-2.5}$ at this sampling site

Han *et al.* (2005)	Gosan	The site is know to be the ideal location for the study of long-range transport of air pollutants	March 29th-May 29th 2002	More than 60% of the major soil components (Al, Si, Fe, Ca, Ti, Cr, Cu, Br, K, Mn, Zn, As, Rb) were distribuited in stage 1 and 3 (1.15-12 μm)
				About 30% of S, Br and Pb was found in stage 4 (0.75-1.15 μm)
				About 20% of S, V and Ni was distribuited between stages 6 and 8 (0.09-0.34 μm)
				Especially S, Zn, As, Pb, Cu, Se, V, Ni, Br had their maximum concentrations in stage 6 (0.34-0.56 μm) during the AD period
Gokhale and Patil. (2004)	Mumbai	Traffic and industrial area	October, November, December	The fraction sof the PM_{10} adn that of Pb showing a tendency of trimodal distributions with the first peak at coarse mode (9.0-10.0 μm), second at 5.8 μm and the third at coarse mode (1.1 μm)
				Average PM_{10} concentraytions values were found 258 and 528 $\mu g/m^3$ in AQCR1 and AQCR2 respectively
				The $PM_{1.1}$ concentration (fine mode) has been found contributing between 20 to 30% of the total PM_{10} in both sites
				In AQCR1 the % of Pb in coarse mode is 27%, in medium mode 32% and in fine mode it is high as 41%
				In ACQR2, the % of Pb in corse mode is as low as 8%, in medium mode it is 44 % and in fine mode it is 48%
Pakkenen *et al.* (2001)	Helsinki	Two sites: urban and rural (3.5 meters above ground)	June 12th 1996- June 5th 1997	The average particulate mass concentration was higher at the urban site, especially for the coarse and accumulation size ranges
				At both sites, especially As, B, Bi, Cd, Ni, Tl, V were enriched in fine particles (<2.3 μm)

		At both sites As and Pb had similar accumulation modes to sulphates suggests that long range transport is important for these components
		V, Ni, Mo, Co fromed another group of similar accumulation modes at btoh sites
		The average fine-particles concentrations of B, Ba, Ca, Cu, Fe, Li, Mn, Mo, Ni, Sb, V, Zn were higher at the urban site than the rural site. Only Se showed a higher fine-particle concentration at the rural site
		The average coarse-particles concentrations were clearly higher at the urban site for nearly all components. Exceptions were coarse Pb and Se, wich showed similar average concnetrations in both sites
		At both sites Ag, Bi, Co, Mo, NI, Se, Sr, Zn had about 10% or more of their fine-particles mass in the Aitken mode
		Most components showed two modes, called the lower and the upper accumulation mode, in the size range 0.15-1 μm
		In uban site similar accumulation modes were observed: 1)Pb, As, Co, Tl; 2) Ca, Ba, Sr; 3) Bi, Tl; 4) Cd, Pb, K, Rb; 5)Mo, No, V, Fe, Co
		At rural site the shape of the accumulation size renage was similar for the groups:1)As, Pb; 2)Bi, Ag, Cd, Na, Tl, Zn, Rb; 3)Cu, Cd; 4)Fe, Mg, Ti; 5) Co, Mo, Ni, V; 6) Na, Rb, K, As
		At the urbansite, the average relative local contributions of several common soil and roa dus components (Al, Ba, Ca, Fe, Mg, Ti, U) were estimeted to be above 90% in PM2,3. The elements As, Cd, Pb, Tl had the lowest average relative down-wind local contributions in $PM_{2.3}$ (23-33%)

Allen *et al.* (2001)	Central England + southern Scotland	Three backgroun sites	February 1999-November 1999	The size distribution obtained in Scotland, wich were typically trimodal, difered from those in central England, where modes were more variable	Metlas whose mass resided mainly whitin the accumulation mode (0.5 μm): Cd, Sn, Pb, Se
					Metals wich were distribuited between fine, intermediate and coarse modes (Ni, Zn, Cu, Co, Mn, Hg)
					Metals wich were mainly found within coarse particles (3-4 μm): Fe, Sr, Ba

Figures

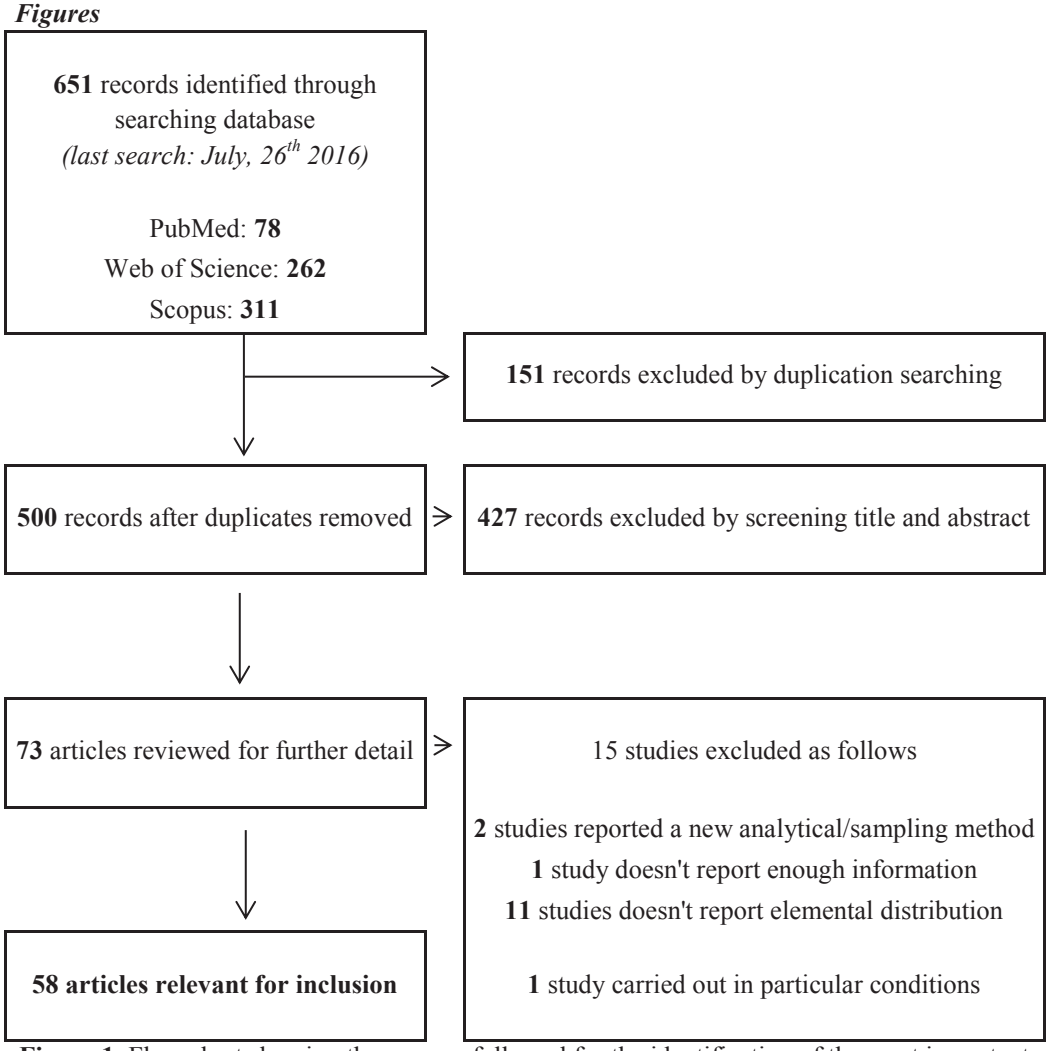

Figure 1. Flow chart showing the process followed for the identification of the most important research studies on the elemental characterization of size-segregated PM.

Chapter 2 – *Mass Concentration and Size-Distribution of Atmospheric Fine and Ultrafine Particles in an Urban Environment*

This chapter is based on a pre-copyedited, author-produced version of an article accepted for publication in *Aerosol and Air Quality Research* following peer review. The article in press [**Rovelli, S.**, Cattaneo, A., Borghi, F., Spinazzè, A., Campagnolo, D., Limbeck, A. and Cavallo, D.M. Mass Concentration and Size-Distribution of Atmospheric Particulate Matter in an Urban Environment. *Aerosol Air Qual. Res.,* doi: 10.4209/aaqr.2016.08.0344] is available online at: http://aaqr.org/Articles_In_Press.php.

Abstract

This chapter is focused on the development of an experimental approach specifically designed to investigate the ambient mass concentration, size-distribution and temporal variability of atmospheric particulate matter (PM), from coarse particles to the smallest particulate ranges. In this context, a long-term monitoring campaign was undertaken at an urban background site in Como, Northern Italy, from May 2015 to March 2016. A 13-stage Low Pressure Impactor (DLPI) was used for the collection of size-segregated particulates in the 0.028–10 µm size range. The results revealed a good level of agreement between DLPI and a co-located Harvard-type $PM_{2.5}$ Impactor used in the study as a gold standard for the fine particulate fraction, allowing them to be classified as comparable and characterized by a reciprocal predictability, at least in the concentration range under investigation. The PM concentration levels varied greatly between the different sampling sessions, with higher mean mass concentrations during the heating season. Appreciable seasonal differences were found for particles between 0.15 and 1.60 µm that, on average, registered concentration levels 3.5 times higher during the heating period (mean: 28.2 µg m^{-3}; median: 24.4 µg m^{-3}) compared to the non-heating season (mean: 8.3 µg m^{-3}; median: 7.6 µg m^{-3}). No relevant and significant differences were detected for the coarser ranges (> 1.60 µm). Temporal variabilities were influenced by typical PM urban sources (e.g., household heating, traffic), that significantly affected fine and submicrometer particles, and were related to meteorological factors. Ambient air particles exhibited a trimodal distribution: a first and sharp peak more pronounced during the heating period was identified between 0.4 and 0.5 µm and two other slight peaks in the coarse mode were centered on approximately 3 and 8 µm. No relevant differences were found in the shape of the size-distribution between the two investigated periods. The average $PM_{2.5}$ (22.4 µg m^{-3}) and PM_{10} (27.7 µg m^{-3}) concentrations monitored in the study area exceeded the annual Air Quality Guideline Values (respectively equal to 10 µg m^{-3} and 20 µg m^{-3}) established by the World Health Organization.

1. Introduction

Numerous epidemiological and toxicological studies have documented strong correlations between measured particulate matter (PM) levels and adverse health outcomes (Erdinger *et al.*, 2005; Schwarze *et al.*, 2006; Brook *et al.*, 2010; Stafoggia *et al.*, 2013; Raaschou-Nielsen *et al.*, 2016). Although current International Guidelines are focused on PM_{10} and $PM_{2.5}$ (World Health Organization, WHO, 2006), increasing toxicological and epidemiological evidences have suggested consistent associations between health endpoints and particles characterized by

smaller aerodynamic diameters (D*p*) (Ibald-Mulli *et al.*, 2002; Oberdörster *et al.*, 2005; Karakoti *et al.*, 2006; Ostro *et al.*, 2015).

The relationships between PM concentrations, chemical characteristics and the potential hazardous effects on human health are related to the penetration, deposition and clearance of particles into the human respiratory tract (Lippmann *et al.*, 1980). The transfer and deposition in lung airways are in turn dependent mainly on particle size and shape (Donaldson *et al.*, 2002). As extensively documented in the literature (Lippmann *et al.,* 1980; Heyder *et al.*, 1986; Donaldson *et al.*, 2002), particles > 10 μm are only deposited in the extrathoracic region by inertial impaction and they are not able to reach the nonciliated tract of the respiratory system. Particles in the 1–10 μm size range are deposited due to impaction in the extrathoracic and upper bronchial airways, while sedimentation governs their deposition in the lower bronchial and alveolar region. The impaction deposition increases with increasing particle size whereas sedimentation is higher around 3 μm. For particles having Dp between 0.1 μm and 1 μm, the deposition in the conducting airways is generally very small. Indeed, these particles are mainly deposited by gravitational and diffusional transport in the alveolar tract and their total deposition therefore approximates the alveolar deposition. Finally, particles < 0.1 μm deposit by diffusion mainly in the lower bronchial and alveolar region. Their total deposition probability tends to increase with decreasing particle size and these particles are more difficult to eliminate by mucociliary clearance and physiological leaching mechanisms (Lippmann *et al.*, 1980). Therefore, information about the size-distribution of airborne PM, from coarse particles to the smallest particulate ranges, represent an important knowledge in terms of health concern. Moreover, unlike PM_{10} or $PM_{2.5}$ for which there are lots of continuous or time-integrated mass data (Ye *et al.*, 2003; Vecchi *et al.*, 2004; Gerasopoulos *et al.*, 2006; Zhao *et al.*, 2009), significantly less is known about the spatial and seasonal variation of size-fractionated particles.

Multistage cascade impactors at low pressure are generally used in this type of studies (Cass et *al.*, 2000; Pakkanen *et al.*, 2001; Fang *et al.*, 2005; Lin *et al.*, 2005; Mbengue *et al.*, 2014) because size cut-points can be reduced at these operating conditions, allowing the additional collection of smaller fractions (Chow and Watson, 2007).

Different researches were carried out in the last decade in the United States (Sardar *et al.*, 2005; Ning *et al.*, 2007; Ntziachristos *et al.*, 2007), Asia (Deshmukh *et al.*, 2012; Fang *et al.*, 2014; Liu *et al.*, 2015) and Europe (Mbengue *et al.*, 2014). In Italy, similar investigations were undertaken in Turin (Malandrino *et al.*, 2016), Genoa (Cuccia *et al.*, 2010) and Rome (Canepari *et al.*, 2008). However, such information is even more scarce and limited at a local scale. Moreover, most of these researches were focused on restricted time periods or low sample numbers, which makes it difficult to estimate seasonal and temporal variations in the mass concentration and size-distribution. Therefore, to improve this knowledge and provide further insights on the topic, a long-term monitoring campaign was performed at an urban background site in Como, Northern Italy.

The aims of this paper are to i) evaluate the performance of a multistage cascade impactor for a typical urban aerosol by comparison with a co-located Harvard-type Impactor; ii) assess ambient mass concentration and size-distribution of atmospheric PM in the 0.028–10 μm size range; iii) assess temporal and seasonal variations; and iv) evaluate the influence of meteorological and environmental conditions on the measured PM concentration levels.

2. Experimental Method

2.1 Sampling Area Description and Sampling Strategy

In this study, a long-term monitoring campaign investigating the ambient PM mass concentration and size-distribution in the 0.028–10 μm range was undertaken in the urban area of Como. Como is a medium-sized provincial town (85,000 inhabitants; 873 inhabitants Km^{-2}; 97 Km^2 of surface area) located in the Lombardy Region, Northern Italy, at 265 m above sea level. The province of Como has more than 500,000 inhabitants and it is surrounded by Switzerland (N), and by the provinces of Sondrio and Lecco (E), Milano and Monza Brianza (S), Varese (W). It covers the SW bank of the Lake of Como and it is characterized by the presence of mountain (2/3 of the total surface area), hilly and flat areas.

The Italian legislation assigned to the Regions the air quality management and Regions acted by dividing the regional territory in different areas for the assessment of ambient air quality and the protection of human health and the environment. Specifically, the Lombardy Region identified i) 3 agglomerates (for the main city of Milano, Bergamo and Brescia) and ii) 4 different zones (A: land with high urbanization; B: land; C: mountain; D: valley) (Fig. 1).

Como is part of zone A, that is characterized by:

i. higher PM_{10} concentrations, especially of primary origin, measured by the fixed site stations of the Regional Air Quality Monitoring Network and confirmed by model simulations
ii. higher PM_{10}, NOx and volatile organic compounds (VOCs) emissions
iii. adverse weather conditions with respect to the pollutants dispersion (limited wind velocity, long periods characterized by high atmospheric pressure and stability, low mixing layer height, frequent thermal inversions at low altitude)
iv. high population density, industrial activities and traffic

Moreover, zone A is further divided into:

- zone A1: urban areas with higher population density and local public transport
- zone A2: urban areas with lower population density and emissions than zone A1

Data from the Regional Air Emissions Inventory (INEMAR, 2012) showed that the main PM_{10} and $PM_{2.5}$ sources in the study area during the year 2012 were characterized by non-industrial combustion processes (domestic heating, wood combustion in residential structures or commercial activities), followed by road transport (especially from cars and heavy vehicles) and other sources.

The collection site was selected on the basis of the Guidelines regarding the Air Quality Monitoring Network (EEA, *Criteria for EUROAIRNET*, 1999). The principal aim was trying to identify an outdoor sampling site that could be considered as an URban Background (URB) station, according to the guidelines criteria, so that the monitoring location could be used to assess the "average" pollution levels in the urban environment (urban background concentration) resulting from transport of air pollutants from outside the urban area and from emissions in the city itself, without dominating or prevailing emission sources like traffic or industrial activities. For this type of monitoring station, the air pollution data should be representative of a surface having a radius between 100 ÷ 2000 m (EEA, February 1999). The represented area is defined as the area in which the pollutant concentrations do not differ for more than 20% from the monitored values (EEA, February 1999). Verification of background concentration levels of air pollutants is a key point for the exposure assessment of the general

population living in the study area in terms of the representativeness of the average levels of air pollution.

The URB monitoring site are used to control average pollution levels within outdoor environments characterized by a continuous urban covering, and they are preferably located inside public green areas or pedestrian areas (e.g. green parks, schools) not directly influenced by specific emission sources, as road traffic or industrial emissions (APAT, 2004). In general, the minimum distances that URB stations must have from emission sources are summarized in Table 1.

As shown in Fig. 2, atmospheric particulate samples were collected at ground level inside the area of the University of Insubria (coordinates: latitude 45°48′05″N, longitude 9°05′42″E, altitude 214 m above the mean sea level). Residential structures and commercial activities surround the sampling location. Different types of industries (textile, printing, mechanical and wood plants) mainly cover the SW/NW sectors within a radius of approximately 4–30 km. A municipal solid waste incinerator is also located approximately 3.5 km SW of the sampling site. The two main roads close to the URB location are Via Castelnuovo and Via Valleggio (Fig. 2). Via Castelnuovo is part of the principal road network of the city and is located at approximately 215 m from the collection site. Via Valleggio is classified as a secondary street with a primary role of distribution and penetration towards the city center, especially from southern locations. It is characterized by a traffic volume of approximately 1,600 vehicles day^{-1} and a speed limit of 50 km h^{-1} and is 25 m from the selected site.

Because of the size, weight and sensitivity of the instrumentation used for particle collection, the sampling equipment was located in a dedicated sampling box, and sampling lines were placed with air inlets at approximately 1.7 m above the ground, which approximately corresponds to the breathing zone of humans. In accordance with the Guidelines Criteria (EEA, *Criteria for EUROAIRNET*, 1999), any type of obstructions, walls or tall trees were not present in the immediate vicinity (< 10 m) of the monitoring devices. The nearest building was located at approximately 25 m from the sampling box.

The experimental approach was designed to integrate different meteorological and environmental conditions that could potentially influence the PM mass and composition in the urban environment. For this reason, the total duration of the planned campaign was 10 months. Atmospheric sampling started at the end of May 2015 and was stopped at the end of March 2016 to obtain a large number of samples that could be used to characterize the study area and investigate temporal variations in the measured PM concentration levels. Measurements generally started between 09:00–10:30 on Monday mornings and lasted until Friday mornings, using a 96-h sampling duration every sampling week. For convenience, the average concentrations obtained each sampling week with a sampling period of 96-h will be indicated in the text as 5-days (5-d) mean concentrations.

2.2 Sampling Equipment

The sampling equipment consisted of different monitoring devices. A 13-stage Low Pressure Impactor (Dekati Low Pressure Impactor, DLPI, DEKATI Ltd., Tampere, Finland) designed for deposition of particles in the 0.028–10 μm size range according to their aerodynamic diameter (12 real stages plus one stage for separating particles > 10 μm) was used for the collection of size-segregated PM. The nominal values for the equivalent aerodynamic 50% cut-

off diameters of the impactor stages are: 0.0283; 0.0559; 0.944; 0.157; 0.262; 0.383; 0.614; 0.950; 1.60; 2.40; 4.00; 6.60 and 9.97 µm.
During operation, a pressure gradient of 900 mbar was applied across the 13 stages, to obtain a pressure of 100 ± 5 mbar under the last impactor stage, thereby ensuring the exact diameter cut points over the measurement period.
Aerosol particles were deposited on high-purity polycarbonate filters (PC, 25-mm; no-holes, Fisher Scientific, S.A.S., Illkirch, France) coated with a thin layer of Apiezon-L grease (DEKATI DS-515 Collection Substrate Spray, DEKATI Ltd., Tampere, Finland) to improve the impactor collection efficiency and prevent bounce- and blow-off effects during separation. Before use, the impactor and all of the accessories needed for handling the substrates and the samples were washed with distilled, de-ionized water and propan-2-ol.
To assess DLPI performance, during 34 of the total 38 5-d samplings, $PM_{2.5}$ was also monitored by a Harvard-type Impactor (HI) (MS&T Area Sampler Air Diagnostic and Engineering, Inc., Harrison, ME, USA) (Marple *et al.*, 1987), operated at 10 L m^{-1} (Leland Legacy pumping unit, SKC, Inc., Eighty Four, PA, USA) and selected in this study as a gold standard for the $PM_{2.5}$ fraction, because of its common use in the scientific literature (Cyrys *et al.*, 2001) and its documented agreement with $PM_{2.5}$ Federal Reference Methods (FRMs) (Babich *et al.*, 2000; Yanosky and Maclntosh, 2001). Fine particles were collected on 37-mm, 2.0-µm polytetrafluoro-ethylene (PTFE) filters with polymethylpentene (PMP) support rings (Pall Life Sciences, New York, NY, USA). The pump flow rates were always checked before and after sampling by a primary standard flow meter (DryCal Defender 520, International Corp., Butler, NJ, USA) to improve the accuracy of the sampling volume estimates and verify that large flux variations did not occur during sampling (percent Coefficient of Variation < 5%). The particle mass collected on PC and PTFE filters was determined gravimetrically following a standard operating procedure (UNI EN 14907; UNI EN 12341). Briefly, each filter was conditioned before weighing at 50% ± 5% relative humidity and 20°C ± 1°C for a minimum of 24 hours in a controlled environment (Bio Activa VE Climatic Cabinet, Aquaria, Lacchiarella, Milan, Italy). The filters were weighed three times (every 20") by a micro-balance with a readability of 1 µg (Gibertini 1000, Novate, Milan, Italy), ensuring a standard deviation ≤ 3 µg. An electrical C-shaped ionizer (HAUG GmbH & CO. KG, Germany) was used to eliminate electrostatic charges from the filter surfaces. This procedure was repeated before and after each sampling, and the particulate masses were determined by differential weighing. Laboratory blanks - two for each type of filter used - were always weighed under the same conditions to verify possible anomalies in the weighing room conditioning (e.g., temperature and humidity variations). The average blank filter masses were then used to correct the filter mass results for each test. Prior to the analysis, the micro-balance was auto-calibrated, and a calibration check was performed using certified standard weights of 1, 100 and 1000 mg, allowing deviations from the true value ≤ 3, 5 and 10 µg, respectively. The quality of the weighing procedure was assessed using the ASTM D 6552 method (ASTM, 2000). The weighing procedure was repeated on three greased PC and three PTFE filters at least three times on the same day for twelve different days to obtain a representative number of repeated weighing (> 30) for each type of collection substrate. Mass limits of detection (LODs) of 0.9 µg and 6.2 µg ($\alpha = 0.05$) were calculated for 25-mm PC filters (DLPI) and 37-mm PTFE membranes (HI), respectively. When referenced to an α-value of 1.1% ($\alpha = 0.011$), LODs increased up to 1.2 µg and 8.7 µg, respectively. The mean LOD (α-value of 1.1%) for the PM

concentrations determined on each DLPI collection plate was 0.0072 μg m^{-3} for an average sampling time of 96-h and a nominal flow rate of 30 L min^{-1}. The mean LOD for the $PM_{2.5}$ collected by HI was 0.2 μg m^{-3} for the same sampling time and a nominal flow rate of 10 L min^{-1}. Mass limits of quantification (LOQs) of 10.7 μg and 75.2 μg were determined for PC and PTFE filters, respectively.

An external weather station (BABUC-ABC, LSI Lastem, Milan, Italy) was also used to characterize and record on-line meteorological conditions (temperature (T), relative humidity (RH), atmospheric pressure (AtP), wind speed (WS) and wind direction (WD)) during the study period at the sampling site. WS and WD data were measured at a height of 3 m above the street level whereas T, RH and AtP sensors were placed at a height of 1.5 m. For each parameter, the weather station was programmed with an acquisition rate of 1 min and an elaboration rate of 60 mins. The acquired data points were thus processed every hour using the programmed statistical mode to provide hourly averages, standard deviations, maximum and minimum values, time of maximum and time of minimum.

Rainfall data were obtained by the nearest monitoring station of the Regional Agency for Prevention and Environment (Agenzia Regionale Protezione Ambiente, ARPA) of Lombardy, located approximately 2.5 km NW of the sampling point. Planetary Boundary Layer (PBL) data related to the sampling location were recovered from the Regional Agency for Prevention and Environment of Emilia-Romagna.

Finally, the average traffic volume on via Valleggio (the nearest street to the sampling site) was estimated for each sampling week by counting for 15 mins the number of vehicles that passed on the street during different times of day (every two hours, from the early morning (07:30) until the late afternoon (19:30); during some days, vehicles were counted also in the late evening).

2.3 Statistical Analysis and Data Treatment

Statistical data analysis was performed using the SPSS software package (SPSS Inc., Chicago, IL, USA). For each 5-d sampling session, PM concentration levels were normalized to the specific conditions (T, RH and AtP) monitored at the sampling site.

For data treatment and analysis, results were differentiated into two main periods: the non-heating season (May 2015–October 15th 2015) and the heating season (October 19th 2015–March 2016), as is often performed in studies on atmospheric pollution (Tecer *et al.*, 2008; Schwarz *et al.*, 2012). For convenience, the separation between these periods was made in accordance with the switching on of the household heating systems during October 2015, as programmed by the Regional Directive of Lombardy.

Descriptive statistics were carried out on size-fractionated PM and meteorological parameters, including histograms of PM fraction contributions. Correlations among variables and differences between DLPI and HI-$PM_{2.5}$ data were assessed by Pearson's correlation coefficients and Paired *t*-test respectively, on *log*-transformed data since data showed a *log*-normal distribution (Kolmogorov-Smirnov test). The Independent-Samples *t*-test was used to explore differences between seasons. Finally, multiple linear regression analyses were performed. In every model, the different DLPI stages were included as dependent variables and the on-situ meteorological (T, RH, AtP, WS and PBL) and environmental (average traffic volume on the closest road) factors as predictors. Only the variables that were found to be

statistically significant in bivariate correlation analysis were included in each model. In all tests, a *p*-value lower than 0.05 was considered to be statistically significant.

To assess DLPI performance, DLPI-$PM_{2.5}$ concentrations were compared with the corresponding average levels monitored by HI according to the indications summarized by Watson *et al.* (1998). Briefly, the agreement between the two methods was defined by linear regression analysis between the y-dependent variable (DLPI-$PM_{2.5}$) and the x-independent variable (HI-$PM_{2.5}$). Comparability and predictability were evaluated as a function of slope (1 ± 3 standard error (s.e.)), intercept (0 ± 3 s.e.) and Pearson correlation coefficient (r) (> 0.9). When r is > 0.9 but slope and intercept criteria are not met, the investigated method can be classified as comparable, but only the dependent variable is predictable from the independent variable. Data with r < 0.9 are classified as not comparable. In addition, $PM_{2.5}$ samplers were also compared by the Bland-Altman plots method (Altman and Bland, 1983; Bland and Altman, 1986).

WS and WD data were analyzed by using the WRPLOT View™ Software (Lakes Environmental Software, ver.7.0.0).

3. Results

3.1 Sampling Information and Meteorological Conditions

Table 2 summarizes the sampling information and the meteorological conditions during the two monitoring periods. The presented information are referred to sampling number and sampling period, T, RH, WS and prevalent WD, AtP, cumulative rainfall and PBL.

During some of the sampling weeks, data from the external weather station were not available because of technical problems. In this case, due to the good correlation and the low relative error between BABUC-data and ARPA-data for T (r = 0.997, $p < 0.001$; 2.4%) and RH (r = 0.963, $p < 0.001$; 11%), hourly T and RH values from ARPA were used at the sampling site. On the contrary, WS was on average 78% lower at the URB location compared with the ARPA monitoring station and the replacement with ARPA-data was not possible.

A variety of meteorological conditions alternated during the study period. As shown in Table 2, the highest T were reached during the central warm weeks, between July and August, when RH dropped to the lowest summer value (53.5%). The non-heating season was generally characterized by high AtP and high T from the beginning of July. These high T values unfortunately caused problems with the sampling pump operation and the sampling campaign was forcedly interrupted until the normal operating conditions were restored. Rainfall was characterized by sporadic rains that increased from late August. The heating season began with high atmospheric stability, characterized by low PBL heights, high AtP, low WS and absence of rainfall from the beginning of November until the end of December. The lowest mean T was reached during the third week of January (–0.9°C). Then, T increased and sporadic rain events occurred in February and March.

The sampling site was characterized by generally low WS, with 5-d mean values always < 1 m s^{-1} (Table 2), probably due to the specific sampling location, far from the banks of Lake Como (approximately 1.8 km) and surrounded by moraine hills on the NE sector. The non-heating season was characterized by an average WS of 0.47 m s^{-1}, with hourly averages < 0.5 m s^{-1} for 59% of the cases. The lowest 5-d means were measured during the first half of the heating season (with 83% of hourly values < 0.5 m s^{-1}), whereas the second half registered higher values, also because of the occurrence of Föhn episodes (e.g., sampling n° 34) accompanied by

decreased RH and increased T (Table 2). In general, hourly WS during the heating season were < 0.5 m s^{-1} for 75% of the cases and the average WS was 0.36 m s^{-1}.
The WD was predominantly from the S/SE sector during the entire study period and it did not change significantly between the heating and the non-heating season. Also for winds characterized by higher intensities, the prevalent WD was from SE, with some rare events from the SW sector (Table 2 and Fig. 3). In this context, it is necessary to underline that the area of Como is characterized by a complex topographic scenario. The presence of the lake, moraine conformations and valleys favour the formation of different meteorological conditions in different areas of the city, with great differences (especially for winds) between urban areas close to the banks of the lake and urban areas located further inland. This could be the main reason of the aforementioned difference between ARPA and BABUC wind data. As shown in Fig. 2, the ARPA monitoring station is located on the SW bank of the lake and it is consequently exposed to winds that blow at higher intensities from the NE sector. Contrariwise, the sampling site was located far from the banks of the lake and winds from N/NE were shielded by the moraine hills located in that direction.

3.2 Comparison Between DLPI and HI-$PM_{2.5}$ Mass Concentration

To assess DLPI performance, DLPI-$PM_{2.5}$ concentrations were compared with the corresponding average levels monitored by HI. The $PM_{2.5}$ levels measured by DLPI were generally lower than those obtained by HI, with statistically significant differences (Paired *t*-test; $p < 0.001$). The 5-d DLPI/HI ratios were mostly below 1 (71% of the cases) and ranged from 0.79 to 1.13 with an overall mean ratio of 0.95 (± 0.08) (Fig. 4).
Agreement between the two sampling methods was first evaluated according to the indications summarized by Watson et al. (1998). HI and DLPI-$PM_{2.5}$ concentrations were analyzed by regression analysis of 34 data pairs (Fig. 3). As previously explained, the level of agreement was defined as a function of slope, intercept and Pearson correlation coefficient. In this study, the $PM_{2.5}$ regression line presented slope = 0.906 (s.e. = 0.013), intercept = 0.816 µg m^{-3} (s.e. = 0.406 µg m^{-3}) and r = 0.997 (Fig. 4).
Additionally, to better assess possible error trends, HI and DLPI-$PM_{2.5}$ concentrations were examined using the Bland-Altman plot (Fig. 5). As shown in Fig. 5, the 95% limit of agreement, calculated as the average difference ± 1.96 x standard deviation of the difference, was ± 4.24 µg m^{-3}. The maximum difference between single measurements was up to –6.83 µg m^{-3} and the average difference was –1.54 µg m^{-3}. A significant correlation (r = –0.78; $p <$ 0.001) was found between $PM_{2.5}$ and DLPI-HI differences, that showed higher (negative) values at the highest concentration levels.

3.3 Ambient PM Mass Concentration and Temporal Trends

During the entire campaign, 38 5-d sampling sessions were performed at the URB station in Como and a total of 221 and 273 DLPI samples were collected for the non-heating and the heating season, respectively. Because of the good agreement between DLPI and HI sampling methods (see paragraph 4.1), only the DLPI particle mass concentrations were subsequently used for data treatment and analysis.
Descriptive statistics of mass concentrations obtained for each DLPI collection plate and for the principal PM sizes during the two monitoring seasons and the whole campaign are reported in Table 3. For the standard PM fractions, concentration levels were obtained summing up the

particulate masses collected on filter substrates, with respect to the aerodynamic diameter of particles (stages 1–12 for PM_{10}; stages 1–9 for $PM_{2.5}$; stages 1–7 for PM_1). DLPI stages 1 and 2 were considered as the ultrafine fraction, because of the absence of a backup filter stage for the collection of particles < 0.028 μm.

A great variability can be observed in the dataset and mean mass concentrations for all size ranges were higher during the heating season, as expected (Table 3 and Fig. 6). Statistically significant differences between the two investigated periods were found for all DLPI stages (Independent-Samples *t*-test, $p < 0.01$) except for stages 1, 10, 11 and 12, namely for the finest particle fraction ($PM_{0.028–0.055}$) and for the coarse size range ($PM_{2.5–10}$). The greatest increase effect was found for particles whose D*p* was between 0.15 and 1.60 μm (collected on DLPI-stages 4, 5, 6, 7 and 8) that, on average, registered concentration levels 3.5 times higher during the heating season (mean: 28.2 μg m^{-3}; median: 24.4 μg m^{-3}) compared with the non-heating season (mean: 8.3 μg m^{-3}; median: 7.6 μg m^{-3}). For the $PM_{2.5–10}$ fraction, the main differences, although not statistically significant and almost negligible with respect to the finest fractions, were noticed in the 2.4–4.0 and 6.6–9.9 μm size ranges, whereas the ultrafine component ($PM_{0.1}$) showed a significant increase only in $PM_{0.055–0.094}$ (Table 3).

On average, 75% of the PM_{10} mass consisted of $PM_{2.5}$, with a minor contribution of the $PM_{2.5–10}$ fraction (33% and 16% during the non-heating and the heating season, respectively). PM_1 was the major component of $PM_{2.5}$ (83% and 87% during the non-heating and the heating season, respectively), with a primary contribution of the accumulation mode ($PM_{0.1–1}$) during both periods (77% and 84%, respectively). $PM_{0.1–1}$ accounted for more than 50% of the PM_{10} mass and all of the size fractions included in this mode were mutually and significantly correlated (Table 4). Lower correlation coefficients, although statistically significant, were found with coarser particles, especially with $PM_{2.5–10}$. $PM_{0.1}$ played only a minor role in the particulate mass concentration, accounting for 7%, 6% and 4% of PM_1, $PM_{2.5}$ and PM_{10}, respectively, during the non-heating season and for 3.0%, 2.7% and 2.3% in the same PM fractions during the heating season. The contribution of $PM_{0.03–0.05}$ was even lower and less relevant (30.0 %, 2.4%, 1.9% and 1.3% for $PM_{0.1}$, PM_1, $PM_{2.5}$ and PM_{10}, respectively, during the non-heating season and 23.1%, 0.8%, 0.7% and 0.6% during the heating season).

The measured levels of outdoor $PM_{2.5}$ and PM_{10} are not strictly comparable with the 1-y WHO Guidelines (WHO, 2006) because of the absence of weekends and some sampling weeks. However, it is reasonable to consider the $PM_{2.5}$ and PM_{10} average concentrations as cautionary surrogates of the annual means in the study area (Table 3). Therefore, considering this assumption, it could be said that the 1-y WHO Guidelines of 10 μg m^{-3} and 20 μg m^{-3} established for $PM_{2.5}$ and PM_{10} were exceeded by approximately 124% and 38.5%, respectively, on average and during the monitoring period.

To explain the great variability of size-fractionated PM levels, the influence of local meteorological conditions was analyzed and a bivariate correlation analysis between PM concentrations and meteorological parameters was performed (Table 5). Significant and negative correlations were found with PBL and WS for most of the DLPI size fractions. T was negatively correlated, especially with particles between 0.055 and 0.95 μm. Negative correlations were also found with rainfall. Finally, positive correlations were found for all size ranges with AtP and, to a lesser extent, with RH (Table 5).

Moreover, despite the relatively low number of samples, the structure of the dataset and the number of independent variables, multiple linear regression analyses were performed, to more

deeply investigate the complex relationship between PM concentrations and meteorological and environmental factors that could potentially influence the atmospheric concentration levels. This preliminary analysis found the mixing layer height as the most important predictor of ambient concentrations, at least for particles between 0.09 and 0.9 μm and between 1.6 and 2.4 μm, followed in certain cases by rainfall, that, on the contrary, seemed to be the main determinant for the coarser range ($PM_{6.6–9.9}$) (Table 6).

3.4 Particle Mass Size-Distribution

The median mass size-distributions between 0.028 and 10 μm obtained with the multistage impactor during the non-heating and the heating season are depicted in Fig. 7.

During the non-heating season, ambient air particles exhibited a trimodal distribution, with a first and sharp peak clearly identified in the accumulation mode between 0.3 and 0.5 μm and two other slight and less-marked peaks centered on approximately 3 and 8 μm in the coarse mode. The accumulation mode-peak greatly increased during the heating period, whereas, at the same time, the two peaks in the coarse range remained roughly unchanged. No relevant differences were found in the shape of the particle size-distribution between the two investigated periods.

4. Discussion

4.1 Comparison Between DLPI and HI-$PM_{2.5}$ Mass Concentration

To evaluate the performance of the multistage impactor, a comparison between DLPI- and HI-$PM_{2.5}$ mass concentrations was performed. DLPI-$PM_{2.5}$ concentrations were, on average, lower than those simultaneously monitored by HI, with DLPI-HI disagreements that increased with increasing ambient concentration levels (Fig. 5). Considering the entire data-set, the Bland-Altman plot showed a clear negative trend for concentration levels > 30 μg m^{-3} (Fig. 5). According to the inter-comparison criteria set forth by Watson *et al.* (1998) and based on a first evaluation, DLPI and HI seemed to be classified as comparable, although not characterized by a reciprocal predictability, because of non-compliance with the slope-criterion. The absence of the DLPI backup filter stage could hardly explain the discrepancy with the HI method, because particles less than 0.028 μm are known to have a negligible role in the total PM mass concentration (Tuch *et al.*, 1997). Additionally, the approximation of DLPI-$PM_{2.4}$ to DLPI-$PM_{2.5}$ is equally negligible because the $PM_{2.4–2.5}$ fraction accounted, on average, for 0.8 and 0.5% of PM_{10} during the non-heating and the heating season, respectively. One possible explanation could be the particle deposition effect on the internal impactor walls (particle wall loss) following an excessive loading of filters. As explained by Fujitani *et al.* (2006), this effect is mainly because of particles that rebound from previously collected particulates and may be i) carried away by the air stream on subsequent stages, with a consequent distortion of the mass size-distribution towards smaller mode diameters (not observed in this study, as roughly visible in Fig. 7) or ii) deposited on the impactor's interior walls. The wall loss effect is expected to increase with increasing particle loading on the impactor collection substrates because the magnitude of particle-bounce increases under these conditions. To prevent particle-bounce and ensure the DLPI collection efficiency, a maximum mass per stage of approximately one milligram is recommended by the manufacturer. During some winter sampling weeks this recommended value was exceeded on stages 5, 6 and 7 because of the long sampling time used for particle collection (96-h) and the elevated ambient PM concentrations. Therefore, to

evaluate the DLPI performance at the recommended operating conditions, the method comparison was also performed excluding those data that did not respect the manufacturer recommendations (Figs. 8 and 9). In this case, the regression line presented slope = 0.993 (s.e. = 0.028), intercept = –0.367 μg m^{-3} (s.e. = 0.508 μg m^{-3}) and r = 0.991 (Fig. 8). The 95% limit of agreement was ± 2.15 μg m^{-3}, with an average difference between DLPI and HI equal to –0.48 μg m^{-3} (Fig. 9). These results showed that the multistage impactor still seemed to slightly underestimate the $PM_{2.5}$ concentrations under the operating conditions provided by the manufacturer, with a mean DLPI/HI ratio of 0.96 ± 0.09 (Fig. 8). Most of the ratio values were around 1 and fell within the considered range of ± 1 standard deviation. The higher relative errors, although acceptable, were found for $PM_{2.5}$ concentrations < 15 μg m^{-3} probably because of an increased difficulty and inaccuracy in the gravimetric determination of impactor stages with very low particles mass loadings. However, the strong correlation (r = 0.991; $p < 0.01$) and the good level of agreement between the two methods allowed them to be classified as comparable and characterized by reciprocal predictability, at least in the $PM_{2.5}$ concentration range under investigation (5–40 μg m^{-3}).

In light of these results, further experiments covering a wider range of ambient concentrations (> 40 μg m^{-3}) are suggested to confirm the impactor predictability and comparability and verify the potential equivalence with EN or EPA Reference Standards.

4.2 Ambient PM Mass Concentration, Size-Distribution and Temporal Trends

As was previously mentioned, large temporal differences can be observed in the dataset, with higher mean mass concentrations for all size ranges during the heating season. This behavior was expected and could be mainly explained by a combined effect of meteorological factors, thermodynamic conditions of the atmosphere and variations in type and/or number of emission sources. Other studies close to Como reported strong seasonal variations in the air pollutant levels because of differences in the atmospheric dispersion conditions between summer and winter time (Vecchi *et al.*, 2004).

The most critical scenario was registered at the beginning of the heating season when a sharp increase in the concentration levels was clearly identified (Fig. 6) and maximum levels of 75.5, 67.3 and 57.3 μg m^{-3} were reached for PM_{10}, $PM_{2.5}$ and PM_1, respectively. From the first week of November (20^{th} sample) until the end of December (27^{th} sample), the study area was characterized by extraordinary meteorological conditions (total absence of rainfall, high atmospheric stability and low PBL height; Centro Meteorologico Lombardo, 2016), that promoted the accumulation of air pollutants in the lower atmosphere. Only at the beginning of the last week of November (23^{rd} sample) the high atmospheric stability was interrupted by cold air masses that decreased ambient T and AtP and increased WS and PBL height (Table 2), with a clear reduction in PM concentration levels (Fig. 6), before the previous atmospheric conditions were restored (Centro Meteorologico Lombardo, 2016). The same episode was also registered at the beginning of January (28^{th} sample). Then, a condition of higher atmospheric dispersion and vertical circulation characterized the last weeks of the heating period (Table 2).

Bivariate correlation analysis with meteorological factors confirmed the previously mentioned qualitative evaluation. Negative correlations were found with the PBL height, which seemed to more greatly affect the fine particulate fractions (Table 5). Different studies documented that the evolution of the PBL has a significant effect on the concentration levels of air pollutants (Baumbach and Vogt, 2003; Velasco *et al.*, 2008), also because of a positive feedback loop

between PBL height and aerosol loadings. As well described by Quan *et al.* (2013), the enhancement of atmospheric aerosol tends to decrease the solar radiation, thus reducing the development of PBL. At the same time, the repressed structure of PBL will in turn decrease the diffusion of surface air pollutants, with a consequent increase of aerosol concentrations at the lowest layers of the atmosphere.

Although the sampling site was characterized by very low WS, often < 0.5 m s^{-1}, the PM concentrations were found to considerably decrease when the WS increased as a result of dilution effects. No obvious relationship was shown for particles ranging from 6.6 to 9.9 μm, probably because of low WS that could not promote the transport and dilution of coarser particles (Kim *et al.*, 1997).

Additionally, T was negatively correlated with PM concentrations. Correlations were statistically significant only for the finest fractions (0.06–0.95 μm), while insignificant associations were showed with particles > 1.6 μm (Table 5). This could be because cold T favor the formation of secondary aerosols in the aerosol particle phase (Putaud *et al.*, 2004) and promote the formation of ultrafine particles (mainly particles > 0.05 μm) (Bukowiecki *et al.*, 2003; Charron and Harrison, 2003). Indeed, it has been shown that the mixing of two air parcels with different temperatures (e.g., the mixing of hot exhaust vapors with cool air) increases significantly the nucleation rates (Nilsson and Kulmala, 1998), with the formation of new particles during the cooling and dilution of the vehicle exhausts (Charron and Harrison, 2003). Ultrafine aged particles can subsequently evolve towards larger size fractions (> 0.1 μm) through condensation and aggregation phenomena which enhanced under these T conditions.

RH was unexpectedly found to positively affect the PM concentration levels. A possible explanation may be that high RH conditions, together with low T and low WS, can promote the formation of lower PBL heights, which hamper the dispersion of air pollutants, as occurred in this study at the beginning of the heating season. Similar findings were showed by Deshmukh *et al.* (2012) and Elminir (2005), that noticed the highest PM_{10} average concentrations at RH values > 80%.

Results from the multiple linear regression analysis have to be interpreted with caution, mainly because of the dataset structure and the low number of samples incorporated in the analysis (n = 25). Among all of the aforementioned meteorological factors, the PBL height seemed to exert the main influence on PM concentrations, which further confirmed the strong correlation found in the bivariate analysis. As already explained, it is known that the seasonal effect on PM mass concentrations is mainly due to differences in the atmospheric dispersion conditions, mostly related to the PBL height. At the same time, the PBL height is in turn dependent on different meteorological factors, including T, RH and WS, that could explain the reason for which these variables disappeared in the multivariate analysis. Furthermore, the effect of PBL seemed to be relevant for smaller particles, whereas the coarser fraction ($PM_{6.6–9.9}$) appeared to be mainly influenced by rainfall (Table 6). In any event, the quality of this evaluation does not permit definitive conclusions and it would be necessary to include more samples to develop a more robust analysis to support and improve these preliminary findings.

Large and statistically significant differences on mass concentration levels were registered for particles having D*p* values between 0.15 and 1.60 μm (Table 3 and Fig. 6), as is also shown in the particle mass size-distribution (Fig. 7), where a first and sharp peak was clearly identified in the accumulation mode between 0.3 and 0.5 μm. Similar findings were found at an urban

site in Vienna, where a marked peak was equally identified in the accumulation mode at 0.5 μm (Horvath *et al.*, 1996).
In a typical urban environment, fine, submicrometer and ultrafine particles may partially result from traffic emissions, because of incomplete combustion processes of gasoline, diesel and other fuels (Knibbs and Morawska, 2012). Although the monitoring location was not a traffic sampling site close to a heavily traffic road, positive correlations were found between the average traffic volume on the closest trafficked road (via Valleggio) and particles ranging from 0.055 to 0.95 μm ($r = 0.5$; $p < 0.05$).
The large and marked peak registered in the accumulation mode may be associated with a combined influence of the aforementioned emission source together with household heating emissions that led to a sharp growth of the peak during the heating period when the heating system was switched on and the traffic intensity increased. Indeed, as explained by Vecchi *et al.* (2004), domestic heating is an additional source for particles < 1 μm and it contributes to primary PM as well as secondary aerosol because of its high emissions of gaseous precursors during the cold season.
On the other hand, traffic related re-suspension phenomena, soil re-suspension phenomena and the presence of industrial activities, such as the mechanical and wood plants upwind of the sampling site, may have led to the formation of larger particles, that could otherwise explain the presence of peaks in the coarse mode fraction (Fig. 7). Mbengue *et al.* (2014) identified a bimodal distribution for an urban-traffic site, with peaks centered on 0.5 and 2.5 μm, whereas a trimodal distribution with a third maximum at 8 μm was only observed downwind of industrial emissions. Also Tecer *et al.* (2008) attributed the most important anthropogenic $PM_{2.5–10}$ sources to the coal processing and mining industries located close and upwind to the sampling location.

4.3 Comparison of Ambient PM Concentrations with Literature Data

For a comparison of our findings with the scientific literature, it must be noticed that the PM concentration levels shown in this study are not always strictly comparable with other similar investigations carried out in Europe and all over the world. Indeed, these researches are often performed at different sampling sites (under urban, traffic or industrial influences), that could determine different PM concentration levels because of different distances from various emission sources. Moreover, the comparability between other studies might be hampered and impaired because of differences in sampling periods, collection intervals and type of monitoring devices used, which may be characterized by different particle cut-off diameters. Only one survey was recently carried out in the Como urban area (Spinazzè *et al.*, 2015). In this study, the quasi-ultrafine particles (QUFPs, referred as $PM_{0.25}$) mass concentrations were measured in different urban microenvironments along a fixed route. The results found in our survey at the URB station for $PM_{0.26}$ (2.6 ± 0.6 and 6.1 ± 2.4 μg m^{-3} during the non-heating and the heating season, respectively) were from 2 to 3 times lower than the corresponding $PM_{0.25}$ concentrations measured along urban traffic routes by Spinazzè *et al.* (2015), mainly because of the specific monitoring protocol that was properly designed to include road and transit microenvironments.
The $PM_{0.1}$ annual average shown in our survey can be compared with the average concentration of 0.5 μg m^{-3} found between April 1996 and June 1997 at an urban and rural site in Helsinki (Pakkanen *et al.*, 2001), whereas the heating mean of 0.8 μg m^{-3} is in line with the

winter urban levels found in the past in Pasadena (Hughes *et al.*, 1998) and in different sites of California (Cass *et al.*, 2000). Lower concentration levels were found by Ntziachristos *et al.* (2007) during winter/spring time for PM_{10}, $PM_{2.5}$ and $PM_{0.18}$ at an urban sampling site in Los Angeles and by Mbengue *et al.* (2014) for winter levels of PM_{10}, PM_1 and QUFPs both at an industrial and an urban-traffic sector in Northern France. Comparable values were shown by Sardar *et al.* (2005) for an urban mix of industrial and traffic sources in Los Angeles. Ramgolam *et al.* (2008) found in Paris PM_{10} concentration values typically observed at European urban background sites.

On the contrary, research studies carried out in some Asian countries showed, as expected, generally higher concentration levels than those measured in this study. Gugamsetty *et al.* (2012) registered summer/fall PM_{10}, $PM_{2.5}$ and $PM_{0.1}$ average concentrations more than two times higher than our non-heating results at an urban area under industrial and traffic influence in New Taipei City. The winter $PM_{0.1}$ mean level reported by Lin *et al.* (2005) for a traffic site in Taiwan was two orders of magnitude higher than our value of 0.8 μg m^{-3}. However, in this case it must be noticed that UFPs emitted from motor vehicles were more efficiently collected because the sampling site was a near-ground sampling (0.6 m above the road surface) close to the intersection of a major road with a high vehicle flow per day (approximately 72,000 vehicles day^{-1}). Moreover, Liu *et al.* (2015) found relatively high concentrations, with the dominant fraction in the size range < 2.1 μm, that accounted for almost 60% of the total PM mass. Similar findings were also obtained by Duarte *et al.* (2008) and Gnauk *et al.* (2008). Only Chen *et al.* (2013) reported lower PM_{10}, $PM_{2.5}$ and $PM_{0.1}$ concentrations for a rural background station in East Asia. See Table 7 for detailed information about the PM mass concentration values reported in the previously mentioned studies.

4.4 Strengths and Limitations of the Study

One of the main limitations of this study is the long sampling period used for particle collection (approximately 96-h per week) that did not allow the identification of day-to-day or daytime-to-nighttime variability. Nonetheless, this choice was motivated by the possibility of obtaining sufficient material at each DLPI collection stage for trace element analysis. A pilot study on test samples confirmed the need for a sampling interval of 96-h for chemical characterization purposes.

Weekend days and the months of April and May were not included in the sampling protocol, mainly because of technical and/or logistical problems. Therefore, the average PM concentration levels were not expected to provide an accurate evaluation of the annual mean in the study area.

Finally, the experimental design was carried out at one urban sampling site, which did not permit the assessment of possible spatial variations in the monitored area. Moreover, because of the complex topographic scenario previously described, the meteorological conditions monitored at the URB station were representative of the sampling site but how large may be the actual area of representativeness could not be accurately defined.

Despite these limitations, this study has important strengths. To our knowledge, this is one of the first investigations in which a reasonable number of size-segregated samples were collected by an intensive long-term monitoring campaign. Indeed, in this type of studies where multistage cascade impactors at low pressure are used, the monitoring protocol is often limited to one season (Hughes *et al.*, 1998; Lin *et al.*, 2005; Fang *et al.*, 2014), or few weeks per site

(Sardar *et al.*, 2005) or per season (Chen *et al.*, 2013; Malandrino *et al.*, 2016), or one week per month (Pakkanen *et al.*, 2001). Sometimes, multistage impactors such as DLPI or nano-MOUDI are only used once during the entire sampling campaign (Canepari *et al.*, 2008; Mbengue *et al.*, 2014), probably because of their laborious and time-consuming management. Moreover, in some studies the mass concentration and size-distribution of the lowest particle fractions (e.g., UFPs) are obtained by integration of optical analyzer data using an assumed particle density (Hughes *et al.*, 1998), which could result in loss of accuracy.

In the present investigation, size-fractionated samples were collected every week for 10 consecutive months, unless there were technical or instrumental problems. Obtained findings were used to better characterize the study area in terms of: i) temporal variability; ii) identification of significant differences between, at least, the two selected seasonal periods for each of the 12 size ranges; and iii) discrimination between meteorological factors that really affect PM concentration levels, although more robust statistical analysis will be needed to better confirm our findings.

Moreover, the collected DLPI and HI paired data allowed the evaluation of DLPI performance for $PM_{2.5}$ that, to our knowledge, has never been assessed before on this type of multi-stage low pressure impactor.

Finally, DLPI stages 1–9 have been analyzed for some potentially toxic trace metals with a novel analytical measurement protocol (data presented in the following chapters of the thesis) in order to: i) assess their concentrations and size-distributions; ii) evaluate their potential risk for human health; and iii) evaluate the influence of in-situ meteorological conditions on the measured concentration levels.

5. Conclusions

In this study, the ambient PM mass concentrations and size-distributions in the range of 0.028–10 μm were assessed at an urban background site during an intensive long-term investigation. Temporal variations, from ultrafine to coarse particles, were shown. As expected, the highest PM concentration levels were found during the heating period because of a joint effect of meteorological factors and variations in type and/or number of emission sources. One of the most interesting findings of this study is that the greatest increasing effect was registered on particles having D*p* values between 0.15 and 1.60 μm (and mainly for particles having D*p* values between 0.4 and 0.9 μm), which are more related to the presence of additional sources of submicrometer particles during the cold season. No relevant and significant differences were found for particles > 1.60 μm. The average $PM_{2.5}$ and PM_{10} values measured in the study area suggested that during the monitoring campaign the general population living in the area may have been exposed to PM levels potentially harmful for human health, mainly because of the high concentrations of fine particles reached at the beginning of the heating season.

Results obtained from this investigation could be used as a valid support in epidemiological studies, as an innovative and alternative target with respect the typical PM fractions on which these type of researches are generally focused (PM_{10} or $PM_{2.5}$). Because of the type of sampling site used for particle collection (URB) and the extended time series of size-segregated particle mass concentrations, these data could be used to better assess if the known and documented PM effects exerted on the general population (e.g., increased mortality or morbidity) could be related to specific size fractions of $PM_{2.5,}$ with a particular focus on those

particles that are able to reach the deepest parts of the respiratory tree, and if these effects are really greater than or independent from the effects induced by larger size particulates.

Acknowledgments
The authors would like to extend a special acknowledgment to Dr Luca Del Buono for his contribution to environmental samplings and to Dr Gabriele Carugati for his technical support with the external weather station.

References

Altman, D.G. and Bland, J.M. (1983). Measurement in medicine: the analysis of method comparison studies. *The Statistician*, 307–317.

American Society of Testing and Materials (ASTM) (2000). *ASTM Standard Practice for Controlling and Characterizing Errors in Weighing Collected Aerosols (ASTM D 6552)*, West Conshohoken, PA; USA, ASTM.

Babich, P., Davey, M., Allen, G. and Koutrakis, P. (2000). Method comparison for particulate nitrate, elemental carbon and $PM_{2.5}$ mass in seven U.S. cities. *J. Air & Waste Manage. Assoc.* 50: 1095–1105.

Baumbach, G. and Vogt, U. (2003). Influence of inversion layers on the distribution of air pollutants in urban areas. *Water Air Soil Poll.* 3(5): 67–78.

Bland, J.M. and Altman, D.G. (1986). Statistical methods for assessing agreement between two methods of clinical measurement. *The lancet* 327(8476): 307–310.

Brook, R.D. *et al.* (2010). Particulate matter air pollution and cardiovascular disease an update to the scientific statement from the American Heart Association. *Circulation* 121(21): 2331–2378.

Bukowiecki, N., Dommen, J., Prévôt, A.S.H., Weingartner, E. and Baltensperger, U. (2003). Fine and ultrafine particles in the Zurich (Switzerland) area measured with a mobile laboratory. An assessment of the seasonal and regional variation throughout a year. *Atmos. Chem. Phys. Discuss.* 3: 2739–2782.

Canepari, S., Perrino, C., Olivieri, F. and Astolfi, M.L. (2008). Characterization of the traffic sources of PM through size-segregated sampling, sequential leaching and ICP analysis. *Atmos. Environ.* 42: 8161–8175.

Cass, G.R., Hughes, L.A., Bhave, P., Kleeman, M.J., Allen, J.O. and Salmon, L.G. (2000). The chemical composition of atmospheric ultrafine particles. *Phil. Trans. R. Soc. Lond. A*. 358: 2581–2592.

Centro Meteorologico Lombardo (2016). Available online at: http://www.centrometeolombardo.com/content.asp?CatId=602&ContentType=mappe.

Charron, A. and Harrison, R.M. (2003). Primary particle formation from vehicle emissions during exhaust dilution in the roadside atmosphere. *Atmos. Environ.* 37: 4109–4119.

Chen, S.-C., Hsu, S.-C., Tsai, C.-J., Chou, C.C.-K., Lin, N.-H., Lee, C.-T., Roam, G.-D. and Pui, D.Y.H. (2013). Dynamic variations of ultrafine, fine and coarse particles at the Lu-Lin background site in East Asia. *Atmos. Environ.* 78: 154–162.

Chow, J.C. and Watson, J.G. (2007). Review of measurements methods and compositions for ultrafine particles. *Aerosol Air Qual. Res.* 7: 121–173.

Cuccia, E., Bernardoni, V., Massabò, D., Prati, P., Valli, G. and Vecchi, R. (2010). An alternative way to determine the size-distribution of airborne particulate matter. *Atmos. Environ.* 44: 3304–3313.

Cyrys, J., Dietrich, G., Kreyling, W., Tuch, T. and Heinrich, J. (2001). $PM_{2.5}$ measurements in ambient aerosol: comparison between Harvard Impactor (HI) and the tapered element oscillating microbalance (TEOM) system. *Sci. Total Environ.* 278: 191–197.

Deshmukh, D., Deb, M.K., Verma, D., Verma, S.K. and Nirmalkar, J. (2012). Aerosol size distribution and seasonal variation in an urban area of an industrial city in Central India. *Bull. Environ. Contam. Toxicol.* 89: 1098–1104.

Donaldson, K., Tran, C.L. and ManNee, W. (2002). Deposition and effects of fine and ultrafine particles in the respiratory tract. *Eur. Respir. Monogr.* 21: 77–92.

Duarte, R.M.B.O., Mieiro, C.L., Penetra, A., Pio, C.A. and Duarte, A.C. (2008). Carbonaceous materials in size-segregated atmospheric aerosols from urban and coastal-rural areas at the Western European Coast. *Atmos. Res.* 90: 253–263.

Elminir, H.K. (2005). Dependence of urban air pollutants on meteorology. *Sci. Total Environ.* 350: 225–237.

Erdinger L., Dürr M. and Höpker KA. (2005). Correlations between mutagenic activity of organic extractions of airborne particulate matter, NO_x, and sulphur dioxide in Southern Germany. *Environ. Sci. Pollut. Res.* 12(1): 10–20.

European Environment Agency (EEA). *Criteria for EUROAIRNET*. Technical Report n. 12, February 1999. Available on-line: http://www.eea.europa.eu/publications/TEC12.

Fang, G.-C., Wu, Y.-S., Wen, C.-C., Lin, C.-K., Huang, S.-H., Rau, J.-Y. and Lin, C.-P. (2005). Concentrations of nano and related ambient air pollutants at a traffic sampling site. *Toxicol. Ind. Health* 21: 259–271.

Fang, G.-C., Kuo, Y.-C., Zhuang, Y.-J. and Chen, Y.-C. (2014). Diurnal concentrations variations, size distributions for ambient air particles and metallic pollutants (Cr, Mn, Ni, Cd, Pb) during summer season at a traffic area. *Environ. Monit. Assess.* 186: 4139–4151.

Fujitani, Y., Hasegawa, S., Fushimi, A., Kondo, Y., Tanabe, K., Kobayashi, S. and Kobayashi, T. (2006). Collection characteristics of low-pressure impactors with various impaction substrate materials. *Atmos. Environ.* 40: 3221–3229.

Gerasopoulos, E., Kouvarakis, G., Babasakalis, P., Vrekoussis, M., Putaud, J.P. and Mihalopoulos, N. (2006). Origin and variability of particulate matter (PM_{10}) mass concentrations over the Eastern Mediterranean. *Atmos. Environ.* 40: 4679–4690.

Gnauk, T., Müller, K., Pinxteren, D., He, L.Y., Niu, Y.W., Hu, M. and Herrmann, H. (2008). Size-segregated particulate chemical composition in Xinken, Pearl River Delta, China: OC/EC and organic compounds. *Atmos. Environ.* 42: 6296–6309.

Gugamsetty, B., Wei, H., Liu, C.-N., Awasthi, A., Hsu, S.-C., Tsai, Roam, G.-D., Wu, Y.-C. and Chen, C.-F. (2012). Source characterization and apportionment of PM_{10}, $PM_{2.5}$ and $PM_{0.1}$ by using positive matrix factorization. *Aerosol Air Qual. Res.* 12: 476–491.

Heyder, J., Gebhart, J., Rudolf, G., Schiller, C.F. and Stahlhofen, W. (1986). Deposition of particles in the human respiratory tract in the size range 0.005–15 μm. *J. Aerosol Sci.* 17(5): 811–825.

Horvath, H., Kasahara, M. and Pesava, P. (1996). The size distribution and composition of the atmospheric aerosol at a rural and nearby urban location. *J. Aerosol Sci.* 27: 417–435.

Hughes, L.S., Cass, G.R., Gone, J., Ames, M. and Olmez, I. (1998). Physical and chemical characterization of atmospheric ultrafine particles in the Los Angeles area. *Environ. Sci. Technol.* 32(9): 1153–1161.

Ibald-Mulli, A., Wichmann, H.E., Kreyling, W. and Peters, A. (2002). Epidemiological evidence on health effects of ultrafine particles. *Journal of Aerosol Medicine* 15(2): 189–201.

INEMAR (INventario EMissioni ARia – Regione Lombardia) (2012), available on-line: http://www.inemar.eu/xwiki/bin/view/InemarDatiWeb/Como.

Karakoti, A.S., Hench, L.L. and Seal, S. (2006). The potential toxicity of nanomaterials – The role of surfaces. *JOM – Journal of the Minerals Metals and Materials Society* 58: 77–82.

Kim, K.-H., Kim, D.-S. and Lee, T.-J. (1997). The temporal variabilities in the concentrations of airborne lead and its relationship to aerosol behavior. *Atmos. Environ.* 31: 3449–3458.

Knibbs, L.D. and Morawska, L. (2012). Traffic-related fine and ultrafine particle exposures of professional drivers and illness: an opportunity to better link exposure science and epidemiology to address an occupational hazard? *Environ. Int.* 49: 110–114.

Lin, C.-C., Chen, S.-J., Huang, K.-L., Hwang, W.-I., Chang-Chien, G.-P. and Lin, W.-Y. (2005). Characteristics of metals in nano/ultrafine/fine/coarse particles collected beside a heavily trafficked road. *Environ. Sci. Technol.* 39: 8113–8122.

Lippmann, M., Yeates, D.B. and Albert, R.E. (1980). Deposition, retention and clearance of inhaled particles. *Brit. J. Ind. Med.* 37: 337–362.

Liu, X., Zhai, Y., Zhu, Y., Liu, Y., Chen, H., Li, P., Peng, C., Xu, B., Li, C. and Zeng, G. (2015). Mass concentration and health risk assessment of heavy metals in size-segregated airborne particulate matter in Changsha. *Sci. Total Environ.* 517: 215–221.

Malandrino, M., Casazza, M., Abollino, O., Minero, C. and Maurino, V. (2016). Size-resolved metal distribution in the PM matter of the city of Turin (Italy). *Chemosphere* 147: 477–489.

Marple, V., Rubow, K.L., Turner, W. and Spengler, J.D. (1987). Low flow rate sharp cut impactors for indoor sampling: design and calibration. *J. Air Poll. Control Assoc.* 37: 1303–1307.

Mbengue, S., Alleman, L. Y. and Flament, P. (2014). Size-distributed metallic elements in submicronic and ultrafine atmospheric particles from urban and industrial areas in Northern France. *Atmos. Res.* 135: 35–47.

Nilsson, E.D. and Kulmala, M. (1998). The potential for atmospheric mixing processes to enhance the binary nucleation rate. *J. Geophys. Res.-Atmos.* 103(D1): 1381–1389.

Ning, Z., Geller, M.D., Moore, K.F., Sheesley, R., Schauer, J.J. and Sioutas, C. (2007). Daily variation in chemical characteristics of urban ultrafine aerosols and inference of their sources. *Environ. Sci. Technol.* 41: 6000–6006.

Ntziachristos, L., Ning, Z., Geller, M.D., Sheesley, R.J., Schauer, J.J. and Sioutas, C. (2007). Fine, ultrafine and nanoparticle trace element compositions near a major freeway with a high heavy-duty diesel fraction. *Atmos. Environ.* 41: 5684–5696.

Oberdörster, G., Oberdörster, E. and Obertörster, J. (2005). Nanotoxicology: an emerging discipline evolving from studies of ultrafine particles. *Environ. Health Persp.* 113: 823–839.

Ostro, B., Hu, J., Goldberg, D., Reynolds, P., Hertz, A., Bernstein, L. and Kleeman, M.J. (2015). Associations of mortality with long-term exposures to fine and ultrafine particles,

species and sources: results from the California teachers study cohort. *Environ. Health Persp.* (Online) 123(6): 549.

Pakkanen, T.A., Kerminen, V.-M., Korhonen, C.H., Hillamo, R.E., Aarnio, P., Koskentalo, T. and Maenhaut, W. (2001). Urban and rural ultrafine ($PM_{0.1}$) particles in the Helsinki area. *Atmos. Environ.* 35: 4593–4607.

Putaud, J.-P., Raes, F., Van Dingenen, R., Brüggemenn, E., Facchini, M.C., Decesari, S., Fuzzi, S., Gehrig, H.C., Laj, P., Lorbeer, G., Maenhaut, W., Mihalopoulos, N., Müller, K., Querol, X., Rodriguez, S., Schnider, J., Spindler, G., Ten Brink, H., Tørseth, K. and Wiedensohler, A. (2004). A European aerosol phenomenology-2: chemical characteristics of particulate matter at kerbside, urban, rural and background sites in Europe. *Atmos. Environ.* 38: 2579–2595.

Quan, J., Gao, Y., Zhang, Q., Tie, X., Cao, J., Han, S., Meng, J., Chen, P. and Zhao, D. (2013). Evolution of planetary boundary layer under different weather conditions, and its impact on aerosol concentrations. *Particuology* 11(1): 34–40.

Querol, X., Alastuey, A., Rodriguez, S., Viana, M.M., Artinano, B., Salvador, P., Mantilla, E., Santos, S.G.d., Patier, R.F., Rosa, J.D.L., Campa, A.S.d.l., Menendez, M. and Gil, J.J. (2004). Levels of particulate matter in rural, urban and industrial sites in Spain. *Sci. Total Environ.* 334-335: 359–376.

Raaschou-Nielsen, O. *et al.* (2016). Particulate matter air pollution components and risk for lung cancer. *Environ. Int.* 87: 66–73.

Ramgolam, K., Chevaillier, S., Marano, F., Baeza-Squiban, A. and Martinon, L. (2008). Proinflammatory effect of fine and ultrafine particulate matter using size-resolved urban aerosol from Paris. *Chemosphere* 72: 1340–1346.

Sardar, S.B., Fine, P.M., Mayo, P.R. and Sioutas, C. (2005). Size-fractionated measurements of ambient ultrafine particle chemical composition in Los Angeles using the NanoMOUDI. *Environ. Sci. Technol.* 39: 932–944.

Schwarz, J., Štefancová, L., Maenhaut, W., Smolík, J. and Ždímal, V. (2012). Mass and chemically speciated size distribution of Prague aerosol using an aerosol dryer – The influence of air mass origin. *Sci. Total Environ.* 437: 348–362.

Schwarze, P.E., Øvrevik, J., Lãg, M., Refsnes, M., Nafstad, P., Hetland, R.B. and Dybing, E. (2006). Particulate matter properties and health effects: consistency of epidemiological and toxicological studies. *Hum. Exp. Toxicol.* 25: 559–579.

Spinazzè, A., Cattaneo, A., Scocca, D.R., Bonzini, M. and Cavallo, D.M. (2015). Multi-metric measurement of personal exposure to ultrafine particles in selected urban microenvironments. *Atmos. Environ.* 110: 8–17.

Stafoggia, M., Samoli, E., Alessandrini, E., Cadum, E., Ostro, B., Berti, G., Faustini, A., Jacquemin, B., Linares, C., Pascal, M., Randi, G., Ranzi, A., Stivanello, E., Forastiere, F. and the MED-PARTICLES Study Group. (2013). Short-term associations between fine and coarse particulate matter and hospitalizations in Southern Europe: results from the MED-PARTICLES Project. *Environ. Health Perspect.* 121: 1026–1033.

Tecer, L.H., Süren, P., Alagha, O., Karaca, F. and Tuncel G. (2008). Effect of meteorological parameters on fine and coarse particulate matter mass concentration in a coal-mining area in Zonguldak, Turkey. *J. Air Waste Manage.* 58(4): 543–552.

Tuch, Th., Brand, P., Wichmann, H. E. and Heyder, J. (1997). Variation of particle number and mass concentration in various size ranges of ambient aerosols in Eastern Germany. *Atmos. Environ.* 31(24): 4193–4197.

UNI EN 14907: 2005. Ambient air quality – Standard gravimetric measurement method for the determination of the $PM_{2.5}$ mass fraction of suspended particulate matter.

UNI EN 12341: 2014. Air Quality – Determination of the PM_{10} fraction of suspended particulate matter. Reference method and field test procedure to demonstrate reference equivalence of measurements methods.

Vecchi, R., Marcazzan, G., Valli, G., Ceriani, M. and Antoniazzi, C. (2004). The role of atmospheric dispersion in the seasonal variation of PM_1 and $PM_{2.5}$ concentration and composition in the urban area of Milan (Italy). *Atmos. Environ.* 38: 4437–4446.

Velasco, E., Márquez, C., Bueno, E., Bernabè, R.M., Sánchez, A., Fentanes, O., Wöhrnschimmel, H., Cárdenas, B., Kamilla, A., Wakamatsu, S. and Molina, L.T. (2008). Vertical distribution of ozone and VOCs in the low boundary layer of Mexico City. *Atmos. Chem. Phys.* 8: 3061–3079.

Watson, J.G., Chow, J.C., Moosmuller, H., Green, M., Frank, N. and Pitchford, M. (1998). Guidance for using continuous monitors in $PM_{2.5}$ monitoring networks. U.S. Environ. Prot. Agency, Off Air Qual Plann Stand, [Tech. Rep.] EPA, ii-xv, 1.

WHO. (2006). Air Quality Guidelines: Global Update 2005. Particulate Matter, Ozone, Nitrogen Dioxide and Sulfur Dioxide. World Health Organization.

Yanosky, J.D. and Maclntosh, D.L. (2001). A comparison of four gravimetric fine particle sampling methods. *J. Air & Waste Manage. Assoc.* 51: 878–884.

Ye, B., Ji, X., Yang, H., Yao, X., Chan, C.K., Cadle, S. H., Chan, T. and Mulawa, P.A. (2003). Concentration and chemical composition of $PM_{2.5}$ in Shanghai for a 1-year period. *Atmos. Environ.* 37: 499–510.

Zhao, X., Zhang, X., Xu, X., Xu, J., Meng, W. and Pu, W. (2009). Seasonal and diurnal variations of ambient $PM_{2.5}$ concentration in urban and rural environments in Beijing. *Atmos. Environ.* 43: 2893–2900.

This chapter is based on:

- **Rovelli, S.**, Cattaneo, A., Borghi, F., Spinazzè, A., Campagnolo, D., Limbeck, A. and Cavallo, D.M. Mass Concentration and Size-Distribution of Atmospheric Particulate Matter in an Urban Environment. *Aerosol Air Qual. Res.* doi: 10.4209/aaqr.2016.08.0344, available online at: http://aaqr.org/Articles_In_Press.php.

- **Rovelli, S.**, Cattaneo, A., Borghi, F., Cavallo, D.M. Mass concentration and size-distribution of atmospheric fine, ultrafine and nanoparticles in the urban area of Como, Northern Italy. In: Conference Proceedings of the 2nd International Conference on Atmospheric Dust, Castellaneta Marina (TA), Italy, June 12th-17th, 2016, Vol. 5: p. 134, ISSN 2464-9147.

- **Rovelli, S.**, Borghi, F., Cattaneo, A., Cavallo, D.M., Campagnolo, D., Del Buono, L., Spinazzè, A. Analisi del particolato fine e ultrafine nell'area urbana di Como. In: Conference Proceedings of the 33rd AIDII National Conference, Lucca (Italy), June 16th-17th, 2016, pp. 326-332.

Tables

Table 1. Minimum distances from emission sources for URB station (EEA, February 1999)

Type	Distance	Comments
Traffic	>50 m	Not more than 2500 vehicles per day within a radius of 50 m
Industrial point sources	-	Expert judgement, depending on emission characteristics and prevailing wind direction, direct influence should be avoided
Small scale domestic heating with coal, fuel oil or wood, small boiler houses	>50 m	Should be avoided as much as possible

Table 2. Sampling information and weekly weather conditions at the URB site in Como, from May 2015 to March 2016.

Sample No.	Sampling period (mm/dd/yy–mm/dd/yy)	T (°C) Mean (Min.–Max.)[a]	RH (%) Mean (Min.–Max.)[a]	WS (m s^{-1}) Mean (Min.–Max.)[a]	Prevalent WD[b]	AtP (hPa) Mean (Min.–Max.)[a]	PBL (m) Mean (Min.–Max.)[a]	Cumulative rainfall (mm)[c]
				Non-heating season				
1	05/25/15–05/29/15	18.9 (11.6–26.1)*	66.1 (26.8–99.4)*	n.a.	n.a.	n.a.	608 (87–2088)	0.4
2	05/29/15–06/02/15	20.7 (14.3–30.1)*	79.5 (38.7–99.4)*	n.a.	n.a.	n.a.	434 (87–1782)	5.8
3	06/08/15–06/12/15	22.7 (17.0–30.9)*	73.2 (44.9–99.4)*	n.a.	n.a.	n.a.	589 (87–2241)	9.0
4	06/15/15–06/19/15	20.9 (15.6–28.6)*	84.9 (49.5–99.4)*	n.a.	n.a.	n.a.	451 (87–1310)	16.0
5	06/22/15–06/26/15	22.1 (14.6–28.7)*	65.2 (26.9–99.4)*	n.a.	n.a.	n.a.	686 (87–2500)	0.0
6	07/27/15–07/31/15	24.8 (18.6–31.0)*	75.8 (47.6–99.4)*	n.a.	n.a.	n.a.	676 (87–1694)	14.2
7	08/03/15–08/07/15	27.4 (21.4–37.2)	58.4 (26.6–82.1)	0.50 (0.20–1.03)	S/ESE	1005.2 (1003.5–1006.8)	708 (87–2098)	0.0
8	08/10/15–08/14/15	26.7 (18.4–36.6)	53.5 (21.4–86.3)	0.59 (0.19–1.34)	SE/SW	1004.2 (1005.0–1007.5)	754 (87–2500)	0.0
9	08/17/15–08/21/15	21.7 (14.5–30.4)	66.3 (30.5–94.0)	0.54 (0.05–1.23)	S	1003.6 (996.4–1011.3)	587 (87–2201)	11.2
10	08/24/15–08/28/15	21.7 (16.3–31.7)	74.6 (34.2–95.2)	0.49 (0.03–1.39)	S/SSE	1005.8 (1001.3–1009.5)	427 (87–1680)	33.6
11	08/31/15–09/04/15	22.5 (14.5–34.5)	66.6 (27.5–93.4)	0.52 (0.12–1.25)	SE/SW	1002.1 (999.3–1007.7)	553 (87–2280)	9.4
12	09/07/15–09/11/15	18.5 (11.1–26.1)	60.3 (28.1–89.5)	0.44 (0.02–1.26)	S/SSE	1007.7 (1004.4–1011.8)	572 (87–1498)	0.6
13	09/14/15–09/18/15	19.0 (16.1–26.0)	84.1 (41.2–95.2)	0.37 (0.01–1.91)	SE	999.4 (995.6–1003.7)	192 (87–1055)	11.4
14	09/21/15–09/25/15	15.3 (6.6–26.5)	73.0 (29.7–96.4)	0.65 (0.02–4.73)	SSE	1000.3 (991.6–1006.1)	357 (87–1245)	63.2
15	09/28/15–10/02/15	14.8 (8.8–21.1)	62.1 (35.3–85.8)	0.43 (0.01–1.29)	SE/SSW	1015.4 (1013.1–1017.4)	480 (87–1564)	0.0
16	10/05/15–10/09/15	17.1 (12.4–26.0)	81.2 (46.7–96.5)	0.28 (0.01–1.03)	S/SSE	n.a.	220 (87–724)	5.4
17	10/12/15–10/16/15	13.3 (6.6–23.3)	87.7 (46.0–97.2)	0.34 (0.01–0.94)	SE	999.3 (995.0–1004.4)	246 (87–909)	67.8

n.a.: data not available; *: data from the Regional Agency for Prevention and Environment of Lombardy; [a]: average, minimum and maximum values of hourly data for each 5-d monitoring session; [b]: prevalent WD during each 5-d monitoring session; [c]: cumulative rainfall during each 5-d monitoring session.

Table 2 (continues). Sampling information and weekly weather conditions at the URB site in Como, from May 2015 to March 2016.

Sample No.	Sampling period (mm/dd/yy–mm/dd/yy)	T (°C) Mean (Min.–Max.)[a]	RH (%) Mean (Min.–Max.)[a]	WS (m s^{-1}) Mean (Min.–Max.)[a]	Prevalent WD[b]	AtP (hPa) Mean (Min.–Max.)[a]	PBL (m) Mean (Min.–Max.)[a]	Cumulative rainfall (mm)[c]
				Heating season				
18	10/19/15–10/23/15	10.7 (4.5–20.8)	79.6 (39.5–97.7)	0.27 (0.02–1.05)	S	1005.5 (1001.1–1011.0)	299 (87–1010)	0.2
19	10/26/15–10/30/15	12.2 (5.8–22.7)	85.7 (32.9–97.7)	0.20 (0.00–0.84)	SE	1008.1 (1001.9–1013.9)	179 (87–672)	31.0
20	11/02/15–11/06/15	11.5 (4.1–21.6)	80.9 (40.8–98.1)	0.17 (0.00–0.74)	SSE	1014.3 (1008.9–1021.7)	140 (87–372)	0.0
21	11/09/15–11/13/15	11.7 (5.6–24.1)	82.9 (37.6–98.0)	0.17 (0.00–0.88)	S	1014.2 (1011.3–1017.4)	116 (87–222)	0.0
22	11/16/15–11/20/15	9.1 (5.0–16.8)	88.4 (59.2–97.8)	0.38 (0.05–1.23)	SSE	1010.0 (1006.1–1013.1)	134 (87–508)	0.0
23	11/23/15–11/27/15	4.2 (–2.1–15.1)	67.1 (14.4–97.1)	0.51 (0.00–2.81)	SSE	1003.7 (994.4–1014.3)	239 (87–621)	0.0
24	11/30/15–12/04/15	4.7 (–0.7–15.3)	83.5 (33.6–98.2)	0.18 (0.02–0.76)	SE	1017.3 (1011.8–1022.6)	109 (87–238)	0.0
25	12/09/15–12/11/15	4.6 (0.9–10.8)*	93.7 (52.7–99.5)*	n.a.	n.a.	n.a.	154 (87–340)	0.0
26	12/14/15–12/18/15	4.8 (0.1–15.0)	85.1 (48.0–98.3)	0.14 (0.01–0.52)	SSE	1017.6 (1013.4–1020.8)	90 (87–148)	0.0
27	12/21/15–12/23/15	7.2 (4.2–12.6)	83.7 (56.2–96.7)	0.19 (0.02–0.58)	SE	1022.3 (1019.4–1025.0)	96 (87–157)	0.0
28	01/11/16–01/15/16	4.2 (–2.2–14.2)	78.6 (22.6–98.9)	0.42 (0.05–1.61)	SSE/SW	997.6 (983.0–1006.8)	207 (87–679)	5.8
29	01/18/16–01/22/16	–0.9 (–5.6–8.4)	60.3 (18.5–94.0)	0.25 (0.02–1.29)	SSE	1010.1 (1004.5–1022.2)	169 (87–915)	0.0
30	01/25/16–01/29/16	7.0 (2.2–13.2)*	93.3 (62.8–99.5)*	n.a.	n.a.	n.a.	127 (87–538)	0.0
31	02/01/16–02/05/16	8.4 (0.6–16.8)	66.2 (12.2–95.2)	n.a.	SSE	1011.1 (1000.6–1016.3)	215 (87–964)	16.2
32	02/08/16–02/12/16	6.4 (3.6–10.9)*	72.1 (28.8–99.5)*	n.a.	n.a.	n.a.	248 (87–890)	23.8
33	02/15/16–02/19/16	6.5 (3.1–11.0)*	98.3 (70.3–99.5)*	n.a.	n.a.	n.a.	234 (87–884)	10.2
34	02/29/16–03/04/16	9.8 (2.1–19.6)	50.0 (14.0–96.7)	0.83 (0.02–2.35)	S	994.8 (985.2–1002.7)	327 (87–1384)	15.6
35	03/07/16–03/11/16	6.6 (–1.3–17.5)	64.4 (15.6–94.8)	0.44 (0.02–1.50)	SSE	998.4 (989.5–1006.3)	376 (87–1260)	0.0
36	03/14/16–03/18/16	7.8 (1.2–16.6)	66.6 (30.6–93.2)	0.53 (0.02–1.98)	SE	1010.4 (1000.4–1016.8)	349 (87–1402)	13.4
37	03/21/16–03/25/16	11.9 (1.8–20.7)	54.6 (15.4–91.3)	0.63 (0.01–2.23)	SW	996.4 (986.7–1006.0)	438 (87–2127)	0.0
38	03/29/16–04/01/16	14.1 (11.4–20.4)	73.9 (37.9–92.1)	0.37 (0.02–1.31)	SSE	1005.5 (1002.4–1008.4)	235 (87–1126)	1.8

n.a.: data not available; *: data from the Regional Agency for Prevention and Environment of Lombardy; [a]: average, minimum and maximum values of hourly data for each 5-d monitoring session; [b]: prevalent WD during each 5-d monitoring session; [c]: cumulative rainfall during each 5-d monitoring session.

Table 3. Descriptive statistics on mass concentrations (µg m^{-3}) for the 12 DLPI-size ranges and for the principal PM fractions during the non-heating season (May 2015–October 15th 2015), the heating season (October 19th 2015–March 2016) and the whole campaign.

DLPI collection plate	***Non-heating season (n = 17)***	***Heating season (n = 21)***	***Total data (n = 38)***	***Ratio[b]***
(particle size range [µm])	***Mean ± SD[a] (Median; Min.–Max.)***	***Mean ± SD[a] (Median; Min.–Max.)***	***Mean ± SD[a] (Median; Min.–Max.)***	
1 (0.0283– 0.559)	0.2 ± 0.1 (0.2; 0.1–0.3)	0.2 ± 0.2 (0.2; 0.1–1.2)	0.2 ± 0.2 (0.2; 0.1–1.2)	1.2
2 (0.0559– 0.944)	0.4 ± 0.1 (0.4; 0.3–0.6)	0.6 ± 0.2 (0.6; 0.2–1.0)	0.5 ± 0.2 (0.4; 0.2–1.0)	1.6[c]
3 (0.0944–0.157)	0.7 ± 0.2 (0.7; 0.5–1.2)	1.4 ± 0.5 (1.4; 0.7–2.0)	1.1 ± 0.5 (0.9; 0.5–2.0)	1.9[c]
4 (0.157–0.262)	1.3 ± 0.4 (1.2; 0.6–2.3)	3.9 ± 1.7 (3.8; 1.2–6.8)	2.8 ± 1.8 (2.2; 0.6–6.8)	3.1[c]
5 (0.262–0.383)	2.0 ± 0.8 (2.1; 0.7–3.7)	6.3 ± 3.1 (5.7; 1.6–11.7)	4.4 ± 3.2 (3.4; 0.7–11.7)	3.1[c]
6 (0.383–0.614)	3.0 ± 1.5 (2.6; 0.6–5.6)	10.2 ± 5.6 (8.8; 2.5–24.3)	7.0 ± 5.6 (5.3; 0.6–24.3)	3.4[c]
7 (0.614–0.950)	1.2 ± 0.7 (1.0; 0.4–3.4)	5.1 ± 3.4 (4.0; 0.9–14.3)	3.3 ± 3.2 (2.3; 0.4–14.3)	4.2[c]
8 (0.950–1.60)	0.8 ± 0.4 (0.7; 0.3–1.9)	2.6 ± 1.8 (2.1; 0.5–7.2)	1.8 ± 1.6 (1.1; 0.3–7.2)	3.3[c]
9 (1.60–2.40)	1.0 ± 0.3 (0.9; 0.6–1.6)	1.5 ± 0.7 (1.5; 0.7–2.8)	1.3 ± 0.6 (1.0; 0.6–2.8)	1.6[c]
10 (2.40–4.00)	1.9 ± 0.6 (1.8; 1.1–3.1)	2.2 ± 0.8 (2.1; 1.0–3.6)	2.0 ± 0.7 (2.0; 1.0–3.6)	1.2
11 (4.00–6.60)	1.5 ± 0.3 (1.4; 1.1–2.5)	1.6 ± 0.5 (1.6; 0.7–2.3)	1.6 ± 0.5 (1.6; 0.7–2.5)	1.1
12 (6.60–9.97)	1.5 ± 0.4 (1.5; 0.9–2.4)	1.8 ± 0.5 (1.9; 0.9–2.4)	1.7 ± 0.5 (1.6; 0.9–2.4)	1.2
Particle size fraction				
$PM_{0.028–0.1}$	0.6 ± 0.1 (0.5; 0.3–0.8)	0.8 ± 0.4 (0.7; 0.2–2.1)	0.7 ± 0.3 (0.6; 0.2–2.1)	1.5[c]
$PM_{0.1–1}$	8.3 ± 3.1 (7.7; 3.0–14.2)	27.0 ± 13.3 (22.4; 7.3–56.1)	18.6 ± 13.7 (14.3; 3.0–56.1)	3.3[c]
PM_1	8.8 ± 3.2 (8.5; 3.5–14.9)	27.8 ± 13.6 (23.2; 7.8–57.3)	19.3 ± 14.0 (14.9; 3.5–57.3)	3.2[c]
$PM_{1–2.5}$	1.8 ± 0.5 (1.5; 0.9–3.0)	4.1 ± 2.4 (3.6; 1.2–10.0)	3.1 ± 2.2 (2.2; 0.9–10.0)	2.4[c]
$PM_{2.5}$	10.6 ± 3.4 (10.2; 5.0–16.9)	31.9 ± 15.7 (26.4; 9.0–67.3)	22.4 ± 15.9 (16.8; 5.0–67.3)	3.0[c]
$PM_{2.5–10}$	4.9 ± 1.1 (4.8; 3.4–8.0)	5.6 ± 1.7 (5.6; 2.7–8.2)	5.3 ± 1.5 (5.1; 2.7–8.2)	1.1
PM_{10}	15.5 ± 3.7 (15.5; 8.4–21.4)	37.5 ± 17.0 (31.2; 12.4–75.5)	27.6 ± 16.9 (21.1; 8.4–75.5)	2.4[c]

[a]: standard deviation

[b]: ratio between the heating and the non-heating average levels

[c]: significant difference ($p < 0.01$) in heating vs non-heating levels by Independent-Samples *t*-test on *log*-normal parameters

Table 4. Correlation analysis between PM fractions. Pearson correlation coefficients (r) and levels of significance (*p*) are shown.

DLPI Stage (µm)		***1 (0.0283–0.0559)***	***2 (0.0559–0.0944)***	***3 (0.0944–0.157)***	***4 (0.157–0.262)***	***5 (0.262–0.383)***	***6 (0.383–0.614)***	***7 (0.614–0.950)***	***8 (0.950–1.60)***	***9 (1.60–2.40)***	***10 (2.40–4.00)***	***11 (4.00–6.60)***
2 (0.0559–0.0944)	r	.386*										
	p	.018										
3 (0.0944–0.157)	r	.323	.925**									
	p	.051	.000									
4 (0.157–0.262)	r	.199	.874**	.956**								
	p	.239	.000	.000								
5 (0.262–0.383)	r	.283	.831**	.930**	.966**							
	p	.089	.000	.000	.000							
6 (0.383–0.614)	r	.268	.748**	.839**	.885**	.942**						
	p	.109	.000	.000	.000	.000						
7 (0.614–0.950)	r	.208	.647**	.731**	.785**	.847**	.959**					
	p	.216	.000	.000	.000	.000	.000					
8 (0.950–1.60)	r	.179	.602**	.677**	.736**	.785**	.906**	.979**				
	p	.288	.000	.000	.000	.000	.000	.000				
9 (1.60–2.40)	r	.140	.533**	.572**	.644**	.691**	.787**	.839**	.887**			
	p	.407	.001	.000	.000	.000	.000	.000	.000			
10 (2.40–4.00)	r	.179	.504**	.463**	.472**	.529**	.591**	.594**	.626**	.843**		
	p	.290	.001	.003	.003	.001	.000	.000	.000	.000		
11 (4.00–6.60)	r	.283	.459**	.408*	.403*	.476**	.504**	.485**	.508**	.724**	.905**	
	p	.089	.004	.011	.012	.002	.001	.002	.001	.000	.000	
12 (6.60–9.97)	r	.392*	.469**	.494**	.501**	.588**	.586**	.533**	.527**	.663**	.682**	.810**
	p	.016	.003	.002	.001	.000	.000	.001	.001	.000	.000	.000

*: correlation is significant at the 0.05 level

**: correlation is significant at the 0.01 level

Table 5. Correlation analysis between PM fractions and meteorological parameters monitored at the URB site. Pearson correlation coefficients (r) and levels of significance (*p*) are shown.

DLPI stage (μm) or PM fraction		***Rainfall***	***PBL***	***T***	***RH***	***WS***	***AtP***
1 (0.0283–0.0559)	r	–.360*	.090	–.091	–.116	–.120	.226
	p	.029	.598	.626	.534	.552	.257
2 (0.0559–0.0944)	r	–.443**	–.710**	–.452**	.414*	–.709**	.679**
	p	.005	.000	.009	.018	.000	.000
3 (0.0944–0.157)	r	–.551**	–.730**	–.535**	.362*	–.680**	.685**
	p	.000	.000	.002	.042	.000	.000
4 (0.157–0.262)	r	–.538**	–.798**	–.548**	.426*	–.675**	.664**
	p	.000	.000	.001	.015	.000	.000
5 (0.262–0.383)	r	–.575**	–.742**	–.565**	.362*	–.628**	.636**
	p	.000	.000	.001	.042	.000	.000
6 (0.383–0.614)	r	–.514**	–.727**	–.519**	.367*	–.593**	.547**
	p	.001	.000	.002	.039	.001	.003
7 (0.614–0.950)	r	–.444**	–.773**	–.482**	.419*	–.588**	.498**
	p	.005	.000	.005	.017	.001	.008
8 (0.950–1.60)	r	–.411*	–.761**	–.391*	.433*	–.621**	.559**
	P	.010	.000	.027	.013	.001	.002
9 (1.60–2.40)	r	–.401*	–.649**	–.228	.363*	–.523**	.543**
	p	.013	.000	.210	.041	.005	.003
10 (2.40–4.00)	r	–.313	–.524**	–.136	.379*	–.629**	.535**
	p	.055	.001	.456	.032	.000	.004
11 (4.00–6.60)	r	–.431**	–.327*	–.112	.198	–.587**	.461*
	p	.007	.045	.541	.277	.001	.016
12 (6.60–9.97)	r	–.634**	–.238	–.312	-.074	–.253	.457*
	p	.000	.149	.082	.687	.203	.017
$PM_{0.03–0.1}$	r	–.460**	–.546**	–.379*	.358*	–.617**	.631**
	p	.004	.000	.032	.044	.001	.000
$PM_{0.1–1}$	r	–.530**	–.760**	–.532**	.384*	–.621**	.581**
	p	.001	.000	.002	.030	.001	.001
PM_1	r	–.534**	–.761**	–.533**	.384*	–.623**	.587**
	p	.001	.000	.002	.030	.001	.001
$PM_{1–2.5}$	r	–.415**	–.742**	–.348	.422*	–.613**	.568**
	p	.010	.000	.051	.016	.001	.002
$PM_{2.5}$	r	–.525**	–.773**	–.520**	.399*	–.636**	.593**
	p	.001	.000	.002	.024	.000	.001
$PM_{2.5–10}$	r	–.478**	–.403*	–.178	.199	–.554**	.526**
	p	.002	.012	.331	.276	.003	.005
PM_{10}	r	–.547**	–.768**	–.502**	.400*	–.656**	.614**
	p	.000	.000	.003	.023	.000	.001

*: correlation is significant at the 0.05 level

**: correlation is significant at the 0.01 level

Table 6. Summary of the regression model results, segregated for each DLPI size range. Results show the standardized coefficients for the independent variables that were found to be statistically significant in each model, with the standardized Beta, 95% confidence interval - upper and lower bounds - (95% C.I.) and *p* value. The last two rows provide an overview of the linear regression model for each dependent variable, presenting the R squared value (r^2), the standard error (Std. error) and the *p* value. Only the regression model with statistically significant independent variables are shown.

Dependent variable (n = 25)	Stage 3 (0.0944–0.157 µm)				Stage 4 (0.157–0.262 µm)				Stage 5 (0.262–0.383 µm)				Stage 6 (0.383–0.614 µm)			
Independent variables	Beta	95% C.I.		*p*	Beta	95% C.I.		*p*	Beta	95% C.I.		*p*	Beta	95% C.I.		*p*
		Lower	Upper			Lower	Upper			Lower				Lower	Upper	
PBL	–0.584	–0.412	–0.004	0.046	–0.702	–0.893	–0.150	0.009	–0.586	–0.997	–0.667	0.032	–0.667	–1.473	0.019	0.040
Rainfall					–0.314	–0.177	–0.022	0.014	–0.382	–0.245		0.006				
Temperature									–0.355	–0.346		0.019				
Regression model statistics	r^2	Std. error		*p*	r^2	Std. error		*p*	r^2	Std. error		*p*	r^2	Std. error		*p*
	0.795	0.051		0.000	0.845	0.093		0.000	0.827	0.118		0.000	0.709	0.187		0.001

Dependent variable (n = 25)	Stage 7 (0.614–0.950 µm)				Stage 9 (1.60–2.40 µm)				Stage 12 (6.60–9.97 µm)			
Independent variables	Beta	95% C.I.		*p*	Beta	95% C.I.		*p*	Beta	95% C.I.		*p*
		Lower	Upper			Lower	Upper			Lower	Upper	
PBL	–0.772	–1.489	–0.102	0.027	–0.623	–0.445	–0.040	0.021				
Rainfall	–0.316	–0.284	0.005	0.058					–0.533	–0.099	–0.021	0.004
Regression model statistics	r^2	Std. error		*p*	r^2	Std. error		*p*	r^2	Std. error		*p*
	0.718	0.174		0.001	0.559	0.078		0.004	0.451	0.054		0.001

Table 7. PM mass concentrations for research studies citied in the paragraph: *Comparison of Ambient PM Concentrations with Literature Data.*

Reference	*Location*	*Sampling period*	*Sampling site*	*Concentration (μg m^{-3}) – [Mean ± SD[a]] or [Min–Max]*			
				PM_{10}	*$PM_{2.5}$*	*PM_{1}*	*UFPs or QUFPs[b]*
This study	Como (Italy)	Non-heating	Urban background	15.5 ± 3.7	10.6 ± 3.4	8.8 ± 3.2	0.6 ± 0.1 ($PM_{0.028–0.1}$)
		Heating		37.5 ± 17.0	31.9 ± 15.7	27.8 ± 13.6	0.8 ± 0.4 ($PM_{0.028–0.1}$)
		Total data		27.7 ± 16.9	22.4 ± 15.9	19.3 ± 14.0	0.7 ± 0.3 ($PM_{0.028–0.1}$)
Cass et al. (2000)	California (USA)	Different periods	Different sites				0.55–1.16 ($PM_{0.06–0.1}$)
Chen et al. (2013)	East Asia	Summer-fall	Rural background	5.5 ± 2.7	4.1 ± 2.1		0.1 ± 0.1 ($PM_{0.1}$)
Duarte et al. (2008)	Portugal	Summer	Urban	46.0 ± 19.4			
			Coastal-rural	24.7 ± 3.8			
Gnauk et al. (2008)	China	Fall	Rural/coastal background	89.3			
Gugamsetty et al. (2012)	New Taipei City (Taiwan)	Summer-fall	Urban	39.5 ± 11.6	21.8 ± 7.5		1.4 ± 0.6 ($PM_{0.1}$)
Hughes et al. (1998)	Pasadena (CA-USA)	Winter	Urban		20.2 ± 5.4 ($PM_{1.8}$)		0.80–1.58 ($PM_{0.017–0.1}$)
Lin et al. (2005)	Taiwan	Winter-spring	Traffic	191.0 ± 53.0	140.0 ± 41.0		31.0 ± 19.0 ($PM_{0.1}$)
Liu et al. (2015)	Changsha (China)	Spring	Urban-traffic	184.4 ± 76.9 (PM_{9})	136.5 ± 46.7 ($PM_{3.3}$)	57.7 ± 29.1	7.7 ± 12.1 ($PM_{0.4}$)
Mbengue et al. (2014)	Dunkirk region (France)	Winter	Industrial sector	23.6 ± 6.0		10.1 ± 4.1	0.8 ($PM_{0.1}$) 2.4 ± 1.1 ($PM_{0.29}$)
			Urban-traffic sector	29.8 ± 4.1		16.6 ± 3.9	0.5 ($PM_{0.1}$) 5.8 ± 2.1 ($PM_{0.29}$)
Ntziachristos et al. (2007)	Los Angeles (CA -USA)	Winter-spring	Traffic	21.0 ± 3.5	10.9 ± 0.9		2.6 ± 0.5 ($PM_{0.18}$)
			Urban	13.8 ± 2.5	7.5 ± 1.6		1.7 ± 0.7 ($PM_{0.18}$)
Pakkanen et al. (2001)	Helsinki (Finland)	1-y (~ 1 sample per month)	Urban				0.49 ($PM_{0.1}$)
			Rural				0.52 ($PM_{0.1}$)
Ramgolam et al. (2008)	Paris (France)	Winter-spring	Urban background	12–42	10–36		

[a]: standard deviation; [b]: quasi-ultrafine particles

Table 7 (continues). PM mass concentrations for research studies citied in the paragraph: *Comparison of Ambient PM Concentrations with Literature Data.*

Reference	*Location*	*Sampling period*	*Sampling site*	*Concentration (μg m^{-3}) – [Mean ± SD[a]] or [Min–Max]*			
				PM_{10}	*$PM_{2.5}$*	*PM_1*	*UFPs or QUFPs[b]*
Sardar et al. (2005)	Los Angeles (CA-USA)	Fall	Urban mix of industrial and traffic sources				3.5 ± 0.1 ($PM_{0.18}$)
			Traffic				3.1 ± 0.1 ($PM_{0.18}$)
			Residential area				2.9 ± 0.1 ($PM_{0.18}$)
		Winter	Residential area				2.9 ± 0.07 ($PM_{0.18}$)
			Urban mix of industrial and traffic sources				1.5 ± 0.06 ($PM_{0.18}$)
			Traffic				1.2 ± 0.05 ($PM_{0.18}$)
			Residential area				1.3 ± 0.09 ($PM_{0.18}$)
			Residential area				1.4 ± 0.06 ($PM_{0.18}$)
		Summer	Urban mix of industrial and traffic sources				2.1 ± 0.08 ($PM_{0.18}$)
			Traffic				0.9 ± 0.1 ($PM_{0.18}$)
			Residential area				1.5 ± 0.06 ($PM_{0.18}$)
			Residential area				1.4 ± 0.05 ($PM_{0.18}$)
Spinazzè et al. (2015)	Como (Italy)	Winter	Urban traffic routes				12.7 ± 4.8 ($PM_{0.25}$)
		Spring					14.1 ± 1.6 ($PM_{0.25}$)
		Summer					9.5 ± 2.6 ($PM_{0.25}$)
		Fall					13.8 ± 3.6 ($PM_{0.25}$)

[a]: standard deviation; [b]: quasi-ultrafine particles

Figures

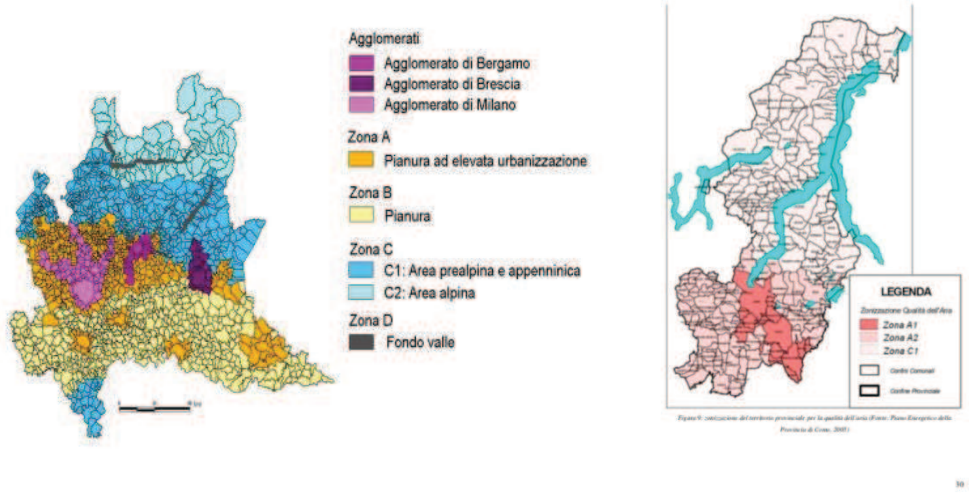

Figure 1. Urban agglomerates and zones for the air quality management identified in the Lombardy Region (figures obtained from the website of the Lombardy Region: www.regione.lombardia.it).

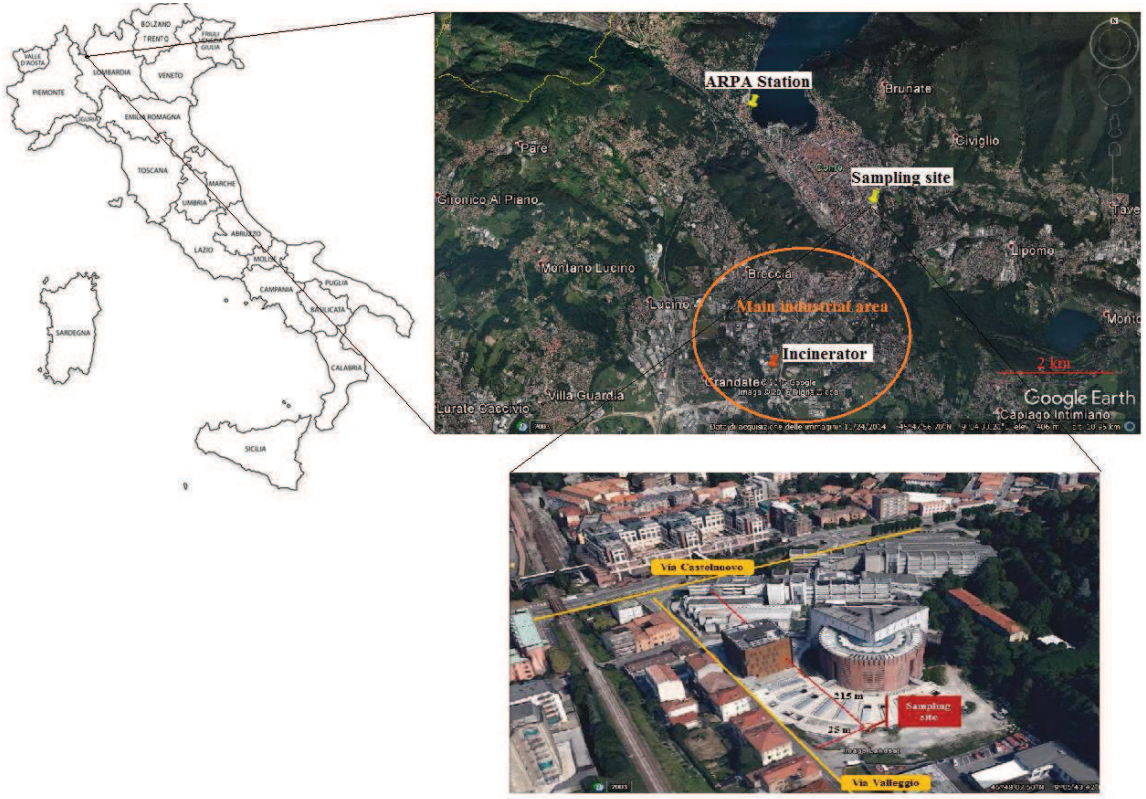

Figure 2. Sampling site location (obtained by Google Earth). The main industrial area (including mainly textile, printing, mechanical and wood plants) and the minimum distances from the nearest streets are shown.

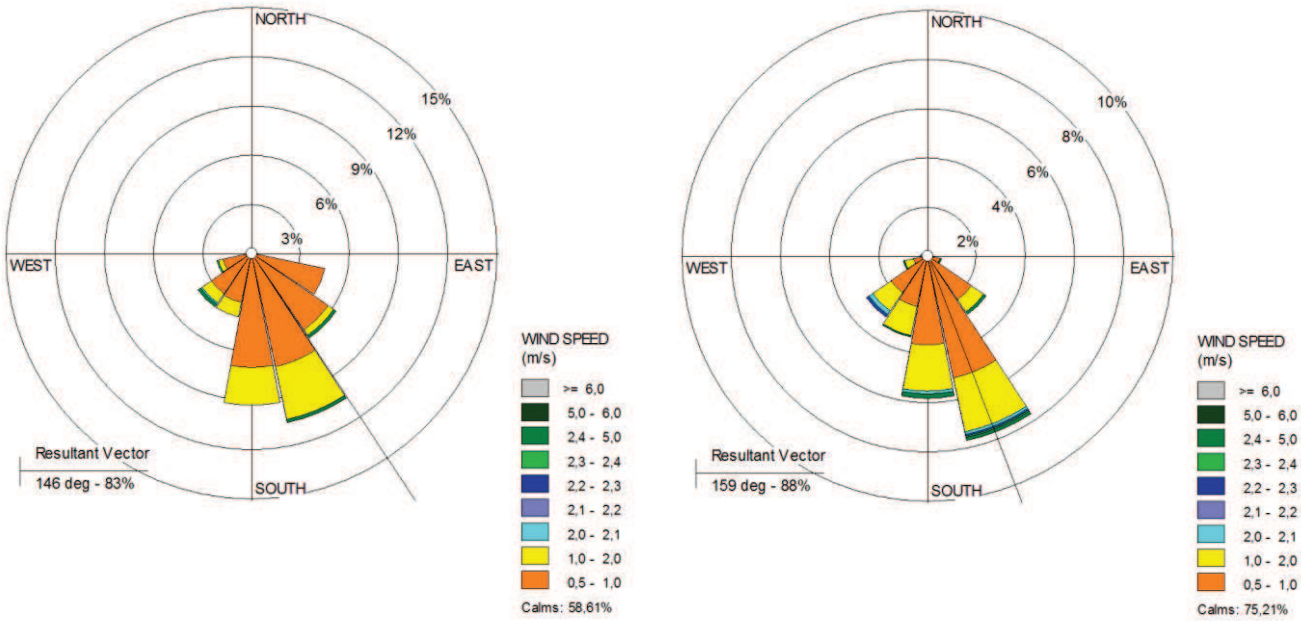

Figure 3. Wind intensity and direction data for the non-heating (left) and the heating (right) season.

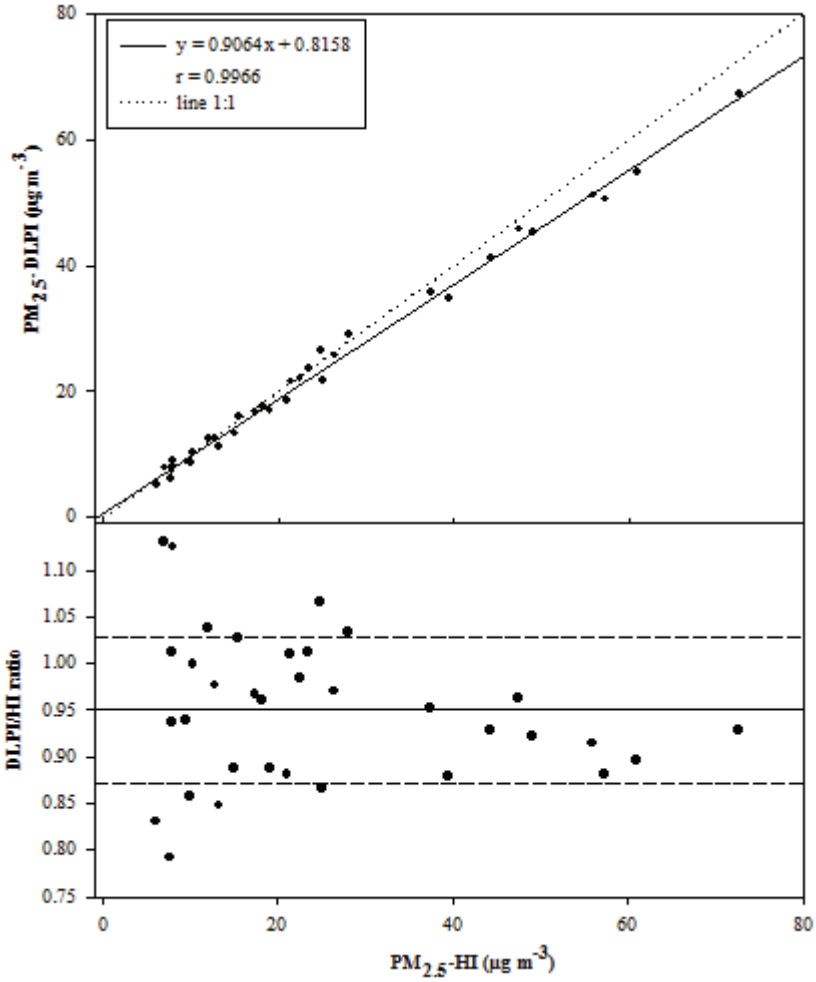

Figure 4. Linear regression between $PM_{2.5}$ concentrations (n = 34) determined via HI and DLPI. In the bottom panel, the DLPI/HI ratios as a function of $PM_{2.5}$-HI concentrations are shown. The mean ratio and its standard deviation (0.95 ± 0.08) are indicated by the solid and dashed lines, respectively.

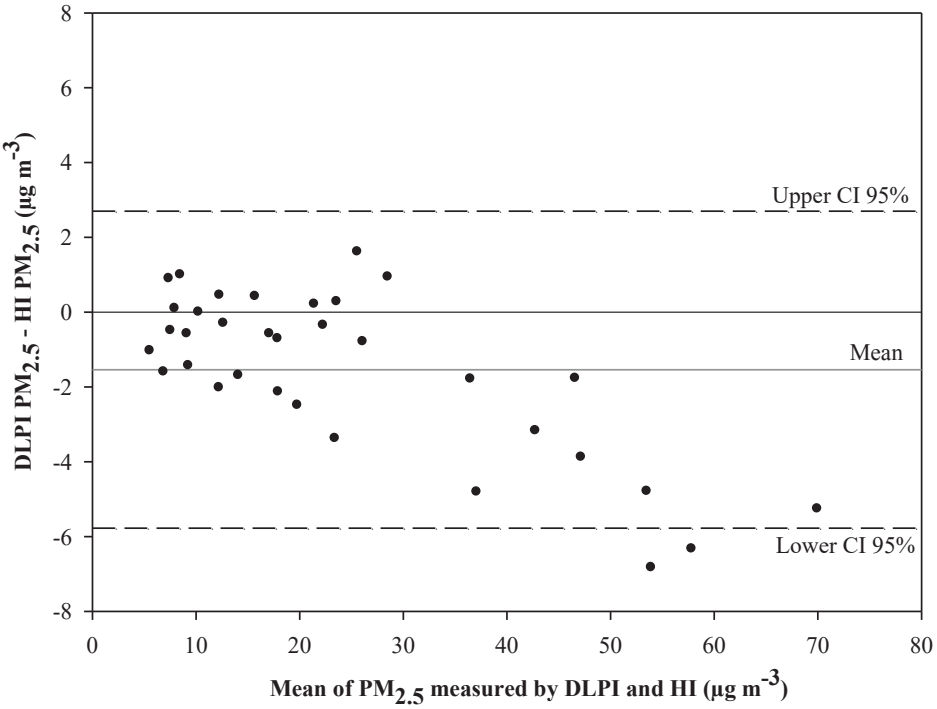

Figure 5. Comparison of $PM_{2.5}$ sampled with DLPI and HI using the Bland-Altman plot. The solid black line represents the ideal agreement between the two methods, the solid grey line represents the observed average error (–1.54 µg m^{-3}), whereas broken lines correspond to the upper and lower 95% limits of agreement.

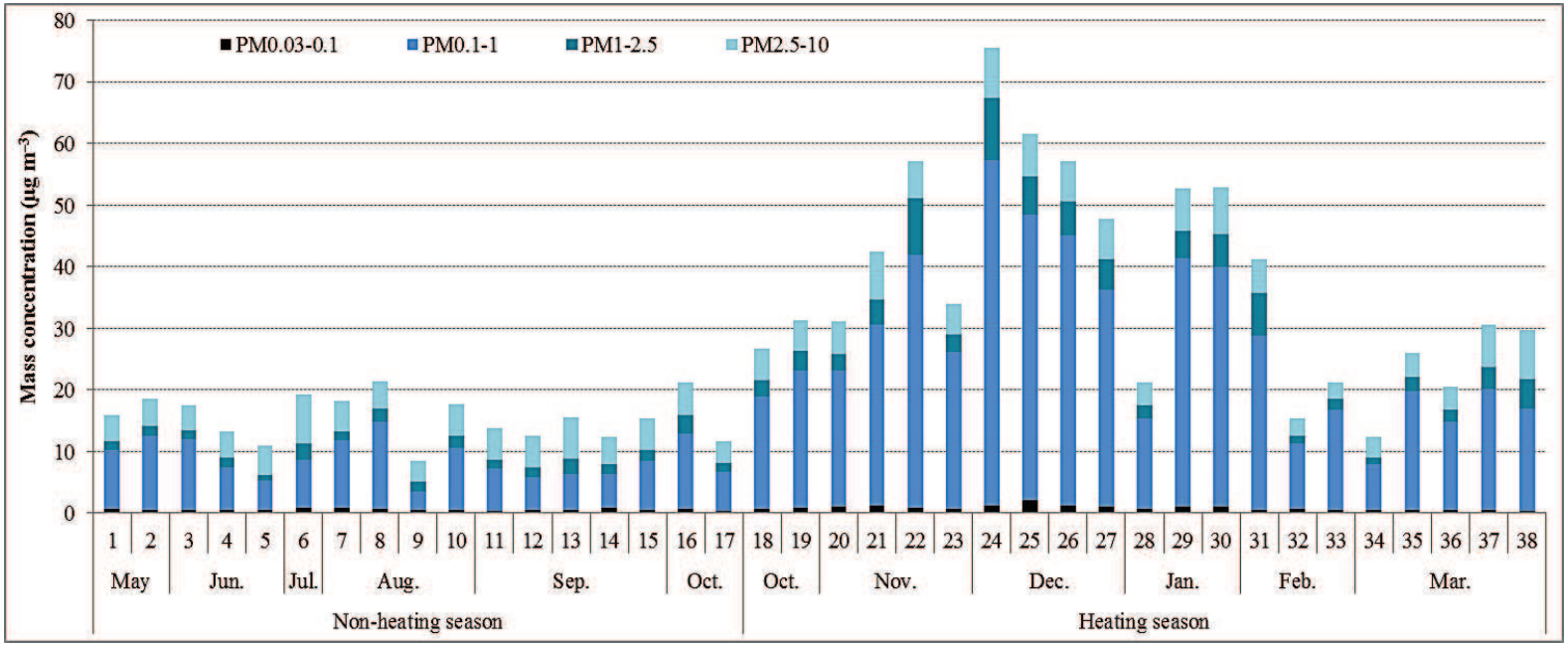

Figure 6. Mean contribution of the principal PM fractions to the total PM_{10} during each weekly sampling session. The sample number is displayed on the x-axis.

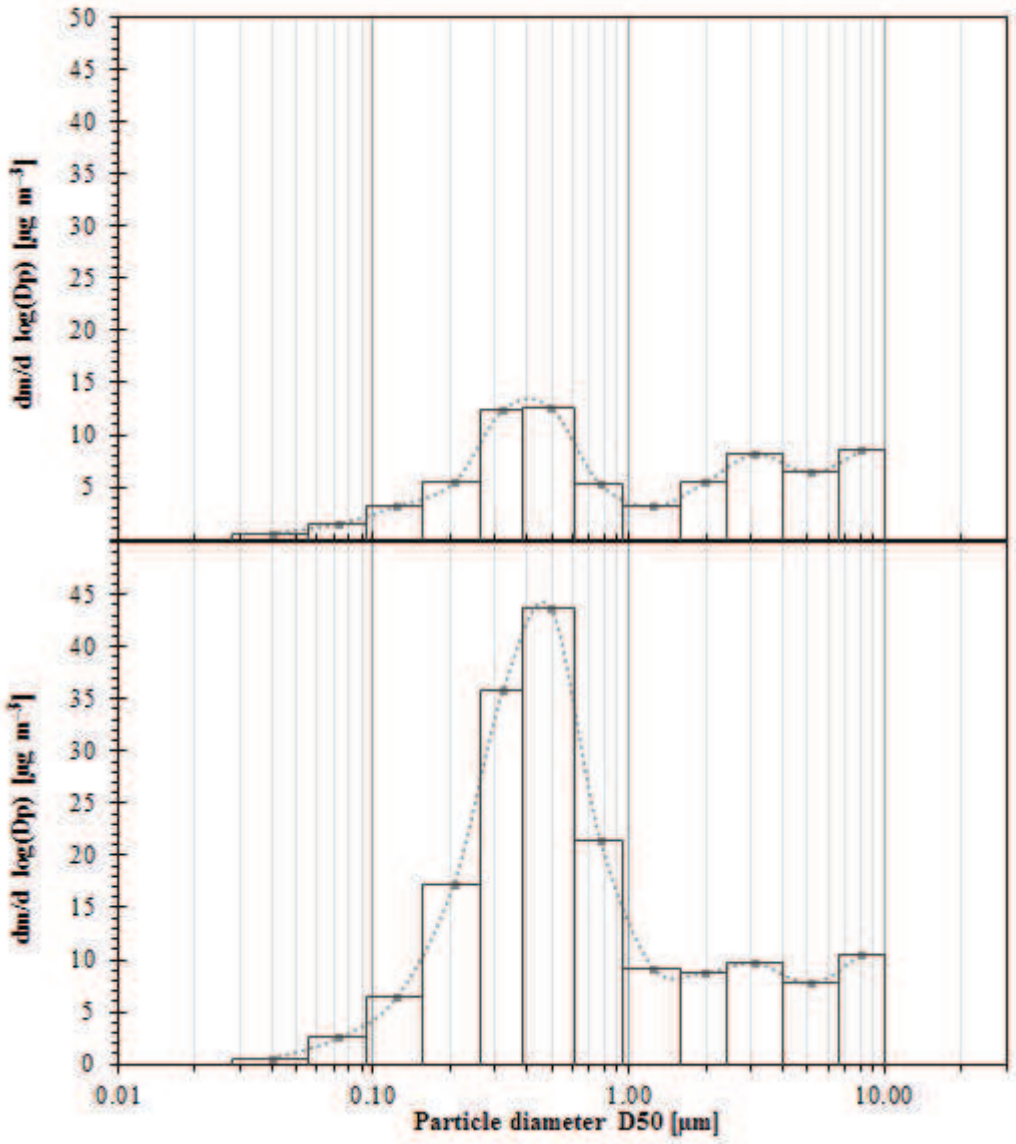

Figure 7. Median mass size-distributions at the URB station during the non-heating (upper panel) and the heating (lower panel) season for particles between 0.028 and 10 µm.

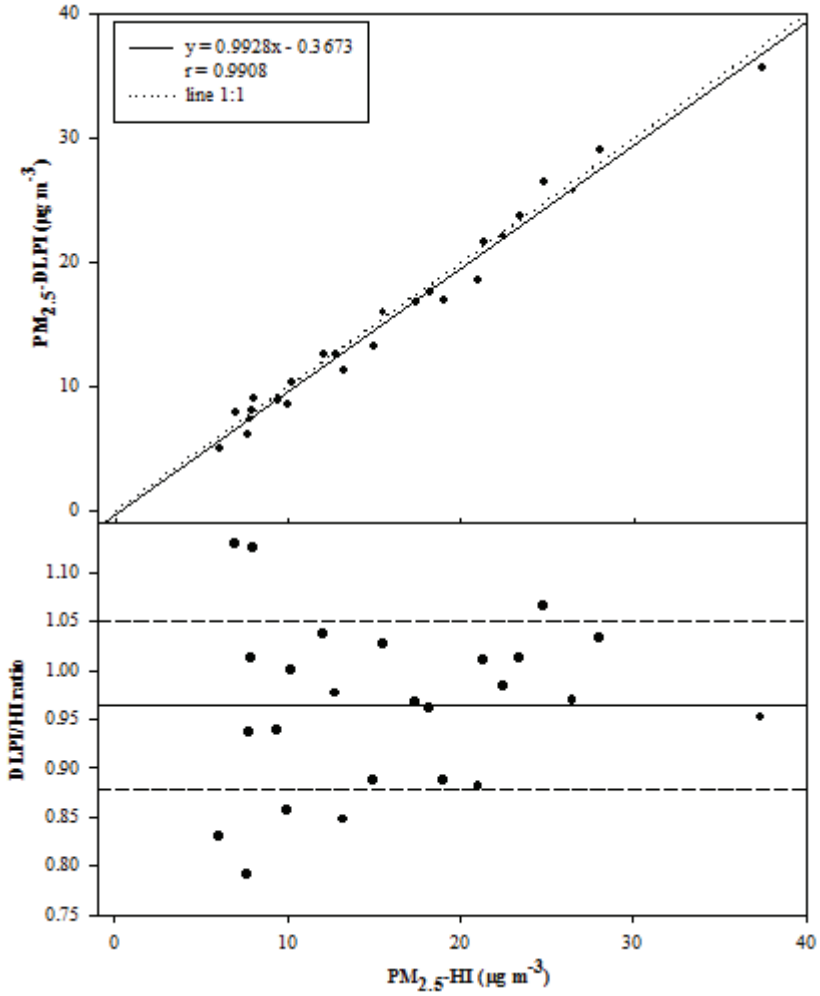

Figure 8. Linear regression between $PM_{2.5}$ concentrations (n = 25) determined via HI and DLPI. Only $PM_{2.5}$ data responding to the DLPI recommended operating conditions are reported in the graph. In the bottom panel, the DLPI/HI ratios as a function of $PM_{2.5}$-HI concentrations are reported. The mean ratio and its standard deviation (0.96 ± 0.09) are indicated by the solid and dashed lines, respectively.

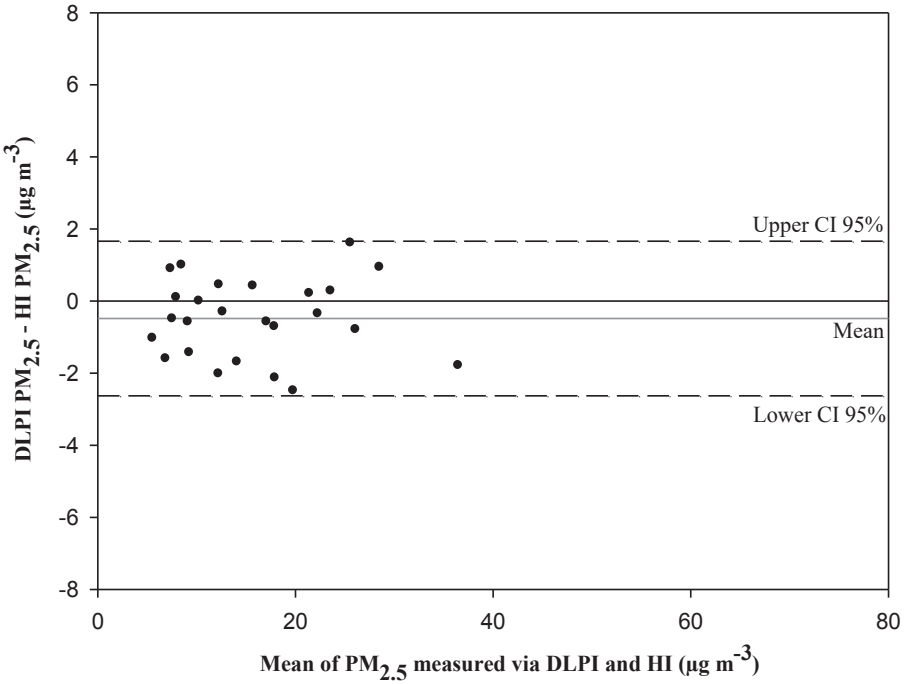

Figure 9. Comparison of $PM_{2.5}$ sampled with DLPI and HI using the Bland-Altman plot. Only $PM_{2.5}$ data responding to the DLPI recommended operating conditions are reported in the graph. The solid black line represents the ideal agreement between the two methods, the solid grey line represents the observed average error (–0.48 µg m^{-3}), whereas broken lines correspond to the upper and lower 95% limits of agreement.

Chapter 3 – *Multi-Element Analysis of Size-Segregated Fine and Ultrafine Particulate via Laser Ablation-Inductively Coupled Plasma-Mass Spectrometry*

Abstract

This chapter focuses on the development and optimization of a novel and reliable Laser Ablation-Inductively Coupled Plasma-Mass Spectrometry (LA-ICP-MS) measurement protocol for the elemental characterization of size-segregated fine and ultrafine particles collected by means of a multi-stage cascade impactor (DLPI). Special efforts were made to improve and optimize sample pre-treatment steps and LA operating conditions in order to avoid some critical drawbacks encountered during analysis and make the particulate samples suitable for an accurate and reproducible LA-ICP-MS analysis, regardless of the mass loading on each dust filter. Under the optimum conditions, dust samples as well as blank filters and standards for calibration were analyzed by multiple line scan of each sample spot and quantitative analysis was accomplished with dried-micro droplets of aqueous standard solutions. The accuracy of LA-ICP-MS results was verified by comparison with conventional ICP-MS analysis of selected PM samples after complete sample mineralization with mineral acids. In this context, an alternative approach for sample pre-treatment in liquid ICP-MS analysis was developed, since the conventional microwave-assisted digestion approach utilizing *aqua regia* does not allow the complete dissolution of the filters used for particle collection in this study. Results revealed a general good agreement between the LA-ICP-MS approach and the conventional method. The LA treatment procedure identified for sample preparation allowed accurate and reproducible analysis with a simple and fast sample preparation, thus overcoming the laborious pre-treatment approach required for wet chemical digestion of polycarbonate filters. With the proposed LA-ICP-MS approach, risks associated with sample contamination were minimized and the time needed for the application of the whole measurement protocol was reduced; the sample throughput could be increased, with the possibility to analyze a greater number of samples with several sample replicates in the same time required for the established ICP-MS protocol. Moreover, the better sensitivity of the LA-ICP-MS approach provided more complete information about the mass concentration and size-distribution of the investigated elements, thus allowing to deeper investigate the composition of the most dangerous PM fractions in terms of health concern.

1. Introduction

Increasing epidemiological and toxicological evidences associated adverse effects on human health with the exposure to atmospheric particulate matter (PM) (Oberdörster *et al.*, 2005; Ostro *et al.*, 2015). In particular, submicronic (PM_1) and ultrafine particles (UFPs, generally defined as particles with aerodynamic diameter < 0.1 μm) attracted the scientific attention in the last decades because of their documented ability to induce oxidative stress, inflammation in cells and cardiovascular diseases (Donaldson *et al.*, 2002), with potential adverse outcomes that appear to be greater than or independent from the effects caused by larger size particles (Li *et al.*, 2003). Because of their small sizes and their higher deposition efficiency, UFPs can penetrate deeper into the lungs, thus being able to transport bound-toxic substances until alveolar regions.

Although trace metals account for a very small percentage of the total PM composition (Terzi *et al.*, 2010), they are an important component of PM because of their toxic characters. Several

works suggested correlations between PM-bound metals and pulmonary toxicity (Sun *et al.*, 2001; Raaschou-Nielsen *et al.*, 2016). Some of the metallic elements are highly toxic (Cr, Mn, Fe, Ni, Zn, Pb) (Dreher *et al.*, 1997; Hartwig and Schwerdtle, 2002; Garçon *et al.*, 2006; Beyersmann and Hartwig, 2008) and are known as human carcinogens (Cr, As, Cd, Ni) (IARC, 1980; IARC, 1990). In summary, the size-distribution of atmospheric trace metals is a key knowledge in terms of health concern.

Wet chemical analysis via Inductively Coupled Plasma-Mass Spectrometry (ICP-MS) or ICP-Optical Emission Spectrometry (ICP-OES) combined with microwave assisted digestion has become one of the most applied techniques for metals quantification in airborne PM, for both total suspended or size-segregated particles (Robache *et al.*, 2000; Lin *et al.*, 2005; Pekney and Davidson, 2005; Herner *et al.*, 2006; Hassan *et al.*, 2007; Ntziachristos *et al.*, 2007; Toscano *et al.*, 2009). ICP-MS, in particular, offers low limits of detection (LODs), wide linear dynamic range, multi-element capability, rapid scanning and high sample throughput. Nonetheless, the traditional ICP-MS systems require the dissolution of solid sample before analysis, thus resulting in enhanced possibility of contamination or losses of trace elements during sample manipulation and pre-treatment. Moreover, this type of analysis generally requires laborious, time-consuming and quite expensive sample preparation (i.e., high reagent consumption).

Solid-sampling techniques as alternative analytical techniques are acquiring increasing interest because they do not need laborious sample pre-treatment, thereby reducing the possibility of contaminations or analyte losses. Techniques often applied for trace element analysis of airborne PM include instrumental neutron activation analysis (INAA) (Cass *et al.*, 2000), proton-induced X-ray emission spectrometry (PIXE) (Miranda and Tomaz, 2008) or X-ray fluorescence spectrometry (XRF) (Viksna *et al.*, 2004, Wagner *et al.*, 2008; Wagner and Mages, 2010). PIXE, XRF and INAA are direct and non-destructive analytical techniques, but the analytical sensitivity is lower than ICP-MS (PIXE, XRF), or they require expensive equipment (INAA).

Laser Ablation combined with ICP-MS (LA-ICP-MS) is one of the increasingly applied techniques in the field of solid sampling. In addition to the aforementioned advantages, this method provides very low detection limits and it is well suited when the amount of sample is limited, as for UFPs. Indeed, UFPs are known to have a negligible role in the total PM mass concentration (<< mg) (Tuch *et al.*, 1997). Since some toxic trace metals commonly account for less than 0.5%, their determination might be difficult when using conventional analytical methods which require additional dissolution steps prior to analysis. Nevertheless, one of the main problem with LA-ICP-MS in the analysis of real dust samples is the quality and homogeneity of sample distribution on the substrate and the difficulty of obtaining matrix-matched standards for signal quantification.

In this study, a multi-stage low pressure impactor was used to collect particles into different size ranges, from ultrafine to coarse fractions. With this type of particulate sampler, airborne particulates are segregated by inertial separation according to their aerodynamic diameter and collected on filter substrates in single spots. Dust spots are generally well-separated and suitable for LA-ICP-MS analysis under appropriate ablation conditions. Although a similar analytical approach was recently published (Hsieh *et al.*, 2011), the presented work aimed to develop and optimize an improved LA-ICP-MS procedure, to overcome and avoid some critical drawbacks (well described in the paper) that were encountered during method development. Therefore, in this article a novel measurement protocol for the analysis of trace

metal contents in size-segregated PM using LA-ICP-MS is presented. Dried-droplet-standards were prepared for calibration curves and signal quantification. The accuracy of LA-ICP-MS results was verified by comparison with conventional ICP-MS analysis of selected PM samples after complete sample mineralization with mineral acids. In this context, an alternative approach for sample pre-treatment in liquid ICP-MS analysis was developed, since the conventional microwave-assisted digestion approach utilizing *aqua regia* does not allow the complete dissolution of the filters used for particle collection in this study.

2. Experimental

2.1 Collection of Size-Segregated Particles

Airborne particles were collected at an outdoor urban background site in Como, Northern Italy, at ground level. A 13-stage Low Pressure Impactor (Dekati Low Pressure Impactor, DLPI, DEKATI Ltd., Tampere, Finland), designed for deposition of particles in the 0.028–10 μm size range according to their aerodynamic diameter (12 real stages plus one stage for separating particles > 10 μm), was used for the collection of size-segregated PM. The nominal values for the equivalent aerodynamic 50% cut-off diameters (D50%) of the impactor stages are reported in Table 1, together with the number of spots per stage and the PM mass collected on each DLPI collection plate during a typical winter sampling campaign. As shown in Table 1 and Fig. 1, the various DLPI impactor stages are characterized by different number of spots, different spot sizes and different particle mass loadings. Generally, the mass collected on DLPI stages 1 and 2 (designed for UFPs collection) is always < 200 μg, especially during summer time when the average PM concentrations are expected to be lower than winter values. Atmospheric sampling, started at the end of May 2015 until the end of March 2016, were generally performed once a week, from Monday to Friday morning, to obtain a large number of samples that could be used to characterize the study area and investigate temporal variabilities in the measured concentration levels. For the validation of the proposed LA-ICP-MS method, two sets of the weekly size-segregated PM samples were used. Specifically, the test samples were collected during wintertime (December 2015) using a sampling duration of 48 h, for a total of 75 m^3 of air volume collected.

During operation, a pressure gradient of 900 mbar was applied across the 13 stages, to obtain a pressure of 100 ± 5 mbar under the last impactor stage, thereby ensuring the exact diameter cut points over the measurement period. Aerosol particles were deposited on high-purity polycarbonate filters (PC, 25-mm; no-holes, Fisher Scientific, S.A.S., Illkirch, France) fixed onto each collection plate by means of a specific holder ring (Fig. 1). Before each sampling session, the PC filters were coated with a thin layer of Apiezon-L grease provided by the manufacturer (DEKATI DS-515 Collection Substrate Spray, DEKATI Ltd., Tampere, Finland) to improve the impactor collection efficiency and prevent bounce- and blow-off effects during separation. The Apiezon-L grease was applied in a form of spray, following a standardized procedure that suggested a double spray application in two different directions, keeping the same grease mass per filter area, as far as possible. Before use, the impactor and all the accessories needed for handling the substrates were washed with distilled, de-ionized water and propan-2-ol. The particle mass collected on PC filters was determined gravimetrically following a standard operating procedure (UNI EN 14907; UNI EN 12341). Briefly, the collection substrates were weighed before and after sampling under controlled temperature (20 ± 1°C) and relative humidity (50 ± 5%) conditions by a micro-balance with a readability of 1

μg (Gibertini 1000, Novate, Milan, Italy). The collected mass was then calculated by differential weighing. After being weighed, particulate samples were stored in clean plastic boxes, in the dark and at 4°C until elemental analysis. Blank and sample PC filters were always handled with plastic tweezers to minimize contamination and a ceramic knife was used to cut every blank and sample PC filter into four equal pieces. Each pre-cut section was then weighed again to ensure the exact weight value after partitioning. Three quarters of each PC filter were subsequently used for the wet chemical digestion whereas the remaining section was analysed via LA-ICP-MS for comparison with the conventional analytical method. DLPI stages 1–9 were analyzed for elemental determination to obtain the mass concentration and size-distribution of fine PM ($PM_{2.5}$, with 9 size fractions in the 0.03–2.5 μm size range).

2.2 Reagents, Standards and Reference Material

1-Methyl-2-pyrrolidone 99.5% for analysis (ACS, Applichem, Germany) was used to dissolve PC filters. Nitric acid (HNO_3) 65% (Merck, EMSURE), hydrofluoric acid (HF) 40% (Merck, EMSURE), perchloric acid ($HClO_4$) 70% (ACS, Applichem, Germany) and hydrogen peroxide (H_2O_2) 30% (Merck, EMSURE) were used for the wet chemical digestion of PC blank filters, dust samples and Standard Reference Material. High-purity water obtained by an Easypure water purification system (Thermo, USA, 18.2 MΩ cm) was used to prepare the 1% (v/v) HNO_3 solution. Standard solutions for aqueous and matrix-matched calibration were prepared by diluting a multi-element stock solution for ICP-MS analysis (ICP-Multielement Standard VIII, 100 mg l^{-1}, Merck, Darmstadt, Germany). Glycerol 99.5% (AnalaR NORMAPUR), ethanol (absolute for analysis, Merck, EMSURE) and acetone 99.5% (Sigma-Aldrich) were used for sample preparation before LA-ICP-MS analysis. NIST Standard Reference Material (SRM) 1648a (Urban Particulate Matter), stored and handled as instructed by the manufacturer, was used to test the precision and accuracy of the proposed digestion procedure (see below).

2.3 Wet Chemical Digestion and Conventional ICP-MS Analysis

Sample preparation. Preliminary experiments on PC blank filters proved that this type of substrates cannot be completely destroyed via conventional microwave-assisted digestion using mixtures of nitric acid, hydrochloric acid and hydrogen peroxide, neither with standard conditions for sample pre-treatment nor with strong acid-digestion conditions. For these reasons, an open-vessel alternative approach consisting of different pre-treatment steps was newly developed. A quarter of a filter was transferred into a pre-cleaned Teflon beakers (HDPE, Nalgene, USA) and treated with 1-Methyl-2-pyrrolidone (500 μL), that was found to entirely dissolve the polycarbonate material. After ultrasonication (5 mins) and complete filter dissolution, H_2O_2 (1 mL) was added to the resulting liquid solution, in order to decompose the dissolved polymer, before evaporation to dryness by means of an heating block (analab, Germany). The dried residue was treated 30 mins more at 90°C with a mixture of HNO_3 (3 mL), H_2O_2 (1.5 mL) and HF (50 μL) to dissolve silicates for the complete digestion of particulate sample and was dried again, in order to eliminate the acid excess that could cause damage to quartz and glass. The final sample treatment was conducted overnight at 90°C with closed caps and an $HClO_4$ (100 μL)-HNO_3 (400 μL) acid mixture to further oxidize remaining organics. After evaporation of the more volatile nitric acid, the remaining digest was diluted to a final volume of 6 mL with 1% (v/v) HNO_3. The Teflon beakers were cleaned after each digestion run using 6 mL of *aqua regia* at 90°C for 60 mins and then rinsed well with high-

purity water. The cleaning procedure was repeated two times, in order to ensure an accurate cleanliness of each container and avoid any kind of cross contamination.
The described open-vessel approach was applied on a quarter of seven different blank filters and on dust filters. In order to evaluate the precision and accuracy of the proposed method, the described protocol was also applied on NIST SRM 1648a. Briefly, a certain amount of NIST SRM 1648a was dried at 28°C for 48h to eliminate any residual moisture, as recommended. After cooling to room temperature, ~ 30 mg of the dried reference material were accurately weighed twice, transferred into Teflon tubes and diluted to a final volume of 10 mL with 1% (v/v) HNO_3. The dust suspensions were then sonicated for 10 mins and shaken for homogenization. A volume of 100 µL was subsequently pipetted five times from each suspension and transferred into different Teflon beakers, for a total of ten replicates. In this way, the various elements should be present at concentration levels similar to those expected, on average, in real size-fractionated PM samples. After evaporation to dryness, the dried residues were treated with the same approach described above, together with two procedural blanks (only reagents and acids) in order to monitor the cleanliness of the Teflon beakers and to account for possible contaminations during the treatment procedure.

Multi-element standard solutions and calibration. Standard solutions for aqueous calibration were prepared by diluting with 1% (v/v) HNO_3 a multi-element stock solution of 100 mg L^{-1} containing the elements of interest (Cr, Mn, Fe, Ni, Cu, Zn, Ba and Pb). Because of the large difference in concentration levels of different metals in the particulate samples, calibration curves were obtained using a blank and seven calibration solutions covering the expected concentration range for all the investigated elements (0.05; 0.5; 1; 2; 5; 10 and 20 µg L^{-1}). Matrix-matched calibration solutions were prepared together with aqueous standard solutions to check for possible variations in the slope of the calibration curves. For these purposes, blank and dust PC filters were dissolved and treated as previously described. The resulting PC blank and dust solutions were subsequently divided into equal aliquots and suitable amounts of multi-element standard solutions were added to each aliquot to obtain PC blank-matched calibration and dust-matched calibration. Unspiked aliquots of PC blank solution and dust solution were kept as a blank. Before starting with analysis, Indium was always added as internal standard to each calibration solution (final concentration: 2 µg L^{-1}).

ICP-MS Analysis and Figures of Merit. Measurements for wet chemical analysis were performed using a Thermo Scientific iCAP Q ICP-MS system (ThermoFisher Scientific GmbH, Bremen, Germany) equipped with ESI SC-2DX autosampler for liquid samples (Elemental Scientific, Inc., Omaha, NE). The ICP-MS QTegra Software provided by the manufacturer (v. 1.5.1189.31) was used to control all instrument operations and performance, including tuning, data acquisition and data analysis. The instrument was tuned in collision cell mode before each set of daily analysis with a tuning solution containing elements at a concentration of 1 µg L^{-1} and instrument parameters were optimized for maximum ^{115}In signal and minimum $^{140}Ce^{16}O/^{140}Ce$ ratio (below 1.9%). The matrix induced interferences were checked with the analysis of matrix-matched calibration solutions, prepared as described above. Spectral interferences were minimized by choosing a non-interfered isotope and by using a collision cell system with a mixture of He and H_2 as the collision gas. ^{115}In was used to correct for instrumental drifts and non-spectral interferences. The typical operating conditions

optimized for liquid analysis are shown in Table 2, together with the list of elemental isotopes under investigation.
For method validation, the precision and accuracy of liquid ICP-MS measurements were checked with the analysis of ten replicates of NIST SRM 1648a prepared with the same open-vessel digestion procedure of blank filters and dust samples. Accuracy was evaluated as the percent ratio between the calculated concentrations and the SRM certified concentrations (percentage of recovery). Precision was expressed as the coefficients of variation (RSD%) of replicates. Moreover, during the analysis of real size-fractionated PM samples, each dust filter was analyzed in triplicate (three sections per filter) to confirm the overall uncertainty of ICP-MS results.
For each element, limits of detection (LODs) and quantification (LOQs) of the ICP-MS analysis were determined as three and ten times the standard deviation of seven PC blank filters treated in the same way as dust samples. For concentration in air, LODs and LOQs were recalculated by using the air volume sampled during particulate collection (75 m^3).

2.4 LA-ICP-MS Procedure

Sample preparation. LA-ICP-MS measurement generally requires less-laborious sample preparation than that needed for wet chemical digestion. The approach presented here is the final result of exploratory experiments improved step by step with the primary aim of reducing sample handling and treatment procedures to the minimum necessary to make the particulate samples suitable for an accurate and reproducible LA-ICP-MS analysis. The improvement and optimization of analytical pre-treatment steps will be described and discussed in detail under Results and Discussion.
For laser ablation, a quarter of each PC blank and dust filter was attached on the surface of poly(methylmethacrylate) slides (Betzold, Austria) by means of a spray glue (3M), applied to the slides surface with a single application in order to create an homogeneous and thin sticky layer. The spray was selected as holding material instead of double-sided tapes because it made the attachment procedure easier and its contribution to the signal intensities of the analyte elements was found to be negligible. Once attached onto the slides, the filters were dipped in a solution of pure glycerol (3%) diluted in ethanol (60%) and acetone (40%). Whereas the volatile solvents ethanol and acetone evaporated immediately, glycerol remained on the sample spots. This was found to be a key step during sample preparation in order to keep dust spots wet and soft, thus avoiding an inconvenient and problematic effect (well described later) for which sometimes during ablation part of the collected dust was broken off and did not reach the ICP-MS detector. Contrariwise, after the abovementioned dipping treatment, the filters remained slightly wet also during measurement and the thin layer of glycerol covering each dust spots was found to be thick enough to avoid the aforementioned effect without causing sample contamination. Filters were then dried for 30 mins under a tilted glass petri-dish to avoid contamination. After solvent evaporation, poly(methylmethacrylate) slides were placed inside the ablation chamber for analysis or kept in a dedicated slide-container for subsequent analysis.

Dried-droplet standards and calibration. As for the conventional ICP-MS method, calibration is essential for quantitative analysis. In this study, the quantification of derived transient signals was accomplished with dried droplets of standard solutions prepared on the

surface of the same poly(methylmethacrylate) slides used for sample filters. Exploratory experiments on real PM samples via conventional ICP-MS allowed the definition of the ideal concentration range for LA-ICP-MS calibrations. Based on ICP-MS results, the expected mass per spot on each DLPI collection plate was calculated for all of the elements under investigation by dividing the total elemental mass of each stage with the number of spots per stage. The expected mass per spot varied greatly, ranging from few picograms (e.g., 0.05 ng for Pb) to hundreds of nanograms (e.g., 200 ng for Fe). Therefore, taking into account the volume used for dried-droplets preparation (5 μL), eleven aqueous standard solutions were prepared to cover the expected mass range (0.05; 0.1; 0.15; 0.2; 1; 3; 5; 7; 20 and 50 mg L^{-1}) by diluting with 1% (v/v) HNO_3 a multi-element stock solution of 100 mg L^{-1}. Indium was always added as internal standard to each calibration solution (final concentration: 5 μg L^{-1}). Moreover, in order to simulate the glycerol coverage on dust spots, 100 μL of 400-fold diluted glycerol were added to blank and standard solutions.
For dried-droplets preparation, slides surfaces were ablated in order to create a 12 x 3 micro-cavities grid (Fig. 2). Standards for calibration were then prepared by dropping with an Eppendorf micropipette 5 μL of standard solutions into the center of each micro-cavity, for a total of three replicates per standard. In this way, standard droplets were distributed in a well-defined grid pattern across the slide surface, simplifying the localization and measurement of the residues without any dyed solution. Micro-droplets were subsequently dried under environmental conditions in a VFT 1525 ultraclean laminar flow hood (WEISS Technik, Austria) under a tilted glass petri-dish. Once dry, the residues were analyzed with the same ablation schemes optimized for dust spots.

System configuration and operating conditions. Laser ablation was performed with a New Wave 213 system equipped with a frequency quintupled 213 nm Nd:YAG laser and a fast washout ablation cup (New Wave 213, ESI, Fremont, CA, USA). During ablation, a helium gas flow of 0.8 L min^{-1} was flushed through the cell. The LA-system was directly connected to the ICP-MS-torch with a PTFE tube (1 m x 4 mm inner diameter) by which the ablated particulate matter was transported to the plasma. After the ablation chamber, an Ar gas flow of 0.8 L min^{-1} was added via a Y-connector. Analysis was always performed in collision cell mode.
LA parameters (e.g., ablation scheme, laser power, scan speed, repetition rate), that will be deeply discussed in the next paragraph, were optimized to obtain standard operating conditions that could ensure a complete and reproducible ablation of dust spots in the shortest data acquisition time, regardless of the mass loading on each DLPI stage (directly dependent on the PM ambient concentration levels and the sampling time). For these purposes, size-fractionated PM samples were firstly divided into two main groups, namely DLPI stages 1-7 (group I) and DLPI stages 8-9 (group II), mainly because of the great difference in the spot sizes between the two sets of samples. The two groups were analyzed separately: all dust filters were prepared as previously described but for each group a suitable ablation scheme was optimized and separate calibration curves were prepared.
Laser ablation was performed using a focused laser beam with 150 μm beam diameter along line scan patterns specifically created to completely cover the whole sample spots. Figs. 3 and 4 show a schematic representation of the line scan patterns used to ablate a single spot of group I and II, respectively. As drawn in Fig 3, for group I a scan line of 1 mm length was created

and duplicated in order to obtain a first rectangular line scan pattern (yellow pattern: 1000 μm x 1050 μm) over the spot surface. The scan direction was set so that every line had a reverse scan direction compared to the previous one. A second line scan pattern slightly lower than the yellow one (blue dotted pattern: 800 μm x 900 μm) was created with the same approach and positioned so that the blue rows overlapped the yellow line edges in order to ensure the removal of any material not carried away during the previous ablation (Fig. 3). The final ablation scheme was set as follow: a first scan on the yellow pattern to pre-ablate the surface material of each spot and two scans following the blue pattern for ablating the majority of dust material. The yellow pattern was finally scanned again to remove any residual. This complex ablation scheme was found to be necessary for PM samples of group I because of the large amount of collected material (especially for DLPI stages 4-7) that could not be quantitatively ablated otherwise. For detailed explanations see Results and Discussion.

Dust spots of group II were analyzed with a similar ablation scheme. As shown in Fig. 4, the ablation area was increased because of the bigger spot size (yellow line scan pattern: 2000 μm x 1950 μm) and a second rectangular scan pattern (blue dotted pattern: 1000 μm x 1050 μm) was positioned in the central section of dust spots. The final ablation scheme included a first scan on the yellow pattern and a second ablation following the blue rows.

In case of extraordinary heavily loaded spots, ablation schemes I or II were scanned two times and the second scan was considered as a new ablated spot for blank correction and elemental mass determination. The calculated mass for each analyte was subsequently added to the amount determined from the first scan only if values were > LOQ.

For both ablation schemes, the total scan time was adjusted to be 15 s longer that the total time needed for ablating one spot, to ensure that the laser ablation of a single spot was ended and the ablated material from the last ablated spot was entirely transported to the plasma before starting with the next ablation. Data acquisition with the QTegra Software was performed over the whole scan time. A summary of the final LA-ICP-MS parameters used for analysis is presented in Table 3.

For each element, LODs and LOQs of the LA-ICP-MS procedure were determined as three and ten times the standard deviation of six different spots on PC blank filters, that were attached on poly(methylmethacrylate) slides and dipped in the glycerol solution in the same way as for dust filters. For samples of group I blank spots were analyzed following the ablation scheme I, whereas the ablation scheme II was used to determine the blank contribution for samples of group II. LODs and LOQs expressed as concentration in air were recalculated by using the air volume sampled during particulate collection.

The precision and stability of the proposed LA-ICP-MS protocol was determined by the analysis of four different spots on each DLPI collection stage.

3. Results and Discussion

As explained in the Introduction, the main goal of this paper was to develop and optimize a suitable LA-ICP-MS procedure for the analysis of trace metals in size-segregated airborne PM. To verify the accuracy and applicability of the proposed method, LA-ICP-MS results were compared with results obtained by conventional ICP-MS analysis. In this perspective, samples were firstly treated with an alternative wet chemical digestion approach and analyzed by ICP-MS. After method validation, ICP-MS results were used as reference values to improve and optimize the LA-ICP-MS measurement protocol in order to obtain accurate and reliable results.

3.1 Validation of the Conventional ICP-MS Procedure

Calibration curves, limits of detection and quantification. Matrix-matched calibrations and aqueous standard calibrations were prepared as described above to check for any possible matrix effects. Fig. 5 represents the signal intensities (normalized to ^{115}In) plotted against the actual lead concentrations with the least-squares regression lines. Calibration curves obtained from dust solution, PC blank solution and aqueous solution are shown. The PC blank-matched calibration curve overlapped with that of aqueous standards because of the negligible amount of Pb in PC blank filters, as expected. For the dust-matched calibration, the intercept was clearly higher since, in this case, calibration standards were prepared from a solution obtained after digestion of real particulate samples containing a certain amount of Pb, in order to reproduce the complex airborne PM matrix. The calculated slope of aqueous calibration differed by 1.9% and 2.6% compared to those of PC blank-matched calibration and dust-matched calibration, respectively. The resulting differences fell within the RSD of replicate measurements on each calibration and can be considered negligible. Data for lead were reported as an example and results for the other investigated elements confirmed these observations (Table 4). In conclusion, no significant variations in the slope of the calibration curves were observed and quantitative analysis were consequently performed using aqueous standard calibrations.

Low limits of detection and stable blank values are crucial points in the analysis of trace metal contents, especially when concentrations are very low and the amount of sample is limited, as in the case of UFPs size fractions. Contamination effects from blank samples could be due to several factors (purity of reagents/containers, cleaning procedures, sample transport and manipulation during preparation) that may potentially affect LODs values. Therefore, all these factors were always carefully controlled, together with instrumental characteristics (e.g., instrumental noise, interferences). PC filters were selected for particle collection because they are well suited for the multi-stage cascade impactor used in this study and, from literature data, they should have low elemental blank values (Chow and Watson, 2007).

LODs expressed as concentration in air for each investigated element are shown in Table 5, together with the coefficients of variation derived from the analysis of replicates. LODs ranged from 0.01 ng m^{-3} (Pb) to 1.6 ng m^{-3} (Fe), whereas LOQs varied between 0.05 ng m^{-3} (Pb) and 5.4 ng m^{-3} (Fe). RSDs of the blank values were always < 10% (except for Fe) indicating quite stable blank contributions.

Recovery from NIST SRM: precision and accuracy. Before starting with the analysis of NIST SRM 1648a, in order to preventively check for any possible analyte losses or sample contaminations during the proposed digestion approach, exploratory experiments were performed on PC blank filters spiked before and after digestion at concentration levels comparable to those expected in particulate samples. The elemental recoveries for the spiked PC blank filters ranged between 85% and 115%, indicating that no significant contaminations or elemental losses should be expected.

The analysis of NIST SRM 1648a used as a quality control material for the evaluation of the digestion protocol efficiency confirmed these preliminary findings. It must be noticed that the estimation of metals' recoveries should be performed on SRMs with similar structure and composition as well as elemental concentrations of the same order of magnitude to that of the samples under investigation. The NIST SRM 1648a typifies the composition of airborne

particulates with aerodynamic diameter up to 53 μm and it is not a size-fractionated PM. The different PM size fractions are generally characterized by a different chemical composition (e.g., different amount of silicates) that could result in possible different behaviors during sample treatment. Nonetheless, to date, no size-fractionated SRMs for PM are available, so that the NIST SRM 1648a was selected as the most suitable Reference Material to check for the analytical problems that could be encountered during the analysis of atmospheric particulate samples.

Elemental recoveries obtained from the digestion and analysis of NIST Reference Material are reported in Table 6. For each element, quantitative analysis was performed using external aqueous calibrations (EAC), since no significant variations in the slope of the calibration curves due to matrix effects were observed, as previously described. Because the concentrations of elements vary considerably between each other (one or more orders of magnitude), each NIST SRM solution was diluted 2-, 50- and 250-fold with 1% (v/v) HNO_3 before ICP-MS analysis to obtain the ideal concentration range for each analyte of interest. Additionally, for quality assurance all concentration levels were also calculated via standard addition (SA). For all of the elements, the quantifications with both external aqueous calibration and standard addition were in agreement. No significant differences were found between EAC and SA results (Paired *t*-test, $p > 0.05$). All recoveries were around 100% ± 5% except for Fe and Cr that registered slightly lower percentages of recovery, even though always within the acceptable range defined by the Association of Analytical Communities (AOAC, 2002).

Cr is generally one of the most critical element to digest. For example, Celo *et al.* (2010) found a 56% recovery when using a microwave-assisted acid digestion method with a HF-HNO_3-H_3BO_3 acid mixture. Higher values were obtained by Toscano *et al.* (2009) (79%) whereas Karthikeyan *et al.* (2006) reported different % recoveries for different amounts of HF, reaching a maximum recovery of 82% with 0.2 mL HF. In our pre-treatment approach, dust and Standard Reference samples were treated for several hours on a heating block with appropriate acid mixtures (HNO_3-H_2O_2-HF and $HClO_4$-HNO_3) that probably allowed a complete sample digestion and mineralization. Also Dreetz and Lund (1992) reported good Cr recoveries with an open digestion system by heating the Reference samples on a hot plate with an $HClO_4$-HNO_3 acid mixture for many hours. Similar findings were also showed by Wang *et al.* (1989).

The precision of analytical measurements, expressed as coefficients of variation of ten replicates, ranged from 1.2% (Pb) to 8.1% (Mn), that can be considered a satisfactory interval taking into account the complexity of the matrix analyzed and the number of manipulations performed. Moreover, it should be remembered that small amounts of Reference Material were used in this study for method validation, to simulate the amount of particles in real size-fractionated ultrafine samples. Therefore, it could be reasonable to attribute deviations of recovery values not only to digestion and analysis procedures but also to the small amounts of material involved in the analysis (well below the recommended sample intake of 5 mg) as well as to reference material heterogeneity.

3.2 Development of an Accurate and Reproducible LA Procedure

3.2.1 Method improvement and optimization

After validation of the wet chemical procedure, ICP-MS results were used as reference values to demonstrate the accuracy of the LA-ICP-MS measurement protocol. Preliminary LA

experiments were performed on dust filter attached on the surface of poly(methylmethacrylate) slides without any type of covering treatment, as performed by Hsieh *et al.* (2011). Laser ablation was carried out using a focused laser beam with 100 µm beam diameter along a single line scan pattern (700 x 700 µm) covering the main sample spot and LA parameters were set at maximum values (laser power: 100%; scan speed: 100 µm s^{-1}; repetition rate: 20 Hz). Quantification of derived ICP-MS signals was performed as described in the experimental section. Data from the first LA-ICP-MS experiments revealed a great discrepancy with liquid ICP-MS results. Concentration levels obtained via LA-ICP-MS were from 2 to 10 times lower than the corresponding values resulting from conventional analysis for all of the elements under investigation. The main differences were found for DLPI stages with the highest mass loadings, that registered relative standard deviations of replicates analysis always > 50%. Therefore, because of the significant underestimation of LA concentrations, special efforts were made to improve the analytical approach with the primary aim of obtaining accurate and reliable results. Three main problems were identified during analysis. As shown in Fig. 1, part of the collected dust could also deposit in the vicinity of the main dust spot. For this reason, the investigated spot area was increased in order to cover the main spot as well as particles possibly deposited in the vicinity, without creating overlaps between the ablation areas of different spots. The final ablation areas reported in Figs. 3 and 4 for sample of group I and II were found to be the best compromise of the aforementioned requirements. In this way, some improvements were achieved (not more than 5%), but results of the LA-ICP-MS method remained still significantly lower than those of the reference method. The most problematic drawback that caused the main discrepancies with ICP-MS results was visually identified during the ablation of the spots with higher dust loads. Specifically, it was found that sometimes during ablation the majority of the collected dust was broken off and thrusted aside. Consequently, most of the dust did not reach the ICP-MS detector in such cases. The use of a focused laser beam instead of defocused conditions was crucial to allow the identification of this problem that probably could not be identified otherwise. In order to find a solution to this challenge, LA parameters (laser beam diameter, laser power, scan speed and repetition rate) were firstly adjusted to try to obtain a final laser fluence that could avoid this effect, without finding any ideal operating conditions. Therefore, some efforts were made to identify a simple pre-treatment approach for dust filters that could help to make the particulate samples suitable for a reproducible LA-ICP-MS analysis. The main reason of this "blow off" effect was due to the high amount of collected dust that created a sort of hard and compact particulate layer easily breakable when ablated. Dust spots were therefore fixed in preliminary experiments with a clear varnish sprayed on the surface of dust filters and, under the optimum LA parameters summarized in Table 3, sample losses were greatly reduced, even though sometimes still present. The problem was completely solved with the pre-treatment procedure well described in the experimental section and finally applied for the analysis of size-segregated PM samples. The 3% glycerol solution used for sample preparation permeated the dust spot (Fig. 6), and after solvent evaporation the remaining glycerol was found to keep the dust spot soft and wet. In this way, due to a combined effect of sample treatment and optimized LA conditions, sample losses were circumvented during sample ablation. Finally, the last improvement step was found to be necessary in order to guarantee a complete ablation of sample spots. Indeed, due to the different mass loads on the various DLPI stages, dust spots were characterized by different thickness that sometimes caused an incomplete ablation of the sample spot when

using a single line scan pattern. For this reason, the ablation schemes were optimized in order to perform multiple ablations of the spot area. As shown in Fig. 7, a significant amount of the collected dust could remain on the filter surface after the first ablation. The addition of a second rectangular pattern in the central section of the ablation area, where the majority of collected particles was concentrated, allowed quantitative ablation of sample spots. Transient signals recorded during consecutive ablation runs (see Figs. 3 and 4) were integrated using the software provided with the ICP-MS instrument. The integral area thus obtained was then used for all further quantitative calculations.

3.2.2 Analytical performance

Calibration curves, limits of detection and quantification. In this study, LA quantitative analysis was accomplished with dried micro-droplet standards prepared on the surface of the same poly(methylmethacrylate) slides used for sample filters. For each element, two sets of calibration curves were obtained from replicate analysis (n = 3) of dried-droplet standards under the optimized conditions used for dust samples of group I and II, respectively. Signal intensities (normalized to ^{115}In) were then plotted against the actual mass per spot for each element. Table 7 lists the resulting calibration curves, that were appropriately referred to the expected mass range for each element, and the corresponding correlation coefficients (R^2). Within the mass ranges under investigation, all calibration curves were linear. The amount of glycerol added to blank and standard solutions was found to be important to avoid the same blow off effect of dust spots sometimes observed during the analysis of the most concentrated standard residues, without causing any variations in the slope of calibration curves.

LODs of the analyte elements, as ng per spot, together with the RSDs from replicate measurements under the optimum conditions are summarized in Table 8. For concentration in air, LODs and LOQs (ng m^{-3}) were calculated by multiplying the LOD and LOQ per spot with the number of spots per stage, as well as by considering the sampled air volume, thus resulting in different concentration values because of the different number of spot per DLPI stage (Table 9). Detection and quantification limits obtained by LA-ICP-MS were, on average, one order of magnitude lower than those obtained by sample digestion and conventional liquid ICP-MS for all of the analytes under investigation (Tables 5 and 9), including some critical elements (e.g., Fe or Zn) that could be more easily subject to contamination during the analytical process. This is a crucial advantage, especially if considering the low concentration values of some trace metals and the limited amount of PM mass on the smallest DLPI stages. Blank contributions of LA-ICP-MS were found to be slightly more variable than those of liquid ICP-MS, even though the RSDs of blank replicates (n = 6) were always < 13% (Table 8).

Comparison of LA-ICP-MS and conventional ICP-MS methods: precision and accuracy. To verify the accuracy and applicability of the proposed LA-ICP-MS method under the optimized conditions, LA results were compared with data obtained from the analysis of the same size-segregated PM samples via conventional ICP-MS. As previously mentioned, LA-ICP-MS analysis was performed on four different spots on each dust filter, in order to determine the stability and precision of the analytical protocol on real samples. The total elemental amount at each stage was then calculated by multiplying the average elemental mass per spot with the number of spots on the corresponding collection plate. For the same reasons, in order to check the overall uncertainty of ICP-MS results, the same selected filters were

analyzed in triplicate with the conventional ICP-MS method. Table 10 compares the average concentration values obtained via LA-ICP-MS and ICP-MS for each DLPI stage together with the RSDs of replicates. The average RSDs from replicate measurements of dust spots by LA-ICP-MS were < 10% for most of the elements and DLPI stages. RSDs > 10% were observed in rare cases, mostly for very low concentration levels (e.g. few pg m^{-3}). These results revealed a good overall stability and precision of the LA-ICP-MS approach under the optimized conditions, with RSDs that were always comparable, and in some cases better than RSDs obtained with the conventional procedure (Table 10). Fig. 8 displays the slopes and correlation coefficients for the concentration levels of Mn, Fe, Ni, Zn, Ba and Pb determined with both techniques. For each element, only the concentration values > LOQs in both analyses were considered for correlation. Correlation coefficients of the investigated analytes varied between 0.9126 (Ni) and 0.9990 (Fe), while the slope of regression lines ranged from 0.8431 (Ni) to 1.1947 (Fe). Cr and Cu were not depicted because of the few data pairs available for comparison, since the sensitivity of the standard procedure was not low enough to allow quantitative determinations. Results revealed a general good agreement between the LA-ICP-MS approach and the conventional method. Ratios between the average concentration levels obtained via ICP-MS and LA-ICP-MS were quite always around unity and in any case between 0.8 and 1.3, with mean LA-ICP-MS values that fell within the RSDs of ICP-MS replicates. The main discrepancies were found for very low concentration values or for concentration values close to the respective quantification limits. The elemental mass size-distributions of $PM_{2.5}$ obtained from the compared LA-ICP-MS and ICP-MS analysis of real size-segregated samples are depicted in Fig. 9. As mentioned above, it is clear that the better sensitivity of the LA-ICP-MS approach provided more complete information about the mass concentration and size-distribution of the investigated elements, thus allowing to deeper investigate the composition of the most dangerous PM fractions in terms of health concerns. Moreover, the lower detection and quantification limits could enable a shorter sampling period for particles collection, thus improving time resolution in air contamination studies.

In conclusion, the good agreement between LA-ICP-MS and ICP-MS results confirmed the accuracy of analysis under the operating conditions optimized on real samples. The LA treatment procedure identified for sample preparation on poly(methylmethacrylate) slides allowed accurate and reproducible analysis with a simple and fast sample preparation, thus overcoming the laborious pre-treatment approach required for wet chemical digestion of polycarbonate filters, in which also the critical step of cutting the filter into three equal pieces for replicate analysis may affect the precision and reproducibility of conventional measurements. With the proposed LA-ICP-MS approach, risks associated with sample contamination were minimized and the time needed for the application of the whole measurement protocol was reduced. Indeed, as summarized in Table 11, the sample throughput could be increased, with the possibility to analyze a greater number of samples with several sample replicates in the same time required for the established ICP-MS protocol.

4. Conclusions

In this study a novel and reliable LA-ICP-MS measurement protocol for the elemental characterization of size-segregated fine and ultrafine particles was developed. Special emphasis was placed on the optimization of sample pre-treatment steps and LA operating conditions in order to avoid some critical drawbacks and make the particulate samples suitable for an

accurate and reproducible LA-ICP-MS analysis, regardless of the mass loading on each dust filter. Using this approach, eight elements (Cr, Mn, Fe, Ni, Cu, Zn, Ba and Pb) were quantified in nine different particles size ranges. This method provided precise and accurate results, with a better sensitivity than the conventional ICP-MS protocol properly developed for polycarbonate filters. Because of the less-laborious and fast sample preparation and analysis, this method could be used for routine application in order to monitor the elemental concentration and size-distribution of airborne particulates with a suitable precision and accuracy for health and sanitary purposes. In this context, the proposed LA-ICP-MS protocol was applied for the analysis of the extended set of size-segregated PM samples collected in Como, as described in the next chapter.

References

AOAC Guidelines for single laboratory validation of chemical methods, Report, 2002.

Beyersmann, D. and Hartwig, A. (2008). Carcinogenic metal compounds: recent insight into molecular and cellular mechanisms. *Arch. Toxicol.* 82: 493–512.

Cass, G.R., Hughes, L.A., Bhave, P., Kleeman, M.J., Allen J.O. and Salmon, L.G. (2000). The chemical composition of atmospheric ultrafine particles. *Philos. Trans. R. Soc. London, Ser. A* 358: 2581–2592.

Celo, V., Dabek-Zlotorzynska, E., Mathieu, D. and Okonskaia I. (2010). Validation of a simple microwave-assisted acid digestion method using microvessels for analysis of trace elements in atmospheric $PM_{2.5}$ in monitoring and fingerprinting studies. *The Open Chemical and Biomedical Methods Journal* 3: 143–152.

Chow, J.C. and Watson, J.G. (2007). Review of measurements methods and compositions for ultrafine particles. *Aerosol Air Qual. Res.* 7:121–173.

Donaldson, K., Brown, D., Clouter, A., Duffin, R., MacNee, W., RenwickTran, L. and Stone, V. (2002). The pulmonary toxicology of ultrafine particles. *J. Aerosol Med.* 15: 213–220.

Dreetz, C.D. and Lund W. (1992). Air-intake filters used for multi-element analysis of airborne particulate matter by inductively coupled plasma atomic emission spectrometry. *Anal. Chim. Acta* 262: 299–305.

Dreher, K.L., Jaskot, R.H., Lehmann, J.R., Richards, J.H., McGee, J.K., Gio, A.J. and Costa, D.L. (1997). Soluble transition metals mediate residual oil fly ash induced acute lung injury. *J. Toxicol. Environ. Heal*th 50: 285.

Garçon, G., Dagher, Z., Zerimech, F., Ledoux, F., Courcot, D., Aboukais, A., Puskaric, E. and Shirali, P. (2006). Dunkerque City air pollution particulate matter-induced cytotoxicity, oxidative stress and inflammation in human epithelial lung cells (L132) in culture. *Toxicol. in Vitro* 20: 519–528.

Hartwig, A. and Schwerdtle, T. (2002). Interactions by carcinogenic metal compounds with DNA repair processes: toxicological implications. *Toxicol. Lett.* 127(1): 47–54.

Hassan, N., Rasmussen, P., Dabek-Zlotorzynska, E., Celo, V. and Chen, H. (2007). Analysis of environmental samples using microwave-assisted acid digestion and inductively coupled plasma mass spectrometry: maximizing total elemental recoveries. *Water Air Soil Pollut.* 178(1–4): 323–334.

Herner, J.D., Green, P.G. and Kleeman, M.J. (2006). Measuring the trace elemental composition of size-resolved airborne particles. *Environ. Sci. Technol.* 40(6): 1925–1933.

Hsieh, Y.-K., Chen, L.-K., Hsieh, H.-F., Huang, C.-H. and Wang, C.-F. (2011). Elemental analysis of airborne particulate matter using an electrical low-pressure impactor and laser ablation/inductively coupled plasma mass spectrometry. *J. Anal. At. Spectrom.* 26: 1502–1508.

International Agency for Research on Cancer. (1980). Monograph on the evaluation of the carcinogenic risk of chemicals to humans, vol. 23, Some metals and metallic compounds. IARC, Lyon.

International Agency for Research on Cancer. (1990). Monograph on the evaluation of the carcinogenic risk to humans, vol. 49, Chromium, nickel and welding. IARC, Lyon.

Karthikeyan, S., Joshi, U.M. and Balasubramanian, R. (2006) Microwave assisted sample preparation for determining water-soluble fraction of trace elements in urban airborne particulate matter: Evaluation of bioavailability. *Anal. Chim. Acta* 576(1): 23–30.

Li, N., Sioutas, C., Cho, A., Schmitz, D., Misra, C., Sempf, J., Wang, M., Oberley, T., Froines, J. and Nel, A. (2003). Ultrafine particulate pollutants induce oxidative stress and mitochondrial damage. *Environ. Health Persp.* 111(4): 455–460.

Lin, C.-C., Chen, S.-J., Huang, K.-L., Hwang, W.-I., Chang-Chien, G.-P. and Lin, W.-Y. (2005). Characteristics of metals in nano/ultrafine/fine/coarse particles collected beside a heavily trafficked road. *Environ. Sci. Technol.* 39: 8113–8122.

Miranda, R. and Tomaz, E. (2008). Characterization of urban aerosol in Campinas, São Paulo, Brazil. *Atmos. Res.* 87(2): 147–157.

Ntziachristos, L., Ning, Z., Geller, M.D., Sheesley, R.J., Schauer, J.J. and Sioutas, C. (2007). Fine, ultrafine and nanoparticle trace element compositions near a major freeway with a high heavy-duty diesel fraction. *Atmos. Environ.* 41: 5684–5696.

Oberdörster, G., Oberdörster, E. and Obertörster, J. (2005). Nanotoxicology: an emerging discipline evolving from studies of ultrafine particles. *Environ. Health Persp.* 113: 823–839.

Ostro, B., Hu, J., Goldberg, D., Reynolds, P., Hertz, A., Bernstein, L. and Kleeman, M.J. (2015). Associations of mortality with long-term exposures to fine and ultrafine particles, species and sources: results from the California teachers study cohort. *Environ. Health Persp.* (Online) 123(6): 549.

Pekney, N.J. and Davidson, C.I. (2005). Determination of trace elements in ambient aerosol samples. *Anal. Chim. Acta* 540: 269–277.

Raaschou-Nielsen, O. *et al.* (2016). Particulate matter air pollution components and risk for lung cancer. *Environ. Int.* 87: 66–73.

Robache, A., Mathé, F., Galloo, J.C. and Guillermo R. (2000). Multi-element analysis by inductively coupled plasma optical emission spectrometry of airborne particulate matter collected with a low-pressure cascade impactor. *Analyst* 125: 1855–1859.

Sun, G., Crissman, K., Norwood, J., Richards, J., Slade, R. and Hatch, G.E. (2001). Oxidative interactions of synthetic lung epithelial lining fluid with metals-containing particulate matter. *Am. J. Physiol. Lung Cell. Mol. Physiol.* 281: L807–L815.

Terzi, E., Argyropoulos, G., Bougatioti, A., Mihalopoulos, N., Nikolaou, K. and Samara, C. (2010). Chemical composition and mass closure of ambient PM_{10} at urban sites. *Atmos. Environ.* 44(18): 2231–2239.

Toscano, G., Gambaro, A., Capodoglio, G., Cairns, W.R.L. and Cescon, P. (2009). Assessment of a procedure to determine trace and major elements in atmospheric aerosol. *J. Environ. Monitor.* 11(1): 193–199.

Tuch, Th., Brand, P., Wichmann, H. E. and Heyder, J. (1997). Variation of particle number and mass concentration in various size ranges of ambient aerosols in Eastern Germany. *Atmos. Environ.* 31(24): 4193–4197.

UNI EN 14907: 2005. Ambient air quality – Standard gravimetric measurement method for the determination of the PM2.5 mass fraction of suspended particulate matter.

UNI EN 12341: 2014. Air Quality – Determination of the PM10 fraction of suspended particulate matter. Reference method and field test procedure to demonstrate reference equivalence of measurements methods.

Viksna, A., Lindgren, E.S., Standzenieks, P. and Jakobsson, J. (2004). EDXRF and TXRF analysis of elemental size distributions and environmental mobility of airborne particles in the city of Riga, Latvia. *X-ray Spectrom.* 33(6): 414–420.

Wagner, A., Boman, J. and Gatari, M.J. (2008). Elemental analysis of size-fractionated particulate matter sampled in Göteborg, Sweden. *Spectrochim. Acta, Part B* 63: 1426–1431.

Wagner, A. and Mages, M. (2010). Total-reflection X-ray fluorescence analysis of elements in size-fractionated particulate matter sampled on polycarbonate filters - Composition and sources of aerosol particles in Göteborg, Sweden. *Spectrochim. Acta, Part B* 65: 471–477.

Wang, C.-F., Miau, T.T., Perng, J.Y., Yeh, S.J., Chiang, P.C., Tsai, H.T. and Yang, M.H. (1989). Multi-element analysis of airborne particulate matter by inductively coupled plasma atomic emission spectrometry. *Analyst* 114: 1067–1070.

This chapter is based on:

- **Rovelli, S.**, Nischkauer, W., Cavallo D.M. and Limbeck, A. Multi-element analysis of size-segregated fine and ultrafine particulate via Laser Ablation-Inductively Coupled Plasma-Mass Spectrometry*, in preparation.*

- Limbeck, A., **Rovelli, S.**, Bonta, M., Nischkauer, W., Cavallo, D.M. Analysis of toxic trace metals in ultrafine airborne particulates using LA-ICP-MS. In: Conference Proceedings of the European Symposium on Atomic Spectrometry (ESAS 2016), Eger, Hungary, 31st March – 2nd April, 2016 (http://www.esas2016.mke.org.hu/images/downloads/ESAS2016_book_of_abstracts_web.pdf).

Tables

Table 1. Number of spots and cut points (D50%) for each DLPI collection stage. The particle loadings (mass per stage and mass per spot on each stage) collected during a typical winter monitoring session are also reported.

DLPI stage	Number of spots	D50% (µm)	PM mass loading (µg)	
			Per stage	Per spot on each stage
1	207	0.0283	36	0.2
2	174	0.0559	149	0.9
3	63	0.0944	297	4.7
4	57	0.157	889	15.6
5	81	0.262	1313	16.2
6	150	0.383	1718	11.5
7	144	0.614	734	5.1
8	60	0.950	402	6.7
9	51	1.60	305	6.0
10	42	2.40	504	12.0
11	9	4.00	376	41.8
12	1	6.60	412	412.0
13	1	9.97	1113	1113.0

Table 2. Operating parameters of the ICP-MS instrumentation for wet chemical analysis.

ICP-MS	**Thermo iCAP Q**
Plasma power	1550 W
Plasma gas flow rate	15 L min^{-1}
Nebulizer gas flow rate	0.94 L min^{-1}
Auxiliar gas flow rate	3.00 L min^{-1}
Dwell time per isotope	0.01 s
Measured isotopes in KED modus	^{53}Cr, ^{55}Mn, ^{57}Fe, ^{60}Ni, ^{65}Cu, ^{66}Zn, ^{138}Ba, ^{206}Pb, ^{115}In (Internal Standard)

Table 3. Final operating parameters of the LA-ICP-MS instrumentation.

LA	**NWR 213 nm Nd:YAG**	
	Group I	**Group II**
Scan pattern	Line scan	Line scan
Spot diameter	150 µm	150 µm
Laser power	60%	80%
Scan speed	70 µm s^{-1}	80 µm s^{-1}
Laser fluence	3.1 J cm^{-2}	6.4 J cm^{-2}
Repetition rate	20 Hz	20 Hz
Carrier gas flow	0.8 L min^{-1} He	0.8 L min^{-1} He
Total time of LA process	354 s	435 s
ICP-MS	**Thermo iCAP Q**	
Plasma power	1550 W	
Plasma gas flow rate	15 L min^{-1}	
Nebulizer gas flow rate	0.8 L min^{-1}	
Auxiliar gas flow rate	3.00 L min^{-1}	
Dwell time per isotope	0.01 s	

Table 4. Slopes and percentage of variation between aqueous calibration, PC blank-matched calibration and dust-matched calibration.

Element	Slope [counts ppb^{-1}]			% variation (aqueous vs PC blank-matched)	% variation (aqueous vs dust-matched)
	Aqueous calibration	PC blank-matched	dust-matched		
^{53}Cr	8717	8619	8595	1.1	1.4
^{55}Mn	10074	10159	9986	0.8	0.9
^{57}Fe	320	308	310	3.8	3.1
^{60}Ni	2947	2913	2916	1.2	1.1
^{65}Cu	3772	3753	3727	0.5	1.2
^{66}Zn	3035	2958	2995	2.5	1.3
^{138}Ba	50691	49902	48743	1.6	3.8

Table 5. Limits of detection (ng m^{-3}) obtained after PC blank digestion and ICP-MS analysis (n = 7). The relative standard deviations (RSDs) of replicates are also reported.

Element	LOD (3σ)	RSD (%)
^{53}Cr	0.1	5.5
^{55}Mn	0.08	4.0
^{57}Fe	1.6	11.7
^{60}Ni	0.04	6.7
^{65}Cu	0.9	2.5
^{66}Zn	0.5	5.3
^{138}Ba	0.06	3.0
^{206}Pb	0.01	2.5

Table 6. Elemental recoveries from NIST SRM 1648a after sample pre-treatment and ICP-MS analysis (n = 10). Concentration values obtained using external aqueous calibration (EAC) and standard addition (SA) are both reported.

Element	SRM certified concentration [mean ± SD]	Results from ICP-MS analysis [mean ± SD (RSD)]		% Recovery (SD)[a]
		EAC	SA	
	%			
^{57}Fe	3.92 ± 0.21	3.42 ± 0.10 (3.0%)	3.41 ± 0.18 (5.2%)	87 (2.6)
^{206}Pb	0.655 ± 0.033	0.677 ± 0.008 (1.2%)	0.671 ± 0.011 (1.6%)	103 (1.3)
	mg Kg^{-1}			
^{53}Cr	402 ± 13	364 ± 14 (3.8%)	358 ± 30 (8.5%)	90 (3.4)
^{55}Mn	790 ± 44	791 ± 64 (8.1%)	793 ± 33 (4.2%)	100 (8.1)
^{60}Ni	81.1 ± 6.8	85.4 ± 4.0 (4.7%)	92.0 ± 6.5 (7.0%)	105 (5.0)
^{65}Cu	610 ± 70	602 ± 29 (4.9%)	617 ± 61 (9.8%)	99 (4.8)
^{66}Zn	4800 ± 270	4635 ± 213 (4.6%)	5136 ± 448 (8.7%)	97 (4.4)
^{138}Ba[b]	546–577	597 ± 13 (2.2%)	600 ± 23 (3.8%)	106 (2.3)

[a] The percent ratios are referred to the concentration values obtained via external aqueous calibration; [b] Non certified value: concentrations from the Database on Geochemical, environmental and biological Reference Materials (GeoReM).

Table 7. Calibration curves and correlation coefficients for all the elements under investigation obtained with the optimized conditions for samples of group I and II.

Element	Range for calibration curve (mass per spot [ng])	Slope (x 10^4) [counts ng^{-1}]	Intercept (x 10^3) [counts]	Correlation coefficient (R^2)
Group I (DLPI stages 1-7)				
^{53}Cr	0–5	63.2	1.6	0.9994
^{55}Mn	0–5	936.1	–270.9	0.9996
^{57}Fe	0–25	18.2	19.2	0.9993
^{60}Ni	0–5	124.1	–7.2	0.9992
^{65}Cu	0–15	148.1	138.3	0.9956
^{66}Zn	0–25	155.7	81.9	0.9959
^{138}Ba	0–5	2600.4	–825.0	0.9994
^{206}Pb	0–15	1242.0	–384.8	0.9997
Group II (DLPI stages 8-9)				
^{53}Cr	0–5	43.4	–0.1	0.9991
^{55}Mn	0–5	353.4	–15.5	0.9989
^{57}Fe	0–250	8.3	104.6	0.9986
^{60}Ni	0–5	108.1	1.9	0.9998
^{65}Cu	0–25	125.4	129.3	0.9966
^{66}Zn	0–25	36.1	79.0	0.9900
^{138}Ba	0–25	1750.0	7.1	0.9997
^{206}Pb	0–5	930.2	38.2	0.9998

Table 8. Limits of detection (ng) obtained after LA-ICP-MS analysis under the optimum conditions for samples of group I and II. The relative standard deviations (RSDs) of blank replicates (n = 6) are also reported.

Element	Group I		Group II	
	LOD (3σ)	RSD (%)	LOD (3σ)	RSD (%)
^{53}Cr	0.02	4.3	0.03	9.3
^{55}Mn	0.001	5.2	0.002	8.7
^{57}Fe	0.06	9.4	0.06	11.2
^{60}Ni	0.004	12.3	0.002	7.8
^{65}Cu	0.03	5.6	0.007	12.2
^{66}Zn	0.02	8.3	0.03	4.0
^{138}Ba	0.002	11.7	0.003	8.6
^{206}Pb	0.001	7.2	0.002	8.3

Table 9. Limits of detection and quantification (ng m^{-3}) obtained after LA-ICP-MS analysis under the optimum conditions for each DLPI stage.

DLPI stage (Particle mass range [µg])	^{53}Cr	^{55}Mn	^{57}Fe	^{60}Ni	^{65}Cu	^{66}Zn	^{138}Ba	^{206}Pb
	LOD (3σ)							
1 (0.0283–0.0559)	0.06	0.003	0.2	0.01	0.07	0.06	0.005	0.003
2 (0.0559–0.0944)	0.05	0.002	0.1	0.009	0.06	0.05	0.005	0.002
3 (0.0944–0.157)	0.02	0.001	0.05	0.003	0.02	0.02	0.002	0.001
4 (0.157–0.262)	0.02	0.001	0.04	0.003	0.02	0.02	0.002	0.001
5 (0.262–0.383)	0.02	0.001	0.06	0.004	0.03	0.03	0.002	0.001
6 (0.383–0.614)	0.04	0.002	0.1	0.008	0.05	0.05	0.004	0.002
7 (0.614–0.950)	0.04	0.002	0.1	0.008	0.05	0.04	0.004	0.002
8 (0.950–1.6)	0.03	0.002	0.05	0.002	0.006	0.02	0.002	0.002
9 (1.6–2.4)	0.02	0.001	0.04	0.001	0.005	0.02	0.002	0.001
	LOQ (10σ)							
1 (0.0283–0.0559)	0.2	0.005	0.5	0.03	0.2	0.2	0.02	0.005
2 (0.0559–0.0944)	0.2	0.005	0.4	0.03	0.2	0.2	0.01	0.005
3 (0.0944–0.157)	0.06	0.002	0.2	0.01	0.07	0.06	0.005	0.002
4 (0.157–0.262)	0.05	0.002	0.1	0.009	0.06	0.06	0.005	0.002
5 (0.262–0.383)	0.08	0.002	0.2	0.01	0.1	0.09	0.006	0.002
6 (0.383–0.614)	0.1	0.004	0.4	0.02	0.2	0.2	0.01	0.004
7 (0.614–0.950)	0.1	0.004	0.4	0.02	0.2	0.1	0.01	0.004
8 (0.950–1.6)	0.08	0.004	0.2	0.006	0.02	0.08	0.009	0.004
9 (1.6–2.4)	0.07	0.003	0.1	0.005	0.02	0.07	0.007	0.003

Table 10. Elemental concentration values (ng m^{-3}) obtained from the analysis of size-segregated PM samples via LA-ICP-MS and conventional ICP-MS for each DLPI stage. Relative standard deviations (RSDs) are referred to n = 3 replicates for ICP-MS and n = 4 replicates for LA-ICP-MS.

DLPI stage (Particle mass range [µg])	^{53}Cr				^{55}Mn				^{57}Fe				^{60}Ni			
	ICP-MS		LA-ICP-MS		ICP-MS		LA-ICP-MS		ICP-MS		LA-ICP-MS		ICP-MS		LA-ICP-MS	
	Conc.	RSD (%)	Conc.	RSD (%)	Conc.	RSD (%)	Conc.	RSD (%)	Conc.	RSD (%)	Conc.	RSD (%)	Conc.	RSD (%)	Conc.	RSD (%)
1 (0.0283–0.0559)	< LOQ	–	0.17	5.0	< LOQ	–	< LOQ	–	< LOQ	–	< LOQ	–	< LOQ	–	< LOQ	–
2 (0.0559–0.0944)	< LOQ	–	0.16	6.8	< LOQ	–	0.01	11.1	< LOQ	–	< LOQ	–	< LOQ	–	0.06	11.4
3 (0.0944–0.157)	< LOQ	–	0.07	3.9	< LOQ	–	0.02	12.1	< LOQ	–	0.44	8.3	0.25	12.7	0.18	8.0
4 (0.157–0.262)	< LOQ	–	0.15	6.0	< LOQ	–	0.22	4.6	< LOQ	–	2.35	5.5	0.62	8.2	0.53	3.8
5 (0.262–0.383)	< LOQ	–	0.24	5.4	0.51	5.5	0.45	7.1	5.55	17.7	4.66	11.4	0.45	12.7	0.41	8.2
6 (0.383–0.614)	< LOQ	–	0.38	3.5	1.17	1.6	1.18	3.8	14.16	9.4	13.28	3.2	0.40	10.5	0.44	5.4
7 (0.614–0.950)	< LOQ	–	0.35	5.0	0.89	2.7	0.80	6.7	28.17	4.3	24.82	5.8	0.17	3.6	0.17	7.4
8 (0.950–1.6)	< LOQ	–	0.75	5.3	1.56	8.3	1.36	4.9	130.26	3.7	140.86	4.5	0.16	14.2	0.20	6.1
9 (1.6–2.4)	0.92	9.9	0.98	5.7	1.92	8.9	1.76	2.3	187.71	9.7	201.84	3.3	0.27	11.1	0.24	4.6
DLPI stage (Particle mass range [µg])	^{65}Cu				^{66}Zn				^{138}Ba				^{206}Pb			
	ICP-MS		LA-ICP-MS		ICP-MS		LA-ICP-MS		ICP-MS		LA-ICP-MS		ICP-MS		LA-ICP-MS	
	Conc.	RSD (%)	Conc.	RSD (%)	Conc.	RSD (%)	Conc.	RSD (%)	Conc.	RSD (%)	Conc.	RSD (%)	Conc.	RSD (%)	Conc.	RSD (%)
1 (0.0283–0.0559)	< LOQ	–	< LOQ	–	< LOQ	–	< LOQ	–	< LOQ	–	< LOQ	–	0.11	2.3	0.09	2.3
2 (0.0559–0.0944)	< LOQ	–	0.08	12.7	< LOQ	–	< LOQ	–	< LOQ	–	< LOQ	–	0.35	11.5	0.31	6.6
3 (0.0944–0.157)	< LOQ	–	0.10	7.1	< LOQ	–	0.74	10.2	< LOQ	–	0.01	3.4	0.76	2.1	0.59	3.1
4 (0.157–0.262)	< LOQ	–	0.45	4.6	7.07	11.3	6.46	3.5	< LOQ	–	0.04	0.7	2.56	14.0	2.29	4.0
5 (0.262–0.383)	< LOQ	–	0.52	7.8	8.12	11.9	7.46	7.8	< LOQ	–	0.07	3.1	2.88	15.1	2.71	7.3
6 (0.383–0.614)	< LOQ	–	0.98	5.3	12.83	4.7	13.03	6.5	0.35	0.9	0.32	1.7	3.95	1.8	4.22	4.1
7 (0.614–0.950)	< LOQ	–	1.07	7.4	8.37	11.0	8.58	8.9	0.77	7.0	0.85	3.2	1.65	1.3	1.85	3.5
8 (0.950–1.6)	3.93	10.8	3.66	6.4	6.75	9.3	5.92	4.5	3.47	8.5	3.74	6.0	1.01	11.2	0.96	5.0
9 (1.6–2.4)	6.83	10.2	6.57	6.3	3.67	8.4	2.97	5.8	5.21	5.2	5.06	2.6	0.44	10.0	0.34	3.3

– data not available

Table 11. Schematic comparison of times required for sample preparation and analysis with the conventional ICP-MS method and the proposed LA-ICP-MS approach.

		ICP-MS		**LA-ICP-MS**	
		Lab procedure	**Time required**	**Lab procedure**	**Time required**
Per DLPI stage	**Sample preparation**	Beaker cleaning	5h	Sample application on poly(methylmethacrylate) slides	40 mins
		Sample pre-treatment	24h		
		Sample dilution for liquid analysis	4h	Identification of spots for LA	1h
	Sample analysis	–	3 mins per liquid solution	–	about 7 mins per spot about 30 mins for 4 spots
For 21 DLPI stages		Considering an heating block of 24 places for sample pre-treatment (21 samples + 3 PC blank filters)	About 34h (**4 working days**) **without any replicate per stage**	Considering 7 filters per slide, 2 filter-slides in the laser chamber + 1 slide for calibration	About 14h (**less than 2 working days**) with **4 replicates per stage**

Figures

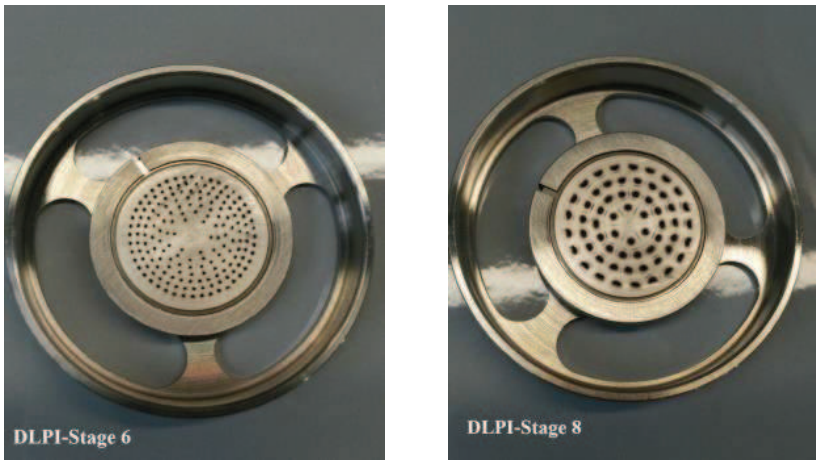

Figure 1. Polycarbonate dust filters fixed onto the DLPI collection plates.

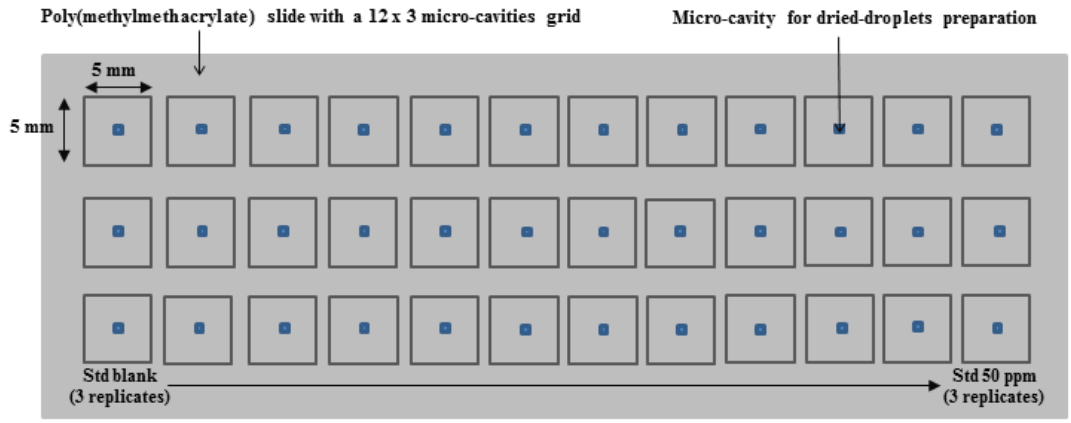

Figure 2. Schematic representation of the arrangement used for the preparation of dried micro-droplets of standard solutions.

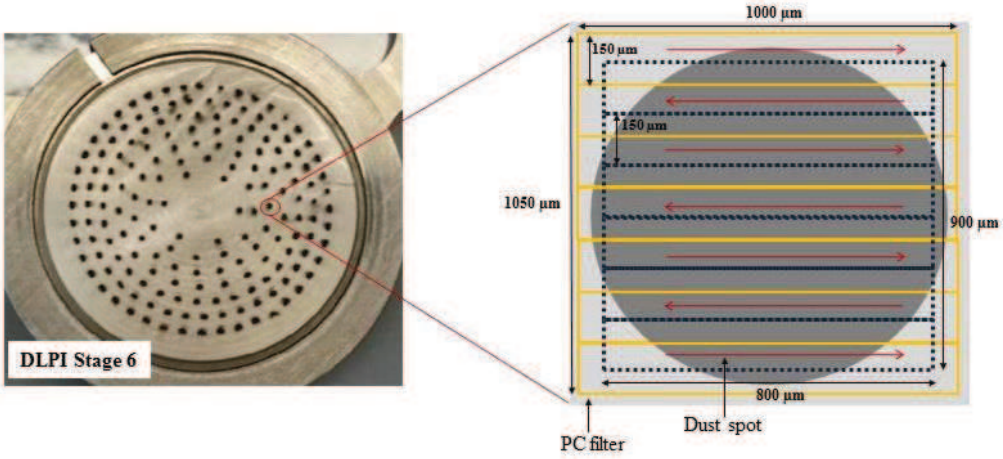

Figure 3. Ablation scheme I used for dust spots of group I (DLPI stages 1-7).

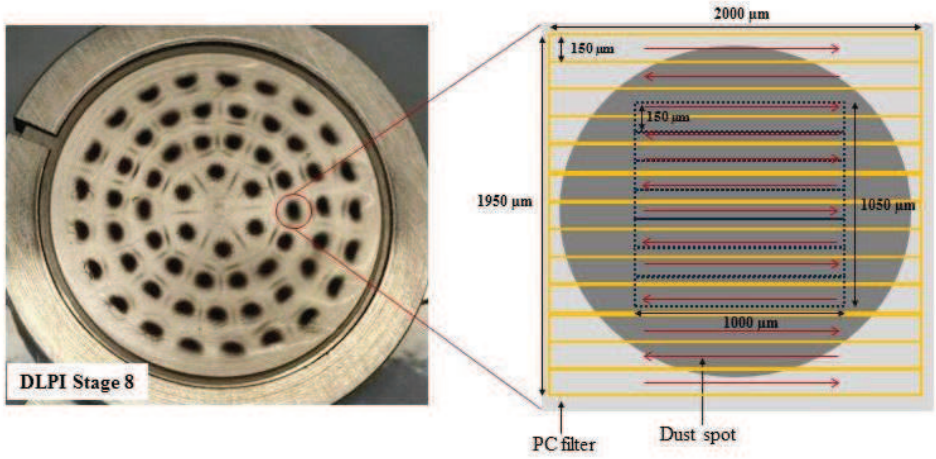

Figure 4. Ablation scheme II used for dust spots of group II (DLPI stages 8 and 9).

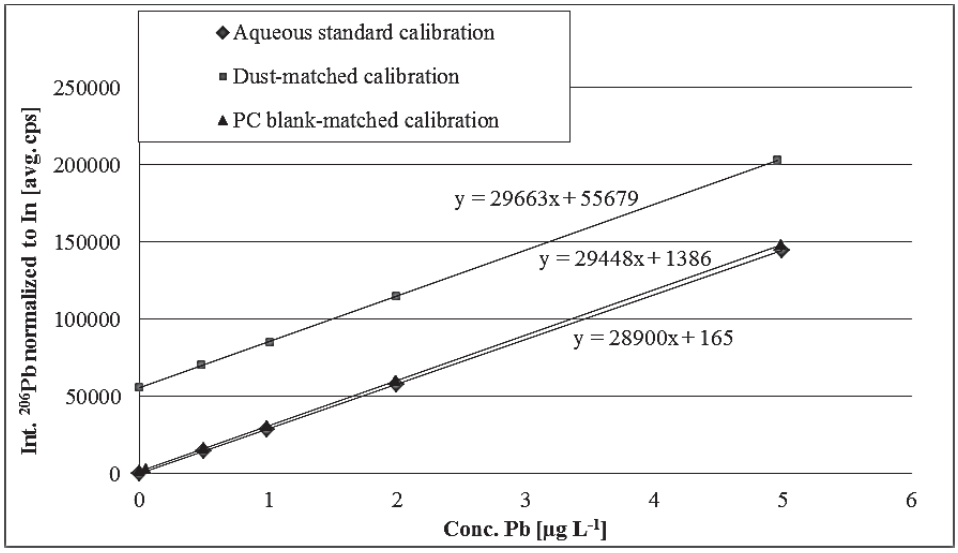

Figure 5. Comparison between aqueous standard calibration and matrix-matched calibrations. Signal intensities (normalized to ^{115}In) plotted against the actual concentrations of lead are reported as example.

Figure 6. Schematic representation of the treatment approach applied on PM samples before LA-ICP-MS analysis.

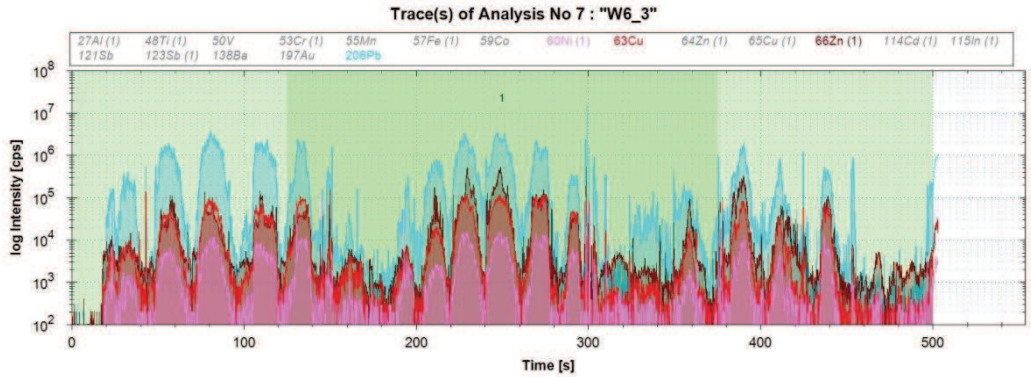

Figure 7. Transient signals derived from the analysis of one spot of DLPI stage n° 6 with the proposed ablation scheme for group I and the optimized LA operating conditions.

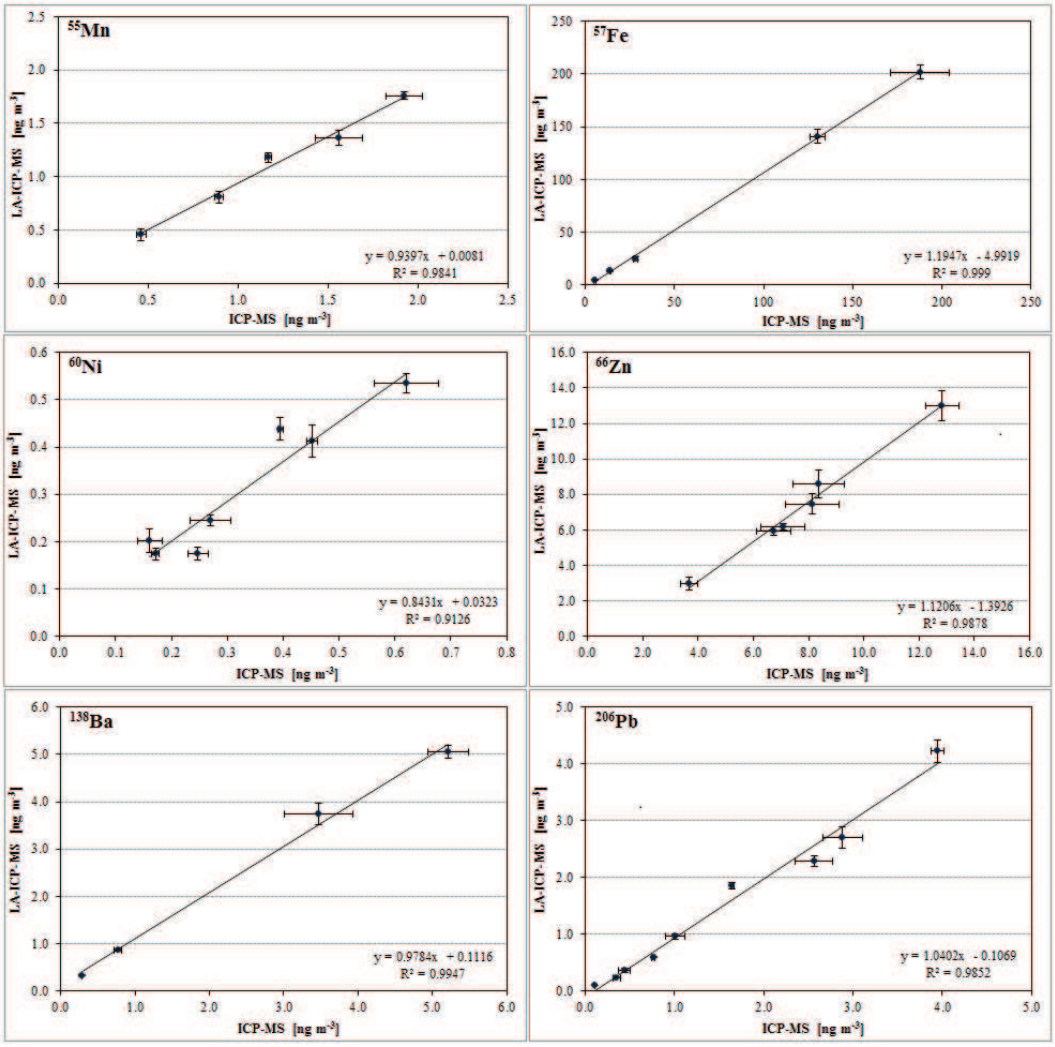

Figure 8. Correlation between the concentration values obtained via conventional ICP-MS (n = 3) and LA-ICP-MS (n = 4). Error bars correspond to 1 standard deviations of replicates.

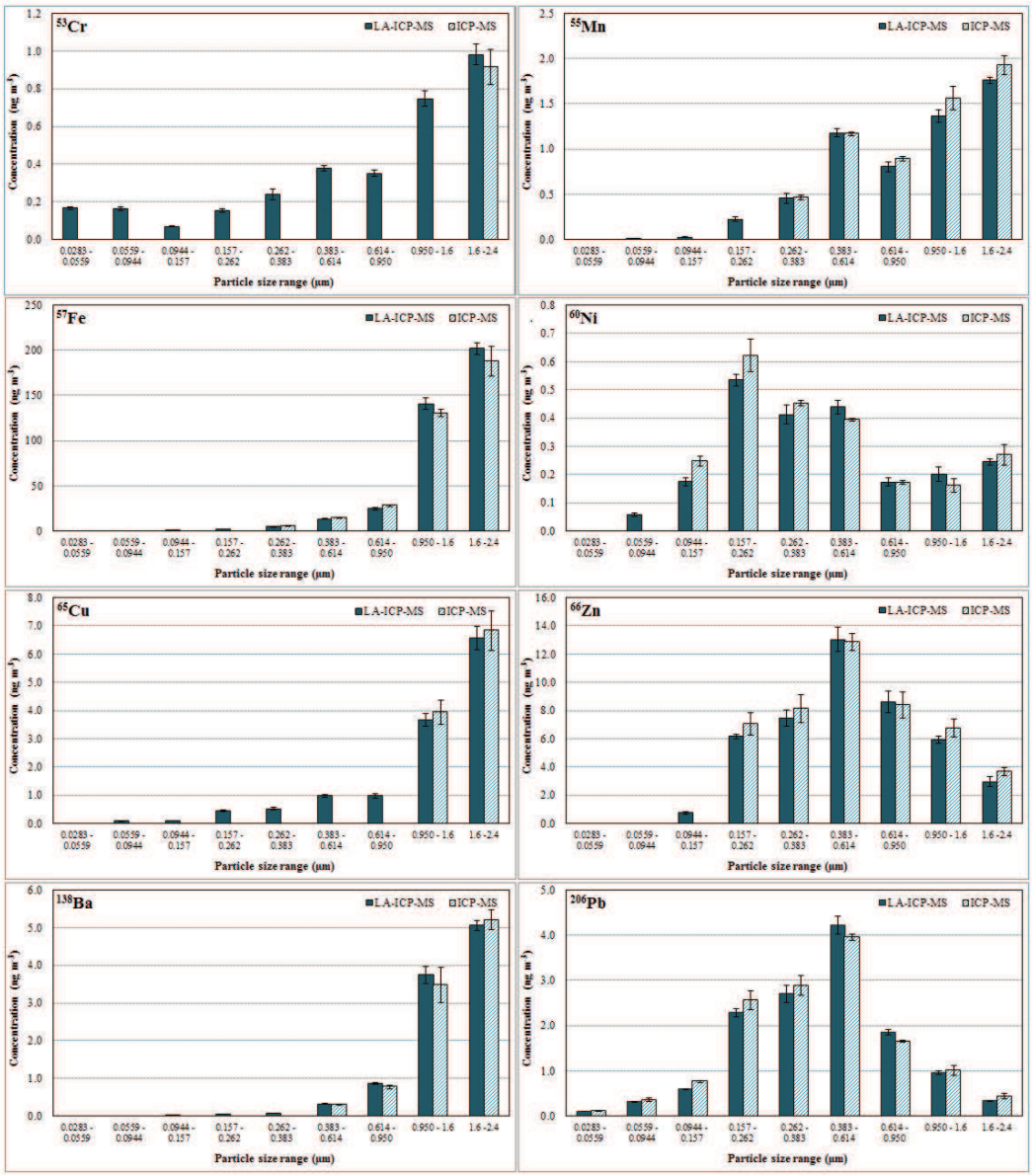

Figure 9. Mass size-distribution for all the elements under investigation. Results from LA-ICP-MS (n = 4) and conventional ICP-MS (n = 3) methods are both reported. Error bars correspond to 1 standard deviation of replicates. Only concentration values > LOQs were depicted in the histograms.

Chapter 4 – *Toxic Trace Metals in Airborne Particulates: Mass Concentration, Size-Distribution and Health Risk Assessment*

Abstract

In this chapter the mass concentrations of selected trace metals (Cr, Mn, Fe, Ni, Cu, Zn, Ba and Pb) measured on the extended set of PM samples collected at the URB site in Como are presented. Size-segregated $PM_{2.5}$ samples were analyzed with a novel LA-ICP-MS method specifically developed, as outlined in the previous chapter. On average, the investigated elements accounted for a very small percentage of the total $PM_{2.5}$ mass concentration (< 0.7 %) and results revealed great variations in the concentration levels of the analyzed toxic metals, with values differing by one or more orders of magnitude from element to element and between the different sampling periods. Obtained findings showed distinct differences for the analyzed elements, with different and characteristic size-distributions in the fine, submicrometric and ultrafine fractions. The studied elements were variously enriched in the particulate sizes, suggesting that local emission sources may exist for these chemical species. Moreover, from a health and sanitary perspective, the hazard quotient and index values calculated for all of the studied elements suggested no non-carcinogenic health risks via the inhalation exposure route. Also the carcinogenic risks of Cr and Ni were within the acceptability range.

Nevertheless, only preliminary and qualitative evaluations have been performed, since the extended dataset has to be deeply investigate with further analysis in order to gain further insights and contribute to a better evaluation of seasonal variabilities, possible influences of meteorological parameters as well as to the quali-quantitative identification of possible emission sources in the study area.

*1. **Introduction***

As well documented in the scientific literature, the adverse effects of airborne particulate matter (PM) on human health are associated with its size and chemical composition (Harrison and Yin, 2000; Valavanidis *et al.*, 2008; Polichetti *et al.*, 2009), although the precise biological mechanisms of PM toxicity are not completely clear (Oeder *et al.*, 2012). These effects range from minor upper respiratory irritation to chronic respiratory and hearth disease, lung cancer, acute respiratory infection in children and chronic bronchitis in adults (Kampa and Castanas, 2008; Peled, 2011). Fine particles ($PM_{2.5}$), and especially submicrometric (PM_1) and ultrafine particles (UFPs, $PM_{0.1}$), can penetrate deeper into the lungs and stay there for a long time, thus being able to enter more easily the blood circulation system. The presence of different chemical compounds may pose serious health concerns and, in terms of adverse health effects, the distribution of toxic compounds among the various size fractions is of primary relevance. Although PM is a complex and heterogeneous mixture of different substances, trace metals represent an important source of PM toxicity because of their toxic characters, as well documented in the scientific literature. Several works suggested correlations between PM-bound metals and pulmonary toxicity (Sun et al., 2001; Raaschou-Nielsen et al., 2016). According to the International Agency for Research on Cancer (IARC), As, Cd, Cr (VI) and Ni compounds are classified as carcinogenic to humans (IARC Working Group on the Evaluation of Carcinogenic Risks to Humans, 2012) whereas inorganic Pb compounds are classified as probable carcinogens (IARC Working Group on the Evaluation of Carcinogenic Risks to

Humans, 2006). Accumulation in fatty tissues and circulatory system, negative effects on central nervous system and internal organs as well as acting as cofactors in other diseases are some of the health effects associated with the exposure to these metals (Chen and Lippmann, 2009; Kurt-Karatus, 2012). On the other hand, less toxic elements, such as Fe, Zn or Mn, seem to play an important role in the formation of oxidants within the lung which in turn produce tissue damage (Ghio *et al.*, 1996).

Literatures studies about the size-segregated metal composition of PM were conducted worldwide in the United States (Sardar et al., 2005; Ning et al., 2007; Ntziachristos et al., 2007), Asia (Li *et al.*, 2012; Sun *et al.*, 2013; Liu *et al.*, 2015), Europe (Pakkanen *et al.*, 2001; Mbengue *et al.*, 2014; Malandrino *et al.*, 2016). Among all these investigations, researches about the health risk for humans associated with PM-bound toxic elements are few and even fewer are those studies concerning the health risk characterization of size-segregate PM, with the aim of assessing the contribution of the various PM fractions to the total $PM_{2.5}$ or PM_{10} health risk. Greene and Morris (2006) found that $PM_{2.5}$ in the Washington area posed notable deleterious risks to subpopulations. Cao *et al.* (2012) and Liu *et al.* (2015) showed that the particle size had a significant influence on the human exposure risk assessment.

In this study, the mass concentrations of size-segregated trace metals (Cr, Mn, Fe, Ni, Cu, Zn, Ba and Pb) were measured on the extended set of size-segregated PM samples collected during an intensive long-term monitoring campaign at an urban background site in Como, as described in Chapter 2. In addition to the assessment of ambient concentration levels, enrichment factors and size-distributions of the selected trace elements, results were used to evaluate their potential non-carcinogenic and carcinogenic risks for human health via the inhalation exposure route. It has to be noticed that the findings showed in this chapter are derived from a preliminary and general data treatment, which has to be deeply investigated with further analysis in order to gain further insights and contribute to a better evaluation of seasonal variabilities, possible influences of meteorological parameters as well as to the identification of possible emission sources in the study area.

2. Materials and Methods

2.1. Size-Segregated PM Collection and Analysis

Airborne PM was collected at an outdoor urban background site in Como, as well described in chapter 2. A 13-stage Low Pressure Impactor (DLPI, DEKATI Ltd., Tampere, Finland) was used for the collection of size-segregated particles in the 0.028–10 μm size range, with 9 collection stages in the $PM_{2.5}$ fraction. Atmospheric samplings were performed once a week, from Monday to Friday morning, using an average sampling period of 96-h. The monitoring campaign started at the end of May 2015 and was stopped at the end of March 2016, thus obtaining a large number of samples (38 weekly sampling sessions) covering an extended time period in order to gain sufficient information for assessing temporal variabilities and differences in the elemental mass concentration and composition of airborne particulates. Aerosol particles were deposited on high-purity polycarbonate filters (PC, 25-mm; no-holes, Fisher Scientific, S.A.S., Illkirch, France) coated with a thin layer of Apiezon-L grease provided by the manufacturer (DEKATI DS-515 Collection Substrate Spray, DEKATI Ltd., Tampere, Finland) to improve the impactor collection efficiency and prevent bounce- and blow-off effects during separation. The particle mass collected on PC filters was determined gravimetrically following a standard operating procedure (UNI EN 14907; UNI EN 12341).

The collection substrates were weighed before and after sampling under controlled temperature (20 ± 1°C) and relative humidity (50 ± 5%) conditions by a micro-balance with a readability of 1 μg (Gibertini 1000, Novate, Milan, Italy). The collected mass was then calculated by differential weighing. After being weighed, particulate samples were stored in clean plastic boxes, in the dark and at 4°C until elemental analysis. Two sets of the collected PM samples were used for the improvement and optimization of the LA-ICP-MS method presented in chapter 3. For all of the other weekly samples, each $PM_{2.5}$ size fraction was then directly analyzed with the proposed LA-ICP-MS measurement protocol and eight elements were determined (Cr, Mn, Fe, Ni, Cu, Zn, Ba and Pb). Briefly, size-fractionated PM samples were divided into two main groups, namely DLPI stages 1-7 (group I) and DLPI stages 8-9 (group II), and analyzed separately, with proper LA operating conditions and calibration curves. One quarter of each polycarbonate filter was cut by means of a ceramic knife and attached on the surface of poly(methylmethacrylate) slides, for a total of seven different samples per slide, together with one quarter of PC blank filter. After the pre-treatment procedure with a 3% glycerol solution (well described in the previous chapter), dust filter were analyzed in LA-ICP-MS under the optimized conditions. Because of the elevated number of size-segregated samples under investigation (a total of 324 dust filters), in routine analysis calibration curves and quality control standards were always analyzed with unknown samples. A typical analytical sequence consisted of a calibration curve followed by the analysis of unknown dust samples (four spots per stage) along with two quality control standards (typically 0.15 and 1 mg L^{-1}) and a second calibration curve. Moreover, when using a new calibration for quantitative analysis, one dust samples already analyzed with the previous calibration curve was analyzed again as a new unknown sample to verify the overall stability of the measurement protocol. Dust samples as well as blank PC filters and standards for calibration were analyzed by multiple line scan of each sample spot and quantitative analysis was accomplished with dried-micro droplets of aqueous standard solutions prepared on the same slides used for sample filters. All concentration values for dust samples were obtained after subtraction of their appropriate blank contributions, if blank values were > LOQs. For detailed information about the optimized laser ablation schemes and the final operating parameters of the LA-ICP-MS instrumentation see chapter 3.

2.2. Exposure Dose and Health Risk Assessment

Generally, the population exposure to airborne metals can potentially occur through three main exposure pathways: i) direct inhalation of atmospheric particulates via mouth and nose; ii) dermal absorption of trace elements from skin adhered dust particles and iii) direct ingestion of atmospheric particulates due to their deposition on food, drinks or other surfaces (more frequent in indoor environments) (Kurt-Karakus, 2012). In this study, only the health risk via inhalation exposure was characterized since the inhalation exposure is typically the primary route of direct exposure to atmospheric PM-bound toxic metals.

For a risk characterization, it's important to know or to estimate, as in this case, the average daily dose assumed for each investigated substance. The model used in this study to calculate the human exposure to airborne metals is based on that developed by the United States Environmental Protection Agency (US EPA). According to the Exposure Factors Handbook (US EPA, 1997), the average daily dose (ADD) of a pollutant via inhalation can be estimated using Eq. 1:

$$\mathrm{ADD} = \frac{C\ x\ InhR\ x\ ED}{\mathrm{BW\ x\ AT}} \quad (1)$$

where ADD is the average daily exposure amount of each metal through inhalation [mg (kg day)$^{-1}$], C is the metal concentration analyzed in each PM size-fraction [mg m^{-3}], InhR is the inhalation rate [m^3 day^{-1}], ED is the exposure duration [days], BW is the body weight [kg] and AT is the averaging time [days] (for carcinogenic or chronic effects AT = 70 years or 25,500 days). Since the potential risks for humans were intended to be assessed for carcinogenic or chronic effects and with the great assumption that the general population living in the study area is exposed every day over a lifetime to the average concentration levels measured during the monitoring campaign, the exposure duration and the averaging time were referred to the average lifetime (70 years or 25,500 days) and the ADD for each element were specifically calculated for an adult (InhR = 20 m^3 day^{-1}; BW = 70 kg) (US EPA, 2011).

Risk characterization was then quantified separately for non-carcinogenic and carcinogenic effects. The potential non-carcinogenic risk was evaluated by the use of hazard quotients (HQs), calculated as the ratio between the average daily dose and a specific threshold value (Eq. 2), generally identified with the Reference (acute, sub-chronic or chronic) Dose (RfD). As defined by the US EPA, the acute or chronic reference dose is an estimate of a daily exposure for an acute (24h or less) or chronic (up to lifetime) duration for the human population (including sensitive subgroups) that is likely to be without an appreciable risk of deleterious effects during a lifetime (IRIS EPA, 2016). In this study the potential non-carcinogenic risk was evaluated for a potential chronic exposure (over a lifetime) and the Tolerable Daily Intake via inhalation exposure (TDI_{inh}) was used as threshold value in place to the RfD. TDI_{inh} has the same meaning of Acceptable Daily Intake (ADI) and is defined as the amount of a substance in air that can be assumed on a daily basis over an extended period of time (usually a lifetime) without suffering deleterious effects. TDIs are usually based on long-term laboratory toxicological studies that are intended to mimic the human assumption over a lifetime. If the ADD value is lower than the TDI_{inh} (HQ < 1), this is indicative that no adverse health effects should occur. Otherwise, if the ADD is higher that the corresponding TDI_{inh} (HQ > 1), it is likely that the exposure pathway could cause adverse human health effects during lifetime (US EPA, 1993). The sum of multiple-chemicals (or multiple-exposure pathways) HQs defined the hazard index (HI), that is used to assess the overall potential for non-carcinogenic effects posed by more than one chemical (US EPA, 2009). As for HQ, an HI below unit indicates that there is no significant risk of non-carcinogenic effects. Conversely, an HI above unit indicates that there is a chance that non-carcinogenic effects may occur, with a probability that tends to increase with increasing HI values (US EPA, 2009).

Finally, the exposure estimation of potential carcinogenic risks was assessed by the use of cancer risks (CR), as calculated in Eq. 4. It has to be noticed that, when evaluating a cancer risk for a carcinogenic substance, an effect threshold limit value cannot be estimated since, theoretically, there should not be a limit below which the carcinogenic response is not manifested. For this reason, according to the US EPA Guidance (IRIS, US EPA), the lifetime cancer risk was calculated by multiplying the estimate of lifetime exposure [mg (kg day)$^{-1}$] with the cancer slope factor (CSF) that is an estimate of the increased cancer risk due to the exposure to a dose of 1 mg (kg day)$^{-1}$ for a lifetime. The CR defines the probability of an individual to develop any kind of cancer during lifetime. In terms of regulatory purposes, both

10^{-6} or 10^{-5} levels (risk of one additional occurrence of cancer in one million and one hundred thousand people, respectively, at a given exposure assumptions) may be considered acceptable for the general population, including susceptible individuals, while highly exposed populations should not exceed a 10^{-4} (risk of one additional occurrence of cancer in ten thousand people) risk level (US EPA, 2009). In this study, the carcinogenic risks were investigated for Cr and Ni since, according to the classification group orders defined by IARC, these metals are classified as carcinogenic element of Group I (IARC, 2011). Cr toxicity is directly dependent on its valence states and in this study, following a worst-case scenario approach, the cancer slope factor of Cr(VI) was assumed as for total Cr.

$$HQ = \frac{ADD}{\text{TDIinh}} \tag{2}$$

$$HI = \sum_{i}^{n} HQi \tag{3}$$

$$CR = ADD\ x\ CSF \tag{4}$$

where ADD is the average daily dose of the investigated trace metals in each size-segregated PM fraction [mg (kg day)$^{-1}$] as previously calculated, TDI_{inh} is the Tolerable Daily Intake by inhalation [mg (kg day)$^{-1}$] and CSF is the cancer slope factor [mg (kg day)$^{-1}$]$^{-1}$. The TDI_{inh} and CSF values used in this study are tabulated in Table 1 and all the presented equations referred to US EPA methods and scientific literature (US EPA, 1997; Du *et al.*, 2013; Slezakova *et al.*, 2014; Liu *et al.*, 2015).

2.3 Statistical Analysis and Data Treatment

Statistical data analysis was performed using the SPSS software package (SPSS Inc., Chicago, IL, USA). Descriptive statistics were carried out for all of the elements under investigation on each PM size fraction. Gaussian distributions of the variables were verified by the Kolmogorov-Smirnov test. The Independent-Samples *t*-test was used to explore differences between groups on *log*-transformed data.

Moreover, for each element Enrichment Factors (EFs) relative to the average composition of the upper continental crust (UCC) were calculated according to Eq. (5):

$$EF = \frac{Eatm/Ratm}{Ecrust/Rcrust} \tag{5}$$

where E_{atm} and R_{atm} are the concentrations of the investigated element and the reference element, respectively, calculated for the aerosol samples, whereas E_{crust} and R_{crust} are the concentration levels of the same elements in the Earth's upper continental crust, as reported by Wedepohl (1995). EFs are generally employed in the atmospheric chemistry to classify the natural or anthropogenic origin of metals in the atmosphere (Alleman *et al.*, 2010; Mbengue *et al.*, 2014; Malandrino *et al.*, 2016). It is usually assumed that elements with EFs values close to unity are predominantly associated with crustal sources whereas elements with EFs values between 5 and 10 may have a significant contribution from non-crustal sources. Finally,

elements having high EFs (> 10) are considered mainly of anthropogenic origin, with anthropogenic contributions that tend to increase with increasing EF values (Gharaibeh *et al.*, 2010; Mbengue *et al.*, 2014). Elements like Al or Si are generally used as reference element because of their abundance in the Earth's crust composition, together with other metals (e.g., Ti, Mn, Fe) (Basha *et al.*, 2010; Dai *et al.*, 2015; Malandrino *et al.*, 2016). In the present study, Fe was used as reference element, since the other possible geogenic elements (e.g., Al, Si, Ti) were not quantitatively determined. It has to be noticed that soil is considered the major source of Fe in the atmosphere, even though Fe can have also non-crustal sources, that could have slightly reduced EFs values. Anyway, Fe is the fourth most abundant element in the upper continental crust and its natural concentration is orders of magnitude higher than the natural concentration levels of those metals having a great toxicological concern (e.g., Ni, Pb, Cr).

3. Results and Discussion

3.1. Elemental Mass Concentrations and Size-Distributions

For data treatment and analysis, results about the elemental mass concentrations and size-distributions were divided into the same main periods considered for PM data, namely the non-heating season (May 2015–October 15th 2015) and the heating season (October 19th 2015–March 2016). For specific details about the sampling information and the meteorological parameters monitored at the sampling site during the whole campaign, see chapter 2. For each element under investigation, descriptive statistics of mass concentrations obtained on each DLPI collection plate and for the principal PM fractions during the two monitoring periods and the whole campaign are reported in Table 2. Concentration levels referred to the standard PM fractions were obtained summing up the elemental masses collected on filter substrates with respect to the aerodynamic diameter of particles. Fig. 1 depicts the average metal size-distributions obtained during the two monitored periods and during the whole campaign.

Higher mean mass concentrations were found during the heating period compared to the non-heating season, with greatly variations in the concentration levels and concentration values differing by one or more orders of magnitude from element to element. As expected, the most abundant element among all of the investigated metals was Fe, followed by Zn, Pb, Cu, Ba and Mn. The lowest concentration levels were showed for Cr and Ni. On average, the investigated elements accounted for a very small percentage of the total $PM_{2.5}$ mass concentration (< 0.7 %). The calculated contribution to the fine particulate corresponded to 0.53, 0.08, 0.04, 0.02, 0.013, 0.011, 0.005 and 0.004 % for Fe, Zn, Pb, Cu, Ba, Mn, Cr and Ni, respectively. Table 3 summarizes the average percentage contributions of each element to the average PM mass concentrations during the non-heating period, the heating period and the whole campaign.

The analyzed elements were characterized by distinct and characteristic size-distributions in the fine, submicronic and ultrafine particles, without relevant differences in the shape of the average size-distributions between, at least, the two main investigated periods (Fig. 1).

According to their size-distributions, elements could be roughly divided into three groups: I) metals mostly concentrated in the largest particles fraction, including Fe, Ba and Cu, with more than 70% in the $PM_{1\text{-}2.5}$ size range; II) metals showing higher contributions in the accumulation mode ($PM_{0.1\text{–}1}$) (with more than 60% of the total $PM_{2.5}$ mass), including Pb, Zn and Ni, with a clear peak between 0.3 and 0.6 μm (at least for Pb and Zn) and III) metals more spread throughout the size-distribution, without considering the lowest DLPI stages (Cr and Mn), with rather similar contributions for the smaller and coarser fractions to the total $PM_{2.5}$ (Fig. 2).

These results are consistent with those of Fernandez-Espinosa *et al.* (2001), which observed the predominance of some toxic trace metals (Pb, Cd and V) in submicronic particles. Also Mbengue *et al.* (2014) showed higher percentage of Pb and Zn in $PM_{1,}$ whereas elements such as Fe, Ba, Cu and Ti were found to be most abundant in the supermicron fraction (> 1 μm).
The ultrafine component showed always very low concentration levels, without any relevant peak in the most critical PM fraction in terms of sanitary concern and contributions to the total $PM_{2.5}$ mass were always < 5% (Table 2 and Fig. 1). Different findings were contrarily showed by Lin *et al.* (2005), that registered Aitken modes for Pb, Zn, Ba and Ni with secondary peaks < 0.1 μm-size strongly associated with vehicle emissions and fossil fuel combustions and mainly due to the specific location of sampling site, close to a heavily trafficked road.
Enrichment Factors (EFs) relative to the average composition of the upper continental crust were calculated for each element according to Eq. (5) presented in the previous paragraph, considering the two main fraction (submicronic particles (PM_1) and coarser particles ($PM_{1–2.5}$)). As already explained, Fe was used as reference element in the present study. Soil is considered the major source of Fe in the atmosphere, even though Fe can have also non-crustal sources, that could have slightly reduced EFs of elements characterized by both crustal and non-crustal origin. Moreover, it has to be noticed that EFs were employed to assess the extent of non-crustal contributions to the atmospheric concentration levels for the elements under investigation taking into account that they only provided general and qualitative information on the element origins in the study area, also because of the wide variations in the UCC composition.
As shown in Fig. 3, elements classified in group I presented different enrichment factors. EFs around 1 were found for Ba, suggesting a predominant crustal origin, whereas notably higher EFs were showed for Cu (in both PM_1 and $PM_{1–2.5}$), probably due to anthropogenic sources influencing both the coarse and the accumulation modes.
Very high EFs were also found for Pb, Zn and Ni, especially in the finest fraction, for which EFs increased by approximately one order of magnitude compared to $PM_{1–2.5}$ EFs, suggesting an increased anthropogenic contribution in the smallest PM size range.
Finally, for elements of group III, EFs around 1 were identified for Mn in $PM_{1–2.5}$, while higher EFs, suggesting a more influence of anthropogenic sources, were found for PM_1. Cr showed EF values indicating potential anthropogenic influences especially on the finest fraction.

3.2 Risk Characterization of Trace Metals in Size-Segregated PM via the Inhalation Exposure Route

As already explained in the introduction, results about the average concentration levels of the investigated metals were used to evaluate their potential non-carcinogenic and carcinogenic risks via inhalation exposure for the population living in the study area. It is important to noticed that this study cannot be considered a real exposure study, because the experimental design did not involve any kind of personal sampling but concentration levels were measured at an outdoor fixed-site monitoring station, specifically selected according to the Guideline Criteria (EEA, Criteria for EUROAIRNET, 1999) to assess urban background concentrations and be representative of the average levels of air pollution, as already explained in chapter 2. Moreover, people generally spend their time in different indoor and outdoor environments, where concentration levels could be different. Therefore, this type of risk characterization should only be considered as a rough estimate of health risks based on the assumption that

people living in the study area are chronically exposed to the average metal concentrations monitored during the whole campaign.

The non-carcinogenic risks associated with inhalation exposure to particulate trace elements were calculated according to the US EPA methodology. The HQs estimated for individual elements in each size fraction of $PM_{2.5}$ are reported in Table 4, together with the size-fractionated HI calculated as the sum of multiple-elements HQs. For the main PM fractions, HQs were estimated summing up the calculated HQs in all size ranges for each element. HQs and HI were assessed for all of the investigated metals except for Fe, since the US EPA has not established a tolerable daily intake for this element, as already shown in Table 1. The calculated $PM_{2.5}$-HQs for all of the elements were always < 1; the lowest HQ values were found for Cu and Zn, whereas Cr and Mn showed the highest HQs.

Considering the main PM fractions, UFPs always registered low values and the lowest percentage contributions to the total $PM_{2.5}$-HQs for all of the elements under investigation (Table 4). HQ values for the accumulation mode ($PM_{0.1–1}$) were following the order Mn > Cr > Ba > Pb > Ni > Zn > Cu, whereas in the coarser fraction ($PM_{1–2.5}$) HQs decreased in the order Mn > Cr > Ba > Pb > Ni > Cu > Zn. $PM_{2.5}$-HQs for Pb, Zn and Ni were found to be mainly dependent from $PM_{0.1-1,}$ with the highest contributions in the 0.3–0.6 μm PM size range, that accounted for 31, 28 and 21% for Pb, Zn and Ni, respectively. On the contrary, Ba and Cu registered the highest contributions in the coarser fraction ($PM_{1-2.5}$), mainly from particles between 1.6 and 2.4 μm. Finally, for Cr and Mn, accumulation and coarser fractions displayed more homogeneous contributions, with anyway higher percentage values for particles > 0.3 μm (Table 4).

As for the single HQs, also the estimate of the overall potential for non-carcinogenic effects posed by all of the metals under investigations (HI) was < 1, suggesting no significant risks for the exposed population. Aerosol particles > 0.3 μm seemed to play the major role in the characterization of the overall non-carcinogenic risk, whereas lower contribution were found for particles < 0.3 μm, with percentage contribution values decreasing with decreasing aerosol particle size (Table 4).

The cancer risks calculated from the ADD of the inhalation pathway for those elements known as human carcinogens (Cr and Ni) are shown in Table 5. The estimated CR values in the fine particulate ($PM_{2.5}$), that resulted from the sum of size-segregated CRs, were equal to 2.32E-07 (Ni) and 1.43E-05 (Cr) and showed distinct contributions from the different size-segregated PM fractions for the two investigated metals. As depicted in Fig. 4, the $PM_{0.1}$ component showed the lowest contribution to the total $PM_{2.5}$-CRs for both elements. More than 70% of $PM_{2.5}$-CR for Ni came from the accumulation mode ($PM_{0.1–1}$), mainly from particles having aerodynamic diameter between 0.15 and 0.61 μm (59%), whereas the $PM_{2.5}$-CR for Cr was more equally distributed between accumulation mode and coarse mode ($PM_{1–2.5}$), accounting for about 52% in $PM_{1–2.5}$ (Table 5).

In conclusion, the estimated $PM_{2.5}$ carcinogenic risks were below (Ni) or within (Cr) the acceptable range established in terms of regulatory purposes for the general population (10^{-6} or 10^{-5}), thus indicating a negligible cancer risk for people living in the study area. Nevertheless, it could be important taking into account that, although the estimated CRs for Ni were two orders of magnitude lower that the calculated CRs for Cr, the higher contributions to the total $PM_{2.5}$-CR for Ni were found to be mainly related to airborne particles that are able to more deeply penetrate into the respiratory system.

4. Conclusions and Future Developments

In this study, the mass concentrations of selected trace metals (Cr, Mn, Fe, Ni, Cu, Zn, Ba and Pb) were measured on the extended set of size-segregated PM samples collected during an intensive long-scale monitoring campaign at an urban background site in Como with a LA-ICP-MS method properly developed. On average, the investigated elements accounted for a very small percentage of the total $PM_{2.5}$ mass concentration (< 0.7 %) and results revealed greatly variations in the concentration levels of the analyzed toxic metals, with values differing by one or more orders of magnitude from element to element and between the different sampling periods. Obtained findings showed distinct differences for the analyzed elements, with different and characteristic size-distributions in the fine, submicronic and ultrafine fractions. The studied elements were variously enriched in the particulate sizes, suggesting that local emission sources may exist for these chemical species. In this context, only preliminary and qualitative evaluations have been performed, since the extended dataset has to be deeply investigate with further analysis in order to gain further insights and contribute to a better evaluation of seasonal variabilities, possible influences of meteorological parameters as well as to the quali/quantitative identification of possible emission sources in the study area (source apportionment studies).

From a health and sanitary perspective, the hazard quotient and index values calculated for all of the studied elements suggested no non-carcinogenic health risks via inhalation exposure. Also the carcinogenic risks of Cr and Ni were within the acceptability range.

References

Alleman, L.Y., Lamaison, L., Perdrix, E., Robache, A. and Galloo, J.-C. (2010). PM_{10} metal concentrations and source identification using positive matrix factorization and wind sectoring in a French industrial zone. *Atmos. Environ.* 96: 612–625.

Basha, S., Jhala, J., Thorat, R., Goel, S., Trivedi, R., Shah, K., Menon, G., Gaur, P., Mody, K.H. and Jha, B. (2010). Assessment of heavy metal content in suspended particulate matter of coastal industrial town, Mithapur, Gujarat, India. *Atmos. Res.* 97: 257–265.

Cao, Z.G., Yu, G., Chen, Y.S., Cao, Q.M., Fiedler, H., Deng, S.B., Huang, J. and Wang, B. (2012). Particle size: a missing factor in risk assessment of human exposure to toxic chemicals in settled indoor dust. *Environ. Int.* 49: 24–30.

Chen, L.C. and Lippmann, M. (2009). Effects of metals within ambient air particulate matter (PM) on human health. *Inhal. Toxicol.* 21: 1–31.

Dai, Q.L:, Bi, X.H., Wu, J.H., Zhang, Y.F., Wang, J., Xu, H., Yao, L., Jiao, L. and Feng, Y.C. (2015). Characterization and source identification of heavy metals in ambient PM_{10} and $PM_{2.5}$ in an integrated iron and steel industry zone compared with a background site. *Aerosol Air Qual. Res.* 15: 875–887.

Du, Y., Gao, B., Zhou, H., Ju, X., Hao, H. and Yin, S. (2013). Health risk assessment of heavy metals in road dusts in urban parks of Beijing, China. *Procedia Environmental Sciences* 18: 299–309.

European Environment Agency (EEA). Criteria for EUROAIRNET. Technical Report n. 12, February 1999. Available on-line: http://www.eea.europa.eu/publications/TEC12.

Fernandez-Espinosa, A.J., Rodriguez, M.T., de la Rosa, F.J.B. and Sanchez, J.C.J. (2001). Size distribution of metals in urban aerosols in Seville (Spain). *Atmos. Environ.* 35: 2595–2601.

Gharaibeh, A.A., El-Rioob, A.-W.O. and Harb, M.K. (2010). Determination of selected heavy metals in air samples from the northern part Jordan. *Environ. Monit. Assess.* 160: 425–429.

Ghio, A.J., Stonehuerner, J., Pritchard, R.J., Piantadosi, C.A., Quigley, D.R., Dreher, K.L. and Costa, D.L. (1996). Humic-like substances in air pollution particulates correlate with concentrations of transition metals and oxidant generation. *Inhal. Toxicol.* 8(5): 479–494.

Greene, N.A. and Morris, V.R. (2006). Assessment of public health risks associated with atmospheric exposure to $PM_{2.5}$ in Washington, DC, USA. *Int. J. Environ. Res. Public Health* 3(1): 86–97.

Harrison, R.M. and Yin, J. (2000). Particulate matter in the atmosphere: which particle properties are important for its effects on health? *Sci. Total Environ.* 249: 85–101.

IARC Working Group on the Evaluation of Carcinogenic Risks to Humans (2006). Inorganic and organic lead compounds. IARC *Monogr. Eval. Carcinog. Risks Hum.* 87: 1–471.

IARC (International Agency for Research on Cancer). (2011). Agents classified by the IARC Monographs, vol. 1–102.

IARC Working Group on the Evaluation of Carcinogenic Risks to Humans (2012). Arsenic, metals, fibers, and dusts. IARC *Monogr. Eval. Carcinog. Risks Hum.* 100(Pt C): 11–465.

IRIS Glossary, EPA. "Integrated Risk Information System Glossary. United States Environmental Protection Agency" Available on-line: https://iaspub.epa.gov/sor_internet/registry/termreg/searchandretrieve/glossariesandkeywordlists/search.do?details=&vocabName=IRIS%20Glossary.

IRIS EPA. "Integrated Risk Information System". United States Environmental Protection Agency, available on-line: https://www.epa.gov/iris.

Kampa, M. and Castanas, E. (2008). Human health effects of air pollution. *Environ. Pollut.* 151: 362–367.

Kurt-Karakus, P.B. (2012). Determination of heavy metals in indoor dust from Istanbul, Turkey: estimation of the health risk. *Environ. Int.* 50: 47–55.

Li, X.R., Wang, L.L., Wang Y.S., Wen, T.X., Yang, Y.J., Zhao, Y.N. and Wang, Y.F. (2012). Chemical composition and size distribution of airborne particulate matters in Beijing during the 2008 Olympics. *Atmos. Environ.* 50: 278–286.

Lin, C.-C., Chen, S.-J., Huang, K.-L., Hwang, W.-I., Chang-Chien, G.-P. and Lin, W.-Y. (2005). Characteristics of metals in nano/ultrafine/fine/coarse particles collected beside a heavily trafficked road. Environ. Sci. Technol. 39: 8113-8122.

Liu, X., Zhai, Y., Zhu, Y., Liu, Y., Chen, H., Li, P., Peng, C., Xu, B., Li, C. and Zeng, G. (2015). Mass concentration and health risk assessment of heavy metals in size-segregated airborne particulate matter in Changsha. *Sci. Total Environ.* 517: 215–221.

Malandrino, M., Casazza, M., Abollino, O., Minero, C. and Maurino, V. (2016). Size resolved metal distribution in the PM matter of the city of Turin (Italy). *Chemosphere* 147: 477–489.

Mbengue, S., Alleman, L.Y. and Flament, P. (2014). Size-distributed metallic elements in submicronic and ultrafine particles from urban and industrial areas in Northern France. *Atmos. Environ.* 135: 35–47.

Ning, Z., Geller, M.D., Moore, K.F., Sheesley, R., Schauer, J.J. and Sioutas, C. (2007). Daily variation in chemical characteristics of urban ultrafine aerosols and inference of their sources. *Environ. Sci. Technol.* 41: 6000-6006.

Ntziachristos, L., Ning, Z., Geller, M.D., Sheesley, R.J., Schauer, J.J. and Sioutas, C. (2007). Fine, ultrafine and nanoparticle trace element compositions near a major freeway with a high heavy-duty diesel fraction. *Atmos. Environ.* 41: 5684-5696.

Oeder, S., Dietrich, S., Weichenmeier, I., Schober, W., Pusch, G., Jörres, R.A., Schierl, R., Nowak, D., Fromme, H., Behrendt, H. and Buters, J.T. (2012). Toxicity and elemental composition of particulate matter from outdoor and indoor air of elementary schools in Munich, Germany. *Indoor Air* 22: 148–158.

Pakkanen, T.A., Kerminen, V.-M., Korhonen, C.H., Hillamo, R.E., Aarnio, P., Koskentalo, T. and Maenhaut, W. (2001). Urban and rural ultrafine (PM0.1) particles in the Helsinki area. *Atmos. Environ.* 35: 4593–4607.

Peled, R. (2011). Air pollution exposure: who is at high risk? *Atmos. Environ.* 45: 1781–1785.

Polichetti, G., Cocco, S., Spinali, A., Trimarco, V. and Nunziata, A. (2009). Effects of particulate matter (PM_{10}, $PM_{2.5}$ and PM_1) on the cardiovascular system. *Toxicology* 261(1): 1–8.

Raaschou-Nielsen, O. et al. (2016). Particulate matter air pollution components and risk for lung cancer. *Environ. Int.* 87: 66–73.

Sardar, S.B., Fine, P.M., Mayo, P.R. and Sioutas, C. (2005). Size-fractionated measurements of ambient ultrafine particle chemical composition in Los Angeles using the NanoMOUDI. *Environ. Sci. Technol.* 39: 932–944.

Slezakova, K., Morais, S. and do Carmo Pereira, M. (2014). Trace metals in size-fractionated particulate matter in a Portuguese hospital: exposure risks assessment and comparison with other countries. *Environ. Sci. Pollut. Res.* 21: 3604–3620.

Sun, G., Crissman, K., Norwood, J., Richards, J., Slade, R. and Hatch, G.E. (2001). Oxidative interactions of synthetic lung epithelial lining fluid with metals-containing particulate matter. *Am. J. Physiol. Lung Cell. Mol. Physiol.* 281: L807–L815.

Sun, Z.Q., Mu, Y.J., Liu, Y.J. and Shao, L.Y. (2013). A comparison study on airborne particles during haze days and non-haze days in Beijing. *Sci. Total. Environ.* 456: 1–8.

UNI EN 14907: 2005. Ambient air quality – Standard gravimetric measurement method for the determination of the $PM_{2.5}$ mass fraction of suspended particulate matter.

UNI EN 12341: 2014. Air Quality – Determination of the PM_{10} fraction of suspended particulate matter. Reference method and field test procedure to demonstrate reference equivalence of measurements methods.

U.S: Environmental Protection Agency. (1993). Reference dose (RfD): description and use in health risk assessments. Background Document 1A. Integrated Risk Information System (IRIS).

U.S. Environmental Protection Agency. (1997). Exposure factors handbook. EPA/600/P-95/002F. Ishington D.C.: National Center for Environmental Assessment, Office of Research and Development.

U.S. Environmental Protection Agency. (2009). Risk Assessment Guidance for Superfund Volume I: Human Health Evaluation Manual (Part F, Supplemental Guidance for Inhalation Risk Assessment). Office of Superfund Remediation and Technology Innovation, Washington, D.C.

U.S. Environmental Protection Agency. (2011). Exposure factors handbook: 2011 edition. EPA/600/R-09/052F, Office for Research and Development, Washington, DC.

Valavanidis, A., Fiotakis, K. and Vlachogianni, T. (2008). Airborne particulate matter and human health: toxicological assessment and importance of size and composition of particles for oxidative damage and carcinogenic mechanisms. *J. Environ. Sci. Heal. C* 26(4): 339–362.

Wedepohl, K.H. (1995). The composition of the continental crust. *Geochim. Cosmochim. Acta* 59: 1217–1232.

This chapter is based on:

- **Rovelli, S.**, Limbeck, A., Nischkauer, W., Bonta, M., Borghi, F., Cattaneo, A., Cavallo, D.M. Characterization of toxic trace metals in size-segregated fine and ultrafine particles within an urban environment. In: Conference Proceedings of the 2nd International Conference on Atmospheric Dust, Castellaneta Marina (TA), Italy, June 12th-17th 2016, Vol. 5, p. 227, ISSN 2464-9147.

Tables

Table 1. Recommended values for the Tolerable Daily Intake (TDI) and Cancer Slope Factor (CSF) in equations of the health risk characterization.

	TDI [mg (kg day)$^{-1}$]	**CSF [mg (kg day)$^{-1}$]$^{-1}$**
Cr	3.00E-05	4.10E+01
Mn	1.43E-05	–
Fe	–	–
Ni	1.30E-03	8.40E-01
Cu	1.41E-01	–
Zn	5.66E-01	–
Ba	1.40E-04	–
Pb	3.60E-03	–

Table 2. Descriptive statistics on the elemental mass concentrations for the 9 DLPI size-ranges and for the main PM fractions during the non-heating period, the heating period and the whole campaign.

	Concentration in air (ng m^{-3}) - Mean (min–max)							
	Non-heating period							
Size range (µm)	**Cr**	**Mn**	**Fe**	**Ni**	**Cu**	**Zn**	**Ba**	**Pb**
0.0283–0.0559	0.03 (0.01–0.13)	0.005 (0.002–0.01)	0.05 (0.02–0.11)*	0.01 (0.002–0.04)	0.01 (0.005–0.02)	0.04 (0.02–0.13)	0.003 (0.001–0.01)*	0.05 (0.02–0.10)
0.0559–0.0944	0.03 (0.01–0.10)	0.01 (0.002–0.04)*	0.09 (0.02–0.24)	0.01 (0.003–0.04)	0.02 (0.004–0.05)*	0.14 (0.02–0.49)*	0.01 (0.001–0.02)*	0.11 (0.03–0.32)
0.0944–0.157	0.02 (0.01–0.05)	0.03 (0.003–0.08)	0.27 (0.08–0.85)*	0.04 (0.01–0.08)*	0.05 (0.01–0.13)*	0.43 (0.02–1.27)*	0.01 (0.003–0.01)*	0.30 (0.04–0.87)*
0.157–0.262	0.03 (0.005–0.06)*	0.06 (0.002–0.16)*	0.65 (0.13–1.58)*	0.08 (0.02–0.17)*	0.08 (0.005–0.23)*	0.81 (0.08–1.82)*	0.01 (0.01–0.02)*	0.57 (0.05–1.48)*
0.262–0.383	0.06 (0.02–0.13)*	0.12 (0.01–0.31)*	1.16 (0.28–3.45)*	0.10 (0.04–0.21)*	0.08 (0.01–0.24)*	1.19 (0.08–2.36)*	0.03 (0.01–0.08)*	0.69 (0.06–1.61)*
0.383–0.614	0.11 (0.03–0.21)*	0.29 (0.04–0.71)*	3.06 (0.98–7.47)*	0.11 (0.04–0.23)*	0.15 (0.03–0.34)*	2.13 (0.21–4.08)*	0.12 (0.04–0.56)*	0.68 (0.07–1.19)*
0.614–0.950	0.10 (0.05–0.16)*	0.20 (0.05–0.45)*	5.24 (2.13–9.55)*	0.05 (0.03–0.08)*	0.16 (0.07–0.28)*	1.40 (0.05–2.69)*	0.21 (0.09–0.74)*	0.32 (0.04–0.67)*
0.950–1.6	0.18 (0.06–0.26)*	0.29 (0.09–0.49)*	21.40 (9.96–30.04)*	0.06 (0.03–0.10)*	0.59 (0.26–0.92)*	1.38 (0.26–2.31)*	0.53 (0.36–0.88)*	0.25 (0.02–0.58)*
1.6–2.4	0.24 (0.12–0.30)*	0.36 (0.15–0.69)*	36.29 (18.77–51.08)*	0.08 (0.03–0.10)*	1.12 (0.61–1.44)*	1.12 (0.32–1.77)	0.78 (0.47–1.01)*	0.14 (0.02–0.25)*
PM fraction								
$PM_{0.1}$	0.06 (0.01–0.23)	0.02 (0.02–0.05)	0.13 (0.04–0.36)	0.02 (0.01–0.08)	0.03 (0.01–0.07)	0.17 (0.04–0.62)	0.01 (0.01–0.02)	0.16 (0.06–0.38)
$PM_{0.1–1}$	0.32 (0.10–0.52)	0.70 (0.11–1.63)	10.38 (3.95–19.00)	0.38 (0.13–0.71)	0.53 (0.12–1.13)	5.97 (0.43–11.25)	0.38 (0.15–1.40)	2.55 (0.26–4.94)
PM_{1}	0.37 (0.12–0.67)	0.72 (0.11–1.64)	10.51 (3.99–19.06)	0.40 (0.14–0.72)	0.56 (0.13–1.17)	6.14 (0.47–11.53)	0.39 (0.17–1.41)	2.70 (0.33–5.09)
$PM_{1–2.5}$	0.42 (0.18–0.56)	0.65 (1.23–1.01)	57.69 (28.73–75.81)	0.14 (0.05–0.19)	1.70 (0.86–2.36)	2.51 (0.58–4.08)	1.31 (0.84–1.79)	0.39 (0.04–0.83)
$PM_{2.5}$	0.80 (0.48–1.11)	1.37 (0.35–2.50)	68.20 (32.71–87.13)	0.54 (0.29–0.91)	2.26 (0.99–3.37)	8.65 (1.05–14.93)	1.70 (1.11–3.19)	3.09 (0.38–5.41)

* Significant difference ($p < 0.05$) in heating vs non-heating levels by Independent-Samples *t*-test on log-normal parameters

Table 2 (continues). Descriptive statistics on the elemental mass concentrations for the 9 DLPI size-ranges and for the main PM fractions during the non-heating period, the heating period and the whole campaign.

	Concentration in air (ng m^{-3}) - Mean (min–max)							
	Heating period							
Size range (µm)	**Cr**	**Mn**	**Fe**	**Ni**	**Cu**	**Zn**	**Ba**	**Pb**
0.0283–0.0559	0.02 (0.01–0.17)	0.004 (0.002–0.02)	0.08 (0.02–0.17)*	0.01 (0.003–0.04)	0.02 (0.05–0.09)	0.07 (0.02–0.45)	0.001 (0.001–0.003)*	0.05 (0.001–0.09)
0.0559–0.0944	0.02 (0.01–0.16)	0.01 (0.002–0.02)*	0.16 (0.03–0.37)	0.03 (0.003–0.06)	0.05 (0.05–0.12)*	0.27 (0.06–0.99)*	0.003 (0.001–0.01)*	0.15 (0.03–0.31)
0.0944–0.157	0.02 (0.003–0.07)	0.02 (0.01–0.04)	0.52 (0.20–0.96)*	0.08 (0.01–0.18)*	0.10 (0.03–0.18)*	0.88 (0.17–2.06)*	0.01 (0.003–0.02)*	0.50 (0.09–0.99)*
0.157–0.262	0.07 (0.01–0.15)*	0.13 (0.02–0.22)*	2.18 (0.46–4.12)*	0.25 (0.02–0.53)*	0.31 (0.06–0.56)*	3.27 (0.40–6.74)*	0.03 (0.01–0.07)*	1.91 (0.22–4.62)*
0.262–0.383	0.13 (0.03–0.28)*	0.32 (0.06–0.61)*	4.65 (1.01–9.28)*	0.26 (0.02–0.59)*	0.41 (0.07–0.85)*	5.15 (0.53–12.39)*	0.07 (0.02–0.13)*	3.34 (0.35–10.76)*
0.383–0.614	0.27 (0.06–0.76)*	0.93 (0.19–2.38)*	12.53 (2.99–28.53)*	0.30 (0.04–0.84)*	0.71 (0.11–1.98)*	7.96 (0.95–23.47)*	0.22 (0.06–0.42)*	4.11 (0.57–13.90)*
0.614–0.950	0.22 (0.02–0.62)*	0.68 (0.15–2.19)*	17.37 (3.01–38.82)*	0.14 (0.03–0.42)*	0.63 (0.09–1.64)*	4.64 (0.40–18.08)*	0.49 (0.11–0.89)*	1.47 (0.20–3.52)*
0.950–1.6	0.36 (0.12–0.75)*	0.70 (0.20–1.91)*	47.93 (12.77–140.86)*	0.13 (0.04–0.29)*	1.61 (0.33–3.66)*	3.43 (0.49–12.76)*	1.30 (0.38–3.74)*	0.63 (0.07–1.61)*
1.6–2.4	0.47 (0.14–0.98)*	0.67 (0.19–1.76)*	74.76 (20.60–201.84)*	0.13 (0.04–0.25)*	2.60 (0.60–6.57)*	1.78 (0.57–4.30)	1.94 (0.53–5.06)*	0.28 (0.04–0.81)*
PM fraction								
$PM_{0.1}$	0.04 (0.01–0.33)	0.01 (0.01–0.03)	0.24 (0.06–0.52)	0.03 (0.01–0.09)	0.07 (0.01–0.20)	0.35 (0.08–1.12)	0.004 (0.001–0.009)	0.20 (0.03–0.40)
$PM_{0.1–1}$	0.72 (0.15–1.86)	2.07 (0.43–5.29)	37.25 (9.11–76.70)	1.03 (0.11–2.43)	2.16 (0.45–5.22)	21.91 (2.64–62.74)	0.81 (0.21–1.45)	11.32 (1.48–33.29)
PM_{1}	0.76 (0.16–2.05)	2.08 (0.44–5.31)	37.49 (9.39–77.20)	1.07 (0.13–2.52)	2.23 (0.46–5.37)	22.26 (2.72–63.80)	0.81 (0.21–1.46)	11.52 (1.54–33.50)
$PM_{1–2.5}$	0.82 (0.26–1.73)	1.37 (0.39–3.24)	122.70 (33.37–342.71)	0.26 (0.09–0.54)	4.21 (0.94–10.24)	5.20 (1.35–17.06)	3.24 (0.91–8.80)	0.91 (0.11–2.33)
$PM_{2.5}$	1.58 (0.43–3.56)	3.45 (0.91–8.55)	160.19 (42.76–388.52)	1.33 (0.21–3.02)	6.44 (1.40–14.49)	27.46 (4.36–76.09)	4.06 (1.12–10.10)	12.43 (1.76–34.49)

* Significant difference ($p < 0.05$) in heating vs non-heating levels by Independent-Samples *t*-test on normal parameters

Table 2 (continues). Descriptive statistics on the elemental mass concentrations for the 9 DLPI size-ranges and for the main PM fractions during the non-heating period, the heating period and the whole campaign.

	Concentration in air (ng m^{-3}) - Mean (min–max)							
	Whole campaign							
Size range (µm)	**Cr**	**Mn**	**Fe**	**Ni**	**Cu**	**Zn**	**Ba**	**Pb**
0.0283–0.0559	0.02 (0.01–0.17)	0.004 (0.002–0.02)	0.06 (0.02–0.17)	0.01 (0.002–0.04)	0.02 (0.005–0.09)	0.06 (0.02–0.45)	0.002 (0.001–0.01)	0.05 (0.001–0.10)
0.0559–0.0944	0.03 (0.01–0.16)	0.01 (0.002–0.04)	0.13 (0.02–0.37)	0.02 (0.003–0.06)	0.04 (0.004–0.12)	0.21 (0.02–0.99)	0.004 (0.001–0.02)	0.13 (0.03–0.32)
0.0944–0.157	0.02 (0.01–0.07)	0.02 (0.003–0.08)	0.40 (0.08–0.96)	0.06 (0.01–0.18)	0.07 (0.01–0.18)	0.67 (0.02–2.06)	0.01 (0.003–0.02)	0.40 (0.04–0.99)
0.157–0.262	0.06 (0.005–0.15)	0.10 (0.002–0.22)	1.48 (0.13–4.12)	0.17 (0.02–0.53)	0.20 (0.05–0.56)	2.14 (0.08–6.74)	0.02 (0.01–0.07)	1.29 (0.05–4.62)
0.262–0.383	0.10 (0.02–0.28)	0.23 (0.01–0.61)	3.05 (0.28–9.28)	0.19 (0.02–0.59)	0.26 (0.01–0.85)	3.33 (0.08–12.39)	0.05 (0.01–0.13)	2.12 (0.06–10.76)
0.383–0.614	0.19 (0.03–0.76)	0.63 (0.04–2.38)	8.18 (0.98–28.53)	0.21 (0.02–0.59)	0.46 (0.03–1.98)	5.29 (0.21–23.47)	0.17 (0.04–0.56)	2.53 (0.07–13.90)
0.614–0.950	0.16 (0.02–0.62)	0.46 (0.05–2.19)	11.80 (2.13–38.82)	0.10 (0.03–0.42)	0.41 (0.07–1.64)	3.16 (0.05–18.08)	0.36 (0.09–0.89)	0.94 (0.04–3.52)
0.950–1.6	0.27 (0.06–0.75)	0.51 (0.09–1.91)	35.74 (9.96–140.86)	0.10 (0.03–0.29)	1.14 (0.26–3.66)	2.49 (0.26–12.76)	0.95 (0.36–3.74)	0.45 (0.02–1.61)
1.6–2.4	0.36 (0.12–0.98)	0.53 (0.15–1.76)	57.09 (18.77–201.84)	0.11 (0.03–0.25)	1.92 (0.60–6.57)	1.47 (0.32–4.30)	1.41 (0.47–5.06)	0.21 (0.02–0.81)
PM fraction								
$PM_{0.1}$	0.05 (0.01–0.33)	0.01 (0.01–0.05)	0.19 (0.04–0.52)	0.03 (0.01–0.09)	0.05 (0.01–0.20)	0.27 (0.04–1.12)	0.01 (0.001–0.02)	0.18 (0.03–0.40)
$PM_{0.1–1}$	0.53 (0.10–1.86)	1.44 (0.11–5.29)	24.91 (3.95–76.70)	0.73 (0.11–2.43)	1.41 (0.12–5.22)	14.58 (0.43–62.74)	0.61 (0.15–1.45)	7.29 (0.26–33.29)
PM_1	0.58 (0.12–2.05)	1.46 (0.11–5.31)	25.10 (3.99–77.20)	0.76 (0.13–2.52)	1.46 (0.13–5.37)	14.85 (0.47–63.80)	0.62 (0.17–1.46)	7.47 (0.33–33.50)
$PM_{1–2.5}$	0.64 (0.18–0.73)	1.04 (0.23–3.24)	92.83 (28.73–342.71)	0.21 (0.05–0.54)	3.06 (0.86–10.24)	3.96 (0.58–17.06)	2.35 (0.84–8.80)	0.67 (0.04–2.33)
$PM_{2.5}$	1.22 (0.43–3.56)	2.50 (0.35–8.55)	117.92 (32.71–388.52)	0.97 (0.21–3.02)	4.52 (0.99–14.49)	18.82 (1.05–76.09)	2.97 (1.11–10.10)	8.14 (0.38–34.49)

Table 3. Summary of the average percentage contributions of each element to the average PM mass concentrations during the non-heating period, the heating period and the whole campaign.

	Cr	Mn	Fe	Ni	Cu	Zn	Ba	Pb
	Non-heating period (%)							
$PM_{0.1}$	0.010	0.003	0.024	0.004	0.006	0.032	0.002	0.028
$PM_{0.1–1}$	0.004	0.009	0.126	0.005	0.006	0.072	0.005	0.031
PM_{1}	0.004	0.008	0.119	0.005	0.006	0.070	0.004	0.031
$PM_{1–2.5}$	0.024	0.037	3.284	0.008	0.097	0.143	0.074	0.022
$PM_{2.5}$	0.008	0.013	0.645	0.005	0.021	0.082	0.016	0.029
	Heating period (%)							
$PM_{0.1}$	0.006	0.001	0.029	0.004	0.009	0.043	0.001	0.025
$PM_{0.1–1}$	0.003	0.008	0.138	0.004	0.008	0.081	0.003	0.042
PM_{1}	0.003	0.007	0.135	0.004	0.008	0.080	0.003	0.041
$PM_{1–2.5}$	0.020	0.033	2.964	0.006	0.102	0.126	0.078	0.022
$PM_{2.5}$	0.005	0.011	0.502	0.004	0.020	0.086	0.013	0.039
	Whole campaign (%)							
$PM_{0.1}$	0.007	0.002	0.027	0.004	0.008	0.039	0.001	0.026
$PM_{0.1–1}$	0.003	0.008	0.134	0.004	0.008	0.078	0.003	0.039
PM_{1}	0.003	0.008	0.130	0.004	0.008	0.077	0.003	0.039
$PM_{1–2.5}$	0.021	0.034	3.020	0.007	0.099	0.129	0.077	0.022
$PM_{2.5}$	0.005	0.011	0.527	0.004	0.020	0.084	0.013	0.036

Table 4. Hazard Quotients (HQs) for each element in size-segregated PM via inhalation exposure and Hazard Index (HI) calculated as the sum of multiple-elements HQs. Results referred to the main PM fractions are also reported, together with the percentage contributions (%) of the size-segregated fractions to the total $PM_{2.5}$-HQs and HI.

	Cr		Mn		Ni		Cu		Zn		Ba		Pb			
Size range [μm]	**HQ**	**%**	**HQ**	**%**	**HQ**	**%**	**HQ**	**%**	**HQ**	**%**	**HQ**	**%**	**HQ**	**%**	**$HI = \sum_{i}^{n} HQi$**	**%**
0.0283–0.0559	2.28E-04	2.0	8.66E-05	0.2	1.50E-06	0.7	3.26E-08	0.4	2.89E-08	0.3	4.29E-06	0.1	3.74E-06	0.6	3.24E-04	0.5
0.0559–0.0944	2.52E-04	2.2	1.60E-04	0.3	4.44E-06	2.1	7.56E-08	0.8	1.07E-07	1.1	8.46E-06	0.1	1.05E-05	1.6	4.36E-04	0.6
0.0944–0.157	2.11E-04	1.8	4.87E-04	1.0	1.37E-05	6.5	1.52E-07	1.7	3.39E-07	3.6	1.49E-05	0.3	3.20E-05	5.0	7.59E-04	1.1
0.157–0.262	5.33E-04	4.6	1.91E-03	3.8	3.75E-05	17.7	4.14E-07	4.5	1.08E-06	11.4	4.77E-05	0.8	1.03E-04	15.9	2.63E-03	3.9
0.262–0.383	9.38E-04	8.1	4.59E-03	9.2	4.16E-05	19.6	5.27E-07	5.8	1.68E-06	17.7	1.00E-04	1.7	1.68E-04	26.1	5.84E-03	8.6
0.383–0.614	1.84E-03	15.9	1.27E-02	25.4	4.66E-05	22.0	9.22E-07	10.1	2.67E-06	28.1	3.43E-04	5.8	2.01E-04	31.1	1.51E-02	22.1
0.614–0.950	1.55E-03	13.3	9.21E-03	18.5	2.14E-05	10.1	8.41E-07	9.2	1.59E-06	16.8	7.16E-04	12.1	7.46E-05	11.6	1.16E-02	16.9
0.950–1.6	2.61E-03	22.4	1.02E-02	20.5	2.23E-05	10.5	2.31E-06	25.2	1.26E-06	13.2	1.90E-03	31.9	3.61E-05	5.6	1.48E-02	21.7
1.6–2.4	3.47E-03	29.8	1.05E-02	21.1	2.32E-05	10.9	3.89E-06	42.4	7.44E-07	7.8	2.81E-03	47.3	1.71E-05	2.6	1.69E-02	24.7
PM fraction																
$PM_{0.1}$	4.80E-04	4.1	2.47E-04	0.5	5.94E-06	2.8	1.08E-07	1.2	1.36E-07	1.4	1.27E-05	0.2	1.43E-05	2.2	7.60E-04	1.1
$PM_{0.1–1}$	5.07E-03	43.6	2.89E-02	57.9	1.61E-04	75.8	2.86E-06	31.2	7.36E-06	77.5	1.22E-03	20.6	5.78E-04	89.6	3.59E-02	52.6
PM_{1}	5.55E-03	47.7	2.91E-02	58.4	1.67E-04	78.6	2.96E-06	32.4	7.50E-06	78.9	1.23E-03	20.8	5.93E-04	91.8	3.67E-02	53.7
$PM_{1–2.5}$	6.08E-03	52.3	2.08E-02	41.6	4.55E-05	21.4	6.19E-06	67.6	2.00E-06	21.1	4.70E-03	79.2	5.31E-05	8.2	3.17E-02	46.3
$PM_{2.5}$	1.16E-02		4.99E-02		2.12E-04		9.16E-06		9.50E-06		5.94E-03		6.46E-04		6.83E-02	

Table 5. Risk characterization for carcinogenic effects assessed by cancer risks (CRs) for Cr and Ni in each size-segregated PM range and in the main PM fractions. The percentage contributions of the size-segregated fractions to the total $PM_{2.5}$-CRs are also reported.

	Cr		**Ni**	
Size range [µm]	**CRs**	**% contributions**	**CRs**	**% contributions**
0.0283–0.0559	2.80E-07	2.0	1.63E-09	0.7
0.0559–0.0944	3.10E-07	2.2	4.85E-09	2.1
0.0944–0.157	2.60E-07	1.8	1.50E-08	6.5
0.157–0.262	6.56E-07	4.6	4.09E-08	17.7
0.262–0.383	1.15E-06	8.1	4.55E-08	19.6
0.383–0.614	2.27E-06	15.9	5.09E-08	22.0
0.614–0.950	1.90E-06	13.3	2.34E-08	10.1
0.950–1.6	3.21E-06	22.4	2.43E-08	10.5
1.6–2.4	4.26E-06	29.8	2.53E-08	10.9
PM fraction				
$PM_{0.1}$	5.90E-07	4.1	6.49E-09	2.8
$PM_{0.1–1}$	6.24E-06	43.6	1.76E-07	75.8
PM_{1}	6.83E-06	47.7	1.82E-07	78.6
$PM_{1–2.5}$	7.47E-06	52.3	4.96E-08	21.4
$PM_{2.5}$	1.43E-05		2.32E-07	

Figures

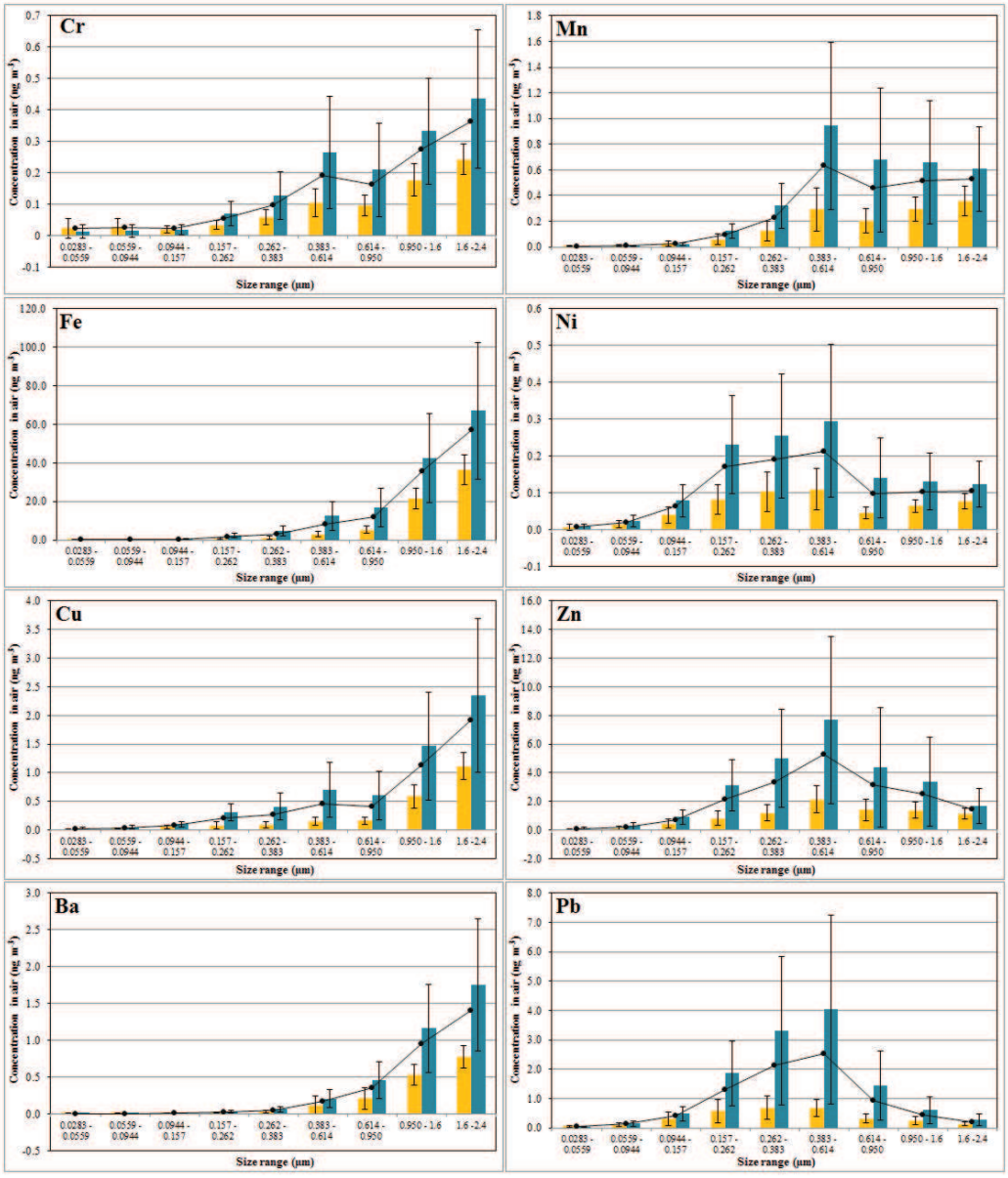

Figure 1. Average size-distributions for the investigated elements during the non-heating (yellow histograms) and the heating (blue histograms) season. Errors bars correspond to 1 standard deviation. The black points indicate the mean concentration values obtained during the whole campaign.

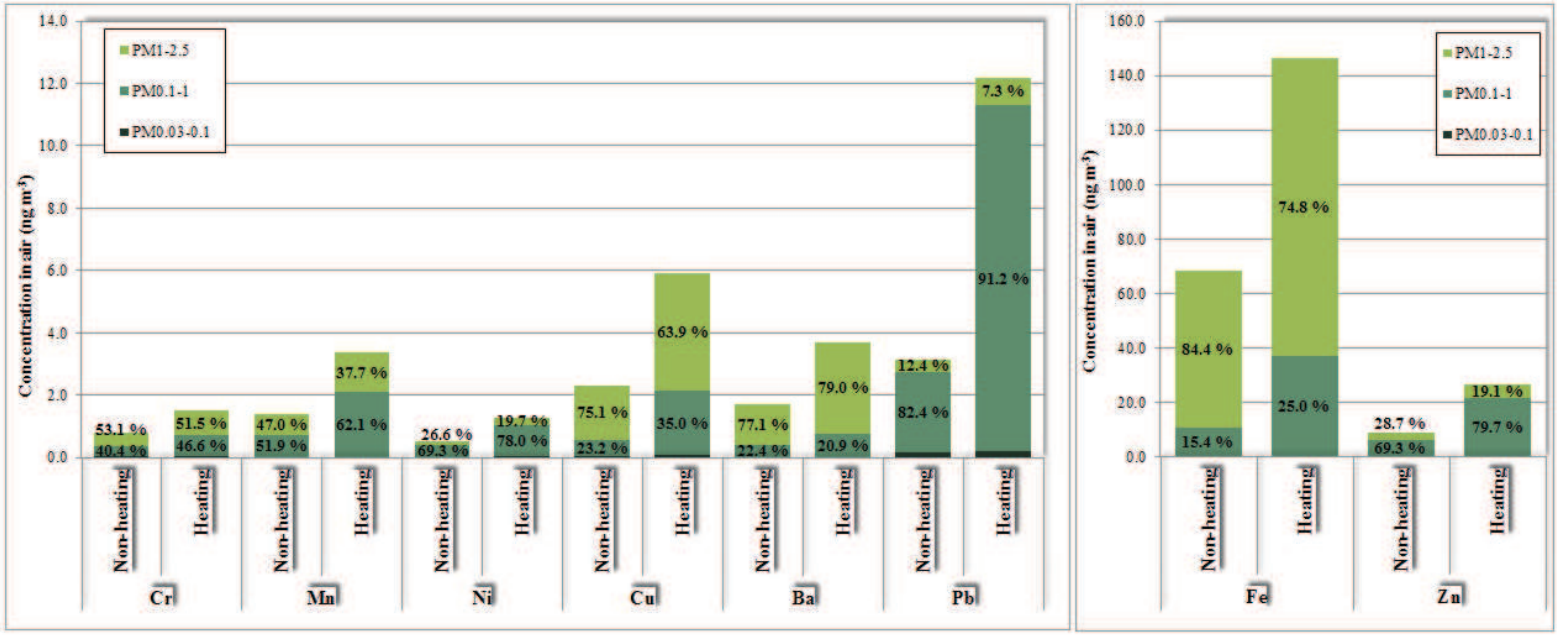

Figure 2. Mean contributions of the size-fractionated metal concentrations (relative values are also reported) to the average $PM_{2.5}$ levels during the non-heating and the heating period. For the 0.03–0.1 μm size range results are always < 5%.

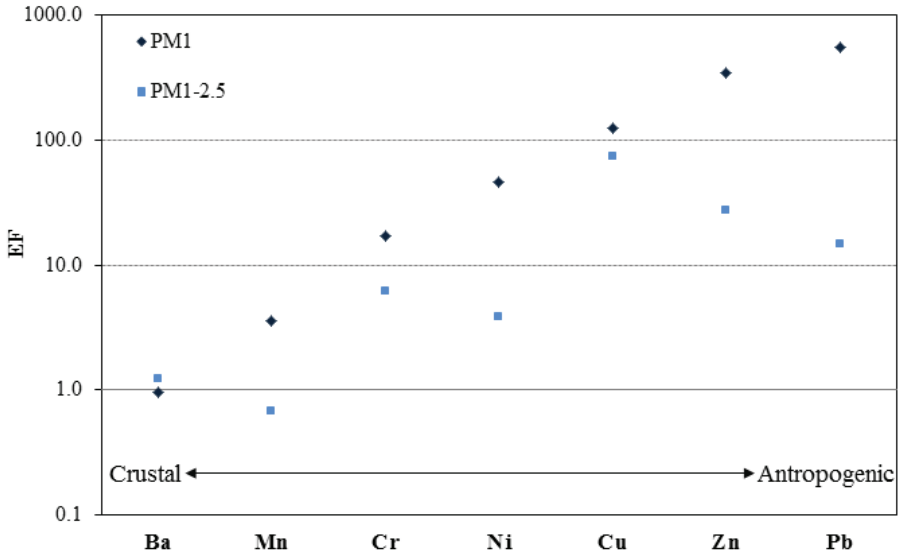

Figure 3. Average Enrichment Factors (EFs) calculated for the smaller (PM_1) and the coarser ($PM_{1\text{-}2.5}$) fractions during the whole campaign. The y-axis is on logarithmic scale.

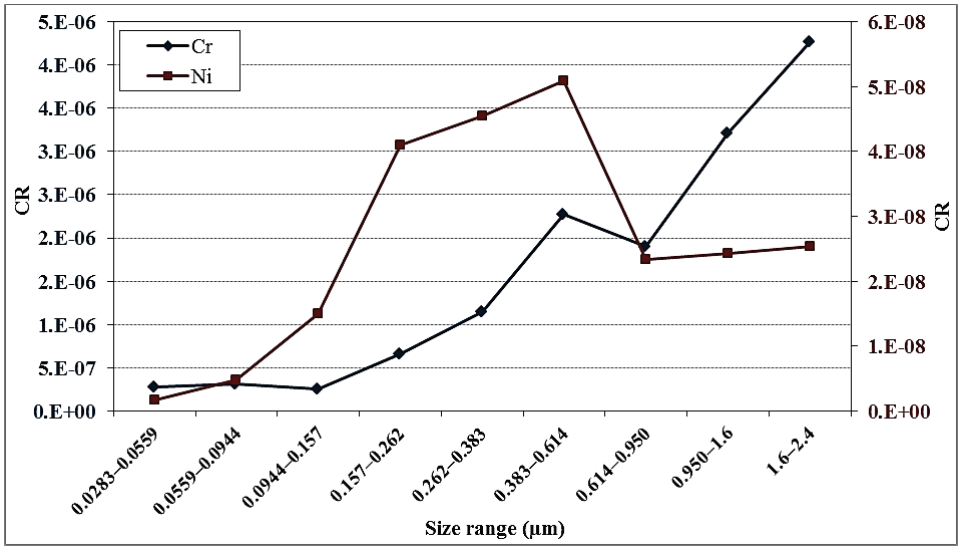

Figure 4. Cancer risk values (CRs) estimated for Cr and Ni via inhalation exposure for each PM size fraction.

Chapter 5 – *Is Particulate Air Pollution at the Front Door a Good Proxy of Residential Exposure?*

This chapter reports the pre-print (pre-refereeing) version of an article that has been accepted for publication in *Environmental Pollution*. The version of record [Zauli-Sajani, S., Trentini, A., **Rovelli, S.**, Ricciardelli, I., Marchesi, S., Maccone, C., Bacco, D., Ferrari, S., Scotto, F., Zigola, C., Cattaneo, A., Cavallo, D.M., Lauriola, P., Poluzzi, V. and Harrison, R.M. (2016). Is particulate air pollution at the front door a good proxy of residential exposure? *Environ. Pollut.* 213: 347–358] is available online at: http://dx.doi.org/10.1016/j.envpol.2016.02.033.

Abstract

The most recent and advanced epidemiological studies on health effects of air pollution assign exposure to individuals based on residential outdoor concentrations of air pollutants measured or estimated at the front-door. In order to assess to what extent this approach could cause misclassification of the important category of highly exposed subjects, measurements were carried out in unoccupied rooms at the front and back of a building which fronted onto a major urban road and adjacent outdoor locations to the front and rear of the building. Two 15-day monitoring campaigns were conducted in the period June-December 2013 in a building located in the urban area of Bologna, Italy. Particulate matter metrics including $PM_{2.5}$ mass and chemical composition, particle number concentration and size distribution were measured. Both outdoor and indoor concentrations at the front of the building substantially exceeded those at the rear. The highest front/back ratio was found for ultrafine particles with outdoor concentration at the front door 3.4 times higher than at the rear. A weak influence on front/back ratios was found for wind direction. Measurements of particle size distribution showed a substantial loss of particles especially within the sub-50 nm size range between the front and rear of the building and a further loss of this size range in the indoor data. The chemical speciation data showed relevant reductions for most constituents between the front and the rear of the building, especially for traffic related elements such as Elemental Carbon, Iron, Manganese and Tin. The main conclusion of the study is that gradients in concentrations between the front and rear, both outside and inside the building, are relevant and comparable to those measured between buildings located in neighbourhoods with high and low traffic volumes. These findings have implications for exposure modeling in epidemiological studies, which has a high potential for exposure misclassification.

1. Introduction

Air pollutants, and airborne particles in particular, pose significant risks to human health (REVIHAAP, 2013). A body of evidence has been accumulating over the last few decades on the effects of air pollution on cardiovascular and respiratory diseases, but there is still considerable uncertainty about the mechanisms of action linked to the health effects and about which physical and/or chemical characteristics of particulate matter (PM) are most important as determinants of health effects (Harrison and Yin, 2000; Kelly and Fussell, 2012).

A key point in assessing the health effects of air pollution is contrasting exposure between people residing in different cities (Pope at *al.*, 2009; Dockery *et al.*, 1993) or different areas within the same city and its surroundings (Raaschou-Nielsen *et al.*, 2013; Beelen *et al.*, 2014). Differences in exposure for people residing in urban areas are mainly related to differences in

proximity to traffic sources and the most recent and advanced epidemiological studies, especially those devoted to long term and traffic-related health effects (Hampel *et al.*, 2015; Wang *et al.*, 2014), assign exposure based on outdoor concentration of air pollutants measured or estimated at the front door. In this respect, Land Use Regression Models and Dispersion Models provide comparable performance (de Hoogh *et al.*, 2014; Beelen *et al.*, 2010) and have been demonstrated to be effective tools to improve exposure assessment compared to the use of data from fixed site monitoring stations. Nitrogen dioxide and particle concentration (usually ultrafine particle number or particles with aerodynamic diameter below 10 μm – PM_{10} – or particles with aerodynamic diameter below 2.5 μm – $PM_{2.5}$) are the most common parameters used as air quality indicators.

While a number of studies have investigated spatial variations of air pollutant concentrations between traffic and urban background sites (Boogard *et al.*, 2011; Naser *et al.*, 2008; Harrison *et al.*, 2004) and in specific locations, such as building-free areas near highways (Patton *et al.,* 2014; Zhu *et al.*, 2002) or inside street canyons (Zhou *et al.*, 2008), only very few studies have addressed specifically the issue of the differences between the concentrations of air pollutants at the front and back of buildings next to busy streets (Weber *et al.,* 2008; Hitchins *et al.*, 2002). Weber *et al.* found differences in particle mass and number concentrations between a busy urban street canyon and an adjacent backyard using optical particle counters. Higher concentrations in the canyon of on average 30 % for PM_{10} and 22 % for PM_1 were found within the street canyon. On the contrary Hitchins *et al.* found no significant gradients from the front to the rear of the building for $PM_{2.5}$ and submicrometer particle number concentrations considering three low-rise buildings at a distance between 11 and 75 m from roads.

The main goal of this paper is to investigate which particle metrics measured at the front door can be used as proxies of residential exposure. More specifically, we would like to investigate how large are the errors in assigning the same exposure to individuals residing in the same building near major roads. This is a key point in epidemiological studies because these individuals represent a very important subpopulation, that constituted by highly exposed subjects. This work is part of a series of monitoring campaigns planned within the "Supersito" project (http://www.arpa.emr.it/supersito) aimed at assessing the variability of exposure within urban areas with a special emphasis on various PM metrics (Zauli Sajani *et al.*, 2015).

2. Methods

2.1 Study Design

To achieve the study aims, two main methodological options were selected a-priori. The first was the choice of going beyond the mere comparison of front/back outdoor particle concentrations by including analyses indoors, where population exposure mostly occurs.

The second was the choice of monitoring uninhabited indoor environments. The main reason for this choice was related to the fact that many studies suggest that particles of outdoor and indoor origin have different physical and chemical characteristics (Brown *et al.*, 2008) and probably can also cause different health effects (Ebelt *et al.*, 2005). In fact, indoor exposure to particles of ambient outdoor origin constitutes the background exposure level, on which possible additive contributions of indoor-generated particles arising from specific indoor sources can superimpose (Urso *et al.*, 2015). Within-city gradients of exposure are assumed to be generated by background ambient exposure.

We selected two indoor environments similar in terms of volume and building materials, with virtually identical Air Exchange Rates (AERs). AERs were controlled by installing in each indoor environment a mechanical system to force air to be exchanged between indoors and outdoors. The system consisted of a fan connected to an air pipe (length = 1.2 m) carrying the air to the centre of the room (at a height of 2 m). Increased indoor air pressure caused the flow to go outwards through a grid. The fan in each room was set at a specific value related to the volume of the room in order to obtain an estimated AER of 0.4 h^{-1} in each room, reflective of a typical level for residential environments (Cattaneo *et al.*, 2011). In a previous work it has been shown that this method is highly effective and does not cause significant loss of particles (Zauli Sajani *et al.*, 2015).

The measurements at the two sides of the building were conducted simultaneously indoors and outdoors (i.e. we had four simultaneous measurement sites). Fig. 1 outlines the size of the building and the location of the monitoring sites. Fig. 1S shows a map of the area and gives a bird's eye view of the surroundings of the monitoring sites. The study building was two-storeyed and located next to a street which surrounds the historical centre of Bologna, a 400,000-inhabitant city in northern Italy. Traffic and domestic heating during the cold season are the dominant air pollution sources in the area and cause high levels of air pollutants. In the period 2011-2013 the city-average annual concentration of $PM_{2.5}$ was about 20 μg m^{-3}. The area near the monitoring site carries a moderate volume of traffic, and the street next to the building is one of the busiest streets of the entire municipal area with a traffic load of 31,000 vehicles (4–5% heavy duty vehicles) each working day. The building is located in a broad (20 m) two-way street canyon.

The indoor monitoring site at the front side (from now on "front site") was on the ground floor (street level). The volume of the room was 119 m^3 with a ceiling height of 3.5 m. The indoor environment at the back (from now on "back site") was on the ground floor as well. The volume of the room was 61 m^3 and the ceiling height was the same as that at the front side. For practical reasons the outdoor $PM_{2.5}$ monitoring site was located next to the building but at about 15 m from the indoor site along the same street (Fig. 1).

Two monitoring campaigns were conducted in the period June-December 2013. Each monitoring campaign lasted 15 days: 1st campaign from 11 to 25 June (often referred to in the text as "hot period"), 2nd campaign ("cold period") from 28 November to 13 December. Due to the availability of a unique filter for each day and measuring site, the chemical speciation was performed sequentially every three days for metals, ions, and carbon (Elemental Carbon and Organic Carbon). During cold periods elemental and organic carbon were measured on an 8 hour basis in order to avoid filter overload.

2.2 Instrumentation and Monitoring Procedure

Meteorological outdoor data were obtained from the meteorological station belonging to the urban meteorological network of ARPA Emilia-Romagna. The station is located close to the monitoring site at an horizontal distance of about 30 m. The station is on the top of a building 25 m above ground level and it measures hourly temperature, relative humidity, and wind speed and direction. Temperature is measured by means of a Pt100 RTD sensing element, while a capacitive sensor is used for humidity; wind speed and direction are measured using a three-cup anemometer and a wind vane respectively. Two digital thermo-hygrometers (Testo

175 H2, Testo AG, Lenzkirch, Deutschland) were used to measure temperature and relative humidity in the two indoor environments.

Four identical samplers (Skypost, TCR TECORA, Corsico – Mi) were operated to measure indoor and outdoor daily $PM_{2.5}$ concentrations at the two sites (flow rate 2.3 $m^3 h^{-1}$). Samples were collected on quartz fiber filters (Whatman, 47 mm diameter) and weighed following the procedure outlined in UNI EN 12341.

$PM_{2.5}$ samples were analyzed for various chemical species. In this paper we present the findings of the chemical species having more than 50% of contemporary data above the limit of quantification (LOQ) for indoor and outdoor samples at both sites. LOQs for chemical components are reported in the Supplementary Information. OC and TC were quantified by means of thermal-optical transmittance (Sunset Laboratory Inc., USA) using the EUSAAR_2 protocol. Inorganic ions were determined by extracting species in 10 mL of ultrapure water. The extracts were filtered and analyzed by Ion Chromatography (Dionex ICS-1000 for anions and ICS-1100 for cations, Thermo Fischer Scientific Inc., USA). Metals were analyzed by Inductively Coupled Plasma – Mass Spectrometry (8800 ICP-MS, Agilent Technologies Inc., USA). Sample digestion was made with nitric acid and hydrogen peroxide in a microwave digestion apparatus, according to UNI14902:2005, with a recovery efficiency over 85%

Two Fast Mobility Particle Sizers (FMPS model 3091; TSI, Shoreview, MN, USA) were used to measure particle size distributions and to estimate UltraFine Particle (UFP) concentrations. The FMPS was developed based on electrical aerosol spectrometer technology from Tartu University (Tammet et al. 2002). The FMPS spectrometer measured the size and number concentration of particles from 5.6 nm to 560 nm with 32 size bins every one second. Size bins below 13 nm were not included in the analysis because of the amount of data below the detection limit and also because of artifacts in the size distribution observed in other studies (Kaminski et al., 2013; Jeong et al., 2009). UFP concentrations were obtained summing the number of particles detected in the channels between 13 and 100 nm. Hourly and daily data were calculated and used in the analyses.

Indoor and outdoor size distributions were obtained with a switching system (Mod 11sc200, Pneumoidraulica Engineering S.r.l., Vicenza, Italy) which allowed for sampling from indoor and outdoor air, switching from one to the other within a time frame set by the user. A valve installed in the system could switch between sampling from the outdoor air, or from the indoor air. After the valve switched, there was a short time delay before the air from the sampled environment reached the instruments, which was the time the air travelled from the valve to the instruments. The system switched every 10 min between the indoor and outdoor measurements. In order to avoid the possibility of mixing of the outdoor and indoor air streams, the 2 min samples taken at the beginning of each 10 min period were deleted from the database.

The Air Exchange Rate in each indoor site was estimated in two ways. Firstly, AERs were estimated based on the air inflow measured at the end of the pipes taking into account the volumes of the rooms. The air inflow was measured with a TESTO 417 Anemometer. The measurements were performed five times at each velocity of the fan. The velocity of fan in each room was chosen in order to obtain an AER equal to 0.4 h^{-1}. Furthermore, in order to verify the estimated AERs, additional measurements based on the tracer gas-decay technique (ASTM Standard E741-95) were carried out. During these measurements, pure CO_2 was released as tracer gas within each indoor environment to obtain a uniform tracer concentration through the spaces being studied (ASHRAE, 1997). The decay in CO_2 concentrations was

continuously (sampling intervals of 1 min) monitored using non-dispersive infrared analyzers (GE sensing Telaire 7001, Goleta, CA, USA) provided with a battery-operated data logger (Hobo U12; Onset Computer Inc., Pocasset, MA, USA). A CO_2 analyzer was placed at each indoor and outdoor sampling site in order to monitor both the indoor gas decay - until the indoor baseline was reached - and the corresponding outdoor CO_2 levels.

2.3 QA/QC and Statistical Analysis

2.3.1 QA/QC

Agreements among gravimetric $PM_{2.5}$ measurements were checked in several intercomparison campaigns carried out in the years 2008-2012. Both correlation levels and tests for differences for slope and intercept of orthogonal regressions between co-located instruments were used as statistical indicators (EC, 2010). Determination coefficients were always higher than 0.972 (mean correlation 0.985). Typical errors (standard deviation of the differences between samplers) were about 2 μg m^{-3} and were quite similar among the various intercomparisons. The differences for slope (from identity) and intercepts (from zero) were usually not significant and not related to specific instruments. Consequently, no corrections were applied to $PM_{2.5}$ data.

In the preliminary phase of the monitoring campaign we carried out four intercomparisons (one before and after each monitoring campaign - mean duration 2 days) between the two FMPS using the same methodology applied for $PM_{2.5}$ samplers. No heteroscedasticity was detected and typical errors (standard deviation of the differences between UFP hourly data from the intercomparison campaigns) were 580 # cm^{-3}. The determination coefficient was 0.976. No correction was applied to the data.

Quality control of $PM_{2.5}$ mass and chemical composition data has been carried out based on residuals calculated by regression analysis between indoor and outdoor data. Data with residuals larger than three times the standard deviation of residuals were identified as anomalous. For FMPS data quality control the following procedure was used: a) applying a log10 function on the UFP minute data; b) stratifying data in time slots of three hours (0–3, 3–6 etc) and calculating the summary statistics for each slot and campaign; c) classifying data as anomalous if they were higher than the mean plus three times the standard deviation for the corresponding campaign and time slot. Then we averaged non-anomalous data on an hourly and daily basis. Statistical data analysis was carried out using the R package (Version 3.0.1).

2.3.2 ***Statistical Analysis***

Summary statistics and paired t-test have been used to investigate differences between series of measurements. Pearson correlation coefficients and regression analysis have been used to address linear relationships between data. An orthogonal regression approach (Fuller, 1987), which is the most suitable when both dependent and independent variable are affected by errors and are not related by a causal relationship, has been adopted.

3. Results and Discussion

3.1 Meteorological Conditions and Air Exchange Rates

The meteorological conditions during the study periods are summarized in Table 1S. The sampling periods were quite representative of the typical annual variability in the area (Table 2S). The mean outdoor temperature measured in the nearby meteorological monitoring station

during the first campaign (hot period) was 25.2°C with hourly values ranging from 15.6°C to 34 °C. Temperatures were much lower during the cold period, as expected, with a mean value of 4.8°C and minimum and maximum equal to -1.4 and 11.7°C, respectively. The area is characterized by low wind intensities and this was a common characteristic of the two monitoring campaigns (mean wind intensities from 1.6 m s^{-1} during the second campaign to 2.5 m s^{-1} during the first campaign). During the sampling periods precipitation events were rare: in fact, only one rainy day during the hot period was recorded with a total of 5.6 mm.
The temperatures measured at the two indoor monitoring sites showed very similar values and temporal patterns. Indoor seasonal differences were clearly reduced compared to those outdoors, especially due to the higher minimum values. Mean indoor temperatures during the hot period were 29.4°C and 29.9°C for the front and back site, respectively. In the cold season, indoor temperatures reached mean values of 16.1°C (front site) and 17.7°C (back site).
Figure 2S shows the wind rose for the campaign periods in 2013 compared to the overall average for the years 2012–2014. It is seen that the campaign period is broadly representative of the longer term average wind rose.
AERs estimated with the tracer gas-decay technique were between 0.2 and 0.3 h^{-1} in both indoor sites. These values were slightly lower than those estimated (0.4 h^{-1}) based on air inflow at the end of the pipes and room volumes.

3.2 Comparison of Front and Back Monitoring Sites

3.2.1 Ultrafine Particles Number Concentrations

Based on the procedure outlined in the methods section, 1.2% and 2.0% of raw data in the back and front site, respectively were classified as outliers and removed from the database. The completeness of hourly data was above 94% at all measurement sites.
Fig. 2 (a) and Table 1 give an overview of the UFP number concentrations during the monitoring campaigns. Mean outdoor UFP concentrations at the front site were 3.5 times higher than at the back site with higher front/back ratios during the cold period (4.2) compared to the hot season (2.5). The highest hourly value at the front site was 120,900 # cm^{-3} while the highest value in the back site was 26,860 # cm^{-3}. Our findings were similar although with gradients generally a little higher than those found in other studies comparing traffic with background sites (Zauli Sajani *et al.*, 2015; Patton *et al.*, 2014; Boogaard *et al.*, 2011; Moore *et al.*, 2009; Rivera *et al.*, 2012). Similar results were also found in a study in Athens (Diapouli *et al.*, 2011) showing a spatial variability ranging from ratios of 1.8 to 2.6 depending on the season. A difference of mean concentrations of UFP between traffic and urban-mean locations estimated with short-term measurements at 60 locations within the Basel urban area, showed a mean ratio of 1.6 (Ragettli *et al.*, 2014). A study on local-scale spatio-temporal variation of particle number in a 1 km^2 area in Braunschweig, Germany, showed during the winter season UFP number concentrations almost double at the roadside sites compared to residential and backyard sites. Reduced gradients were found during the summer season (Ruths *et al.*, 2014). Similar results were also found in Budapest (Salma *et al.*, 2014).
The range of UFP indoor concentrations was much lower than outdoors, at both sites. As for outdoors, large gradients were found in the UFP indoor concentrations between the front and back sites (ratio 2.2), with mean I_{front}/I_{back} ratios ranging from 1.7 during the hot period to 2.5 during the cold season.
The I/O ratio for UFP was higher in the back compared to the front site (0.5 vs 0.3) and

remained almost constant over the two campaigns (Table 1). As shown in the following section, higher I/O ratio at the front side is due to the very effective loss of freshly nucleated particles in the indoor environment. The I/O ratios found in this study are in good agreement with that obtained in the previous SUPERSITO campaign (Zauli Sajani *et al.*, 2015). Kearney *et al.* (2011) found median I/O ratios of hourly data ranging from 0.27 to 0.39. Diapouli *et al.* (2011) found an I/O ratio for particles in the 10–400 nm size range equal to 0.6 with AERs in the 0.5–1 h^{-1} range, while I/O ratios between 0.3–0.4 were found in Erfurt (Germany) (Cyrys *et al.*, 2004) and in other major European urban areas (Hoek *et al*., 2008).

The Pearson correlation coefficient between daily outdoor UFP concentrations at the front and rear was equal to 0.84 (Fig. 3). This value was slightly lower than in the previous SUPERSITO campaign and significantly higher than those reported in other studies focused on particle number concentrations (Puustinen *et al.*, 2007). Correlations between indoor UFP concentrations were lower (R = 0.79). Very similar correlation coefficients were found between indoor and outdoor UFP concentrations at the front and back sites (R = 0.94 and 0.85 respectively).

It was expected that wind direction would influence the relationship between the outdoor concentrations at the front and back of the building and thereby also influence the indoor concentrations. Both indoor and outdoor concentrations of UFP at the front of the building showed no appreciable sensitivity to wind direction (see Figs. 3S and 4S). At the back of the building, both outdoor and indoor UFP concentrations showed a similar wind speed and direction dependence with highest concentrations on stronger winds in the easterly sector. This is probably due to the fact that easterly winds tend to move primary or freshly nucleated particles from the street to the back of the building. The directional pattern of concentration ratios between the front and back of the building for UFP (Figs. 3S and 4S) was broadly similar, with the highest ratios occurring in the sector between north and west. Ratios between the front and back of the building outdoors showed a range from 2 to 4, while those indoors showed a smaller range from 2 to 2.5. Irrespective of wind direction, concentrations were always higher at the front than the rear of the building (Fig. 3S) and the influence of wind direction on the pattern of concentrations was not high. Therefore all the collected data have been presented together without disaggregation according to wind direction.

3.2.2 Particle Size Distribution

Fig. 4 shows the mean indoor and outdoor size distributions at the two sites for the two measurement periods. Multimodal distributions with sharp peaks at 20 and 30 nm in the concentrations were found outdoors at the front site. A second peak can occur at about 60–100 nm. This is typical of heavily trafficked sites, with the modes arising from the semi-volatile nucleation particles and solid graphitic particles respectively (Harrison *et al.*, 2011).

The presence of a bi (or tri)-modal distribution was also shown in previous studies (Morawska *et al.*, 2008; Hussein *et al.*, 2005) and is in line with knowledge of particle emissions and transformation. The 30 nm mode is due to the combination of freshly nucleated particles formed as the exhaust gases are diluted with ambient air and particles directly emitted by vehicles (Charron and Harrison, 2003). Nucleation mode particles are associated with the hot exhaust gases expelled from the tailpipe of a vehicle. These gases cool and condense to form large numbers of very small particles in the air (Shi and Harrison, 1999). On-road dilution of the exhaust plume is very important in the generation of particles in the exhaust plume. These

nucleation processes are favoured by low ambient temperatures and high relative humidity (Charron and Harrison, 2003) which are typical in the area during the cold season (Table 1S). In addition, the gaseous precursors condense or adsorb on to the surface of carbon particles in the accumulation mode.

Upon entry into the building, not only would the nucleation mode fraction show a higher deposition velocity than the coarser graphitic mode (Riley *et al.*, 2002), it would be subject in winter to evaporation at the higher indoor temperatures (Dall'Osto *et al.*, 2011) and the hydrocarbon vapours released would tend to adsorb to indoor surfaces (Weschler and Nazaroff, 2008) and settled indoor dusts (Weschler and Nazaroff, 2010). Such processes would contribute to a relatively rapid loss of the nucleation mode of particles such that shown in the front site between outdoor and indoor and from front outdoor to back.

Indoor size distributions were very similar to the findings of the previous work comparing traffic and residential sites (Zauli Sajani *et al.*, 2015). Similar shapes and differences between sites were also found by Ruths *et al.* (2014). Much lower relative weight of the nucleation mode compared to the accumulation mode was found indoors compared to the outdoor size distributions as was also found in other previous studies (Hussein *et al.*, 2004; Diapouli *et al.*, 2011).

Relevant differences in the shape of the size distributions were found between the cold and the hot period. The front outdoor site showed a much higher relative weight of small particles during the cold period. On the contrary, all other measuring sites showed a shift of the principal mode from about 30 nm towards 60–80 nm. The striking difference in the front outdoor size distributions between the seasons is likely to be due to the rapid loss of the semi-volatile constituents of the particles within the street canyon due to evaporation at the high temperatures occurred during the hot period (Table 1).

3.2.3 $PM_{2.5}$ Mass

Indoor and outdoor $PM_{2.5}$ concentrations during the two monitoring campaigns are shown in Fig. 2 (b) and Table 1. Small but significant differences in $PM_{2.5}$ outdoor concentrations were found, with average $PM_{2.5}$ levels at the front site about 14% higher than those at the back site. The highest outdoor values for daily mean $PM_{2.5}$ concentrations were 68 μg m^{-3} and 64 μg m^{-3} for the front and back site, respectively. As expected, outdoor concentrations during the cold period were, on average, more than three times higher compared to summer, according to the typical PM seasonal trends in some European countries (Oeder *et al.*, 2012).

The outdoor $PM_{2.5}$ ratio between front and back levels was slightly higher than the ratio between traffic and residential sites found in similar monitoring campaigns conducted under the same SUPERSITO project (1.14 vs 1.06) (Zauli Sajani *et al.*, 2015). The $PM_{2.5}$ spatial variability in our study was virtually equal to the mean within-city variability reported in the ESCAPE study, a very large epidemiological survey in Europe which included monitoring campaigns on air pollution spatial variability in urban areas (Eefftens *et al.*, 2012). That survey reported a mean ratio between traffic sites and urban background sites equal to 1.14, with a quite broad range of values (0.96–1.30). Similar $PM_{2.5}$ gradients (from 1.0 to 1.3) were found in a study focused on the comparison between street and background locations within the same cities in the Netherlands (Boogaard *et al.*, 2011).

Differently from UFPs, higher $PM_{2.5}$ ratios were found between front and back indoor concentrations (1.44 on average, 1.82 during the cold period and 1.31 during the hot period).

Mean indoor/outdoor (I/O) ratios for $PM_{2.5}$ during the cold period were equal to 0.57 in the front side and 0.46 at the rear. Differently from UFPs, higher values were found during the hot period with mean I/O ratios of 1.02 and 0.78 for the front and back side, respectively (Table 1). These results were in good agreement with previous studies in indoor settings (Chen *et al.*, 2011; Hanninen *et al.*, 2004). Inter-campaign $PM_{2.5}$ variations in the indoor environments were lower than outdoors. The ratios between the $PM_{2.5}$ indoor concentrations during the cold and the hot period were 1.71 for the front site and 2.38 for the back site. The corresponding ratios for outdoor $PM_{2.5}$ concentrations were markedly higher (3.02 and 3.91 at the front and back site, respectively).

A high correlation (R = 0.98) between outdoor $PM_{2.5}$ concentrations at the two sites was found (Figure 3). Indoor $PM_{2.5}$ concentrations were highly correlated as well (R = 0.95). Somewhat lower correlations were found between indoor and outdoor concentrations with I/O correlation coefficients at the front and back site equal to 0.91 and 0.90, respectively. These findings are similar to those found in other studies (Hanninen *et al.*, 2004) and the high I/O and I/I correlations is probably related to the absence of indoor sources.

3.2.4 Chemical Composition of $PM_{2.5}$

Table 3 shows descriptive statistics for the $PM_{2.5}$ chemical components. Organic carbon (OC) and nitrates were found to be the largest contributors to outdoor $PM_{2.5}$ mass at both sites, followed by elemental carbon (EC), sulfates and ammonium. Indoor data confirmed the primary role of OC and showed a pronounced decrease of nitrates. The contribution of ammonium was more than three times higher at the outdoor sites compared to indoor. Significant differences (p-value < 0.005) were found between outdoor front and back average levels for EC (3.96 and 2.25 μg m^{-3}, respectively) and Mn (7.25 and 5.55 ng m^{-3}, respectively) (Table 2). Large but not statistically significant were the outdoor trends for Fe and Sn (Table 2). The same patterns were confirmed indoors, with indoor differences always higher than outdoors. The largest I_{front}/I_{back} ratios were found for Fe and Sn, with values more than three times at the front door compared to the back site (Table 2).

As reported in the literature, EC is an important component of diesel exhaust particulate matter (Suvendrini Lena *et al.*, 2002; Shi *et al.*, 2000). Mn and Sn are typical markers of vehicle emissions for fine PM (Marcazzan *et al.*, 2001; Monaci *et al.*, 2000). Fe, Mn and also Cu are related with brake wear emissions (Manoli *et al.*, 2002; Gietl *et al.,* 2010). Tyre wear, brake wear, vehicle component detachment and fluid leakage are known sources of Fe (Ball *et al.*, 1991), as well as motor exhausts (Pant *et al.*, 2013). Furthermore, traffic-induced road dust resuspension also plays an important role for some elements (Fe and Mn), including those originated from crustal sources. Although more marked for the coarse size fraction, this can be considered also a contributor to fine fraction aerosol (Manoli *et al.*, 2002; Harrison *et al.*, 2012). Götschi *et al.* (2005) found substantially elevated concentrations of Cu, Fe and Mn in $PM_{2.5}$ particles at a busy street location. A strong elevation in EC, organic compounds and Fe-rich dust was also reported elsewhere (Harrison *et al.*, 2004).

Modestly increased Zn concentrations at the street site (1.11) were found in our survey. This could be due to the fact that Zn may derive from tyre wear (Manoli *et al.*, 2002) but also from a large number of other atmospheric sources (Thorpe and Harrison, 2008).

I/O ratios were < 1 for all the chemical species at both sites, with the exception of strong traffic markers (EC, V, Sn, Sb and Fe) at the front site (Table 3). This could be due to the location of

the outdoor sampling site (Fig. 1), which was placed in a more open space at about 15 m from the indoor environment, and it is likely that slightly higher concentrations of traffic-related pollutants would have been found if the outdoor sampling location was in front of the corresponding indoor sampling site. Low I/O ratios (<0.7) were found for chemical species of typical outdoor origin including nitrates (0.15), ammonium (0.29) and sulfates (0.65) at both sites (Table 3). The very low I/O ratios for nitrate are due to the evaporation of ammonium nitrate indoors, due to deposition of ammonia and nitric acid vapour on indoor surfaces causing destabilisation (see below).

The outdoor and indoor EC/TC ratios were respectively 0.31 and 0.39 at the front site and 0.21 and 0.22 at the back site. These values were similar to those reported by Naser *et al.* (2008) for outdoor urban data.

Table 4 shows the Pearson correlation coefficients among the chemical components. Outdoor data at the two sampling sites were highly correlated. The correlation coefficients were all greater than 0.9 with the exception of Sn (0.70) and Fe (0.38), which further confirms in general the origin of these elements, closely related to the traffic source. The findings for OC, EC, ammonium, nitrates and sulfates were expected as high correlation levels between within-city outdoor concentrations of PM these constituents were found by Bell *et al.* (2011) and Naser *et al.* (2008).

Very high correlations were also found between indoor data, except for Sn (0.69). Correlation levels were also generally high between indoor and outdoor data. Low R values were found only for Fe (0.16) at the front site and for Sn (0.45) at the back site. High correlations between indoor and outdoor levels of OC and EC were found by Sawant *et al.* (2004) in several schools in California . The I/O correlations for ammonium found by the same authors showed large variability in the different schools. Particles of outdoor origin can undergo substantial changes and may be lost to building walls during indoor penetration. A study investigating the transformation of ambient ammonium nitrate aerosols in indoor environments has shown that measured indoor concentrations were considerably lower than the values predicted based only on penetration and deposition losses (Lunden *et al.*, 2003). This was attributed to the semi-volatility of ammonium nitrate, leading to losses as nitric acid and ammonia vapours. This behavior was also highlighted in the previous SUPERSITO campaign (Zauli Sajani *et al.*, 2015).

3.3 Strengths and Weaknesses of the Study

A major strength of the study was the simultaneous measurement of a number of particulate characteristics (mass, size distribution, chemical composition) to assess the variability of exposure between front and back of a building next to a busy street. The simultaneous indoor and outdoor measurements were also a key strength of the study because of the role of the indoor environment in determining exposure. To our knowledge, this is the first study comparing simultaneous indoor and outdoor measurements on the front and back side of the same building taking into account both size distribution and chemical components of particulate matter.

The choice of monitoring uninhabited indoor environments made possible the use of instruments such as instruments for $PM_{2.5}$ mass measurements using reference methods that are rarely used in inhabited house due to their size and noise emissions.

A possible weakness of the study is related to the choice of a unique building to be monitored. Other monitoring campaigns in different settings could be useful but we think that this study should be considered significantly more than a pilot study. As a matter of fact, the selected building is a quite common setting within urban areas even though pure canyon configuration with higher and continuous buildings could produce even higher front/back gradients compared to our findings. In conclusion we think that our study gives important insights about possible misclassification of people residing next to busy streets. The choice of selecting AER to a typical value should be a plus with regards to the generalization of our findings.
Field campaigns in inhabited houses could give supplemental information but would not separate outdoor and indoor origins of particles. Moreover such an approach would suffer from the tremendous variability of indoor characteristics and personal habits of the population. This would represent a substantial problem in being able to identify gradients in population exposure due to particles of ambient origin.
It may also be questioned as to whether the air ventilation system could be a weakness of our study. This question was considered in detail in our earlier paper (Zauli Sajani *et al.*, 2015). In brief, we think that the two identical simple systems installed to impose fixed and equal air exchange rates between sites should be considered a strength and not a weakness of the study. Firstly, this choice provided a good control on the air exchange rate in the two indoor environments. Secondly, the choice eliminated the effect of possibly different specific infiltration factors of each building envelope.

4. Summary and Conclusions

This study focused on the variations of exposure to various particle metrics from the front to the back of a building located next to a trafficked street. In particular, both indoor and outdoor spatial gradients have been analyzed in terms of $PM_{2.5}$ mass and chemical composition, size distribution and particle number concentrations. Large differences in the concentrations of UFP, tin, manganese, iron and elemental carbon were found both indoors and outdoors. Sizeable but less substantial were the spatial gradients for $PM_{2.5}$. Significant differences were also found for the shape of particle size distributions for outdoor particles, while indoor particles showed very similar distributions. Indoor front/back gradients are generally consistent in terms of direction but with remarkable differences in magnitudes between the different particle metrics. Indoor concentrations were much lower than outdoors for $PM_{2.5}$ mass and UFP. Taking into account the chemical components, the building environment was protective especially for nitrates, ammonium, potassium, sulfates, lead and cadmium underlining the different characteristics of indoor particulate matter compared to outdoor independently from the presence of indoor sources.
Our findings show that the variability of exposure to air pollution of people living in the same building next to a busy street may be large i.e. some people could be erroneously classified as highly exposed. The front/back variability is comparable to that found in previous studies involving people residing in buildings in a heavy and low traffic areas. Given that a common way to assess the risks due to exposure to air pollutants, and in particular to the risks associated with proximity to traffic sources, is by contrasting exposure levels within cities, and considering that the assessment of population exposure is usually based on residential outdoor concentrations estimated at the front-door, the impact of exposure misclassification could be important. Epidemiological studies should consider these findings when designing their

strategy for exposure assessment in order to avoid or at least reduce potentially large overestimation (with regards to concentration of some metrics) and mis-estimation (with regards to physical and chemical characteristics of particles) of exposure to air pollutants for people living in the back of buildings close to heavy trafficked roads .

Acknowledgments

This research was conducted as part of the SUPERSITO Project, which was supported and financed by the Emilia-Romagna Region (Deliberation of the Regional Government n. 1971/13) and the Regional Agency for Prevention and Environment (ARPA Emilia-Romagna). Financial contribution for the collaboration between ARPA Emilia-Romagna and the University of Birmingham came from the Kic-Pioneers EU Program which involved the corresponding author. The authors thank Sandra Sangiorgi, Michele Volta and Giuseppe Simoni for the logistic support.

References

ASHRAE, 1997. Evaluating Building IAQ and Ventilation with Indoor Carbon Dioxide. ASHRAE Transactions, Vol. 103, No. 2. Available online: http://fire.nist.gov/bfrlpubs/build97/PDF/b97044.pdf

Ball, D., Hamilton, R. and Harrison, R., (1991). The influence of highway-related pollutants on environmental quality. In: Hamilton R, Harrison R (Eds), Highway Pollution, Elsevier Science, New York, pp. 1–47.

Beelen, R., Voogt, M., Duyzer, J., Zandveld, P. and Hoek, G. (2010). Comparison of the performances of land use regression modelling and disperion modelling in estimating small-scale variations in long-term air pollution concentrations in a Dutch urban area. *Atmos. Environ.* 44: 4614–4621.

Beelen, R., Raaschou-Nielsen, O., Stafoggia, M., Andersen, Z.J., Weinmayr, G., Hoffmann, B., Wolf, K., Samoli, E., Fischer, P., Nieuwenhuijsen, M., Vineis, P., Xun, W.W., Katsouyanni, K., Dimakopoulou, K., Oudin, A., Forsberg, B., Modig, L., Havulinna, A.S., Lanki, T., Turunen, A., Oftedal, B., Nystad, W., Nafstad, P., De Faire, U., Pedersen, N.L., Östenson, C.G., Fratiglioni, L., Penell, J., Korek, M., Pershagen, G., Eriksen, K.T., Overvad, K., Ellermann, T., Eeftens, M., Peeters, P.H., Meliefste, K., Wang, M., Bueno-de-Mesquita, B., Sugiri, D., Krämer, U., Heinrich, J., de Hoogh, K., Key, T., Peters, A., Hampel, R., Concin, H., Nagel, G., Ineichen, A., Schaffner, E., Probst-Hensch, N., Künzli, N., Schindler, C., Schikowski, T., Adam, M., Phuleria, H., Vilier, A., Clavel-Chapelon, F., Declercq, C., Grioni, S., Krogh, V., Tsai, M.Y., Ricceri, F., Sacerdote, C., Galassi, C., Migliore, E., Ranzi, A., Cesaroni, G., Badaloni, C., Forastiere, F., Tamayo, I., Amiano, P., Dorronsoro, M., Katsoulis, M., Trichopoulou, A., Brunekreef, B. and Hoek, G. (2014). Effects of long-term exposure to air pollution on natural-cause mortality: an analysis of 22 European cohorts within the multicentre ESCAPE project. *Lancet* 383: 785–795.

Bell, M.L., Ebisu, K. and Peng, R.D. (2011). Community-level spatial heterogeneity of chemical constituent levels of fine particulates and implications for epidemiological research. *J. Expo. Sci. Env. Epid.* 21: 372–384.

Boogaard, H., Kos, G.P.A., Weijers E.P., Janssen, N.A.H., Fischer P.H., Van der Zee, S.C., De Hartog, J.J. and Hoek, G. (2011). Contrast in air pollution components between major

streets and background locations: Particulate matter mass, black carbon, elemental composition, nitrogen oxide and ultrafine particle number. *Atmos. Environ.* 45: 650–658.

Brown K.W., Sarnat J.A., Suh H.H., Coull B.A., Spengler J.D. and Koutrakis P. (2008). Ambient site, home outdoor and home indoor particulate concentrations as proxies of personal exposures. *J. Environ. Monitor.* 10(9): 1041–1051.

Cattaneo, A., Peruzzo, C., Garramone, G., Urso, P., Ruggeri, R., Carrer, P. and Cavallo, D.M. (2011). Airborne particulate matter and gaseous air pollutants in residential structures in Lodi province, Italy. *Indoor Air* 21: 489–500.

Charron, A. and Harrison, R.M. (2003). Primary particle formation from vehicle emissions during exhaust dilution in the roadside atmosphere. *Atmos. Environ.* 37: 4109–4119.

Chen, C. and Zhao, B. (2011). Review of relationship between indoor and outdoor particles: I/O ratio, infiltration factor and penetration factor [Rivista] // *Atmos. Environ.* 45: 275–288.

Cyrys, J., Heinrich, J., Richter, K., Wölke, G. and Wichmann, H.E. (2000). Source and concentrations of indoor nitrogen dioxide in Hamburg (west Germany) and Erfurt (east Germany). *Sci Total Environ.* 250: 51–62.

Cyrys, J., Pitz, M., Bischof, W., Wichmann, H.E. and Heinrich, J. (2004). Relationship between indoor and outdoor levels of fine particle mass, particle number concentrations and black smoke under different ventilation conditions. *J. Expo. Anal. Env. Epid.* 14: 275–283.

Dall'Osto, M., Thorpe, A., Beddows, D.C.S., Harrison, R.M., Barlow, J.F., Dunbar, T., Williams, P.I. and Coe, H. (2011). Remarkable dynamics of nanoparticles in the urban atmosphere. *Atmos. Chem. Phys.* 11: 6623–6637.

Diapouli, E., Eleftheriadis, K., Karanasiou, A. and Vratolis, S. (2011). Indoor and outdoor particle number and mass concentrations in Athens. Sources, sinks and variability of aerosol parameters. *Aerosol Air Qual. Res.* 11: 632–642.

Dockery, D.W., Pope III, A., Xu, X., Spengler, J.D., Ware, J.H., Fay, M.E., Ferris, B.G. and Speizer, F.E. (1993). An association between air pollution and mortality in six U.S. cities. *The New England Journal of Medicine* 329: 1753–1759.

Ebelt ST, Wilson WE and Brauer M. (2005). Exposure to ambient and nonambient components of particulate matter: a comparison of health effects. *Epidemiology* 16(3): 396–405.

EC, 2010. Guide to the demonstration of equivalence of ambient air monitoring methods. Report by an EC Working Group on Guidance for the Demonstration of Equivalence. - 2010. EN 15267, n 3). URL: http://europa.eu.int/comm/environment/air/pdf/equivalence_report3.pdf.

Eeftens, M., Tsai, M.-Y., Ampe, C., Anwander, B., Beelen, R., Bellander, T., Cesaroni, G., Cirach, M., Cyrys, J., de Hoogh, K., De Nazelle, A., de Vocht, F., Declercq, C., Dėdelė, A., Eriksen, K., Galassi, C., Gražulevičienė, R., Grivas, G., Heinrich, J., Hoffmann, B., Iakovides, M., Ineichen, A., Katsouyanni, K., Korek, M., Krämer, U., Kuhlbusch, T., Lanki, T., Madsen, C., Meliefste, K. and Mölter, A. (2012). Spatial variation of $PM_{2.5}$, PM_{10}, $PM_{2.5}$ absorbance and PM_{coarse} concentrations between and within 20 European study areas and the relationship with NO_2 - results of the ESCAPE project. *Atmos. Environ.* 62: 303–317.

Fuller, W.A. (1987). Measurement Error Models. Wiley, New York.

Gietl, J.K., Lawrence, R., Thorpe, A.J. and Harrison, R.M (2010). Identification of brake wear particles and derivation of a quantitative tracer for brake dust at a major road. *Atmos. Environ.* 44: 141–146.

Götschi, T., Hazenkamp-von Arx, M.E., Heinrich, J., Bono, R., Burney, R., Forsberg, B., Jarvis, D., Maldonadog, J., Norbäckh, D., Sterni, W.B., Sunyerj, J., Torénk, K., Verlatol, G., Villani, S. and Künzli, N. (2005). Elemental composition and reflectance of ambient fine particles at 21 European location. *Atmos. Environ.* 39: 5947–5958.

Hampel, R., Peters, A., Beelen, R., Brunekreef, B., Cyrys, J., de Faire, U., de Hoogh, K., Fuks, K., Hoffmann, B., Hüls, A., Imboden, M., Jedynska, A., Kooter, I., Koenig, W., Künzli, N., Leander, K., Magnusson, P., Männistö, S., Penell, J., Pershagen, G., Phuleria, H., Probst-Hensch, N., Pundt, N., Schaffner, E., Schikowski, T., Sugiri, D., Tiittanen, P., Tsai, M.Y., Wang, M., Wolf, K. and Lanki, T., ESCAPE TRANSPHORM study groups. (2015). Long-term effects of elemental composition of particulate matter on inflammatory blood markers in European cohorts. *Environ. Int.* 82: 76–84.

Hanninen, O.O., Lebret, E., Ilacqua, V., Katsouyanni, K., Kunzli, N., Sram, R.J. and Jantunen, M. (2004). Infiltration of ambient $PM_{2.5}$ and levels of indoor generated non-ETS $PM_{2.5}$ in residences of four European cities. *Atmos. Environ.* 38: 6411–6423.

Harrison, R.M., Jones, A., Gietl, J., Yin, J. and Green, D. (2012). Estimation of the contribution of brake dust, tire wear and resuspension to nonexhaust traffic particles derived from atmospheric measurements. *Environ. Sci. Technol.* 46: 6523–6529.

Harrison, R.M., Beddows, D.C.S. and Dall'Osto, M. (2011). PMF analysis of wide-range particle size spectra collected on a major highway. *Environ. Sci. Technol.* 45: 5522–5528.

Harrison, R.M., Jones, A.M. and Lawrence, R.G. (2004). Major component composition of PM_{10} and $PM_{2.5}$ from roadside and urban background sites. *Atmos. Environ.* 38: 4531–4538.

Harrison, R.M. and J. Yin, 2000. Particulate matter in the atmosphere: Which particle properties are important for its effects on health? *Sci. Total Environ.* 249: 85–101.

Harrison, R.M., Leung, P.L., Somervaille, L., Smith, R. and Gilman, E. (1999). Analysis of incidence of childhood cancer in the West Midlands of the United Kingdom in relation to proximity to main roads and petrol stations. *Occup. Environ. Med.* 56: 774–780.

Hitchins, J., Morawska, L., Gilbert, D. and Jamriska, M. (2002). Dispersion of particles from vehicle emissions around high- and low-rise buildings. *Indoor Air* 12: 64–71.

Hoek, G., Beelen, R., de Hoog, K., Viennau, D., Gulliver, J., Fisher, P. and Briggs, D. (2008). A review of land-use regression models to asses spatial variation of outdoor air pollution. *Atmos. Environ.* 42: 7561–7578.

Hoek, G., Ko,s G., Harrison, R.M., de Hartog, J., Meliefste, K., ten Brink, H., Katsouyanni, K., Karakatsani, A., Lianou, M., Kotronarou, A., Kavouras, I., Pekkanen, J., Vallius, M., Kulmala, M., Puustine,n A., Thomas, S., Meddings, C., Ayres, J., van Wijnen, J. and Hameri, K. (2008). Indoor-outdoor relationships of particle number and mass in four European cities. *Atmos. Environ.* 42: 156–169.

de Hoogh, K., Korek, M., Vienneau, D., Keuken, M., Kukkonen, J., Nieuwenhuijsen, M.J., Badaloni, C., Beelen, R., Bolignano, A., Cesaroni, G., Pradas, M.C., Cyrys, J., Douros, J., Eeftens, M., Forastiere, F., Forsberg, B., Fuks, K., Gehring, U., Gryparis, A., Gulliver, J., Hansell, A.L., Hoffmann, B., Johansson, C., Jonkers, S., Kangas, L., Katsouyanni, K., Künzli, N., Lanki, T., Memmesheimer, M., Moussiopoulos, N., Modig, L., Pershagen, G., Probst-Hensch, N., Schindler, C., Schikowski, T., Sugiri, D., Teixidó, O., Tsai, M.Y., Yli-Tuomi, T., Brunekreef, B., Hoek, G. and Bellander, T. (2014). Comparing land use regression and dispersion modelling to assess residential exposure to ambient air pollution for epidemiological studies. *Environ. Int.* 73: 382–392.

Hussein, T., Hameri, K., Aalto, P., Asmi, A., Kakko, L. and Kulmala, M. (2004). Particle size characterization and indoor-to-outdoor relationship of atmospheric aerosol in Helsinki. *Scandinavian Journal of Work, Environment and Health* 30: 54–62.

Hussein, T., Hameri, K, Aalto, P.P., Paatero, P. and Kulmala, M. (2005). Modal structure and spatial-temporal variations of urban and suburban aerosol in Helsinki - Finland. *Atmos. Environ.* 39: 1655–1668.

Jeong, C.H. and Evans, G. (2009). Inter-comparison of a fast mobility particle sizer and a scanning mobility particle sizer intercorporating an ultrafine water-based condensation particle counter. *Aerosol Sci. Tech.* 43: 364–373.

Kaminski, H., Kuhlbusch, T.A.J., Rath, S., Gotz, U., Sprenger, M., Wels, D., Polloczek, J., Bachmann, V., Dziurowitz, N., Kiesling, H.-J., Schwiegelshohn, A., Monz, C., Dahmann, D. and Asbach, C. (2013). Comparability of mobility particle sizers and diffusion chargers. *J. Aerosol Sci.* 57: 156–178.

Kearney, J., Wallace, L., MacNeill, M., Xu, X., VanRyswyk, K., You, H., Kulka, R. and Wheeler A.J. (2011). Residential indoor and outdoor ultrafine particles in Windsor, Ontario. *Atmos. Environ.* 45: 7583–7593.

Kelly, F.J. and Fussell, J.C. (2012). Size, source and chemical composition as determinants of toxicity attributable to ambient particulate matter. *Atmos. Environ.* 60: 504–526.

Lunden, M.M, Revzana, K.L., Fischer, M.L., Thatcher, T.L, Littlejohn, D., Hering, S.V. and Brown, N.J. (2003). The transformation of outdoor ammonium nitrate aerosols in the indoor environment. *Atmos. Environ.* 37: 5633–5644.

Manoli, E., Voutsa, D. and Samara, C. (2002). Chemical characterization and source identification/apportionment of fine and coarse air particles in Thessaloniki, Greece. *Atmos. Environ.* 36: 949–961.

Marcazzan, G.M., Vaccaro, S., Valli, G. and Vecchi, R. (2001). Characterization of PM_{10} and $PM_{2.5}$ particulate matter in the ambient air of Milan (Italy). Atmos. Environ. 35: 4639–4650.

Monaci, F., Moni, F., Lanciotti, E., Grechi, D. and Bargagli, R. (2000). Biomonitoring of airborne metals in urban environments: new tracers of vehicle emission, in place of lead. *Environ. Pollut.* 107: 321–327.

Moore, K., Krudysz, M., Pakbin, P. Hudda, N. and Sioutas, C. (2009). Intra-community variability in total particle number concentrations in the San Pedro Harbor area (Los Angeles, California). *Aerosol Sci. Technol.* 43: 587–603.

Morawska, L., Ristovski, Z., Jayaratne, E.R., Keogh, D.U. and Ling, X. (2008). Ambient nano and ultrafine particles from motor vehicle emissions: Characteristics, ambient processing and implications on human exposure. *Atmos. Environ.* 42: 8113–8138.

Naser, T.M. Yoshimura, Y., Sekiguchi, K., Wang, Q. and Sakamoto, K. (2008). Chemical composition of $PM_{2.5}$ and PM_{10} and associated Polycyclic Aromatic Hydrocarbons at a roadside and urban background area in Saitama, Japan. *Asian Journal of Atmospheric Environment* 2: 99–101.

Oeder, S., Dietrich, S., Weichenmeir, I., Schober, W., Pusch, G., Jörres, R.A., Schierl, R., Nowak, D., Fromme, H., Behrendt, H. and Buters, J.T.M. (2012). Toxicity and elemental composition of particulate matter from outdoor and indoor air of elementary schools in Munich, Germany. *Indoor Air* 22: 148–158.

Pant, P. and Harrison, R.M. (2013). Estimation of the contribution of road traffic emissions to particulate matter concentrations from field measurements: a review. *Atmos. Environ.* 77: 89–97.

Patton, A.P., Perkins, J., Zamore, W., Levy, J.I., Brugge, D. and Durant, J.L. (2014). Spatial and temporal differences in traffic-related air pollution in three urban neighborhoods near an interstate highway. *Atmos. Environ.* 99: 309–321.

Pope III C.A., Ezzati, M. and Dockery, D.W. (2009). Fine-particulate air pollution and life expectancy in the United States. *New England Journal Medicine* 360:376–86.

Puustinen, A., Hämeri, K., Pekkanen, J., Kulmala, M., de Hartog, J., Meliefste, K., ten Brink, H., Kos, G., Katsouyanni, K., Karakatsani, A., Kotronarou, A., Kavouras, I., Meddings, C., Thomas, S., Harrison, R., Ayres, J., van der Zee, S. and Hoek, G. (2007). Spatial variation of particle number and mass over four European cities. *Atmos. Environ.* 41: 6622–6636.

Ragettli, M.S., Ducret-Stich, R.E., Foraster, M., Morelli, X., Aguilera, I., Basagaña, X., Corradi, E., Ineichen, A., Tsai, M.Y., Probst-Hensch, N., Rivera, M., Slama, R., Künzli, N. and Phuleria, H.C. (2014). Spatio-temporal variation of urban ultrafine particle number concentrations. *Atmos. Environ.* 96: 275–283.

Raaschou-Nielsen O, Andersen ZJ, Beelen R, Samoli E, Stafoggia M, Weinmayr G, Hoffmann B, Fischer P, Nieuwenhuijsen MJ, Brunekreef B, Xun WW, Katsouyanni K, Dimakopoulou K, Sommar J, Forsberg B, Modig L, Oudin A, Oftedal B, Schwarze PE, Nafstad P, De Faire U, Pedersen NL, Ostenson CG, Fratiglioni L, Penell J, Korek M, Pershagen G, Eriksen KT, Sørensen M, Tjønneland A, Ellermann T, Eeftens M, Peeters PH, Meliefste K, Wang M, Bueno-de-Mesquita B, Key TJ, de Hoogh K, Concin H, Nagel G, Vilier A, Grioni S, Krogh V, Tsai MY, Ricceri F, Sacerdote C, Galassi C, Migliore E, Ranzi A, Cesaroni G, Badaloni C, Forastiere F, Tamayo I, Amiano P, Dorronsoro M, Trichopoulou A, Bamia C, Vineis, P. and Hoek, G. (2013). Air pollution and lung cancer incidence in 17 European cohorts: prospective analyses from the European Study of Cohorts for Air Pollution Effects (ESCAPE). *Lancet Oncology* 14: 813–822.

REVIHAAP, 2013. Review of evidence on health aspects of air pollution - REVIHAAP Project. Technical Report, World Health Organization, Regional Office for Europe, Copenhagen.

Riley, Q.J., Mckone, T.E., Lai, A.C.K. and Nazaroff, W.W. (2002). Indoor particulate matter of outdoor origin: importance of size dependent removal mechanisms. *Environ. Sci. Technol.* 36: 200–207.

Rivera, M., Basagana, X., Aguilera, I., Agis, D., Bouso, L., Foraster, M., Medina-Ramón, M., Pey, J., Künzli, N. and Hoek, G. (2012). Spatial distribution of ultrafine particles in urban settings: a land use regression model. *Atmos. Environ.* 54: 657–666.

Ruths, M., von Bismarck-Osten, C. and Weber, S. (2014). Measuring and modelling the local-scale spatio-temporal variation of urban particle number size distributions and black carbon. *Atmos. Environ.* 96: 37–49.

Sawant, A.A., Na, K., Zhu, X., Cocker, K., Butt, S., Song, C. and Cocker III, D.R. (2004). Characterization of $PM_{2.5}$ and selected gas-phase compounds at multiple indoor and outdoor sites in Mira Loma, California. *Atmos. Environ.* 38: 6269–6278.

Shi, J.P., Mark, D. and Harrison, R.M. (2000). Characterization of particles from a current technology heavy-duty diesel engine. *Environ. Sci. Technol.* 34: 748–755.

Shi, J.P. and Harrison R.M. (1999). Investigation of ultrafine particle formation during diesel exhaust dilution. *Environ. Sci. Technol*. 33: 3730–3736.

Suvendrini Lena, T., Ochieng, V., Carter, M., Holguin-Veras, J. and Kinney, P.L. (2002). Elemental carbon and $PM_{2.5}$ levels in a urban community heavily impacted by truck traffic. *Environ. Health Persp.* 110: 1009–1015.

Tammet, H., Mirme, A. and Tamm, E. (2002). Electrical aerosol spectrometer of Tartu University. *Atmos. Res.* 62: 315–324.

Urso , P., Cattaneo, A., Garramone, G., Peruzzo, C., Cavallo, D.M. and Carrer, P. Identification of particulate matter determinants in residential homes. *Build. Environ.* 86: 61–69.

Wang, M., Beelen, R., Stafoggia, M., Raaschou-Nielsen, O., Andersen, Z.J., Hoffmann, B., Fischer, P., Houthuijs, D., Nieuwenhuijsen, M., Weinmayr, G., Vineis, P., Xun, W.W., Dimakopoulou, K., Samoli, E., Laatikainen, T., Lanki, T., Turunen, A.W., Oftedal, B., Schwarze, P., Aamodt, G., Penell, J., De Faire, U., Korek, M., Leander, K., Pershagen, G., Pedersen, N.L., Östenson. C.G., Fratiglioni, L., Eriksen, K.T., Sørensen, M., Tjønneland, A., Bueno-de-Mesquita, B., Eeftens, M., Bots, M.L., Meliefste, K., Krämer, U., Heinrich, J., Sugiri, D., Key, T., de Hoogh, K., Wolf, K., Peters, A., Cyrys, J., Jaensch, A., Concin, H., Nagel, G., Tsai, M.Y., Phuleria, H., Ineichen, A., Künzli, N., Probst-Hensch, N., Schaffner, E., Vilier, A., Clavel-Chapelon, F., Declerq, C., Ricceri, F., Sacerdote, C., Marcon, A., Galassi, C., Migliore, E., Ranzi, A., Cesaroni, G., Badaloni, C., Forastiere, F., Katsoulis, M., Trichopoulou, A., Keuken, M., Jedynska, A., Kooter, I.M., Kukkonen, J., Sokhi, R.S., Brunekreef, B., Katsouyanni, K. and Hoek, G. (2014). Long-term exposure to elemental constituents of particulate matter and cardiovascular mortality in 19 European cohorts: results from the ESCAPE and TRANSPHORM projects. *Environ. Int.* 66: 97–106.

Weber, S. and Weber, K. (2008). Coupling of urban street canyon and backyard particle concentrations. *Meteorologische Zeitshrift* 17: 251–261.

Weschler, C.J. and Nazaroff, W.W. (2008). Semivolatile organic compounds in indoor environments. *Atmos. Environ.* 42: 9018–9040.

Weschler, C.J. and Nazaroff, W.W. (2010). SVOC partitioning between the gas phase and settled dust indoors. *Atmos. Environ.* 44: 3609–3620.

Zauli Sajani, S., Ricciardelli, I., Trentini, A., Bacco, D., Maccone, C., Castellazzi, S., Lauriola, P., Poluzzi, V. and Harrison, R.M. (2015). Spatial and indoor/outdoor gradients in urban concentrations of ultrafine particles and $PM_{2.5}$ mass and chemical components. *Atmos. Environ.* 103: 307–320.

Zhu Y, Hinds WC, Kim, S. and Sioutas, C. (2002). Concentration and size distribution of ultrafine particles near a major highway. *J. Air Waste Manage.* 52: 1032–1042.

Zhu, Y. , Hinds, W.C., Krudysz, M., Kuhn, T., Froines, J. and Sioutas, C. (2005). Penetration of freeway ultrafine particles into indoor environments. *J. Aerosol Sci.* 36: 303–322.

Zhou, Y. and Levy, J.I. (2008). The impact of urban street canyons on population exposure to traffic-related primary pollutants. *Atmos. Environ.* 42: 3087–3098.

This chapter is based on:

- Zauli-Sajani, S., Trentini, A., **Rovelli, S.**, Ricciardelli, I., Marchesi, S., Maccone, C., Bacco, D., Ferrari, S., Scotto, F., Zigola, C., Cattaneo, A., Cavallo, D.M., Lauriola, P., Poluzzi, V. and Harrison, R.M. **(2016)**. Is particulate air pollution at the front door a good proxy of residential exposure? *Environ. Pollut.* 213: 347-358.

- **Rovelli S.**, Zauli Sajani S., Cattaneo A., Ricciardelli I., Trentini A., Bacco D., Poluzzi V., Lauriola P., Cavallo D.M. Indoor and outdoor airborne pollutant levels on the street- and back-side of a building in a trafficked urban area. In: Conference Proceedings of the 21st European Aerosol Conference (EAC),), Milan, 7th-11th September 2015.

- **Rovelli S.**, Zauli Sajani S., Cattaneo A., Ricciardelli I., Trentini A., Bacco D., Poluzzi V., Lauriola P., Cavallo D.M. Valutazione della variabilità spaziale nelle concentrazioni indoor e outdoor di particolato atmosferico e inquinanti gassosi sul fronte strada e sul retro di un edificio nell'area urbana di Bologna. In: Conference Proceedings of the 32nd AIDII National Conference, Varese (Italy), June 24th-26th, 2015, pp. 167-173.

Tables

Table 1. Summary statistics of $PM_{2.5}$ mass (μg m^{-3}) and UFP number (# cm^{-3}) concentrations during the monitoring campaigns.

	Front					Back				
	Outdoor		Indoor		I/O mean	Outdoor		Indoor		I/O mean
	Number of valid data	Mean (min–max)	Number of valid data	Mean (min–max)		Number of valid data	Mean (min–max)	Number of valid data	Mean (min–max)	
$PM_{2.5}$ (24-h data)										
All data	30	33.3 (11.3–68)	30	21.7 (11.5–41)	0.76	30	29.2 (7.5–64)	30	15.1 (3.8–36)	0.6
Hot period	11	15.6 (11.3–23.8)	15	15.5 (11.5–20.1)	1.02	15	11.1 (7.5–16.5)	15	8.5 (3.8–12.8)	0.78
Cold period	15	47.1 (27–68)	14	26.5 (16–41)	0.57	15	43.4 (24–64)	14	20.2 (9–36)	0.46
UFP (1-h data)										
All data	652	25358 (2118–120931)	652	7625 (1472–21142)	0.39	652	7444 (647–26860)	652	3544 (213–8854)	0.55
Hot period	353	15502 (2118–38367)	353	5109 (1472–10773)	0.39	353	6169 (647–24308)	353	2932 (213–7901)	0.52
Cold period	299	36994 (3095–120931)	299	10,595 (2854–21142)	0.38	299	8948 (1781–26860)	299	4266 (1730–8854)	0.58

Sampling period: hot period from 11 to 25 June 2013; cold period from 28 November to 13 December 2013.

Table 2. Gradients of concentrations for different pollutants comparing both indoor and outdoor.

	Outdoor		**Indoor**	
	Front/back	**p-value**	**Front/back**	**p-value**
UFP	3.4	<0.001**	2.2	<0.001**
$PM_{2.5}$	1.1	<0.001**	1.4	<0.001**
Elemental carbon (EC)	1.8	<0.001**	2.5	<0.001**
Iron (Fe)	1.7	0.122	3.7	0.001**
Manganese (Mn)	1.3	0.003**	1.5	0.002**
Tin (Sn)	1.3	0.246	3.0	<0.001**
Total carbon (TC)	1.2	0.016*	1.5	<0.001**
Organic carbon (OC)	1.1	0.038*	1.1	0.008**
Zinc (Zn)	1.1	0.053	1.2	0.008**
Nitrates (NO_3)	1.1	0.073	1.3	0.086
Sulfates (SO_4)	1.0	0.184	1.0	0.889
Ammonium (NH_4)	1.0	0.456	1.1	0.129
Vanadium (V)	1.0	0.741	1.4	0.002**
Arsenic (As)	1.0	0.966	1.1	0.171
Cadmium (Cd)	1.0	0.802	1.1	0.866
Lead (Pb)	1.0	0.782	1.0	0.686
Potassium (K)	1.0	0.012*	1.0	0.279
Antimony (Sb)	0.9	0.591	2.3	0.002**

*p-value < 0.05; **p-value < 0.01.

Table 3. Descriptive statistics and Indoor/Outdoor ratio (I/O) for different chemical components. OC, EC, TC, NH_4, NO_3, SO_4 and K are expressed in µg m^{-3} while the other elements in ng m^{-3}.

	Number of valid data[a]	Front			Back		
		Outdoor mean (min–max)	Indoor mean (min–max)	I/O mean	Outdoor mean (min–max)	Indoor mean (min–max)	I/O mean
Organic carbon (OC)	9	8.84 (3.33–18.89)	6.82 (2.77–13.08)	0.77	7.84 (2.91–15.55)	5.98 (2.5–11.44)	0.76
Elemental carbon (EC)	9	3.96 (1.22–7.65)	4.3 (2.01–7.59)	1.09	2.25 (0.77–4.95)	1.7 (0.5–4.03)	0.76
Total carbon (TC)	9	12.8 (5.02–26.54)	11.12 (5.1–20.67)	0.87	10.64 (3.68–20.67)	7.68 (3–15.47)	0.72
Ammonium (NH_4)	9	2.92 (0.86–5.96)	0.88 (0.44–1.86)	0.3	2.85 (0.92–6.19)	0.77 (0.37–1.33)	0.27
Nitrates (NO_3)	9	8.2 (0.23–20.41)	1.28 (0.16–3.54)	0.16	7.76 (0.18–19.32)	1.02 (0.15–2.37)	0.13
Sulfates (SO_4)	9	3.32 (1.57–5.06)	2.13 (1.01–3.1)	0.64	3.19 (1.46–5.05)	2.11 (1.07–3.41)	0.66
Potassium (K)	5	0.44 (0.24–0.59)	0.36 (0.18–0.49)	0.82	0.45 (0.24–0.6)	0.35 (0.19–0.47)	0.78
Vanadium (V)	8	1.06 (0.33–2.29)	1.24 (0.72–2.1)	1.17	1.05 (0.33–2.29)	0.92 (0.34–1.5)	0.88
Arsenic (As)	8	0.6 (0.21–1.12)	0.48 (0.22–0.88)	0.8	0.6 (0.19–1.1)	0.45 (0.12–0.85)	0.75
Cadmium (Cd)	7	0.19 (0.07–0.33)	0.15 (0.06–0.25)	0.79	0.19 (0.05–0.31)	0.14 (0.04–0.24)	0.74
Tin (Sn)	8	3.18 (0.9–6.41)	3.87 (1.39–5.52)	1.22	2.44 (0.62–5.04)	1.28 (0.56–2.67)	0.52
Antimony (Sb)	8	1.35 (0.36–4.14)	1.44 (0.28–3.19)	1.07	1.53 (0.24–6.21)	0.64 (0.13–1.44)	0.42
Lead (Pb)	8	7.14 (1.57–15.14)	5.29 (1.05–11.36)	0.74	7.21 (1.6–14.62)	5.22 (1.01–11.72)	0.72
Iron (Fe)	6	212.16 (86.48–395.53)	251.19 (141.35–350.87)	1.18	122.74 (84.9–203.99)	68.59 (29.95–127.45)	0.56
Zinc (Zn)	6	38.84 (17.18–52.12)	29.12 (13.5–40.96)	0.75	35.05 (20.62–46.8)	24.2 (13.14–33.77)	0.69
Manganese (Mn)	5	7.25 (5.07–10.33)	5.54 (4.12–7.76)	0.76	5.55 (4.31–8.32)	3.69(2.83–5.86)	0.66

[a] Number of data simultaneously above LOQ in all monitoring sites.

Table 4. Pearson correlation coefficients (R) and orthogonal regression lines for different chemical species. Intercepts for OC, EC, TC, NH_4, NO_3, SO_4 and K are expressed in μg m^{-3}; intercepts for the other elements are expressed in ng m^{-3}.

	Front out vs back out			**Front ind vs back ind**			**Front ind vs front out**			**Back ind vs back out**		
	R	**Slope**	**Intercept**	**R**	**Slope**	**Intercept**	**R**	**Slope**	**Intercept**	**R**	**Slope**	**Intercept**
Organic carbon (OC)	0.99	1.23	—0.79	0.99	1.17	—0.2	0.98	0.65	1.06	1.0	0.69	0.61
Elemental carbon (EC)	0.97	1.4	0.81	0.97	1.7	1.41	0.96	0.99	0.37	1.0	0.82	—0.14
Total carbon (TC)	0.97	1.23	—0.32	1.0	1.0	0	0.98	0.74	1.63	1.0	0.92	1.38
Ammonium (NH_4)	0.99	0.98	0.12	0.94	1.5	—0.28	0.68	0.16	0.41	0.53	0.08	0.53
Nitrates (NO_3)	1.0	1.02	0.32	0.98	1.41	—0.16	0.97	0.14	0.1	0.97	0.1	0.21
Sulfates (SO_4)	0.98	0.99	0.14	0.85	1.01	0	0.89	0.6	0.16	0.94	0.6	0.19
Potassium (K)	1.0	0.99	0	1.0	1.07	—0.02	0.99	0.85	—0.02	1.0	0.79	0
Vanadium (V)	0.99	1.0	0.01	0.93	1.23	0.1	0.99	0.66	0.54	0.9	0.51	0.38
Arsenic (As)	0.98	1.02	—0.01	0.97	0.87	0.09	0.99	0.73	0.04	0.99	0.86	—0.07
Cadmium (Cd)	0.98	1.0	0	0.97	1.03	0	0.99	0.71	0.01	0.96	0.68	0.01
Tin (Sn)	0.7	1.81	—1.25	0.69	2.53	0.63	0.51	0.48	2.34	0.45	0.29	0.56
Antimony (Sb)	0.92	0.64	0.37	0.93	1.77	0.31	0.83	0.65	0.56	0.8	0.22	0.3
Lead (Pb)	0.99	1.03	—0.26	0.99	0.99	0.1	1.0	0.76	—0.11	1.0	0.78	—0.4
Iron (Fe)	0.38	5.97	—521.02	0.94	2.55	76.13	0.16	0.23	201.42	0.94	0.75	—23.75
Zinc (Zn)	0.98	1.31	—7	0.98	1.3	—2.42	0.99	0.72	1.02	0.97	0.72	—1.14
Manganese (Mn)	0.97	1.23	0.41	0.95	1.23	1.0	0.97	0.77	—0.03	0.99	0.78	—0.62

Figures

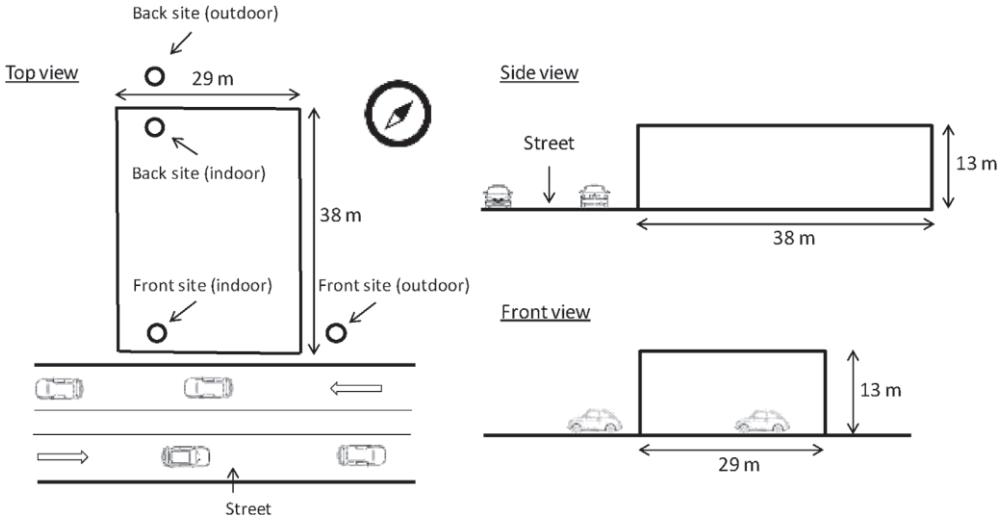

Figure 1. Schematic diagram of the building and location of the sampling points.

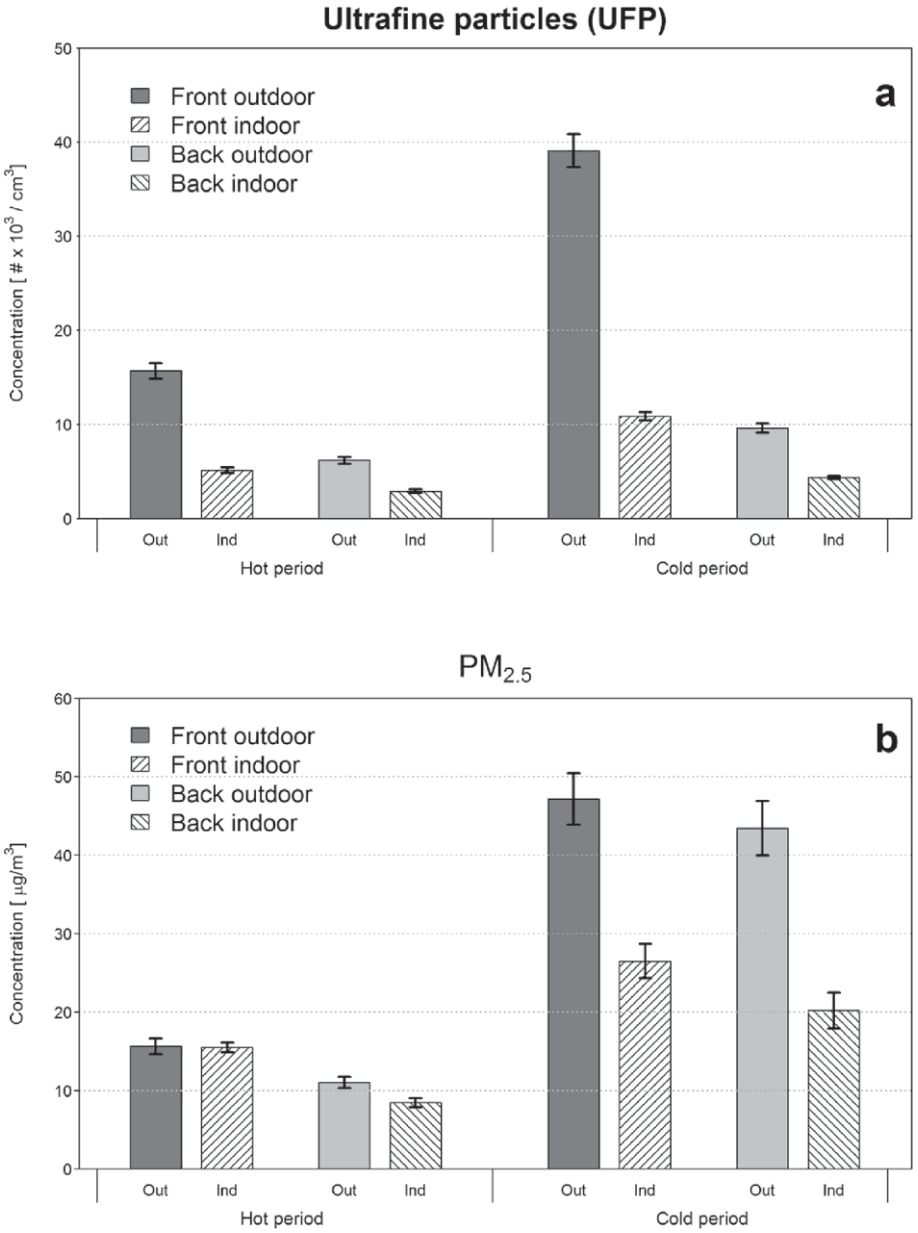

Figure 2. Average value and standard error of $PM_{2.5}$ (a) and UFP (b) during the two monitoring campaign.

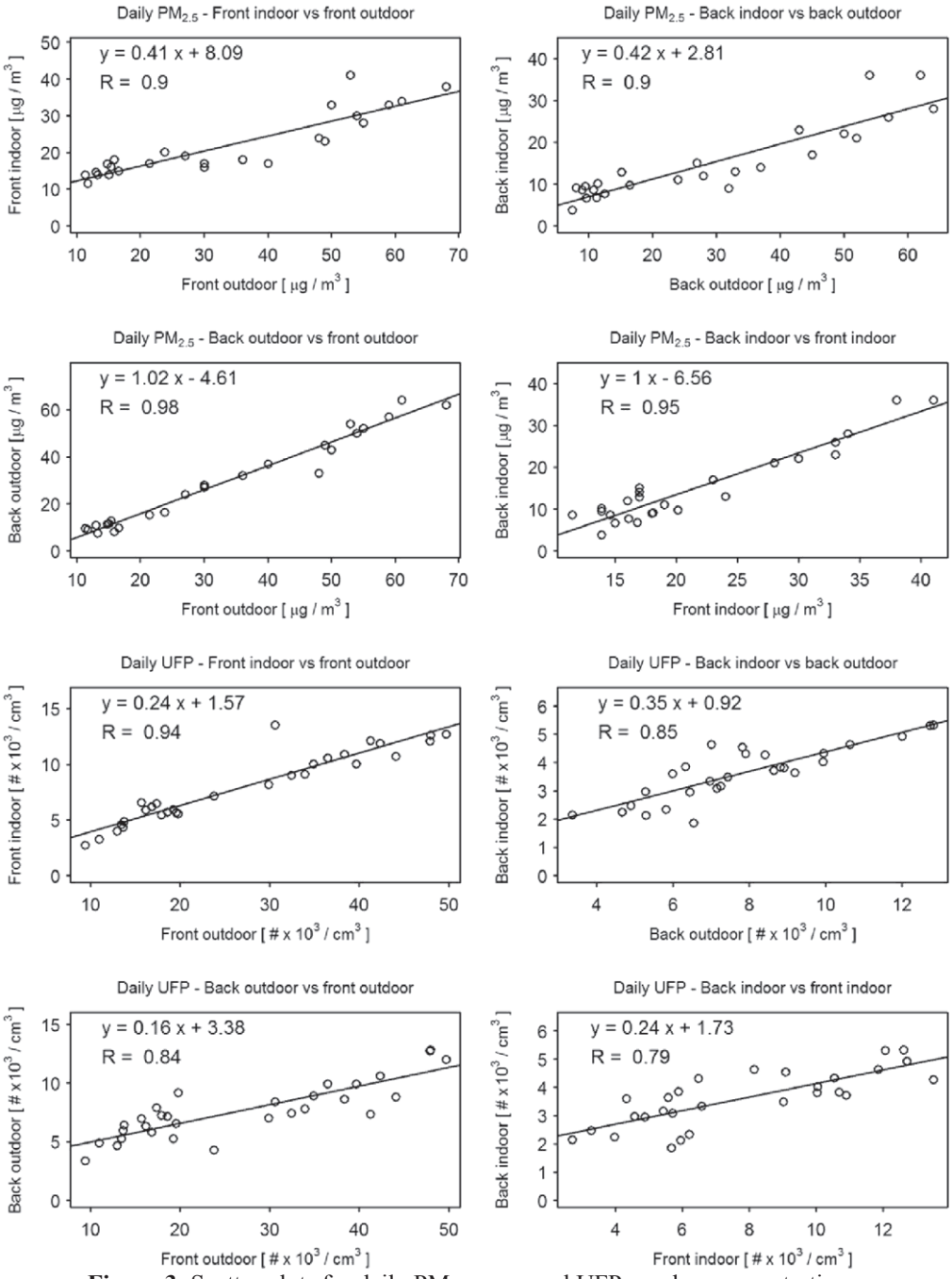

Figure 3. Scatter plots for daily $PM_{2.5}$ mass and UFP number concentrations.

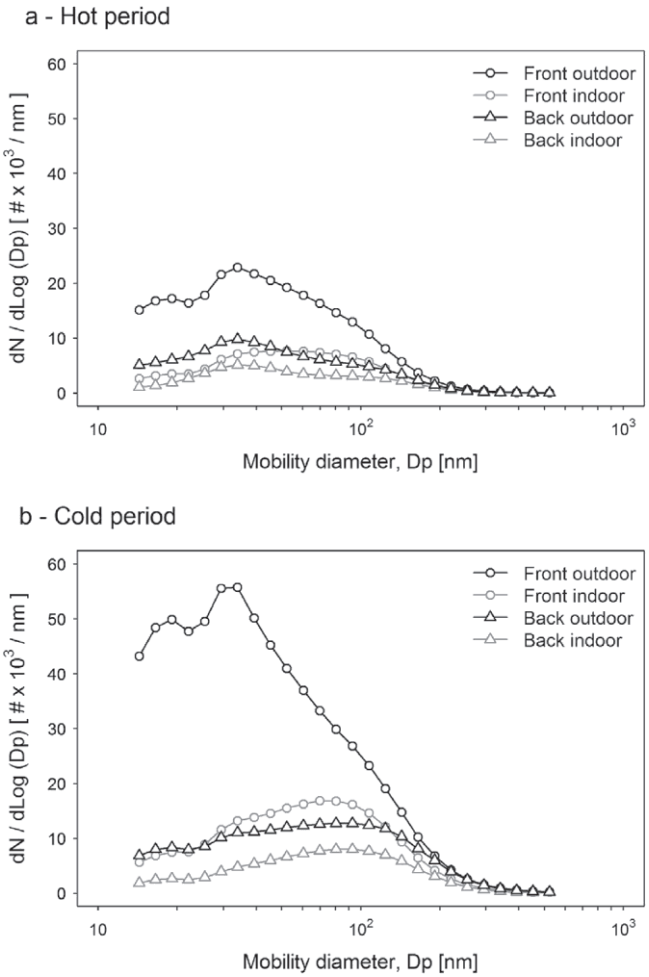

Figure 4. Mean particle size distribution of hourly data for the hot (a) and the cold (b) period. On the x-axis the aerodynamic diameter (Dp) is reported on a logarithmic scale. On the y-axis dN/dlog(Dp) represents the number of particles per unit increment of Dp on a logarithmic scale.

Supplementary Material

Limits of quantification for chemical species

LOQs for chemical components were:

0.03 ng m^{-3}	for Arsenic (As),
0.03 ng m^{-3}	for Vanadium (V),
0.01 ng m^{-3}	for Cadmium (Cd),
0.18 ng m^{-3}	for Lead (Pb),
0.04 ng m^{-3}	for Tin (Sn),
0.14 ng m^{-3}	for Antimonium (Sb),
0.7 ng m^{-3}	for Chromium (Cr),
0.5 ng m^{-3}	for Manganese (Mn),
36 ng m^{-3}	for Iron (Fe),
12.2 ng m^{-3}	for Zinc (Zn),
0.04 µg m^{-3}	for Ammonium (NH_4^+),
0.04 µg m^{-3}	for Potassium (K^+),
0.05 µg m^{-3}	for Nitrate (NO_3^-),
0.09 µg m^{-3}	for Sulfate (SO_4^{2-}),
2.1 µg m^{-3}	for Organic Carbon (OC),
0.3 µg m^{-3}	for Elemental Carbon (EC).

Table 1S. Summary statistics of the meteorological variables during the monitoring campaigns.

	Hot period mean (min–max)	**Cold period mean (min–max)**
Temperature (°C)		
Urban meteorological station	25.2 (15.6–34)	4.8 (-1.4–11.7)
Indoor - Back site	29.9 (24.2–34.4)	17.7 (16.1–19.3)
Indoor - Front site	29.4 (24.6–31.8)	16.1 (15–16.9)
Relative Humidity (%)		
Urban meteorological station	43.0 (18–85)	72.1 (38–103)
Indoor - Back site	41.6 (31.7–50.9)	34.2 (27.9–38.3)
Indoor - Front site	46.9 (38.2–52.7)	39.3 (31.1–44.1)
Wind Speed (m s^{-1})		
Urban meteorological station	2.5 (0–8)	1.6 (0–4)
Precipitation (mm)		
Urban meteorological station	< 0.1 (0–2.6)	< 0.1 (0–0.2)

Table 2S. Comparison between meteorological variables during the monitoring campaigns and the corresponding typical values derived from the years 2012-2014.

	Monitoring campaign Hot period	**Hot months***	**Monitoring campaign Cold period**	**Cold months****
Mean Temperature (°C)	25.2	25	4.8	5.8
Mean Relative Humidity (%)	43.0	47.2	72.1	79
Mean Wind Speed (m s^{-1})	2.5	2.7	1.6	1.9

*June-August 2012-2014; **December-February 2012-2014.

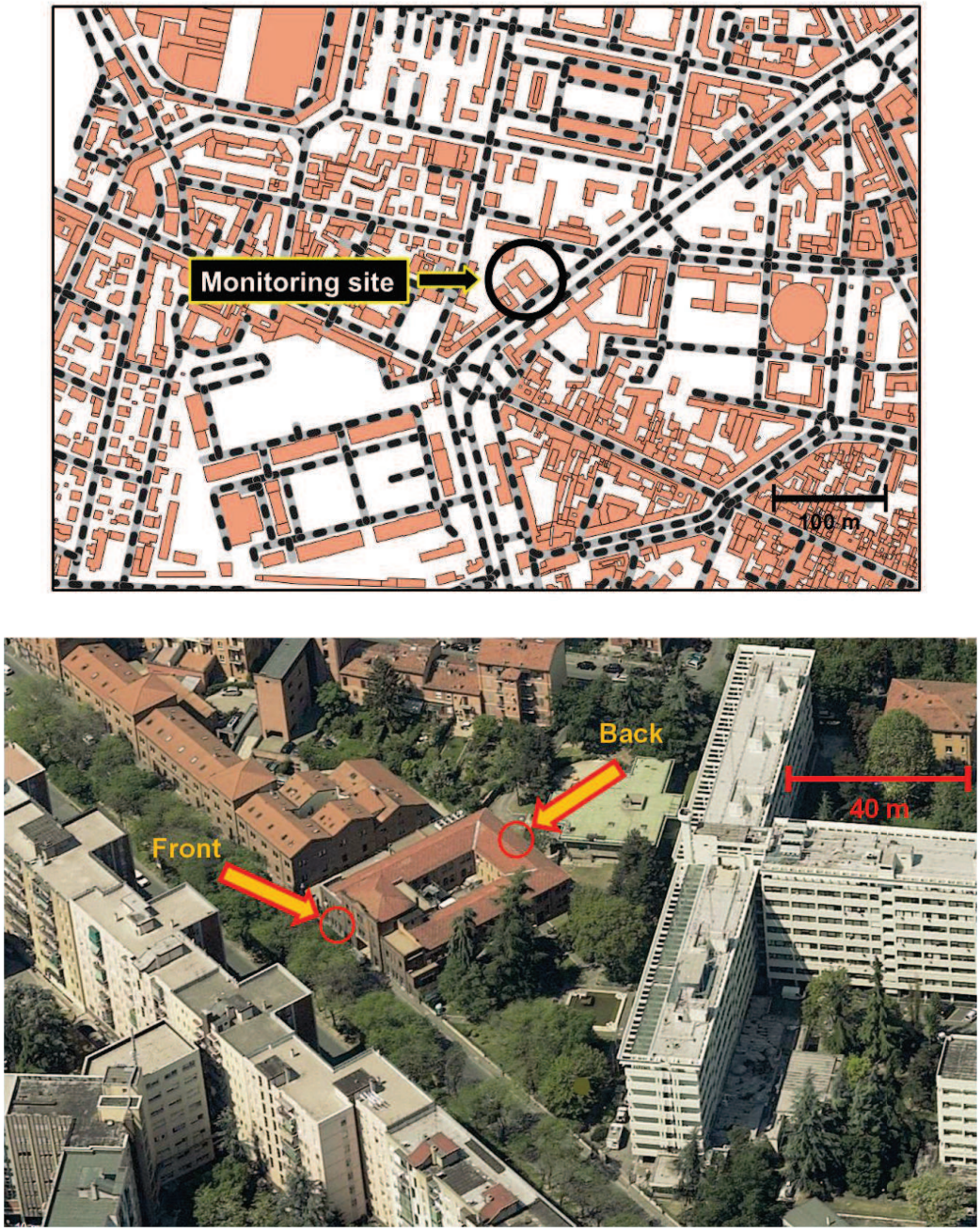

Figure 1S. Map (upper panel) and bird's eye view (lower panel) of the location of the monitoring sites. Dotted grey lines represent traffic flows.

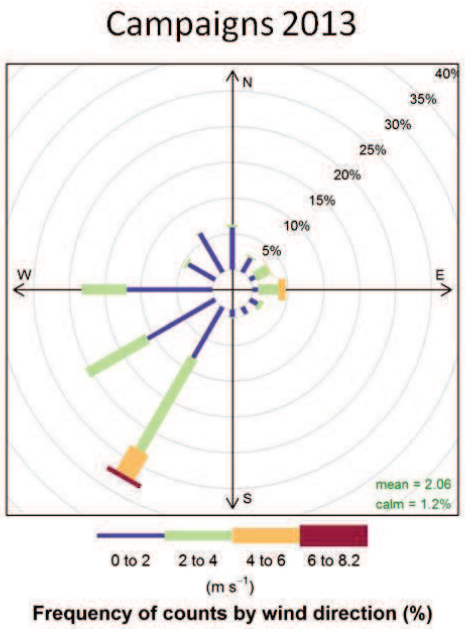

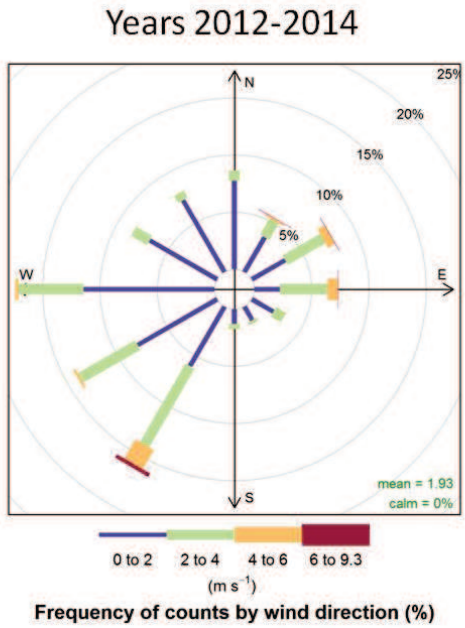

Figure 2S. Wind rose for the measurements period and for the years 2012-2014. Data from the meteorological station located close to the monitoring sites.

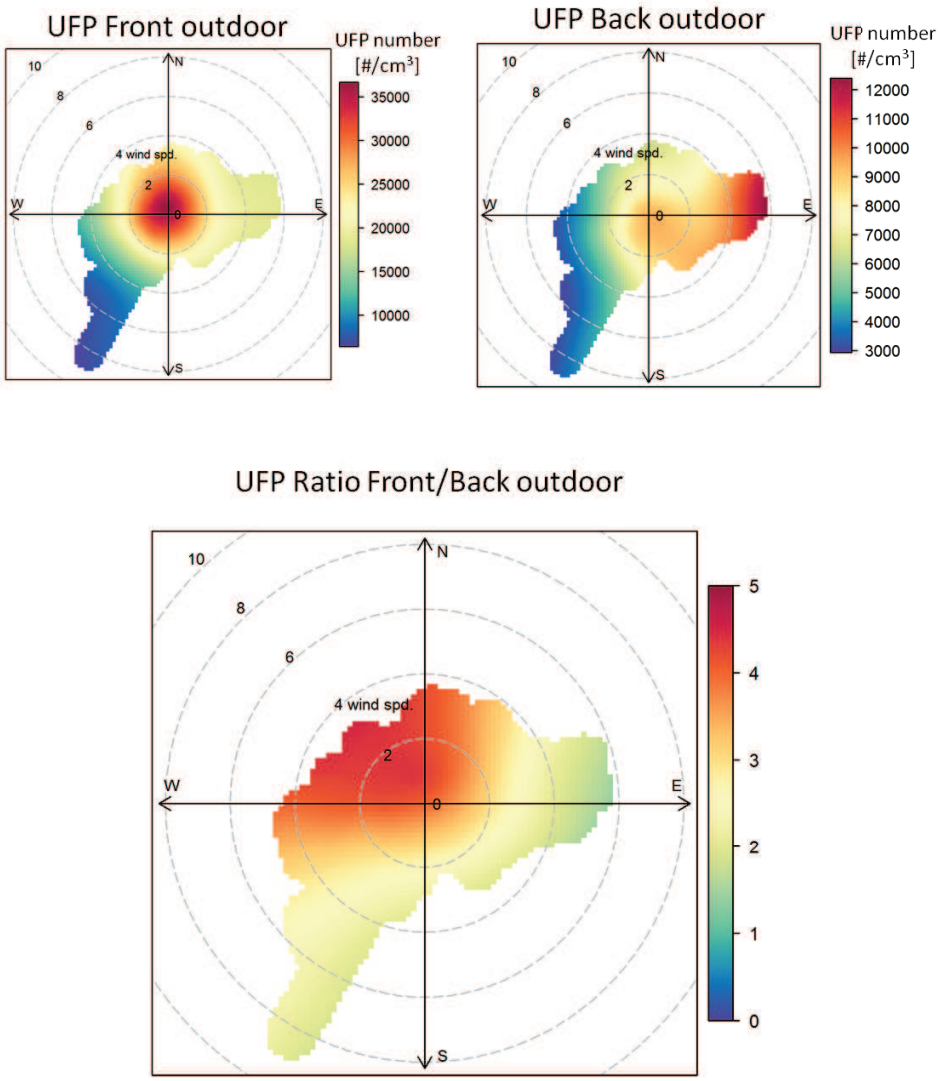

Figure 3S. Impact of wind speed and direction on the Ultrafine Particle concentrations at the front-door and the back and on the front/back ratio. Outdoor sites.

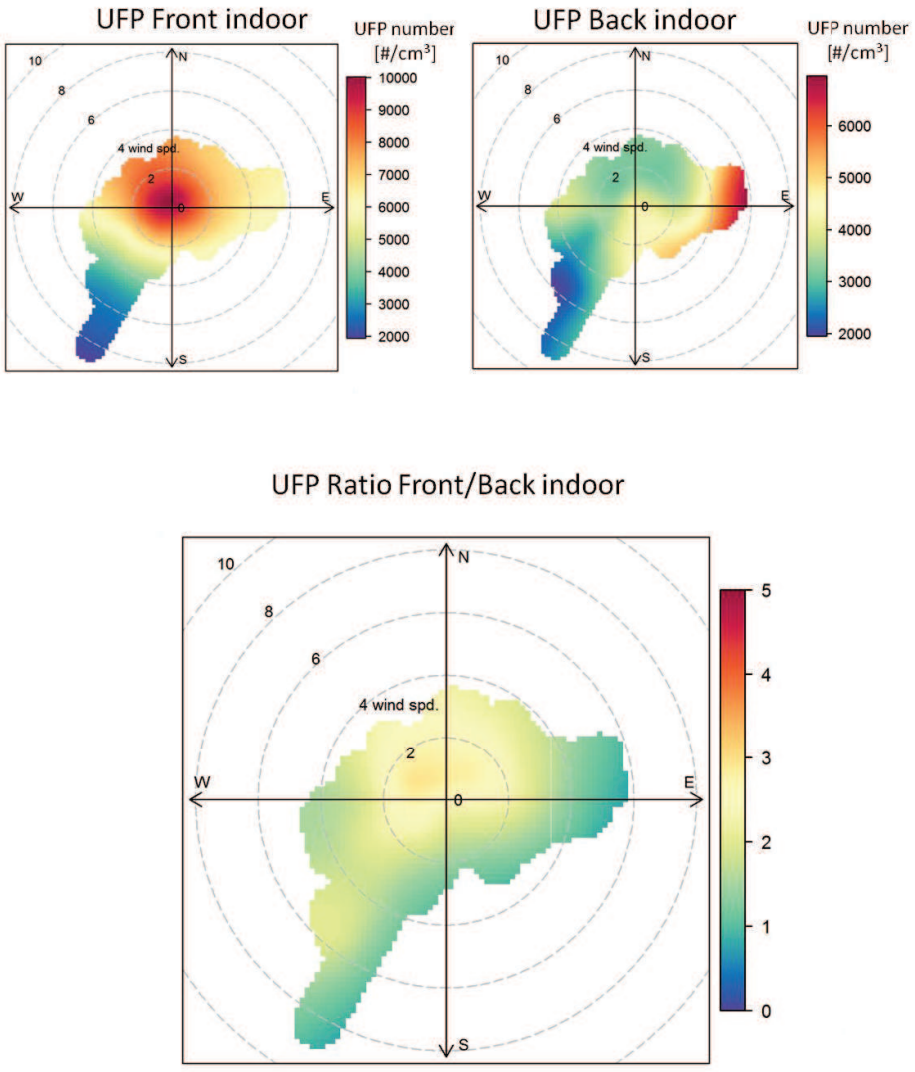

Figure 4S. Impact of wind speed and direction on the Ultrafine Particle concentrations at the front-door and the back and on the front/back ratio. Indoor sites.

Chapter 6 – *Occupational Exposure to Arsenic and Cadmium in Thin-Film Solar Cell Production*

This chapter reports a pre-copyedited, author-produced version of an article accepted for publication in *The Annals of Occupational Hygiene* following peer review. The version of record [Spinazzè, A., Cattaneo, A., Monticelli, D., Recchia, S., **Rovelli, S.**, Fustinoni, S., and Cavallo, D. M. (2015). Occupational Exposure to Arsenic and Cadmium in Thin-Film Solar Cell Production. *Ann. Occup. Hyg.* 59(5): 572–585] is available online at: 10.1093/annhyg/mev002.

Abstract

Workers involved in the production of Cd/As-based photovoltaic modules may be routinely or accidentally exposed to As- or Cd-containing inorganic compounds. For this reason, the workers' exposure to As and Cd was investigated by environmental monitoring following a worst-case approach and biological monitoring from the preparation of the working facility to its decommissioning. Workplace surface contamination was also evaluated through wipe-test sampling.

The highest mean airborne concentrations were found during maintenance activities (As = 0.0068 µg m^{-3}; Cd = 7.66 µg m^{-3}) and laboratory simulations (As = 0.0075 µg m^{-3}; Cd = 11.2 µg m^{-3}). These types of operations were conducted for a limited time during a typical work shift and only in specifically suited containment areas, where the highest surface concentrations were also found (Laboratory: As = 2.94 µg m^{-2}; Cd = 167 µg m^{-2}; Powder Containment Booth: As = 4.35 µg m^{-2}; Cd = 1500 µg m^{-2}). The As and Cd urinary levels (As_u; Cd_u) were not significantly different for exposed (As_u = 6.11 ± 1.74 µg l^{-1}; Cd_u = 0.24 ± 2.36 µg g^{-1} creatinine) and unexposed workers (As_u = 6.11 ± 1.75 µg l^{-1}; Cd_u = 0.22 ± 2.08 µg g^{-1} creatinine).

Despite airborne arsenic and cadmium exposure well below the TLV when the operation is appropriately maintained in line, workers who are involved in various operations (maintenance, laboratory test) could potentially be at risk of significant exposure, well in excess of the TLV. Nevertheless, the biological monitoring data did not show significant occupationally related arsenic and cadmium intake in workers and no significant changes or differences in arsenic and cadmium urinary level among the exposed and unexposed workers were found.

1. Introduction

The technology to fabricate CdTe/CdS-based thin-film solar cells can be considered mature for large-scale production, given that some process innovations were defined in the last few years, such as specific applications of close-space sublimation and radio-frequency sputtering (Bosio *et al.*, 2006). These discoveries are considered useful to simplify the production process, making it easier and more scalable to industrial scale and making the concept of a manufacturing plant as a single inline thin film-processing unit possible.

The aim of the studied production process was to obtain multilayer thin films of different semiconductors deposited on a glass panel that could be treated with laser scribing to obtain electrical connections between all of the cells constituting the module. The production process in the studied company was organised as follows: (I) acceptance of raw materials and quality control and (II) storage; (III) production of the photovoltaic module and (IV) finishing

operations (electrical contacts, coverage); (V) quality control and testing process; and (VI) storage of the complete modules. All of these tasks were performed within a single building, organised to accommodate separated areas for each specific activity. In detail, the production site has a total area of approximately 10200 m^2 (111200 m^3). This building was divided into (I) a non-productive area (e.g., offices, locker room) with a total surface of approximately 500 m^2; (II) warehouses for raw materials and finished products (approximately 1 700 m^2) and (III) a laboratory (100 m^2) for quality control and production test simulation. The production line was situated in a central open-space area (production facility) of approximately 8000 m^2 (85000 m^3). The core of the production line was fully automated with minimal human intervention; only module-finishing and maintenance operations required manual interventions. The production process was organised as follows: the glass panels moved on a rail used to travel into nine process chambers and leave the production machine when the photovoltaic modules were completed. The semi-conductor deposition processes were conducted in high-vacuum (0.001 mbar) or low-vacuum (100 mbar) and high-temperature (250–400 °C) conditions.

Risk Management Strategy

A multilayer approach for preventing and mitigating exposure was implemented to eliminate or control the exposure associated with occupational handling of hazardous materials and reduce their consequences (Mirer, 2008) during the productive period. This risk management strategy was developed to contain arsenic and cadmium on the basis of a hierarchy of controls that includes engineering controls, warnings, training and procedures, specific work practices and Personal Protective Equipment (PPE) for each different work task (table 1). Processes such as maintenance work (e.g., scraping, cleaning) and laboratory tests and simulations (analysis of end products, semi-finished modules or raw semiconductors; pilot-scale deposition simulations) present occupational health risks arising from the emission of fine particles of arsenics- and cadmium-containing compounds (Edelman, 1990). For these activities, specific collective protection devices were also introduced, such as powder containment booths and chemical hoods, to avoid workplace contamination and to minimise workers' exposure. Thus, this type of activity was performed in accordance with specific standard operative procedures (SOP) that included the requirement for sufficient purging time, the use of appropriate techniques to minimise exposure, the introduction of specific workplace and self-cleaning operating procedures (HEPA-filtered vacuum cleaners) and the use of high-level personal protective equipment (e.g. Tyvek® overalls and filtering full-face mask with FFP3-class exhalation valve). The cleaning routine and the decommissioning process required specific SOPs, too. These last addressed the isolation of the contaminated area, the aspiration and abatement of air contamination in the isolated work areas by ventilation systems (HEPA filtered), the protection of uncontaminated surfaces and equipment from possible contamination events and the protection of workers engaged in cleaning work practices with personal protective equipment (PPE).

Some concerns were raised regarding the health aspects linked to the presence of hazardous chemicals (such as CdS, CdTe, As_2Te_3) needed for production process, which are considered carcinogenic or probably carcinogenic by inhalation (CdS and CdTe) (IARC, 1997; NIOSH, 2005; SCOEL, 2010; ACGIH, 2013) or carcinogenic to humans (As_2Te_3) (IARC, 1987; NIOSH, 1997). Exposure to inorganic As and Cd compounds was associated with a higher frequency of skin and lung cancer, and chronic poisoning could lead to a wide range of

symptoms. Thus, chronic exposure to inorganic As and Cd compounds is considered a potential occupational hazard (Aoki *et al.*, 1990; Horng *et al.*, 2002). Generally, the occupational health hazards presented by Cd and As compounds change with their physical state and mode of exposure. The studied workers may be routinely or accidentally exposed to As- or Cd-containing inorganic compounds, and inhalation is probably the most important exposure pathway because of the larger potential for exposure and higher absorption efficiency of Cd- and As-containing compounds in the lung than in the gastrointestinal tract or skin. Processes such as feedstock preparation and maintenance, in which these chemicals are used or produced as fine particles or fumes, present the highest occupational health risks in the semiconductor industry (Fthenakis, 2001).
This study was developed in order to evaluate workers' exposure for different working task and throughout the plant history (from "background" to "restoration"), by means of environmental (air sampling) and biological (end-shift urine samples) monitoring. Further, surface sampling campaigns were performed to qualitatively evaluate the general workplace contamination.

2. Materials and Methods

The exposure assessment was performed during a five-year period, including the beginning of production ("background"–July 2009), the productive period (September 2010–September 2013) and the plant decommissioning and restoration (September 2013–March 2014). The monitoring activity consisted of sampling and analysis of arsenic and cadmium both by environmental (23 sampling sessions) and biological monitoring (5 sampling sessions). Air and surface sample collection were carried out in different workplace environments (production facility, powder containment booths, laboratory, outdoors) and during different operating conditions (background, maintenance work, laboratory tests, end of work-shift, plant shutdown and decommissioning).

2.1 Air Monitoring: Sampling and Analysis

Air samples were collected and analysed by the NIOSH 7300 method (NIOSH, 2003) and in accordance with a standard sampling practice (EN 689:1995). The sampling design consists of the combination of (I) high-flow Total Suspended Particulate (TSP) sampling (Filter-Cassette for TSP, 47 mm Mixed Cellulose Esters (MCE) filter; flow rate = 25,0 L min^{-1}) with (II) low-flow sampling of inhalable fraction (Conical Inhalable Sampler, 25 mm cassette, MCE filter, flow rate = 3.5 L min^{-1}). Low-flow personal samples were collected in the breathing zone of workers for whom high exposures were expected (worst-case exposure scenario). Furthermore, inhalable particles and total suspended particles (TSP) were also monitored by fixed site sampling in different areas of the sampling site; when feasible, these sampling lines were placed at the same time and place of personal sampling. Typically, each sampling campaign consisted of two personal sampling and one or two fixed site sampling points. The aim of this protocol was to characterise the exposure concentration associated with each working task and working place, as well as the general workplace concentration. For this reason, while most of the fixed site sampling refers to eight-hour time weighted average samples, all personal samples and some fixed-site samples were collected on the basis of a worst-case approach: these last must be considered short-term (approximatively from 60 to 120 minutes), task-based samples. Thus, the interpretation of the environmental concentration is limited by the fact that the reported results are not representative of a typical 8-h TWA personal exposure. Microwave

assisted acid digestion was used to digest the samples (procedure now described in a separate NIOSH method (NIOSH, 2014)): ultrapure nitric acid produced by sub-boiling distillation (Milestone Duopur) was used for sample digestion, bottle cleaning, standard and blank preparation. Trace element were simultaneously determined by Inductively Coupled Plasma – Mass Spectrometry (ICP-MS, X Series II from Thermo, Rodano, MI, Italy). A protocol of QA/QC was strictly followed, including allowing a 1 hour warm up time, mass calibration of the instrument, check of sensitivity and signal stability by tune solutions, blank measurements, calibration for each analysis batch, control charts and analysis of synthetic samples.

2.2 Surface Contamination: Sampling and Analysis

Surface samples ("wipe sampling") were collected and analysed according to the NIOSH 9102 method (NIOSH, 2003). Sampling was performed with filter paper (Quantitative Filter Paper - Ashless) moistened with ultrapure water using a 15-cm long square template to define the sampling area. Samples were taken in different positions (especially where higher concentrations were expected – worst-case exposure scenario) and during different plant-life periods (table 3) through a dedicated protocol developed for the standardisation of the sampling activity. Environmental samples were digested with nitric acid in a microwave digestion bomb and analysed by ICP-MS, as described above.

2.3 Biomonitoring: Urine Collection and Analysis

A spot urine specimen was collected from groups of workers at the end of the last working shift of the week (at approximately half-year frequencies). Workers were a priori classified as "unexposed" (N = 8; office administrators - control group) or "exposed", including two group of production workers, "operators" (N = 14; directly involved in laboratory tests or maintenance activities) and "engineers" (N = 16; not involved in laboratory tests or maintenance activities). Office administrators were assumed to be unexposed to arsenic and cadmium, because they did not have an active role in the production activity and they weren't required to enter the production area. Further, drift from productive area into offices were assumed to be negligible, due to the presence of a "decontamination area" at the exit of the production area, in which ventilation systems were placed in order to ensure the aspiration and abatement of air contamination in the isolated work areas by ventilation systems. The collection of biological samples was performed in the context of risk evaluation, according to Italian law for health and safety at the work place (Italy Parliament and Senate, 2008), under the supervision of an occupational health physician. Arsenic was determined as inorganic arsenic and its two major organic metabolites in urine: monomethylarsonic acid and dimethylarsinic acid (As_u). To this aim urine was first submitted to chemical speciation by ion exchange chromatography to remove arsenobetaine; the resulting fraction was analysed by atomic absorption spectrophotometry with electrothermal atomization (GfAAS Soolar M6 Thermo, Rodano, MI, Italy) according to Buratti *et al*., 1984. Cadmium in urine (Cd_u) was determined by atomic absorption spectrophotometry with electrothermal atomization (GF-AAS Solar M60 Thermo Scientific, Rodano, MI, Italy) as previously reported (Angerer, 1988). The certified reference material used for quality control was Seronorm™ Trace Elements Urine L-1 (SERO, Norway, lot 1011644, acceptable range for arsenic: 47–111 μg L^{-1}; acceptable range for cadmium: 0.13–0.28 μg L^{-1}). Analytic work was considered acceptable only when the reference material run within the sample sequence was within the acceptable range. In order to

account for concentration or dilution of urine samples, and to enable accurate interpretation of urinary results, urine samples were accepted only if creatinine concentration were > 0.3 g L^{-1} and < 3.0 g L^{-1} (ACGIH, 2013).

2.4 Limit of Detection and Limit of Quantification

The limits of detection were determined according to the IUPAC recommendation: 3 times the blank standard deviation divided by the sensitivity (Currie, 1995). Operatively, a blank value for the elements of interest was obtained for each batch of analysis by determining the values in the three employed matrices (47 and 25 mm Mixed Cellulose Esters (MCE) filters and filter paper) following the same procedure used for the samples. The standard deviations of these values were subsequently used to calculate the limits of detection. Analytical limits of quantification (LOQ) were considered to be three-fold larger than LOD. Regarding air samples analysis, the LOQ for arsenic in were 0.0014 µg m^{-3} (fixed site) and 0.017 µg m^{-3} (personal); the LOQ for cadmium were 0.0028 µg m^{-3} (fixed site) and 0.0037 µg m^{-3} (personal). Concerning surface analysis, the LOQ were 5.5 µg m^{-2} for arsenic and 3.5 µg m^{-2} for cadmium. For urinary biomarkers LOQ was defined as the concentration corresponding to five times the standard deviation of the signal in the blank sample and was 1 and 0.3 µg l^{-1} for As_u and Cd_u, respectively.

2.5 Statistical Analyses

Statistical analyses ("ANOVA": one-way analysis of variance for normally distributed variables with the Bonferroni post-hoc test; "KW": Kruskal Wallis – one way ANOVA and "MW" – Mann–Whitney U-test for non-normally distributed data) were performed using IBM SPSS 20.0 (IBM, Armonk, NY, USA) to compare the differences between environmental concentrations of arsenic and cadmium as a function of (I) the period of the plant history, (II) working conditions/task and (III) sampling position. Moreover, the differences observed in biological sampling were analysed and discussed as a function of workers' exposure condition and time period. Statistical results were regarded as significant when $\rho < 0.05$. All of the results below the limits of detection (LOD) were replaced by substitution with "LOD/2" (Hornung and Reed, 1990). Results are presented as the geometric mean (G.M.) and geometric standard deviation (Geom. S.D.).

3. Results

In total, N = 108 Particulate Matter (PM) samples, N= 69 urine specimens and N = 147 wipe tests were collected during this study. Data were analysed on the basis of the variables considered hereafter to determine the local and temporal patterns in exposure concentrations and in workplace contamination.

3.1 Air Monitoring

Fixed-site air-monitoring results (table 2) showed statistically significant differences for airborne concentrations of arsenic ($\rho_{KW} < 0.001$) and cadmium ($\rho_{KW} < 0.001$) among different work areas. The mean airborne cadmium concentration in the production facility was one order of magnitude higher than the outdoor background concentration ($\rho_{MW} = 0.001$), and the same order of magnitude for As ($\rho_{MW} = 0.722$). On average, concentrations were higher (up to three orders of magnitude for cadmium) in the containment booths and in the laboratory than in the

rest of the production facility ($\rho_{MW} < 0.001$), for both personal and fixed-site monitoring. Arsenic concentrations were generally lower (mean value on the order of 10^{-3} μg m^{-3}) than cadmium concentrations (mean values ranging from 10^{-2} to 10^{+1} μg m^{-3}) in each location. The results indicated that very high levels of atmospheric and surface contamination were found in some specific environments (laboratory and powder containment booths), but this contamination did not affect the rest of the workplace (production facility and non-manufacturing areas). Differences in the levels of the two metals among different work tasks were also statistically significant (arsenic $\rho_{KW} < 0.001$; cadmium $\rho_{KW} < 0.001$); the highest mean concentration and the widest data variability were observed during maintenance activities and during laboratory tests rather than during the production routine or after the end of the work shift. Statistically significant differences ($\rho_{MW} < 0.001$) were detected between fixed-site and personal monitoring (these last were performed only during the production period). Differences in the personal exposures to cadmium among different work tasks and locations were also statistically significant ($\rho_{MW} < 0.001$).

3.2 Surface Contamination Monitoring

Results from wipe-test sampling (table 3) showed statistically significant differences in surface contamination levels, especially for cadmium (arsenic $\rho_{KW} = 0.044$; Cd $\rho_{KW} < 0.001$). Cadmium surface concentrations were higher in the containment booths (two orders of magnitude; $\rho_{MW} < 0.001$) and in the laboratory (one order of magnitude; $\rho_{MW} = 0.141$) with respect to the rest of the production facility and other connected environments (e.g., locker rooms). The surface contamination for arsenic compounds was on the same order of magnitude in every sampling area, with higher mean concentrations found in the containment booths (same order of magnitude; $\rho_{MW} = 0.039$) with respect to the rest of the production facility. The surface concentration defined during the production phase was consistently and significantly higher ($\rho_{KW} < 0.001$) than background levels. Surface sampling was performed after the end of the production activity and after an early cleaning (plant shutdown/decommissioning) only in areas in which surface contamination was assumed to be high (e.g. powder containment booths, laboratory) and were then repeated after the plant restoration in the general workplace area (production facility).

3.3 Biological Monitoring

Biological monitoring results (table 4) showed that urinary As_u and Cd_u were not significantly different (arsenic $\rho_{ANOVA} = 0.422$; Cadmium $\rho_{ANOVA} = 0.939$) between exposed and unexposed subjects. No significant differences (arsenic $\rho_{ANOVA} = 0.365$; cadmium $\rho_{ANOVA} = 0.937$) were found between different categories of exposed workers (engineers and operators).

3.4 Plant Life-Cycle Stage

Cadmium and arsenic air and surface concentrations (table 2, table 3) defined during the production phase were consistently and significantly higher ($\rho_{KW} < 0.001$) than background levels. The results from wipe-test sampling (table 3) also showed a slight increase in the surface level with respect to background values during the decommissioning period. Concentrations similar to the background levels were then found after the plant shut-down and restoration ($\rho_{MW} > 0.05$). Biological monitoring did not show any statistically significant variations (Arsenic $\rho_{ANOVA} = 0.483$; cadmium $\rho_{ANOVA} = 0.083$) between baseline values and

levels measured during the productive period (1^{st} – 4^{th} sampling session). Figure 1 and figure 2 present the percentual variation of arsenic and cadmium in air, surface and biological samples, during different plant life-cycle stage, providing an indication of the differences in environmental and biological monitoring throughout the plant history.

4. Discussion

4.1 Air Monitoring

Occupational threshold limit values (8-h Threshold Limit Value-Time Weighted Average – TLV-TWA-, PEL, REL) have been established at 10 μg m^{-3} (ACGIH, 2013; OSHA, 2008) or 5 μg m^{-3} (NIOSH, 2005) for As and its inorganic compounds and at μg m^{-3} (ACGIH, 2013) or 5 μg m^{-3} (OSHA, 2010) for Cd and its inorganic compounds. More restrictive occupational exposure limits (OELs) were set for cadmium in the respirable fraction; the 8-h TLV-TWA is set at 2 μg m^{-3} (ACGIH, 2013) or 4 μg m^{-3} (SCOEL, 2010). Workers were exposed to substantially lower As levels than the ACGIH TLV of 10 μg m^{-3} (ACGIH, 2013) and the NIOSH PEL of 5 μg m^{-3} (NIOSH, 1997), with the maximum exposure concentration (0.129 μg m^{-3}), measured at a personal level during maintenance that was two orders of magnitude lower than occupational exposure thresholds. In contrast, workers' exposure to cadmium was found to be higher than the most conservative TLV defined by ACGIH (2 μg m^{-3} - respirable fraction), especially for workers involved in maintenance activity or laboratory tests (table 1). In particular, while As concentrations were always below the proposed occupational threshold limit (ACGIH, 2013; NIOSH, 1997; OSHA, 2010], cadmium concentrations exceeded the threshold (TLV-TWA) defined by different agencies at 2 μg m^{-3} (ACGIH, 2013) (N=26/108), 5 μg m^{-3} (NIOSH, 2005; OSHA, 2010) (N=23/108) and 10 μg m^{-3} (ACGIH, 2013) (N=22/108). The differences in air contamination between arsenic and cadmium compounds reflect the different amounts of raw materials used for the production of thin-film solar cells, which contain a thick layer of CdTe in comparison with very thin layers of CdS and As_2Te_3 (Bosio *et al*., 2006). Moreover, most of the exposure data referred to CdTe (69%) and CdS (21%) deposition chambers, and few samples were collected in As_2Te_3 deposition rooms. Although the Cadmium levels measured during key maintenance or laboratory tasks indicate the potential for very serious exposures, the possibility of significant exposure to arsenic and cadmium compounds is likely to be remote during normal operation if procedures are appropriately maintained in line with engineering controls such as closed-loop production line, enclosure, shielding of the operation equipment and exhaust ventilation (table 4). The maximum exposure levels to arsenic and cadmium measured in the production department in the usual operating conditions were 0.20 and 0.76 μg m^{-3}, respectively, which are far below (at least one order of magnitude) the respective occupational exposure thresholds. This evidence suggests that workers who are regularly or occasionally involved in maintenance work have higher potential for occupational exposure than operators who are in charge of routine production work. Further, exposure levels may vary considerably depending on several factors, such as cleaning frequency, contamination level and presence and efficiency of engineering controls. Statistically significant differences ($\rho_{KW} < 0.001$) were detected between personal and fixed-site monitoring; as expected, the highest mean concentrations were typically observed for personal sampling rather than for fixed-site sampling performed during the same work task and/or in the same location. This difference is probably because operators need to operate very

close to the particles sources and because of the absence of a Local Exhaust Ventilation (LEV) system, which would be useful to reduce occupational exposure.

4.2 Surface Contamination Monitoring

Arsenic- and cadmium-containing compounds were also found to be deposited on various surfaces, primarily in association with maintenance work (powder containment booth) and laboratory tests (table 3). Even when airborne concentrations were below the TLVs, arsenics and cadmium compounds can accumulate on floors, equipment, and work surfaces. Regarding surface contamination, there are no standards or guidelines aimed at defining a well-established assessment criterion. Thus, a literature search was conducted to analyse possible decontamination methods and a maximum allowed surface contamination threshold. The decision to choose 10000 μg m^{-2} as the maximum allowed surface contamination for As and Cd in an occupational environment was made with a precautionary approach; this informal standard was based on analogy to other carcinogenic chemicals, and it is considered acceptable for use in industry practice (except in the case of eating surfaces) (Dufault *et al.,* 2010). As expected, the contamination of work surfaces was linked with the productive period. In this regard, cadmium surface concentrations were also typically higher than the corresponding As concentrations, probably due to the aforementioned greater use of cadmium-based raw materials than arsenic-based in the production process. After the end of the production activities, an increase in surface contamination levels was observed in some specific areas (powder containment boots) with respect to background values. This could be mainly ascribed to the opening, disassembly and disposal of operation chambers, which resulted in significant dispersal of arsenic and cadmium powders. Generally, surface contamination levels were within the adopted informal threshold of 10000 μg m^{-2} (Dufault *et al.*, 2010) both for arsenic and cadmium in the production facility, laboratory and non-productive areas. Nevertheless, in the containment booths, the contamination levels may easily exceed this limit value (for arsenic N = 2/80; for cadmium N = 21/80) (table 2). The afore mentioned informal threshold was widely maintained for almost all of the surfaces after the first cleaning (reduction up to 90%, estimated by field test) and for most of the remaining contamination with a second cleaning (overall reduction over 95%, estimated by field tests) with the standard operating procedure (SOP) for cleaning and decontamination specifically developed to achieve a final surface concentration on the same order of magnitude of background values. The cleaning SOP consists of the following different stages: (I) contaminants were first removed from workplace surfaces by scraping, brushing and vacuuming (HEPA-equipped vacuums); (II) surfaces were then washed and wet wiped with an appropriate solvent (isopropyl alcohol aqueous solution) and (III) re-washed with water. After this protocol was implemented, the decontamination method and procedures were documented during an intervention survey to ensure the achievement of "cleanliness" conditions established a priori. Arsenic and cadmium concentrations appeared to be on the same order of magnitude as the background levels for both surface (Arsenic = 0.36 μg m^{-2}, Cadmium = 0.61 μg m^{-2}) and air (Arsenic = 0.001 μg m^{-3}, Cadmium = 0.004 μg m^{-3}) sampling.

4.3 Biological Monitoring

The biological monitoring data (table 4) showed no significant temporal variation in the biological markers used for surveillance; no statistically significant differences were observed

between the exposed and unexposed groups and between the employees working most intimately on the manufacturing processes (operators) and those who were employed in other activities (engineers). This is in contrast to other studies, which show that urinary biomarkers in exposed groups working in the semiconductor manufacturing industry are generally higher than in non-exposed groups (Park *et al.*, 2010; Byun *et al.*, 2013). Nevertheless, no individual worker has ever shown occupationally related As_u or Cd_u levels above the biological exposure indexes (BEI) recommended for urine samples (end-shift samples), which are 35 μg L^{-1} for As_u and between 2 and 5 μg g^{-1} creatinine for Cd_u (SCOEL, 2010; ACGIH, 2013). Further, mean value for Cd_u both in exposed (0.22 μg g^{-1} creatinine) and unexposed workers (0.32 μg g^{-1} creatinine) are compatible with level found in adult population in the absence of occupational exposure, which are generally below 1 μg g^{-1} creatinine (SCOEL 2010). Finally, As_u values defined both for the exposed and unexposed workers were consistent with levels found in the European general population without occupational exposure to arsenic (Foà *et al.*, 1984; Farmer and Johnson, 1990; Kristiansen *et al.*, 1997).

4.4 Plant Life-Cycle Stage

Cadmium and Arsenic air and surface concentration during the production phase were consistently and significantly higher than background levels (table 2, table 3) and overall mean values (fig. 1, fig. 2). This result should be interpreted with caution because it may also be ascribed to the sampling strategy, which refers to the worst-case scenario during the production activity, resulting in higher mean concentrations. Concentrations similar to the background levels ($\rho_{MW} > 0.05$) were then found after the plant shutdown and restoration both for air and surface samples. The results from wipe-test sampling (table 3, fig. 1, fig. 2) showed a slight increase in surface concentrations during the decommissioning period with respect to background values and to the overall mean. This was ascribed as consequent to the disposal of operation chambers, which resulted in a significant dispersion of arsenic and cadmium powders. After the application of the cleaning procedure described below, surface contamination appeared to be on the same order of magnitude of background levels (As = 0.36 μg m^{-2}; $\rho_{MW} = 0.886$; Cd = 0.61 μg m^{-2}; $\rho_{MW} = 0.029$) and well beyond the overall mean values. Finally, biological monitoring results (table 4) showed no significant changes for the studied period; the biological markers did not show any statistically significant variations (As_u $\rho_{ANOVA} = 0.483$; Cd_u $\rho_{ANOVA} = 0.083$) between baseline values (year 2010) and levels measured during the productive period (1^{st}–4^{th} sampling session; year 2011-12), although a slight decreasing trend in urinary values can be noted during the monitoring period (fig. 1, fig. 2).

4.5 Risk Management

Some occupational activities (mechanical cleaning of deposition chambers and laboratory simulations) may cause serious contamination within the workplace and for specific workers. Exposure levels may vary considerably depending on several factors such as cleaning frequency, contamination level of equipment for cleaning, presence and efficiency of engineering controls, dust-handling techniques, etc. (Park *et al.*, 2010). The development of properly guided procedures for workplace and worker surveillance, together with the improvement of removal and containment systems as well as education and training of production and maintenance workers, assisted by specific monitoring activity, were all helpful

in preventing the absorption of toxic metals by workers. The definition of a specific SOP was part of a comprehensive risk-management program (table 4) that also addressed other issues such as the abatement of air contamination in isolated work areas (HEPA filters), the protection of uncontaminated surfaces and equipment from possible contamination events and the protection of workers engaged in maintenance, laboratory and cleaning work practices with PPE. The introduction of a well-suited risk management protocol in this company ensured adequate protection of workers' health. In this regard, the implementation of up-to-date control strategies, including local exhaust ventilation (LEV) for airborne dust extraction, with mobile HEPA-filtered inlets to be placed in correspondence with the potential sources of cadmium and arsenic dust in laser-scribing stations, laboratories and deposition chambers, was recommended. This additional risk-management action is recommended for future production of CdTe photovoltaic cells because it should contribute to further lowering the air and workplace contamination levels.

4.6 Concluding Remarks

This is the first study of workers' exposure to arsenic and cadmium in an industrial-scale plant devoted to the production of CdTe-based solar cells including both environmental (PM and surface contamination) and biological (urine samples) monitoring. Despite the limitations in monitoring these particular activities because of their irregular schedule and duration, this study reports a fairly wide number of samples. A similar study was performed in a pilot-scale production (Bohland and Smigiclski, 2000), and the results were compatible with the evidence reported in the present study. Environmental cadmium concentrations exceeded the corresponding OEL (5 μg m^{-3}) only during manufacturing activities, but the results are not reported for that study. In contrast, cadmium exposure in other manufacturing processes (semiconductor deposition, finalisation, module recycling, etc.) and biological-monitoring results (blood Cd, urine Cd and urine Beta2-microglobulin) were well below the respective thresholds.

Some limitations and peculiarities in the study design and methods could have an impact on the exposure assessment. First, environmental measurements were collected on the basis of a worst-case approach due to technical needs: exposure levels from maintenance work may vary considerably depending on several factors (i.e. the cleaning frequency, the contamination level of equipment for cleaning, maintenance area, presence and efficiency of engineering controls, and dust-handling techniques, etc) and this may be a source of variability among the measurements. For example, maintenance work in the study industry were characterized by a very irregular schedule and duration: maintenance work normally takes 1 or 2 h for each workers, then, for the remainder of the work shift, the maintenance worker was in facilities where no arsenic and cadmium compounds were handled: thus, 8-h TWA level could be significantly variable, depending on whether or not the remaining time involves work entailing arsenic and cadmium exposure. Thus, since authors decided to perform short-term (1–2 h), task based sampling for laboratory and maintenance worker, the interpretation of the personal exposure concentration is limited by the fact that the some of the reported results are not representative of a typical 8-h TWA exposure. Nevertheless, observed personal concentrations of cadmium compounds were always measured over a period of more than 1 hour and were tipically (76% of cases) almost an order of magnitude higher than the corresponding TLV-TWA. In these cases, TLV-TWA would be exceeded anyway. Secondly, biological monitoring

was not performed in a perfect match with environmental sampling. For this reason, urine Cd_u and As_u levels may only be interpreted as indicative of long-term exposures. In this regard, cadmium is known to be accumulative in the kidneys, and does not begin to excrete in the urine until concentrations become high; however the observation period (all together 2 years), was long enough to show any accumulation trend, if present. Further, although a blood sample rather than a urine sample is the most suitable sample matrix to monitor exposure to cadmium, the determination of Cd_u requires the collection of a non-invasive urine sample; this is much better accepted by workers in comparison with blood sampling. Nevertheless, the patterns in As_u and Cd_u are assumed to be demonstrative of relationships that would remain consistent.

5. Conclusions

This paper provides exposure information for an industry from environmental (airborne and surface concentration) and biological (urinary concentration) monitoring of arsenic and cadmium. Exposure data were taken for the entire life cycle of the plant. The study shows that workers handling normal processes of fabrication operation are exposed to arsenic and cadmium levels substantially lower than the TLVs. Nevertheless, the possibility of significant exposure to arsenic and cadmium inorganic compounds is likely to be considered in other condition (maintenance work, laboratory test). In particular, personal short-term exposure to cadmium compounds by maintenance and laboratory workers and was higher than the TLV and cadmium airborne concentration near key maintenance and laboratory areas on were also higher enough to indicate a potential for very serious exposure, well in excess of the TLV (table 2). Further, the surface sampling results showed that arsenic- and cadmium-containing dust, were found to be deposited on various surfaces (Table 3), but mostly in maintenance-related area (powder containment booths). Thus, maintenance and laboratory personnel could have a higher potential for inhalation exposure than other workers, whose exposure to arsenic during routine production work appears to be controlled below the TLV. In conclusion, airborne arsenic and cadmium exposure were well below the TLV when the operation is appropriately maintained in line with engineering controls such as exhaust ventilation and enclosure (i.e. powder containment booths); workers who are involved in various operations (maintenance, laboratory test) could potentially be at risk of significant exposure. Nevertheless, the biological monitoring data did not show significant occupationally related arsenic and cadmium exposure in workers and no significant changes or differences in arsenic and cadmium urinary level among the exposed and unexposed workers were found.

Acknowledgments

The authors extend a special acknowledgment to Dr. Nicola Tecce, Dr. Andrea Rossotti, Dr. Alessia Rossetti and Dr. Luca Del Buono for their contribution to the environmental samplings and to Dr. Gabriele Carugati for his contribution in the performance of chemical analysis. The authors declare no conflict of interest. This study was performed in collaboration with Melete Srl, a spin-off company of the Università degli Studi di Milano and of the Università degli Studi dell'Insubria. Melete Srl has been charged for consultancy activities in HSE items and consequently received research support (for supplies and equipment) from the organization involved in this study.

References

American Conference of Governmental Industrial Hygienists. (2013). Threshold limit values for chemical substances and physical agents and biological exposure indices. Cincinnati: American Conference of Governmental Industrial Hygienists (ACGIH).

Angerer, J.: Cadmium. In: Analyses of Hazardous Substances in Biological Materials: Methods for Biological Monitoring, pp. 85–96. J. Angerer and K.H. Schaller, Eds. VCH, New York (1988).

Aoki, Y., Lipsky, M.M. and Fowler, B.A. (1990). Alteration of protein synthesis in primary cultures of rat kidney epithelial cells by exposure to Ga, In and As. *Toxicol. Appl. Pharmacol.* 106: 462–468.

Bohland, J. and Smigiclski, K. (2000) First Solar's CdTe module manufacturing experience: environmental, health and safety results. Proceedings of the 28th IEEE Photovoltaic Specialists Conference. Anchorage, AL, New York: Institute of Electrical and Electronics Engineers; 575–578.

Bosio, A., Romeo, N., Mazzamuto, S. and Canevari, V. (2006). Polycrystalline CdTe thin films for photovoltaic applications. *Prog. Cryst. Growth Ch.* 52: 247–279.

Byun, K., Won, Y.L., Hwang, Y.I., Koh, D.H., Im, H. and Kim, E.A. (2013). Assessment of Arsenic Exposure by Measurement of Urinary Speciated Inorganic Arsenic Metabolites in Workers in a Semiconductor Manufacturing Plant. *Ann. of Occup. Environ. Med.* 25(1): 21.

Buratti, M., Calzaferri, G., Caravelli, G., Colombi, A., Maroni, M. and Foà, V. (1984). Significance of arsenic metabolic forms in urine. Part I: Chemical speciation. *Int. J. Environ. Anal. Chem.* 17(1): 25–34.

Dufault, R., Abelquist, E., Crooks, S., Demers, D., Di Berardinis, L., Franklin, T., *et al.* (2010). Reducing environmental risk associated with laboratory decommissioning and property transfer. *Environ. Health Persp.* 108(6): 1015–1022.

Edelman P. (1990) Environmental and workplace contamination in the semiconductor industry: implications for future health of the workforce and community. *Environ. Health Persp.* 86: 291–295.

European Commission Scientific Committee on Occupational Exposure Limits (2010). SCOEL/SUM/136. Recommendation from the Scientific Committee on Occupational Exposure Limits for cadmium and its inorganic compounds. European Commission Scientific Committee on Occupational Exposure Limits (SCOEL)

European committee for Standardization. (1995). EN 689:1995 Workplace atmospheres - Guidance for the assessment of exposure by inhalation to chemical agents for comparison with limit values and measurement strategy. Bruxelles: European committee for Standardization (CEN).

Farmer, J.G., Johnson, L.R. (1990). Assessment of Occupational Exposure to Inorganic Arsenic Based on Urinary Concentrations and Speciation of Arsenic. *Br. J. Ind. Med.* 47:342–348.

Foa, V., Colombi, A., Maroni, M., Buratti, M. and Calzaferri, G. (1984). The Speciation of the Chemical Forms of Arsenic in the Biological Monitoring of Exposure to Inorganic Arsenic. *Sci. Total Environ.* 34: 241–259.

Fthenakis, V.M. (2002). Multilayer protection analysis for photovoltaic manufacturing facilities. *Process Saf. Prog.* 20(2): 87–94.

Horng, C.J., Horng, P.H., Lin, S.C., Tsai, J.L., Lin, S.R. and Tzeng, C.C. (2002). Determination of urinary beryllium, arsenic and selenium in steel production workers. *Biol. Trace Elem. Res.* 88: 235–246

Hornung, R.W. and Reed, L.D. (1990). Estimation of average concentration in the presence of nondetectable values. *Applied Occupational and Environmental Hygiene* 5(1): 46–51.

Kristiansen, J., Christensen, J.M., Iversen, B.S. and Sabbioni, E. (1997). Toxic Trace Element Reference Levels in Blood and Urine: Influence of Gender and Lifestyle Factors. *Sci. Total Environ*. 204:147–160.

International Agency for Research on Cancer. (1987). Arsenic and arsenic compounds. In IARC Monographs on the Evaluation of Carcinogenic Risks to Humans. Vol 23, Suppl. 7. Lyon: International Agency for Research on Cancer (IARC).

International Agency for Research on Cancer. (1997). Monograph on the Evaluation of risks to Humans. Cadmium, Mercury, Beryllium and the Glass Industry. Monograph on the Carcinogenity: An Update of IARC Monograph, vol 58. Lyon: International Agency for Research on Cancer (IARC).

Italy Parliament and Senate. (2008). Decreto Legislativo n. 81. Attuazione dell'articolo 1 della legge 3 agosto 2007, n. 123, in materia di tutela della salute e della sicurezza nei luoghi di lavoro (G.U. n. 101 del 30 aprile 2008). 9th April 2008. Rome: Italy Parliament and Senate.

Currie, L.A. (1995). Nomenclature in evaluation of analytical methods including detection and quantification capabilities (IUPAC Recommendations 1995). *Pure and Applied Chemistry* 67(10): 1699–1723.

Mirer, F.E. (2008). Occupational Safety and Health Protections. In: Heggenhougen K, Quah S (eds). International Encyclopedia of Public Health; Academic Press, Oxford, 2008; pp 658–668, Elsevier Inc. 2008

National Institute for Occupational Safety and Health. (2005). Publication No. 2005-151. Department of Health & Human Services, Centers for Disease Prevention & Control (DHHS). Pocket Guide to Chemical Hazards & Other Databases CD-ROM. Atlanta: National Institute for Occupational Safety and Health (NIOSH)

National Institute for Occupational Safety and Health. (2003). Method 7300, Issue 3. Elements (ICP): Manual of Analytical Methods (NMAM), Fourth Edition, 2003. Atlanta: National Institute for Occupational Safety and Health (NIOSH)

National Institute for Occupational Safety and Health. (2014). Method 7302, Issue 3. Elements by ICP: Manual of Analytical Methods (NMAM), Fifth Edition, 2014. Atlanta: National Institute for Occupational Safety and Health (NIOSH)

National Institute for Occupational Safety and Health. (2003). Method 9102, Issue 1. Elements on Wipes - Manual of Analytical Methods (NMAM), Fourth Edition, 2003. Atlanta: National Institute for Occupational Safety and Health (NIOSH)

National Institute for Occupational Safety and Health. (1997). Publication No. 97-140, 20. 1997. Pocket Guide to Chemical Hazards. DHHS (NIOSH). Atlanta: National Institute for Occupational Safety and Health (NIOSH)

Occupational Safety and Health Administration (2008). 29 CFR 1910.1018. Occupational Safety and Health Standards – Inorganic Arsenic. Washington, DC: Occupational Safety and Health Administration (OSHA)

Occupational Safety and Health Administration (2010). 29 CFR 1910.1027. 2010. U.S. National Archives and Records Administration's Electronic Code of Federal Regulations. Washington, DC: Occupational Safety and Health Administration (OSHA)

Park, D., Yang, H., Jeong, J., Ha, K., Choi, S., Kim, C., et al. (2010). A comprehensive review of arsenic levels in the semiconductor manufacturing industry. *Ann. Occup. Hyg.* 54(8): 869-879.

This chapter is based on:

- Spinazzè, A., Cattaneo, A., Monticelli, D., **Rovelli, S.**, Recchia, S., Fustinoni, S. and Cavallo, D.M. **(2015)**. Occupational exposure to arsenic and cadmium in thin-film solar cell production. *Ann. Occup. Hyg.* 59(5): 572–585

- Spinazzè A., Cattaneo A., **Rovelli S.**, Fustinoni S., Cavallo D.M. Esposizione occupazionale a Arsenico e Cadmio: caso studio nell'industria fotovoltaica. In: Conference Proceedings of the 32nd AIDII National Conference, Varese (Italy), June 24th-26th, 2015, pp. 131-137.

Tables

Table 1. Risk management options used for different work tasks.

<table>
<tr><th></th><th>Production (Regular)</th><th colspan="2">Deposition Chamber Maintenance, Laser scribing of photovoltaic module</th><th>Laboratory test / simulation</th><th>Cleaning / Decommissioning</th></tr>
<tr><td>Organisation, Procedures</td><td colspan="5">Warnings, Training, Specific Operating Procedures (S.O.P.).</td></tr>
<tr><td rowspan="2">Engineering control</td><td rowspan="2">Closed-loop, fully automated production line; General Ventilation; Other (floor sticky mats)</td><td colspan="3">Enclosure of high-exposed potential activity</td><td rowspan="2">Local Exhaust Ventilation; HEPA-filtered Vacuum Cleaners</td></tr>
<tr><td colspan="2">Fixed containment booths: HEPA-filtered, 60 ACH, with double locked-holding area</td><td>Chemical Hoods (EN 14175-compliant)</td></tr>
<tr><td>Personal Protective Equipment</td><td>Tyvek® Coveralls;</td><td colspan="4">Disposable Tyvek® Coveralls; Safety Boots and disposable shoe-covers; Nitrile gloves and disposable safety gloves; Filtering full-face mask with exhalation (FFP3-class valve)</td></tr>
<tr><td>Exposure Assessment</td><td colspan="5">Environmental Monitoring (As and Cd atmospheric sampling; surface sampling); Biological monitoring program (As and Cd urinary levels)</td></tr>
</table>

Table 2. Environmental monitoring results (PM samples): arsenic and cadmium airborne concentrations as a function of sampling location, plant life cycle stage and working task.

				As (μg m^{-3})					Cd (μg m^{-3})				
Sampling Description	*N*			*GM*	*GSD*	*Max*	*N>LOQ*	*N>TLV*	*GM*	*GSD*	*Max*	*N>LOQ*	*N>TLV*
Background													
Outdoor	SF	8h	5	0.003	1.00	0.003	0	0	0.0003	1.00	0.003	0	0
Indoor (Production Facility)	FS	8h	4	0.005	2.64	0.02	1	0	0.0006	3.97	0.0045	1	0
Position[1]													
Powder Containment booth	FS	TB	22	0.003	3.82	0.12	18	0	0.014	41.5	217.9	19	5
	P	TB	21	0.007	2.24	0.13	1	0	7.66	119	1038	18	15
Production Facility	FS	8h	51	0.002	3.48	0.02	30	0	0.006	14.2	0.76	28	0
Laboratory	FS	8h	3	0.001	1.00	0.006	0	0	11.2	1.00	11.2	3	2
	P	TB	4	0.007	1.26	0.01	0	0	5.71	133	1167	4	4
Plant Life-Cycle[1]													
Production	FS	TB	36	0.003	4.42	0.12	26	0	0.025	563	217.9	24	7
	P	TB	25	0.007	2.05	0.13	2	0	7.17	111	1167	22	19
Plant Shutdown	FS	8h	19	0.001	3.03	0.007	10	0	0.032	10.4	0.76	17	0
Decommissioning	FS	8h	11	0.003	1.00	0.003	11	0	0.008	12.4	0.14	8	0
Final (restoration)	FS	8h	8	0.001	1.41	0.002	8	0	0.004	4.27	0.31	8	0
Working Task[1]													
Maintenance Work	FS	8h	25	0.003	5.55	0.12	16	0	0.067	39.3	217.9	25	5
	P	TB	21	0.007	2.24	0.13	2	0	7.66	119	1038	18	15
Laboratory tests	FS	8h	3	0.001	1.00	0.006	0	0	11.2	1.00	11.2	3	2
	P	TB	4	0.007	1.26	0.01	0	0	5.71	133	1167	4	4
After Work Shift End	FS	8h	8	0.003	1.39	0.005	8	0	0.006	10.11	0.015	2	0

[1] = statistically significant ($\rho < 0.05$) differences in As and Cd airborne concentrations among groups of this variable; FS: Fixed-site sampling; P: personal sampling; TB: Short-term, task based sampling; 8h: 8-hour time weighted average sampling; GM = geometric mean; GSD = geometric standard deviation; Max = maximum; As: TLV-TWA = 10 μg m^{-3}; LOQ = 0.0014 μg m^{-3} (fixed site); 0.0028 μg m^{-3}(personal); Cd: TLV-TWA = 2 μg m^{-3}; LOQ = 0.0017 μg m^{-3} (fixed site); 0.0037 μg m^{-3}(personal).

Table 3. Surface contamination results (wipe test): arsenic and cadmium concentrations as a function of location and plant life cycle stage (GM = geometric mean; GSD = geometric standard deviation; Interval: max-min interval).

	N	*As (µg m^{-2})*					*Cd (µg m^{-2})*				
		GM	***GSD***	***Max***	***N>LOQ***	***N>Threshold***	***GM***	***GSD***	***Max***	***N>LOQ***	***N>Threshold***
Position[1]											
Production Facility	36	2.23	3.39	88.9	5	0	36.2	31.2	11377	30	1
Powder Containment booth	80	4.35	7.32	7784	25	2	1500	9.21	116000	80	21
Laboratory	8	2.94	3.35	14.6	3	0	167	9.30	1493	8	0
Other/ non-productive area	19	1.49	2.77	19.9	3	0	14.4	9.78	3822	14	0
Plant Life Cycle Stage[1]											
Background	4	0.36	1.93	0.6	0	0	0.02	1.00	0.2	0	0
Production	119	2.61	4.10	933	23	0	365	19.1	11600	116	22
Shutdown/ Decommissioning	20	13.7	11.5	7784	13	2	407	6.82	1493	20	0
Final (restoration)	4	0.36	1.42	0.59	8	0	0.61	1.38	0.89	4	0

[1] = statistically significant ($\rho < 0.05$) differences in As and Cd surface concentrations among groups of this variable

GM = geometric mean; GSD = geometric standard deviation; Max = maximum.

As: Threshold = 10000 µg m^{-2}; LOQ = *5.46 µg m^{-2}. Cd: Threshold = 10000 µg m^{-2}; LOQ = 3.48 µg m^{-2}.*

Table 4. Biological monitoring results: arsenic and cadmium urinary level (As-u, Cd_u) as a function of job category and plant life-cycle stage and sampling sessions.

	N	As_u (*μg l⁻¹*)					Cd_u (*μg g⁻¹* creatinine)				
		GM	***GSD***	***Max***	***N>LOQ***	***N>BEI***	***GM***	***GSD***	***Max***	***N>LOQ***	***N>BEI***
Worker population											
Reference group	12	6.11	1.77	14.0	12	0	0.24	2.36	0.85	12	0
Exposed group	57	6.11	1.75	15.0	57	0	0.22	2.08	0.83	57	0
Job category											
Administrators	12	6.23	1.75	14.0	12	0	0.23	2.20	0.55	12	0
Engineers	28	6.82	1.57	14.0	28	0	0.21	2.36	0.85	28	0
Operators	29	5.47	1.90	15.0	29	0	0.23	1.86	0.66	29	0
Plant Life cycle stage											
Background	12	7.39	1.67	15.0	12	0	0.21	1.90	0.76	12	0
Production	57	5.87	1.75	14.0	57	0	0.22	2.16	0.85	57	0
Sampling session											
Baseline (May2010)	12	7.41	1.67	15.0	12	0	0.21	1.89	0.76	12	0
1st (2011 – I Semester)	16	6.04	1.53	12.0	16	0	0.28	1.86	0.83	16	0
2nd (2011 – II Semester)	20	6.31	1.95	11.0	20	0	0.27	1.91	0.85	20	0
3rd (2012 – I Semester)	6	6.01	1.29	8.0	6	0	0.31	1.18	0.38	6	0
4th (2012 – II Semester)	15	5.18	1.91	14.0	15	0	0.12	2.42	0.58	15	0

GM = geometric mean; GSD = geometric standard deviation; Max = maximum

As: BEI = 35 μg l^{-1}, LOQ = 1 μg l^{-1}; Cd: BEI = 2 μg g^{-1} creatinine, LOQ = 0.3 (μg l^{-1}).

Figures

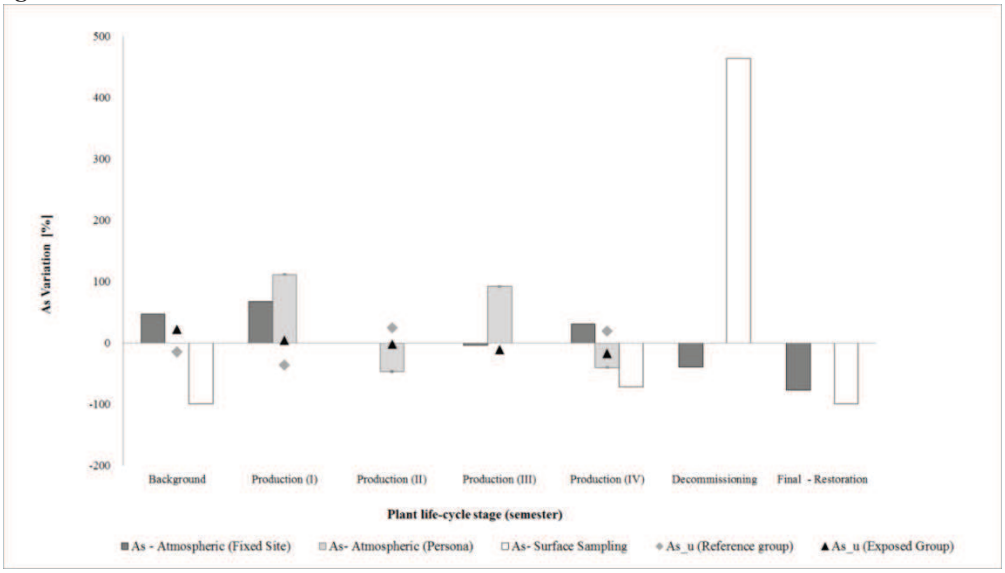

Figure 1. Percentual variation of arsenic in air (fixed site; personal), surface and biological (reference group; exposed group) samples, respectively, during different plant life-cycle stage.

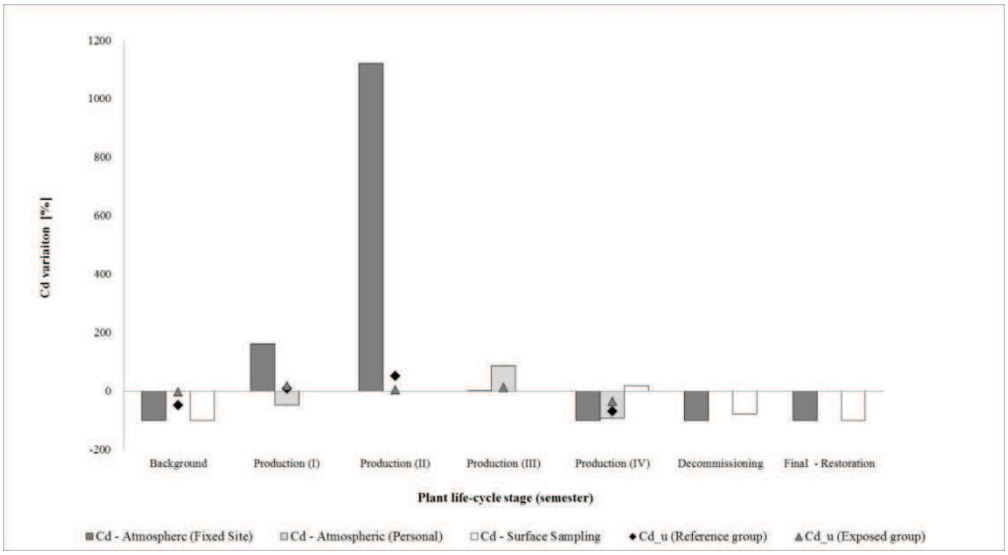

Figure 2. Percentual variation of cadmium in air (fixed site; personal), surface and biological (reference group; exposed group) samples, respectively, during different plant life-cycle stage.

General Conclusions and Future Developments

Despite some limitations, this thesis provides important insights about the mass concentration and size-distribution of airborne particles and metal components, that could be useful in developing larger air pollution and epidemiological studies.

Results obtained from the long-term monitoring campaign carried out in the Como urban area showed that the highest PM concentration levels were found during the heating period, as expected, because of a joint effect of meteorological factors and variations in type and/or number of emission sources. One of the most interesting findings of this investigation was that the greatest increase effect in the PM concentration levels was registered for particles having aerodynamic diameter values between 0.15 and 1.60 μm (and mainly for particles having D*p* values between 0.4 and 0.9 μm - more related to the presence of additional sources of submicronic particles during the cold season), whereas no relevant and significant differences were found for particles > 1.60 μm.

The proposed LA-ICP-MS method for the metal characterization provided precise and accurate results, with a better sensitivity than the conventional ICP-MS technique. The LA treatment procedure identified for sample preparation allowed accurate and reproducible analysis with a simple and fast sample preparation, thus overcoming the laborious pre-treatment approach required for wet chemical digestion. With the proposed LA-ICP-MS approach, risks associated with sample contamination were minimized and the time needed for the application of the whole measurement protocol was reduced, with the possibility to analyze a greater number of samples with several sample replicates in the same time required for the established ICP-MS protocol. Because of the less-laborious and fast sample preparation and analysis, this method could be used for routine application in order to monitor the elemental concentration and size-distribution of airborne particulates with a suitable precision and accuracy for health and sanitary purposes.

Regarding the elemental composition, the investigated elements (Cr, Mn, Fe, Ni, Cu, Zn, Ba and Pb) accounted, on average, for a very small percentage of the total $PM_{2.5}$ mass concentration and results revealed characteristic size-distributions and great variations in the concentration levels of the analyzed toxic metals, with values differing by one or more orders of magnitude from element to element and between the different sampling periods.

Although based on the assumption that people living in the study area are chronically exposed to the average metal concentrations monitored during the whole campaign, the estimated hazard quotients for each element and the overall estimate for non-carcinogenic effects posed by all of the metals under investigations were always < 1, suggesting no significant risks for the exposed population. Nevertheless, aerosol particles > 0.3 μm seemed to play the major role in the characterization of the overall non-carcinogenic risk, whereas lower contribution were found for particles < 0.3 μm, with percentage contribution values decreasing with decreasing aerosol particle size. Moreover, also the estimated $PM_{2.5}$ carcinogenic risks (CR) for Ni and Cr were below or within the acceptable range established in terms of regulatory purposes for the general population (10^{-6} or 10^{-5}), thus indicating a negligible cancer risk for people living in the study area. Nevertheless, it should be important taking into account that, although the estimated CRs for Ni were two orders of magnitude lower that the calculated CRs for Cr, the higher contributions to the total $PM_{2.5}$-CR for Ni were found to be mainly related to airborne particles that are able to more deeply penetrate into the respiratory system.

Therefore, despite some assumptions or limitations, results obtained from this research could represent important tools in epidemiological studies, as an innovative and alternative target with respect to the typical PM fractions on which these types of research are generally focused (PM_{10} or $PM_{2.5}$). Because of the type of sampling site used for particle collection (urban background) and the extended time series of size-segregated particle mass concentrations and elemental composition, these data could be used to better assess if the known and documented PM effects exerted on the general population (e.g., increased mortality or morbidity) could be related to specific size fractions and/or components of $PM_{2.5}$ and if these effects are really greater than or independent from the effects induced by larger size particulates.

Future research studies will consider the possibility to integrate the gathered information with the analysis of other major and trace elements (e.g., Al, K, S, V, As, Cd, Ti, Sb, Be) as well as some ionic species (e.g., NO_3^-, SO_4^{2-}, NH_4^+) to obtain a more complete chemical characterization of the collected size-segregated samples. In this way, the extended information derived from chemical analysis could be used for the identification and quantification of the major sized-aerosol sources in the study area (e.g., via Positiv Matrix Factorization (PMF), Principal Component Analysis (PCA)).
The determination of the bioavailable metal fraction is another relevant task for toxicological and epidemiological studies aiming at the health risk assessment of size-fractionated PM. In this context, a proper LA-ICP-MS analytical measurement protocol including an extraction procedure with Gamble's solution is currently being developed.
Finally, obtained results could help to better investigate the complex relationship between airborne PM (especially those fractions that are of major concern for humans) and adverse health effects. In this perspective, part of each filter could be preserved to consider future investigations in which the size-segregated samples could be used for in-vitro or in-vivo toxicological studies to more deeply examine: i) the critical PM characteristics that may determine the adverse effects on humans; ii) their biological mechanisms and iii) their potential relationship with the measured metal content in the size-segregated PM.

<u>Annex 1</u> – *Participation in Funded Research Projects and Scientific Publication List*

Participation in Funded Research Projects

- **Project:** *The SUPERSITE Project (2013–2015)*
  Promoter/Founded by:.Emilia-Romagna Region and Regional Agency for Prevention and Environment of Emilia-Romagna (ARPA Emilia-Romagna)
  Role: Local team member (University of Insubria, Como)
- **Project**: *SINPHONIE–Schools Indoor Pollution and Health: Observatory Network in Europe (2011–2013)*
  Promoter/Founded by: Directorate General for Health and Consumer
  Role: Local team member (University of Insubria, Como)
- **Project:** *CCM–Indoor School Project*
  Promoter/Founded by: National Center for the Prevention and Control of Disease of the Ministry of Health (Project CCM, 2010)
  Role: Local team member (University of Insubria, Como)

Full Articles - Papers

- **Rovelli, S.**, Cattaneo, A., Borghi, F., Spinazzè, A., Campagnolo, D., Limbeck, A., Cavallo, D.M. Mass Concentration and Size-Distribution of Atmospheric Particulate Matter in an Urban Environment. *Aerosol Air Qual. Res.* doi: 10.4209/aaqr.2016.08.0344, available online at: http://aaqr.org/Articles_In_Press.php.
- Spinazzè, A., Borghi, F., **Rovelli, S.** and Cavallo, D.M. (2017). Exposure Assessment Methods in Studies on Waste Management and Health Effects: an Overview. *Environments* 4: 19.
- Spinazzè, A., Lunghini, F., Campagnolo, D., **Rovelli, S.**, Locatelli, M., Cattaneo, A. and Cavallo, D.M. Accuracy Evaluation of Three Modelling Tools for Occupational Exposure Assessment. (2017). *Ann. Work Expo. Health* doi: 10.1093/annweh/wxx004.
- Spinazzè, A., Fanti, G., Borghi, F., Del Buono, L., Campagnolo, D., **Rovelli, S.**, Cattaneo, A. and Cavallo, D.M. (2017). Field comparison of instruments for exposure assessment of airborne ultrafine particles and particulate matter. *Atmos. Environ.* 154: 274–284.
- Zauli-Sajani, S., Trentini, A., **Rovelli, S.**, Ricciardelli, I., Marchesi, S., Maccone, C., Bacco, D., Ferrari, S., Scotto, F., Zigola, C., Cattaneo, A., Cavallo, D.M., Lauriola, P., Poluzzi, V. and Harrison, R.M. (2016). Is particulate air pollution at the front door a good proxy of residential exposure? *Environ. Pollut.* 213: 347–358.
- Spinazzè, A., Cattaneo, A., Monticelli, D., **Rovelli, S.**, Recchia, S., Fustinoni, S. and Cavallo, D.M. (2015). Occupational exposure to arsenic and cadmium in thin-film solar cell production. *Ann. Occup. Hyg.* 59(5): 572–585.
- **Rovelli, S.**, Cattaneo, A., Nuzzi, C.P., Spinazzè, A., Piazza, S., Carrer, P. and Cavallo, D.M. (2014). Airborne Particulate Matter in School Classrooms of Northern Italy. *Int. J. Environ. Res. Public Health* 11: 1398–1421.

Conference Proceedings

- Limbeck, A., **Rovelli, S.**, Nischkauer, W. and Cavallo, D.M. LA-ICP-MS analysis of size-segregated ultrafine airborne particulates. In Conference Proceedings of the European Winter Conference on Plasma Spectrochemistry (EWCPS, 2017), Sankt Anton am Arlberg, Austria, 19th-24th February 2017
- Zauli Sajani, S., Trentini, A., **Rovelli, S.**, Bacco, D., Maccone, C., Marchesi, S., Ferrari, S., Scotto, F., Cattaneo, A., Lauriola, P., Poluzzi, V. Indoor/Outdoor Seasonal Variability of Different Particle Metrics. In Conference Proceedings of the 28th ISEE Annual Conference (International Society for Environmental Epidemiology), Rome, Italy, September 1st-4th, 2016 (Abstract ID: 3855, http://ehp.niehs.nih.gov/isee/2016-p2-156-3855/).
- Zauli Sajani, S., Trentini, A., **Rovelli, S.**, Ricciardelli, I., Marchesi, S., Bacco, D., Maccone, C., Ferrari, S., Scotto, F., Cattaneo, A., Lauriola, P., Poluzzi, V., Harrison, R. 3D Variability of Different Particle Metrics in Urban Areas. In Conference Proceedings of the 28th ISEE Annual Conference (International Society for Environmental Epidemiology), Rome, Italy, September 1st-4th, 2016 (Abstract ID: 3396, http://ehp.niehs.nih.gov/isee/2016-o-144-3396/).
- **Rovelli, S.**, Limbeck, A., Nischkauer, W., Bonta, M., Borghi, F., Cattaneo, A., Cavallo, D.M. Characterization of toxic trace metals in size-segregated fine and ultrafine particles within an urban environment. In: Conference Proceedings of the 2nd International Conference on Atmospheric Dust, Castellaneta Marina (TA), Italy, June 12th-17th, 2016, Vol. 5: p. 227, ISSN 2464-9147.
- **Rovelli, S.**, Cattaneo, A., Borghi, F., Cavallo, D.M. Mass concentration and size-distribution of atmospheric fine, ultrafine and nanoparticles in the urban area of Como, Northern Italy. In: Conference Proceedings of the 2nd International Conference on Atmospheric Dust, Castellaneta Marina (TA), Italy, June 12th-17th, 2016, Vol. 5: p. 134, ISSN 2464-9147.
- **Rovelli, S.**, Borghi, F., Cattaneo, A., Cavallo, D.M., Campagnolo, D., Del Buono, L., Spinazzè, A. Analisi del particolato fine e ultrafine nell'area urbana di Como. In: Conference Proceedings of the 33rd AIDII National Conference, Lucca (Italy), June 16th-17th, 2016, pp. 326-332.
- Campagnolo, D., Del Buono, L., Cattaneo, A., Keller, M., Borghi, F., Bollati V., **Rovelli, S.**, Spinazzè, A., Cavallo, D.M. Monitoraggio personale di particolato atmosferico nella città di Milano: un approccio su base GIS. In: Conference Proceedings of the 33rd AIDII National Conference, Lucca (Italy), June 16th-17th, 2016, pp. 292-299.
- Del Buono, L., Cattaneo, A., Borghi, F., Campagnolo, D., **Rovelli, S.**, Spinazzè, A., Bollati, V., Cavallo, D.M. Valutazione dell'esposizione media giornaliera a PM_{10} e $PM_{2,5}$ di soggetti residenti in un'area metropolitana italiana. In: Conference Proceedings of the 33rd AIDII National Conference, Lucca (Italy), June 16th-17th, 2016, pp. 137-145.
- Spinazzè, A., Cattaneo, A., Borghi, F., Campagnolo, D., Del Buono, L., Fanti, G., **Rovelli, S.**, Cavallo, D.M. Nanomateriali: problemi nella valutazione dell'esposizione e nella gestione del rischio. In: Conference Proceedings of the 33rd AIDII National Conference, Lucca (Italy), June 16th-17th, 2016, pp. 237-244.
- Limbeck, A., **Rovelli, S.**, Bonta, M., Nischkauer, W., Cavallo, D.M. Analysis of toxic trace metals in ultrafine airborne particulates using LA-ICP-MS. In: Conference

Proceedings of the European Symposium on Atomic Spectrometry (ESAS 2016), Eger, Hungary, March 31st – April 2nd, 2016 (http://www.esas2016.mke.org.hu/images/downloads/ESAS2016_book_of_abstracts_web.pdf).

- **Rovelli S.**, Zauli Sajani S., Cattaneo A., Ricciardelli I., Trentini A., Bacco D., Poluzzi V., Lauriola P., Cavallo D.M. Indoor and outdoor airborne pollutant levels on the street- and back-side of a building in a trafficked urban area. In: Conference Proceedings of the 21st European Aerosol Conference (EAC), Milan, September 7th-11th, 2015.
- Zauli Sajani S., Trentini A., Maccone C., **Rovelli S.**, Ricciardelli I., Marchesi S., Scotto F., Ferrari S., Cattaneo A., Lauriola P., Poluzzi V. Seasonal variation of population exposure to air pollution. In: Conference Proceedings of the 21st European Aerosol Conference (EAC), Milan, September 7th-11th, 2015.
- Marchesi S., Zauli Sajani S., Bacco D., Ferrari S., Maccone C., Ricciardelli I., Scotto F., **Rovelli S.**, De Gennaro G. Vertical profile of air pollutant concentrations in proximity of a high-rise building. In: Conference Proceedings of the 21st European Aerosol Conference (EAC), Milan, September 7th-11th, 2015.
- **Rovelli S.**, Zauli Sajani S., Cattaneo A., Ricciardelli I., Trentini A., Bacco D., Poluzzi V., Lauriola P., Cavallo D.M. Valutazione della variabilità spaziale nelle concentrazioni indoor e outdoor di particolato atmosferico e inquinanti gassosi sul fronte strada e sul retro di un edificio nell'area urbana di Bologna. In: Conference Proceedings of the 32nd AIDII National Conference, Varese (Italy), June 24th-26th, 2015, pp. 167-173.
- Spinazzè A., Cattaneo A., **Rovelli S.**, Fustinoni S., Cavallo D.M. Esposizione occupazionale a Arsenico e Cadmio: caso studio nell'industria fotovoltaica. In: Conference Proceedings of the 32nd AIDII National Conference, Varese (Italy), June 24th-26th, 2015, pp. 131-137.
- Zauli Sajani S., Ricciardelli I., Trentini A., Bacco D., Maccone C., Scotto F., Ferrari S., Marchesi S., Cattaneo A., **Rovelli S.**, Cavallo D., Poluzzi V., Lauriola, P. Gradiente di esposizione all'inquinamento atmosferico sul fronte strada e sul retro di uno stesso edificio: un'indagine nell'area urbana di Bologna. In: Conference Proceedings of the 38th AIE National Conference, Napoli (Italy), November 5th-7th, 2014.
- **Rovelli S.**, Cattaneo A., Nuzzi C.P., Spinazzè A., Piazza S., Fanetti A.C., Carrer P., Cavallo D.M. Airborne particulate matter in school classrooms of Northern Italy. In Conference Proceedings of the Conference on Environment and Health – Conference of ISEE, ISES and ISIAQ", Basilea, Switzerland, August 19th-23rd, 2013 (Abstract: Environ. Health Perspect., http://ehp.niehs.nih.gov/isee/p-1-01-05/).
- **Rovelli S.**, Cattaneo A., Nuzzi C.P., Spinazzè A., Peverelli G., Cavallo D.M. Valutazione delle concentrazioni atmosferiche di polveri aerodisperse provenienti da attività di demolizione e caratterizzazione del contenuto in silice libera cristallina. In: Conference Proceedings of the 30th AIDII National Conference, Maranello (Italy), June 26th-28th, 2013, pp. 289-294.
- **Rovelli S.**, Cattaneo A., Nuzzi C.P., Spinazzè A., Piazza S., Carrer P., Cavallo D.M. Valutazione delle concentrazioni di particolato atmosferico e caratterizzazione della distribuzione dimensionale delle polveri nelle scuole del Nord Italia. In: Conference Proceedings of the 30th AIDII National Conference, Maranello (Italy), June 26th-28th, 2013, pp. 300-306.

- Spinazzè A., Cattaneo A., **Rovelli S.**, Limonta A., Nuzzi C.P., Cavallo D.M. Composti organici volatili e anidride carbonica in edifici scolastici. In: Conference Proceedings of the 29th AIDII National Conference, Pisa (Italy), June 12th-14th, 2012, pp. 205-210.
- Cattaneo A., Spinazzè A., **Rovelli S.**, Limonta A., Nuzzi C.P., Cavallo D.M. Importanza della calibrazione sull'accuratezza delle misure di particolato atmosferico mediante analizzatori ottici. In: Conference Proceedings of the 29th AIDII National Conference, Pisa (Italy), June 12th-14th, 2012, pp. 246-250.
- **Rovelli S.**, Cattaneo A., Spinazzè A., Limonta A., Nuzzi C.P., Cavallo D.M. Particolato atmosferico e co-inquinanti gassosi all'interno di edifici scolastici. In: Conference Proceedings of the 29th AIDII National Conference, Pisa (Italy), June 12th-14th, 2012, pp. 191-196.